(1→3)-β-D-GLUCAN SYNTHASES OF PLANTS

by

Andrew Keith Jacobs, B. Sc. (Hons.)

A thesis submitted in fulfillment of the requirements
for the degree of Doctor of Philosophy

School of Agriculture and Wine
Faculty of Sciences
University of Adelaide, Waite Campus
Glen Osmond, SA 5064
Australia

June 2003

Statement of Authorship

This thesis contains no material that has been submitted or accepted for the award of any other degree or diploma in any university or other tertiary institution. No other person's work has been included without due reference being made in the text.

I give consent to this copy of my thesis, when deposited in the University Libraries, being available for photocopying and loan.

Andrew K. Jacobs
June 2003

Table of Contents

Acknowledgements

I am greatly indebted to my principal supervisor Professor Geoff Fincher for providing me with the scholarship and funding that supported this research from an Australia Research Council grant and for his guidance, patience and support throughout the project. I would also like to thank him for allowing me to pursue a number of experiments, which at the time, seemed to be beyond the immediate aims of the project and providing me with the opportunity to conduct some of these studies at the Max Planck Institute for Plant Breeding Research in Cologne. I wish to thank my other supervisor, Dr. Rachel Burton, for her friendship, guidance and for the many helpful discussions related to the technical aspects of this project. Thanks also to the past and present members of the Fincher laboratory and support staff for providing a friendly and enjoyable working environment and for instilling many fond memories.

I would like to thank Professor Paul Schulze-Lefert for allowing me to pursue my studies in his laboratory at Max Planck Institute and for providing me with a roof over my head during the six months I spent in Germany. There are a number of post-doctoral fellows at the Max Planck Institute to whom I am grateful to for their help, guidance and friendship during my visit, namely, Dr. Ralph Panstruga, Dr. Volker Lipka, Dr. Judith Mueller, Dr. Andreas Hartmann, Dr. Stephane Bieri, Dr. Bekir Uelker and Dr. Stephan Bau.

Without the collaboration, generosity and advice given by a number of people much of the work presented in this thesis would not have been possible. I would therefore like to thank Prof. Bruce Stone, Dr. Neil Shirley, Dr. Tim Adams, Dr. John Forster, Dr. Sergei Lopato, Dr. Joachim Uhrig, Dr. Tim Soellick, Dr. Paul Gooding, Dr. David Gibeaut, Dr. Wojciech Grzemski, Dr. Meredith Wallwork, Ms. Dale Meyer, Ms. Jing Li and Mr. Michael Schober for their contribution and input.

Finally, I would like to thank all my family for their unwavering support and Misha Heyer for her patience, understanding and love.

Publications

Refereed papers

Andrew K. Jacobs, Volker Lipka, Rachel A. Burton, Ralph Panstruga, Nicolai Strizhov, Paul Schulze-Lefert and Geoffrey B. Fincher. (2003). An *Arabidopsis thaliana* callose synthase, GSL5, is required for wound and papillary callose formation. Plant Cell 15(11) In Press. (*Appendix D*).

Conference proceedings

Wardak, A.Z., **Jacobs, A.K.**, Anderson, M.A., Fincher, G.B. and Stone, B.A.
"The (1→3)-β-glucan synthase from suspension-cultured *Lolium multiflorum* (Rye Grass) endosperm."
Presented at ComBio99, Gold Coast, Queensland, Australia, September 27-30, 1999.

Wardak, A.Z., **Jacobs, A.K.**, Li, J., Burton, R.A., Fincher, G.B. and Stone, B.A.
"(1→3)-β-glucan synthase from the endosperm of Ryegrass (*Lolium multiflorum*)"
Presented at the 9th International Cell Wall Meeting, Toulouse, France, September 2-7, 2001.

Wardak, A.Z., **Jacobs, A.K.**, Li, J., Burton, R.A., Fincher, G.B. and Stone, B.A.
"Purification of a (1→3)-β-glucan synthase from suspension cultured endosperm of Ryegrass (*Lolium multiflorum*)."
Presented at the 27th Annual Lorne Conference on Protein Structure and Function, Lorne, Victoria, Australia, February 10-14, 2002.

Jacobs, A.K., Burton, R.A., Schulze-Lefert, P., and Fincher, G.B.
"Functional analysis of plant (1→3)-β-D-glucan synthases."
Presented at the Plant Cell Wall Biosynthesis Meeting, UCLA, Lake Arrowhead Conference Centre, May12-15, 2002.

Jacobs, A.K., Burton, R.A., Schulze-Lefert, P., and Fincher, G.B.
"Functional analysis of plant (1→3)-β-D-glucan synthases."
Presented at the Plant Polysaccharide Workshop, Palm Cove, Queensland, Australia, July 4-6, 2002.

Jacobs, A.K., Lipka, V., Burton, R.A., Panstruga, R., Strizhov, N., Schulze-Lefert, P., and Fincher, G.B.
"Arabidopsis AtGSL5 deposits callose at papillae and wound sites."
Presented at the 7th International Congress of Plant Molecular Biology, Barcelona, Spain, June 23-28, 2003.

Abbreviations

A	Absorbance
AD	Activation domain
Approx.	Approximately
ATP	Adenosine triphosphate
BD	Binding domain
bp	Base pairs
BSA	Bovine serum albumin
cAMP	Cyclic adenosine monophosphate
CaMV	Cauliflower mosaic virus
cDNA	Complementary DNA
cGMP	Cyclic guanosine monophosphate
CTAB	Cetyltrimethylammonium bromide
d	Days
Da	Dalton
dCTP	Deoxycytidine triphosphate
DEAE	Diaminoethyl
DMSO	Dimethylsulphoxide
DNA	Deoxyribonucleic acid
dNTP	Deoxynucletide triphosphate
dsRNA	Double stranded DNA
DTT	Dithiothreitol
EDTA	Ethylene diamine tetra-acetic acid
EGTA	Ethylenebis (oxyethylenenitrilo) tetraacetic acid
EST	Expressed sequence tag
g	Gram
g	Units of relative centrifugal force
Gal4	Yeast transcriptional activator protein
GFP	Green fluorescent protein
GSL	Glucan synthase-like
GTE	Glucose Tris EDTA
GTP	Guanosine triphosphate
GUS	β-Glucuronidase
H	Hour
HEPES	(N-[2-Hydroxyethyl] piperazidine-N'-[2-ethanesulphonic acid])
HPLC	High-performance liquid chromatography
HRP	Horseradish peroxidase
IgG	Immunoglobulin G
IPTG	Isopropylthiogalactoside
kb	Kilo base
LB	Luria-Bertani
M	Molar
MeCN	Acetonitrile
min	Minutes
mRNA	Messenger RNA
MS	Murashige Skoog
PCR	Polymerase chain reaction
PEG	Polyethylene glycol
pI	Isoelectric point
PVP	Polyvinyl pyrilidone
RACE	Randomly amplified cDNA ends
RFLP	Restriction length polymorphism
RNA	Ribonucleic acid
RNAi	RNA interference
rpm	Revolutions per minute
RT-PCR	Reverse transcriptase PCR
SD	Synthetic dropout
SDS	Sodium dodecyl sulphate
SDS-PAGE	SDS-polyacrylamide gel electrophoresis
sec	Seconds
SM	Saline magenesium
SSC	Standard saline citrate
TBS	Tris buffered saline
T-DNA	Transfer DNA
TdT	Terminal transferase
TEAA	Triethylammonium acetate
T_m	Melting temperature
Tris	Tris[hydroxymethyl] amino methane
U	Units
UDP	Uridine diphosphate
UV	Ultraviolet
v/v	Volume for volume
w/v	Weight for volume
X-α-Gal	5-Bromo-4-chloro-3-indolyl-α-D-galactopyranoside
X-β-Gal	5-Bromo-4-chloro-3-indolyl-β-D-galactopyranoside
X-Glu	5-Bromo-4-chloro-3-indolyl-β-D-glucuronide
YPD	Yeast potato dextrose

Abstract

Callose is a (1→3)-β-D-glucan that is widely distributed in higher plants. During normal plant growth and development, callose is found as a transitory component of the cell plate in dividing cells, it is a major component of pollen mother cell walls and pollen tubes, and is found as a structural component of plasmodesmatal canals. Callose is also observed in abscission zones and in the phloem of dormant tissues. In addition to its role in normal growth and development, callose is deposited between the plasma membrane and the cell wall following exposure of plants to a range of abiotic and biotic stresses, including wounding, desiccation, metal toxicity and microbial attack. The involvement of the plant glucan synthase-like or *GSL* genes in the formation of callose at these various locations is investigated in this thesis. Techniques including database screening, bioinformatics, various cloning protocols, heterologous expression, analysis of protein-protein interactions, gain-of-function systems and loss-of-function systems have been used in this project. Gene isolation was conducted in ryegrass where good biochemical data existed for GSLs but subsequent functional analyses were conducted in barley, where better genetic information was available. Ultimately proof of function of a single *GSL* gene was achieved in the plant model *Arabidopsis*.

A full length cDNA of a (1→3)-β-D-glucan synthase termed *LmGSL1*, encoding 1907 amino acid residues, was isolated from *Lolium multiflorum* using molecular techniques. The deduced LmGSL1 protein is predicted to contain 14 transmembrane spanning domains with the NH_2-terminus and a large central loop, thought to contain the catalytic site, located in the cytoplasm. A homologue of this gene was isolated from barley, *HvGSL1*, for the purpose of functional analyses. cDNA fragments of the barley *GSL* gene were expressed in *E. coli* and mammalian cells, and (1→3)-β-D-glucan synthase activity assays were undertaken on purified fractions. No (1→3)-β-D-glucan synthase activity could be attributed to either of the expressed polypeptides, alone or when combined.

The involvement of the barley *GSL* gene in the formation of papillae that result from fungal challenge was investigated in single cells of barley leaf blades using a transient

gene-silencing assay. Double-stranded RNA interference (dsRNAi) constructs with homology to *HvGSL1* were produced and introduced into the epidermal cells of barley leaves using a biolistic approach. The callose deposits found in transformed leaves at papillae were indistinguishable from those found in control leaves, suggesting that HvGSL1 is unlikely to be involved in papillae formation. Regions of the barley GSL protein were further assessed for interactions with other proteins using the yeast two-hybrid system and interactions between the NH_2-terminal region of HvGSL1 and proteins expressed from several plant cDNA libraries were detected.

Deposition of callosic plugs, or papillae, at sites of fungal penetration is a widely recognised early response of host plants to microbial attack and is thought to physically impede entry of the fungus. *Arabidopis* was transformed with dsRNAi constructs designed to silence three putative callose synthase genes (*AtGSL5, 6* and *11*). Both papillary callose and wound callose were absent in lines transformed with *AtGSL5* dsRNAi constructs, and in a corresponding sequence-indexed *AtGSL5* T-DNA insertion line, but were unaffected in *AtGSL6* and *AtGSL11* dsRNAi lines. Depletion of callose from papillae in *gsl5* mutants only slightly enhanced penetration of the grass powdery mildew fungus *Blumeria graminis*. Upon infection of wild type *GSL5* plants with biotrophic powdery mildew fungi or the oomycete *Peronospora parasitica*, callose also encased haustorial complexes, which are intracellular fungal feeding structures that are vital for nutrient uptake. Most importantly, the absence of callose in papillae or at haustorial complexes correlated with effective growth cessation of several normally virulent powdery mildew species and of *P. parasitica*. The enhanced disease resistance phenotype of the previously described *Arabidopsis* mutant *pmr4* to powdery mildew is probably the result of a mutation in *AtGSL5*. It is proposed that biotrophic fungal pathogens exploit wound-inducible GSL5 callose for the maintenance of a biotrophic lifestyle.

CHAPTER 1

GENERAL INTRODUCTION

1.1 INTRODUCTION

The overall aim of the work described in this thesis was to isolate and characterise genes and cDNAs encoding (1→3)-β-D-glucan synthases in higher plants. In plants, (1→3)-β-D-glucan is commonly referred to as callose and its presence has been noted and studied for over 100 years (Mangin, 1890). However, the chemical structure of the (1→3)-β-D-glucan polymer was not determined until Kessler (1958) isolated and characterised the callose pads found at sieve plates of the phloem in grapevine. To date there have been no reports on the successful isolation, in a pure form, of the enzyme responsible for the deposition of callose in plants. A number of groups have reported enrichment of callose synthase activity but there has been much debate regarding the polypeptides that might be actively involved.

Deposits of (1→3)-β-D-glucans have been found in various cellular locations and cell types at different stages of development and following various environmental influences. These observations suggest there is a number of callose synthases in plants, given the range of locations where callose is found and the different cues that stimulate its production. The work presented in this thesis is centred on the study of the biosynthesis of (1→3)-β-D-glucans in plants, especially with respect to linking the putative (1→3)-β-D-glucan synthase genes to specific functions within the plant. (1→3)-β-D-glucan synthase genes will be refered to here using the widely accepted nomenclature of *GSL* for glucan synthase-like genes (http://cellwall.stanford.edu/). To address the complex nature of this polysaccharide synthase and its regulation, which affect some of the more fundamental aspects of plant growth and development, the research described here was conducted using various molecular based techniques and model systems.

The search for a *GSL* cDNA was initially conducted in tissues of ryegrass because the biochemical properties of ryegrass (1→3)-β-D-glucan synthases had been well documented (Henry and Stone, 1982; Meikle *et al.,* 1991; Bulone *et al.,* 1995; Bulone *et al.,* 1999). The study of *GSL* function was subsequently conducted in barley where more genetic information was available and finally in *Arabidopsis* where the complete genome sequence, well defined mutant populations and a highly efficient

transformation system could be utilised. The first chapter of the thesis introduces the properties, locations and presumed functions of (1→3)-β-D-glucans in plants, along with an introduction to some of the techniques utilised in functional studies of putative *GSL* genes.

1.2 (1→3)-β-D-GLUCAN

1.2.1 Structural properties of (1→3)-β-D-glucans

(1→3)-β-D-Glucans of plants are essentially linear, unbranched molecules of (1→3)-linked β-D-glucosyl residues (*Figure 1.1*). The (1→3)-β-linkage causes the polymer to adopt a helical conformation, which enables the formation of a gel-like structure under certain circumstances. (1→3)-β-D-Glucan molecules often form both double and triple helices and these conformational variations alter the solubility, strength and rigidity of the (1→3)-β-D-glucan molecule. Triple helices of (1→3)-β-D-glucan are known to form fibrillar microfibrils in the cell walls of specialised cell types, such as pollen tubes (Anderson *et al.*, 1987; Stone and Clarke, 1992). (1→3)-β-D-Glucans bind tightly to the fluorochrome of the aniline blue dye and this property has proven useful for the detection of callose deposits in various plant tissues, using microscopes equipped with epifluorescent illumination (Eschrich, 1954; Waterkeyn, 1981).

1.2.2 Cellular locations and associated functions

1.2.2.1 Cell plate

Many of the molecular mechanisms involved in the process of cell division in plants remain largely unknown. However, it has long been known that callose is deposited transiently at the cell plate or "phragmoplast" during cell division (Eschrich, 1954; Stone and Clarke, 1992). The callose begins to accumulate in vesicles that are derived from the Golgi apparatus. The vesicles align along the plane of cell division during the early anaphase stage of meiosis (Otegui *et al.*, 2001). Phragmoplastin, a dynamin-like protein, appears at this point and associates with the cell plate vesicles (Verma, 2001). In *Arabidopsis,* phragmoplastin has been shown to interact with both a protein encoded by a putative *GSL* gene, *AtGSL6,* and a protein encoded by a UDP-glucose transferase (*UGT1;* Hong *et al.*, 2001a, 2001b).

The vesicles aligned at the phragmoplast form the earliest part of the new cell wall, and create a fenestrated sheet that extends in a centrifugal manner and ultimately fuses with the existing primary wall of the dividing cell. The rapid increase in the volume

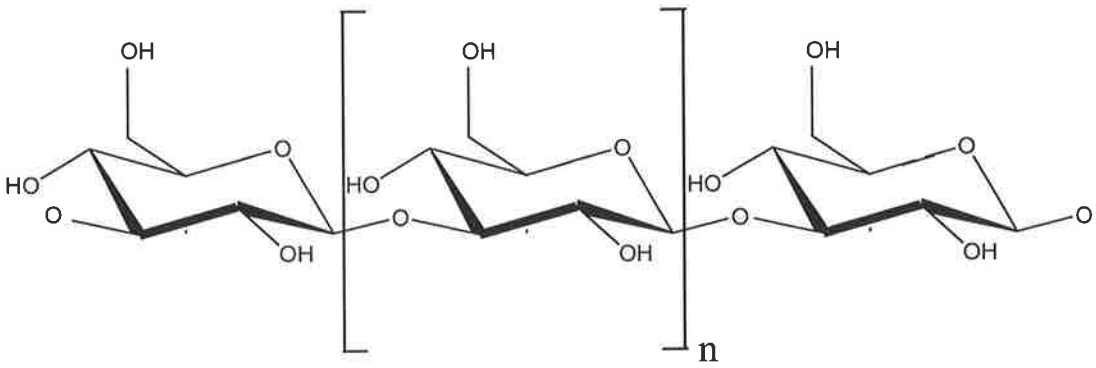

Figure 1.1 Structure of (1→3)-β-D-glucan. n represents the number of β-D glucosyl residues in the (1→3)-β-D-glucan polymer.

of the developing fenestrated sheet during the later stages of cell plate formation is believed to be largely due to the deposition of callose (Otegui *et al.*, 2001). The bulk of this substantial deposition of callose is ultimately degraded as the mature anticlinal wall forms and cell division is completed.

1.2.2.2 Plasmodesmata and sieve plates

As the cell plate forms, some of the numerous microtubules that guide the Golgi-derived vesicles to the cell plate become permanently fixed within the newly formed anticlinal cell wall. These entrapped microtubules preserve cytoplasmic connections between the daughter cells and later become plasmodesmata (Brett and Waldron, 1996). The plasmodesmata of cells that ultimately differentiate into the phloem are termed sieve pores and together they form the sieve plate. In plant species that overwinter in a dormant state, such as grapevine, thick pads of "dormancy" callose are deposited at the sieve plates at the end of the growing season and this callose is degraded at the beginning of the new growing season. Monoclonal antibodies have been used to demonstrate that plasmodesmatal canals contain callose deposits in the neck region of the canal and that the callose deposits are most prominent in the sieve plates of phloem cells (Northcote, 1989). Histochemical staining with aniline blue has also been used to locate callose deposits at the plasmodesmata (Waterkeyn, 1981).

Early studies of the deposition of callose in growing tissues prepared for microscopy by sectioning long confused scientists, because callose was routinely found blocking the neck of plasmodesmata and it seemed illogical for intercellular transport routes to be obstructed. It was later realised that the preparation of the tissue for microscopy was causing the formation of the observed callose deposits. Subsequent experiments in which tissues were prepared in the presence of 2-deoxy-D-glucose, an inhibitor of callose formation, led to substantial reductions of callose deposits observed in the neck regions of plasmodesmata (Radford *et al.*, 1998). Radford *et al.* (1998) also demonstrated that the upper size limit for transport through plasmodesmata is generally around 700-900 Da, but that increases in the concentration of cytosolic Ca^{2+} lead to a reversible reduction in the permeability of the plasmodesmata due to the deposition of callose in the neck of the plasmodesmata. Thus, the deposition of

callose in plasmodesmata involves a Ca^{2+} signal and is often a response to wounding. The involvement of a Ca^{2+} signal as a cue for callose deposition is discussed further in section 1.2.3.1.

Mutant tobacco plants that are deficient for a class I (1→3)-β-glucanase (*GLUI*), which is an enzyme that hydrolyses (1→3)-β-glucosyl linkages, deposit more callose in the neck region of plasmodesmata when compared with wild type plants that have been heat-shocked at 32°C, treated with fungal elicitors or xylanase, or following wounding (Iglesias and Meins, 2000). A noticeable delay in the spread of both tobacco mosaic virus and a recombinant potato virus X was associated with enhanced callose deposition in *gluI* knockout plants (Shimomora, 1982; Iglesias and Meins, 2000). The observed decrease in infection severity in *gluI* knockout plants is believed to result from a reduction in the size exclusion limit of plasmodesmata due to callose deposition. Accordingly, reductions in callose deposits at the plasmodesmata are thought to contribute to the more severe infection phenotype detected in *GLUI* over-expression lines. Tobacco plants over-expressing the *GLUI* gene exhibit more severe symptoms of tobacco mosaic virus infection compared with wild type (Bucher *et al.*, 2001). Together, these observations illustrate the importance of callose as the structural compound responsible for the size exclusion limit of the plasmodesmatal pore and concomitantly for cell-to-cell trafficking.

1.2.2.3 Reproductive tissues

Callose is known to form a protective barrier around sporocytes prior to meiosis and around degenerating megaspores (pollen mother cells) following meiosis (Fincher and Stone, 1981). The deposits, like those at the phragmoplast, are only transitory and the deposition of callose in embryogenic tissues can therefore be used as a marker for the onset of megasporogenesis (Tucker *et al.*, 2001). During the course of pollen development, the callose deposits of the megaspore are progressively dissolved, along with any remaining primary cell wall polysaccharides (Stone and Clarke, 1992). The developing pollen grains are ultimately released as a result of this degradation of the megaspore.

(1→3)-β-D-Glucan is found in the cell walls of other specialised tissues, including pollen tubes. Monoclonal antibodies directed against (1→3)-β-D-glucan, together with aniline blue fluorochrome, have shown that callose is present in the inner wall layer of pollen tubes of *Nicotiana* (Meilke *et al.,* 1991). Later studies suggested that the cell walls of pollen tubes of *Nicotiana* may contain as much as 75-88% (w/w) callose as a total of cell wall carbohydrates (Schlüpmann *et al.*, 1994). When the pollen grain germinates, the pollen tube grows down through the transmission tissue of the style to the embryo sac. One of the unique features of this process is that the growing pollen tube extends from the tip, analogous to the way in which fungal hyphae grow. Most other growth in higher plants occurs via extension of the longitudinal cell walls (Cosgrove, 1997). Callose is deposited sub-apically and transversely at regular intervals across the pollen tube (Steer and Steer, 1989). It is believed that the transverse depositions provide the growing pollen tube with a means to retain the cytoplasmic contents of the cell at the growing tip. Another feature of the callose found in the walls of pollen tubes is that the enzyme responsible for its deposition has biochemical properties that appear quite distinct from the properties of other (1→3)-β-D-glucan synthase enzymes (Schlüpmann *et al.,* 1993, 1994). These differences will be discussed further in section 1.2.3.1.

1.2.2.4 Abiotic stress-associated callose deposits

Callose is synthesized at wound sites whether they are caused by mechanical disruption (Waterkyn and Bienfeit, 1979; Riehl and Jaffe, 1984), chemical stress (Jorns *et al.,* 1991; Wissemeier and Horst, 1987) or are temperature-related (Thomas and Hall, 1979; Dinar *et al.,* 1983). In wounded cells callose is deposited between the plasma membrane and the cell wall, in close proximity to the site of wounding, and appears to emanate from the plasma membrane. The deposition of callose occurs within minutes of damage to the cell and is clearly visible after staining with the aniline blue fluorochrome (Stone and Clarke, 1992). Rapid shaking or DMSO treatment will also induce callose formation in liquid cultured carrot cells (Shea *et al.,* 1989).

Plants exposed to high concentrations of metal ions suffer growth retardation and callose is deposited in the tips of roots exposed to the ions. Callose is detectable in roots of Norway spruce within three hours following exposure to Al^{3+} ions (Jorns *et al.*, 1991). In soybean, Al^{3+} ions inhibit root elongation and callose can be detected in root tips two hours following treatment (Horst *et el.*, 1992). Exposure to Mn^{2+} ions also leads to the formation of callose in the root tips of soybean (Wissemeier *et al.*, 1993) and cowpea (Wissemeier and Horst, 1987). Callose deposits in root tips of soybean exposed to Al^{3+} ions begin to degrade 22 hours after return to Al^{3+} free media. There is a demonstrated Ca^{2+} dependence for callose formation in response to metal ion exposure (Wissemeier and Horst, 1995) and callose deposition in root tips has also been used as a marker for Al^{3+} ion sensitivity in maize (Horst *et el.*, 1997).

1.2.2.5 Biotic stress-associated callose deposits

In leaves, callose deposits are often located at sites of failed penetration attempts by fungal hyphae (Heitefuss and Ebrahim-Nesbat, 1986; Stone and Clarke, 1992) and deposits are induced in plants following infection by other biological agents, including many viruses and bacteria (Beffa *et al.*, 1996; Wenzl and Wodicka, 1981).

The callose deposits that are associated with penetrating fungal structures are commonly referred to as papillae. Particular attention has been focused on callose formation in plant-microbe interactions, during which plant host cells respond to microbial attack by rapidly synthesising and depositing callose as plugs, drops or plates in close proximity to the invading pathogen (Ryals *et al.*, 1996; Donofrio and Delaney, 2001). These callosic deposits may contain, in addition to (1→3)-β-D-glucan, minor amounts of protein, phenolic compounds or other polysaccharides (Smart *et al.*, 1986a, 1986b; Bolwell, 1993). While the precise function of callosic papillae during microbial attack has not been demonstrated unequivocally, it is generally believed that the papillae act as a physical barrier to impede microbial penetration and might also serve to slow or immobilize invading micro-organisms so that the host plant can focus upon them a number of anti-microbial compounds, such as wall-degrading enzymes, phytoalexins and active oxygen species (Brown *et al.*, 1998).

It has been postulated that the timing and frequency of papillae formation following attempted infection in a plant may be crucial in determining whether or not a plant ultimately becomes infected. An example of where the speed of callose deposition would appear to affect the outcome of fungal attack is neatly illustrated in observations of the barley *mlo* mutant (Gold *et al.,* 1986). In *mlo* mutants, broad-spectrum resistance to the powdery mildew fungus, *Blumeria graminis*, is the result of the absence of a single, 60 kDa, wild type MLO protein (Jørgensen, 1992). The MLO protein appears to be a negative regulator of a basic plant defence response, which amongst other things has downstream effects on the speed at which a plant cell senses or responds to infection, and acts by forming papillae at sites of attempted cellular penetration. As a consequence, *mlo* mutants synthesize callose earlier, faster and in greater abundance than their wild type relatives, which might contribute to the observed increase in resistance (Gold *et al.,* 1986).

1.2.3 Biosynthesis

1.2.3.1 Biochemistry

Attempts over the last 50 years to purify the enzyme responsible for the synthesis of (1→3)-β-D-glucans have been largely unsuccessful. The methods employed have mostly been biochemical in nature but they have failed in their ultimate goal of purifying this protein to homogeneity. The major impediment to the purification of callose synthase would appear to be that the enzyme is membrane bound. The enzyme catalyses the following reaction, where G is a glycosyl residue and n is the degree of polymerisation of the (1→3)-β-D-glucan chain:

$$(G)_n + \text{UDPGlc} \rightleftharpoons (G)_{n+1} + \text{UDP}$$

The new glycosidic linkage of the extending glucan chain is formed at the O-3 position of the terminal glucosyl residue at the non-reducing end of the polymer (Henry and Stone, 1982a, 1982b).

Various biochemical methods aimed at isolating the synthase complex have been employed, including detergent solubilisation, rate zonal centrifugation (Lawson *et al.,*

1989; Delmer *et al.,* 1991), native gel electrophoresis (Thelen and Delmer, 1986), isoelectric focussing, substrate affinity labelling assays (Dhugga and Ray, 1994) and immunoaffinity procedures with polyclonal antibodies (Fink *et al.,* 1990) and monoclonal antibodies (Delmer *et al.,* 1991; Meikle *et al.,* 1991). All have led to the co-purification of a number of polypeptides or, alternatively, to the purification of a polypeptide lacking callose synthase activity.

Product entrapment techniques have been used to enrich callose synthase activity from membrane extracts (Bulone *et al.,* 1995; Inoue *et al.,* 1995). Bulone *et al.* (1995) reported a 400-fold purification of (1→3)-β-D-glucan synthase activity from membrane preparations of *Lolium multiflorum* endosperm suspension-cultured cells. The product entrapped enzyme preparation contained six major polypeptides of which the authors suggested the abundant polypeptides of 29-32 kDa and 55 kDa were the most likely candidates for participation in (1→3)-β-D-glucan synthesis. There have been other reports of partially purified polypeptides having callose synthase activity, but there has been some discrepancy in the size reported for the peptides putatively responsible for the activity. Dhugga and Ray (1994) reported the presence of 55 kDa and 70 kDa polypeptides in purified pea membranes and a 65 kDa polypeptide was found to co-localise with callose in the papillae of infected cells of French bean (Brown *et al.,* 1998). A 65 kDa protein was also detected in immunoprecipitated callose synthase active fractions extracted from mung bean, pumpkin and cucumber (Hayashi *et al.*, 1987; Delmer *et al.,* 1993) and found in elicitor-induced suspension cultures of French bean (McCormack *et al.,* 1997). A polypeptide of 190 kDa was enriched in product-entrapped pellets from pollen tube extracts of *Nicotiana alata* (Turner *et al.,* 1998). Three polypeptides of 27, 29 and 31 kDa identified in plasma membrane fractions of *Beta vulgaris* were implicated in the synthesis of callose based upon topology-related protease sensitivity assays (Wu and Wasserman, 1993).

One explanation for the multiple polypeptides found in preparations capable of producing callose may be that the callose synthase enzyme forms a complex with a group of proteins and that the multiple polypeptides observed in gels merely correspond to these ancillary or regulatory proteins. Indeed, the concept of a (1→3)-

β-D-glucan synthase complex has gained significant support over recent years (Bulone *et al.,* 1995; Cui *et al.,* 2001; Hong *et al.,* 2001a, 2001b; Verma, 2001)

In some of the partially purified (1→3)-β-D-glucan synthase preparations mentioned above, it was noted that a higher concentration of the substrate, UDP-glucose (1 mM), preferentially favoured the production of (1→3)-β-D-glucan, as opposed to cellulose or (1→3, 1→4)-β-D-glucan, which predominated under lower concentrations of UDP-glucose (10 μM; Henry and Stone, 1982a). These observations have fuelled the long-running debate surrounding the possibility that cellulose synthase and callose synthase may indeed be the same enzyme. This theory was first proposed as a result of studies on partially purified preparations of cellulose synthase that contained (1→3)-β-D-glucan synthase activity (Delmer, 1987). The identification of separate cellulose synthase genes (Pear *et al.,* 1996; Delmer, 1999; Burton *et al.,* 2000) and callose synthase genes (Cui *et al.,* 2001; Doblin *et al.,* 2001; Hong *et al.,* 2001a, 2001b; Østergaard *et al.,* 2002) from various plant species would seem to have resolved this issue, but in many cases there is no good evidence that callose synthase activity is directly associated with the putative callose synthase gene product, and the possibility that cellulose and callose are synthesized by the same enzyme can not yet be fully discounted. The identification of a large number of putative β-D-glucan synthase-like (*GSL*) genes that encode ~200 kDa proteins (http://cellwall.stanford.edu/), indicates that the smaller polypeptides observed in the early purification studies are only a part of the callose synthase enzyme or are components of a larger callose synthase complex.

Other factors that may explain the observed lack of callose synthase enzyme activity in many of the purified preparations could relate to the loss of critical co-factors during the purification process. Indeed, it has been shown in yeast that the *RHO1P* and *RHO2P* gene products must be present, and in a GTP-bound state, for active synthesis of (1→3)-β-D-glucan to occur (Qadota *et al.,* 1996), and that this activity is also likely to be mediated *via* two protein kinase C homologues *PCK1P* and *PCK2P* (Arellano *et al.,* 1999). In *Arabidopsis,* two plant homologues of the *RHO* yeast genes have been identified (*AtROP4* and *AtROP6*) and the proteins have been located at the cross-wall of root meristems and also at the cell plate (Molendijk *et al.,* 2001)

both are known sites of callose deposition. Furthermore, a Rop GTPase-dependent pathway was found to control the deposition of callose during pollen tube growth in *Arabidopsis* (Li *et al.*, 1999).

There is an increasing body of evidence that suggests the existence of two types of (1→3)-β-D-glucan synthase activity in plants. One is found in somatic cells and appears to bind the substrate, UDP-glucose, in a Ca^{2+}-dependent manner (Amor *et al.*, 1995; Cui *et al.*, 2001; Goubet and Morvan, 1995). The second is found in pollen tubes and is not Ca^{2+}-responsive (Schlüpmann *et al.*, 1993; Li *et al.*, 1997; Doblin *et al.*, 2001). These observations, and results from the sequencing of the rice and *Arabidopsis* genomes, give credence to the idea that a family of (1→3)-β-D-glucan synthases may exist in higher plants. Individual members of the family presumably have specific cellular functions, for the deposition of callose in all its different forms and locations, and in response to different external stimuli.

1.2.3.2 Yeast (1→3)-β-D-glucan synthase genes

Some success in linking putative (1→3)-β-D-glucan genes to specific functions has been achieved over the last ten years using genetic approaches. Douglas *et al.* (1994) reported the cloning of a gene, *FKS1*, from *Saccharomyces cerevisiae* by complementation of yeast mutant containing a lower a (1→3)-β-D-glucan content. Disruption of the *FKS1* gene in the mutant resulted in very slow growth, hypersensitivity to immunosuppressants, a slight increase in sensitivity to echinocandin [a (1→3)-β-D-glucan synthase inhibitor] and, most importantly, a significant reduction in (1→3)-β-D-glucan synthase activity *in vitro*. The *FKS1* nucleotide sequence encodes a 215 kDa polypeptide predicted to be an integral membrane protein with 16 transmembrane helices. A second gene, *FKS2*, has also been cloned from *S. cerevisiae* and encodes a 217 kDa polypeptide that shares 88% peptide sequence identity with *FKS1* (Mazur *et al.*, 1995). The presence of the *FKS2* gene may account for the lack of lethality and slow growth of the *fks1* knockout mutants. Three genes sharing high levels of homology to the yeast *FKS1* gene were subsequently cloned from other microorganisms, including *Aspergillus nidulans*

(Kelly *et al.*, 1996), *Candida albicans* (Douglas *et al.*, 1997; Mio *et al.*, 1997) and *Cryptococcus neoformans* (Thompson *et al.*, 1999).

1.2.3.3 Plant GSL *genes*

At the commencement of this project in 1999 there was no reported or publicly listed gene that was predicted to encode a plant (1→3)-β-D-glucan synthase enzyme. However, in the past two years there have been four publications reporting the characterisation of various plant (1→3)-β-D-glucan synthases (Cui *et al.*, 2001; Doblin *et al.*, 2001; Hong *et al.*, 2001a; Østergaard *et al.*, 2002). If one now conducts a search for plant *GSL* genes in any of the publicly accessible databases a large number of putative DNA sequences are found. All of these putative plant callose synthase genes have been identified on the basis of their nucleotide sequence similarity to the yeast *FKS* genes, discussed in the previous section, which are believed to encode catalytically active (1→3)-β-D-glucan synthases. Analyses of the *Arabidopsis* and rice genomes have revealed the presence of 12 and 13 putative *GSL* genes, respectively (http://cellwall.stanford.edu/). Two recently published papers have made use of the publicly available DNA sequence of putative (1→3)-β-D-glucan synthases to clone and characterise two of the genes from *Arabidopsis*, termed *AtGSL5* and *AtGSL6*, as described below.

Thus, Hong *et al.* (2001a) cloned an *Arabidopsis* gene they termed *CalS1,* which will be referred to here as *AtGSL6*, based on the recommendations of Richmond and Somerville (2000). The *AtGSL6* gene has an open reading frame of 1950 bp that encodes a deduced polypeptide of 226 kDa with 16 transmembrane helices and an NH_2-terminal and large central loop that are both predicted to be cytoplasmic. A recombinant AtGSL6:GFP fusion protein was found at the cell plate in transgenic tobacco BY-2 cells and the AtGSL6 protein was found to interact with phragmoplastin and a UDP-glucose transferase (Hong *et al.*, 2001a). The transgenic tobacco BY-2 cells were also found to have elevated levels of callose synthase activity when compared with wild type cells. As a result of these findings Hong *et al.* (2001a) concluded that the *AtGSL6* gene encodes the catalytic subunit of the

Arabidopsis (1→3)-β-D-glucan synthase enzyme that is involved in cell plate formation.

In the other recent paper on an *Arabidopsis* callose synthase gene, the product of a AtGSL5:GFP fusion construct that was transcriptionally regulated by the constitutive CaMV 35S promoter was located at the plasma membrane of particle bombarded onion cells (Østergaard *et al.*, 2002). Northern analyses of the *AtGSL5* transcript revealed that transcription could be induced by salicylic acid treatment and that a floral organ pattern of gene activation existed, leading the authors to speculate that in addition to a role in callose production in pollen, *AtGSL5* is a likely target of systemic acquired resistance during pathogen attack. Like the *AtGSL6* gene, the deduced peptide sequence was predicted to have 16 transmembrane helices, with an NH_2-terminal and central loop that are probably cytoplasmic. Another feature of the *AtGSL5* sequence is a predicted cytoplasmic UDP-binding motif in a 76 amino acid loop that was located further towards the COOH-terminus than the large central loop. Østergaard *et al.* (2002) also presented data to suggest that the *AtGSL5* cDNA could partially complement the yeast *fks1* mutant.

The *GSL* genes from other plant species have also been characterised. Using RT-PCR, Doblin *et al.* (2001) showed that two genes, designated *NaGSL1* and *NaGSL2*, were expressed in the floral organs of *Nicotiana alata*. *NaGSL1* was expressed abundantly in developing and mature pollen, and in growing pollen tubes, whilst *NaGSL2* was expressed at low levels in immature floral organs. The NaGSL1 enzyme was predicted to have 16 transmembrane helices with a large central loop of 745 amino acid residues and a smaller NH_2-terminal region of 496 amino acid residues, both of which were predicted to be cytoplasmic. The authors suggested that *NaGSL1* is the gene encoding the (1→3)-β-D-glucan synthase enzyme that deposits callose in the cell walls of pollen tubes (Doblin *et al.*, 2001).

A cDNA designated *CFL1*, encoding a 219 kDa protein with 13 deduced transmembrane helices, was cloned from cotton fibres (Cui *et al.*, 2001). The protein has two large hydrophilic regions predicted to be cytoplasmic, namely an NH_2-terminal region of 557 amino acid residues and a large central loop of 729 amino acid

residues. The full-length cotton cDNA has limited (41%) homology to the yeast *FKS1* gene but the hydrophilic central loop has a higher level of similarity (52%) than the rest of the protein. A calmodulin-binding domain was identified in the NH_2-terminal domain of the protein and Northern hybridisation analyses of *CFL1* gene transcription revealed that it was expressed most strongly in cotton fibres during primary wall development. The authors also demonstrated that an *in vitro*-synthesized callose pellet could be labelled with an anti-*CFL1* antibody (Cui *et al.*, 2001).

One of the common features of all the plant genes or cDNAs mentioned in the studies above is the predicted presence of two substantial cytoplasmic domains at the NH_2-terminal and central regions of the deduced proteins, where the central loop appears to share the greatest degree of sequence homology in the genes examined. It is tempting to speculate that the catalytic site of the (1→3)-β-D-glucan synthase enzyme may be contained in one of these regions. It is important to note, however, that to date only Hong *et al.* (2001a) were able to demonstrate, albeit circumstantially by detection of a fusion protein at a site of known (1→3)-β-D-glucan synthase activity, that any kind of (1→3)-β-D-glucan synthase activity was associated with the gene studied. No other group have yet been able to demonstrate unequivocally that (1→3)-β-D-glucan synthase activity is specifically associated with a single gene.

1.3 FUNCTIONAL ANALYSIS OF UNKNOWN GENES

As outlined in the sections above, two difficulties were identified when we embarked on this project to clone and characterise plant genes encoding callose synthases. Firstly, the isolation of putative callose synthase cDNAs and genes had been based upon their homology with the yeast *FKS* genes, which have been implicated in the synthesis of (1→3)- and (1→3, 1→6)-β-D-glucans in yeast cell walls (Douglas *et al.*, 1994; Castro *et al.*, 1995; Mazur *et al.*, 1995). However, the evidence for *FKS* gene function in the synthesis of these polysaccharides has been indirect, and is not universally accepted (Cabib *et al.*, 2001; Dijkgraaf *et al.*, 2002). Thus, there was some doubt as to whether the higher plant FKS homologues were actually (1→3)-β-D-glucan synthases. The second difficulty related to the common occurrence of multi-gene families in higher plants. Indeed, the putative *GSL* gene families from *Arabidopsis* and rice contain at least 12 and 13 genes, respectively (http://cellwall.stanford.edu/). While it might be reasonably expected that the members of the multi-gene family will be expressed in different tissues at different times or under different environmental conditions, it is also possible that some members have slightly different activities. For example, would all the enzymes encoded by the putative *GSL* genes actually synthesize (1→3)-β-D-glucan, or could some be involved in the synthesis of closely related polysaccharides, such as (1→6)-β-D-glucans?

With these possibilities in mind, it was clear that considerable effort would need to be directed to confirming the function(s) of the putative *GSL* genes being targeted in the current project. In the sections below some of the functional analysis procedures commonly used to define plant gene function are summarised in general terms, as background information for much of the work described in this thesis. More specific methods for functional analysis of the putative *GSL* genes will be introduced in greater detail in later chapters, where the experimental data are presented.

1.3.1 Introduction

The completion of the *Arabidopsis* Genome Initiative Sequencing Project in 2000 (Arabidopsis Genome Initiative, 2000), the release of a substantial part of the rice genome sequence from the International Rice Genome Sequencing Project in 2002 (Goff *et al.,* 2002; Yu *et al.,* 2002), coupled with the vast number of cDNA and EST sequences that are publicly available, provide an important resource for studies of plant genes. For example, there are currently more than 800,000 EST sequences available for wheat and barley (Matthews *et al.,* 2003). Thus, it is often possible to retrieve the DNA sequence of a gene of interest, or a close relative, from a database rather than by undertaking laborious protein purification or gene isolation experiments. The DNA sequences generated from these programs will ultimately lead to the identification of almost all *Arabidopsis* and rice genes. In the future, the genomes of other important plant species will be added to the DNA sequence databases. Most of the genes identified as a result of these sequencing programs are likely to have homologues in other plant species. The DNA sequence databases provide a starting point for understanding the function and interrelationships of an estimated 25,000 genes for *Arabidopsis* alone (Chory *et al.,* 2000). The immediate challenge now facing plant biologists is how we might identify a function for each of these genes.

The analysis of gene function is often a more difficult task than the process of gene identification and isolation. Some of the factors that need to be considered before undertaking the functional analysis of a gene include when and where the gene is expressed, whether the gene encodes a product that is essential for plant development or cellular integrity, and the likelihood that other genes may have the same or a similar function. Generally speaking there are three strategies that can be used for the identification of an unknown gene's function. Firstly, the isolated gene can be expressed in a heterologous system and the function of the expressed, purified protein can be measured directly. This is particularly useful where the gene product is an enzyme for which a specific activity assay is available. Secondly, there are a number of "loss-of-function" systems, including transient gene silencing or mutant analysis, through which a phenotype can be reasonably linked to the function of the silenced or mutated gene. Thirdly, "gain-of-function" systems allow gene function to be linked

with a phenotype or activity when the particular candidate gene is over-expressed or expressed in a location that does not normally contain that gene product. More information regarding these three strategies for functional analysis of candidate genes is given in the sections below.

1.3.2 Candidate gene identification

As mentioned above, database screening is commonly undertaken prior to gene isolation experiments and the DNA sequence or deduced peptide sequence of a known gene from one species can often be used as a tool to guide the isolation of the homologous gene of interest in another species. Ultimately the gene or part thereof needs to be cloned and gene isolation has historically been achieved using phage library screening (Sambrook *et al.,* 1987) and/or PCR based techniques (Siebert *et al.,* 1995; Frohman *et al.,* 1998). A successful outcome for these approaches to gene isolation depends upon the homology between the gene of interest and the homologue identified in the database or literature, if one is not trying to isolate a gene that has previously been sequenced. The analysis of homologous genes from different species has led to the observation that within a single gene there are regions of DNA that are quite highly conserved and other regions that are more variable, and the use of restriction mapping (Nass *et al.,* 1981) and direct DNA sequencing of immunoglobulin genes (Hackett and Lis, 1981) has highlighted this. Thus, by targeting conserved regions for PCR primer design, DNA probes with a high probability of success can be generated for the isolation of a gene of interest.

The data from genome-wide analyses of gene expression are becoming increasingly useful for identifying genes of interest and the results of a number of microarray experiments are available in the public domain (www.arabidopsis.org/links/microarrays.html). A search for callose synthase on the Stanford microarray database (http://genome-www5.stanford.edu/MicroArray/SMD/) revealed six sequences of interest (A.K. Jacobs, unpublished data). Of the six, one sequence had been placed on a microarray and its expression profile following abiotic stress and hormonal/drug treatment was retrieved. The sequence on the array corresponds to the *Arabidopsis AtGSL10* gene that encodes a putative (1→3)-β-D-glucan synthase. Expression of this gene appears to be induced following treatment with abscisic acid and cordycepin

(transcription chain terminator), and by exposure to Al^{3+}, Fe^{2+} and K^{+}. Treatment with auxin, cytokinin and gibberellin has no effect on expression levels of the *AtGSL10* gene. The information gleaned from this straightforward search would take a substantial amount of time to generate in experimental terms. These databases are in the early stages of development but ultimately all the genes from *Arabidopsis* and rice will be arrayed and their expression profiles made publicly available (http://genome-www5.stanford.edu/MicroArray).

1.3.3 Heterologous expression

Proteins are frequently present in plant cells in low abundance or associated with other proteins or complexes, and their extraction can be hindered by secondary metabolites in the cell (Tsugita and Kamo, 1999). Heterologous expression systems can be used as a means to produce recombinant proteins in relatively large amounts and in high purity. In this process, a full-length or near full-length cDNA is inserted into an appropriate plasmid vector designed specifically for expression in a particular heterologous system. The plasmid vector containing the cDNA of interest is transferred to a cell in which the expression of the plasmid can be induced. Following proliferation of the transformed cell and induction of the expression plasmid containing the inserted cDNA, the translated protein product can be recovered for analysis of its biological function. In many cases the expressed protein can be modified slightly to assist in its purification. For example, expressed proteins can be modified to carry a short NH_2- or COOH-terminal poly-histidine segment. This enables the expressed protein to be easily purified, using Ni-NTA affinity chromatography, from the large number of other proteins that will be present in the cell homogenate (Janknecht and Nordheim, 1991). Heterologous expression can be undertaken in several different systems, most notably in *E. coli*, *Pichia pastoris*, insect cells and a range of mammalian cell lines.

Thus, a glutathione-dependent formaldehyde dehydrogenase of *Arabidopsis* was recently identified as an S-nitrosoglutathione reductase by studying the kinetics of a recombinant enzyme expressed and purified from *E. coli* (Sakamoto *et al.*, 2002). The yeast *Pichia pastoris* system has been used for expression of a number of plant enzymes including a xyloglucan endotransglycosylase of tomato (Catala *et al.*, 2001),

an arginine decarboxylase of *Arabidopsis* (Hanfrey *et al.*, 2001), a DELTA6-fatty acid desaturase of *Borago officinalis* (Sayanova *et al.*, 2001) and a lipid phosphate phosphatase of *Arabidopsis* (Pierrugues *et al.*, 2001). The baculovirus/insect cell expression system has been used for the expression of an inwardly rectifying potassium channel from potato (Zimmermann *et al.*, 1998), a two-pore potassium channel of *Arabidopsis* (Czempinski *et al.*, 1997) and a stachyose synthase of adzuki bean (Peterbauer *et al.*, 1999). Expressing the KDC1 protein of carrot in Chinese hamster ovary cells identified it as a voltage and pH-dependent inwardly rectifying potassium channel (Downey *et al.*, 2000). Immortalised mammalian cell lines and *Xenopus laevis* oocytes have also been used as expression systems but rarely for plant proteins. The *HKT1* gene of *Arabidopsis* is one of the few plant genes to be expressed in *Xenopus laevis* oocytes and was found to encode a selective Na^+ uptake transporter (Uozumi *et al.*, 2000).

1.3.4 Loss-of-function systems

Loss-of-function analyses require a specific gene of interest to be silenced, either transiently or in stably transformed plants or cell lines, so that the function of the gene can be defined by reference to the phenotype produced. For example, if a putative callose synthase gene were silenced its putative function could be confirmed if the plant was subsequently incapable of synthesising callose.

Silencing can be effected in a number of ways, but most commonly through antisense or RNA interference technology, both of which operate post-transcriptionally. Antisense technology relies upon the binding of a reverse complementary or antisense RNA fragment, which is generally transcribed at high levels from an introduced transgene or plasmid, to the mRNA of the target gene following its transcription. Hybridisation of the antisense fragment to the target mRNA induces sequence-specific degradation of the double stranded RNA (dsRNA) molecules, resulting in reduced expression of the encoded protein (Baulcombe, 1996). RNA interference operates via the same dsRNA degradative mechanism (Fire *et al.*, 1998). The presence of a dsRNA molecule with homology to the target gene is achieved by introducing a plasmid or transgene containing an inverted repeat of the target gene. Following transcription of the DNA construct, the mRNA forms a region of dsRNA

by virtue of the inverted repeat. Again the dsRNA is subjected to sequence-specific degradation in a process that also degrades single stranded mRNA with the same sequence (Hamilton and Baulcombe, 1999). Thus, a DNA construct encoding a dsRNA in which the inverted repeat contains callose synthase sequence would induce degradation of endogenous callose synthase mRNA and thereby "silence" the callose synthase gene.

The cDNA construct that encodes the dsRNA molecule is generally introduced into the plant by common transformation procedures. Transgenic plants can now be produced for a huge number of plant species, usually by particle bombardment or by *Agrobacterium* infection (Chen *et al.*, 1986; Czernilofsky *et al.*, 1986; Wallroth *et al.*, 1986). Particle bombardment can be used for stable or transient gene silencing assays in many plant species. In this technique gold particles are coated with a plasmid engineered for silencing a specific gene and the DNA-coated particles are shot into the cells of the host plant using helium gas. The plasmid is transcribed directly or is integrated into the host's genome where it is subsequently transcribed and silences target gene expression as outlined above. *Agrobacterium tumafaciens* is a natural soil borne pathogen of plants causing crown gall disease. Part of the pathogenic strategy of these bacteria is the integration of DNA encoding virulence factors into the host's genome. This facet of the bacteria's life cycle has been exploited and engineered plasmids can be used to transfer foreign DNA into the plant genome (Leemans *et al.*, 1981). For some plant species, such as *Arabidopsis*, transformation simply requires submersion of leaves in an *Agrobacterium*/detergent solution.

In addition to targeted gene silencing techniques of the type discussed above, naturally occurring mutants and mutagenised plant populations can be used to define gene function, provided the phenotypes of the mutant can be reliably linked with a lesion in a specific gene. Mutant plant populations can be produced by chemical mutagenesis or by random transposon and T-DNA insertions. Large mutant populations exist for important plant species including *Arabidopsis*, rice, barley and maize, many of which are publicly available. Mutants generated using random insertion of transposons or T-DNA are particularly useful because the inserted sequence can be used as a base for PCR analysis of flanking sequences in the genome and this speeds up the identification of the disrupted gene.

1.3.5 Gain-of-function systems

Gain-of-function experiments are achieved by the expression of a gene in a location where, or at a time when, that gene would not normally be expressed. Thus, a new function or phenotype at that location can be directly attributed to the expression of the new gene. As an example, most mammalian cells do not produce (1→3)-β-D-glucan and the expression of a putative (1→3)-β-D-glucan gene in these cells and the subsequent detection of callose with the aniline blue fluorochrome would represent a gain-of-function and provide strong evidence that that gene did, indeed, encode a (1→3)-β-D-glucan synthase. Gain-of-function experiments generally require the expression of a full-length coding sequence and often utilise the techniques of transformation described in the previous section.

Over-expression of an introduced DNA has been used to elucidate gene function in plants (McCormac *et al.*, 1991; Deng *et al.*, 1992; Oonu *et al.*, 1993; Tourneur *et al.*, 1993). As examples, constitutive over expression of the *Arabidopsis* gene *AtGSK1* results in enhanced NaCl tolerance in *Arabidopsis* (Piao *et al.*, 2001) and seed-specific over-expression of an *Arabidopsis* cDNA encoding a diacylglycerol acyltransferase enhances seed oil content and weight (Jako *et al.*, 2001). However, the presence of endogenous versions of the gene proposed for expression or up-regulation can make interpretation of the result difficult, because it might not be obvious whether the over-expression is due to the indirect up-regulation of the endogenous gene, or to expression of the introduced gene that is being analysed. Thus, the gain of an entirely new function in a system where the gene or similar genes are not normally expressed precludes many of these interpretative issues.

In an alternative gain-of-function approach, a mutant phenotype can be complemented by the expression of a gene suspected to be responsible for the mutant phenotype. Complementation has been used extensively to assign gene function in yeast but has rarely been used in plants. However, it has been used to identify genes involved in (1→3)-β-D-glucan synthesis (Douglas *et al.*, 1994) and in cell cycling (Nasmyth and Reed, 1980).

1.4 AIMS OF THE PRESENT STUDY

The overall aim of this project was to isolate and characterise callose synthase genes of higher plants and to undertake the functional analysis of these putative callose synthase genes. Initially, the callose synthase genes of *Lolium multiflorum* were targeted because there was considerable biochemical information available on the corresponding enzymes (Bulone *et al.,* 1995; Henry and Stone, 1982; Meikle *et al.,* 1991). However, as the project progressed the emphasis was shifted to callose synthases in plant species where more extensive genetic and EST information was available, namely in barley and *Arabidopsis*.

Within the overall objective of this project the more specific aims were:

1) To clone a full-length cDNA encoding a *GSL* gene and characterise its expression patterns in *Lolium multiflorum*, with a view to linking transcriptional activity of the gene with known sites of callose synthesis (Chapter 2).
2) To investigate the function of putative plant (1→3)-β-D-glucan synthases by heterologous expression studies in *E. coli* and mammalian cells (Chapter 3), and by altering gene expression levels in living plants utilising RNA interference technology in transiently transformed cells (Chapter 5) and transgenic plants (Chapter 6).
3) To identify and characterise other proteins that may be interacting with the *GSL* gene product as part of a multi-subunit complex by studying the interaction of selected regions of the barley GSL protein using a yeast two-hybrid approach (Chapter 4).

CHAPTER 2

ISOLATION OF A (1→3)-β-D-GLUCAN SYNTHASE cDNA FROM *LOLIUM MULTIFLORUM*

2.1 INTRODUCTION

The main thrust of the research project presented in this thesis was to provide some concrete evidence linking the function of *GSL* genes to the production of callose in plants. By definition therefore the starting point of the project required the isolation of a plant *GSL* gene. It is worth repeating that the plant *GSL* genes referred to here were identified based upon their sequence homology to the yeast *FKS1* gene and that no plant *GSL* gene had been directly linked with (1→3)-β-D-glucan synthase activity. Thus, all the plant genes are "putative" (1→3)-β-D-glucan synthase genes. The discovery and subsequent characterisation of the *FKS1* gene of yeast (Douglas *et al.*, 1994), was an important development for scientists investigating callose formation in plants. In higher plants, homologues of the yeast FKS protein are associated with the cell plate (Hong *et al.*, 2001a), with product-entrapped callosic material generated *in vitro* (Cui *et al.*, 2001) and an *Arabidopsis FKS* gene homologue is reputed to partially complement a yeast *fks1* mutant (Østergaard *et al.*, 2002).

Prior to the start of this research project, the late Nick Paech and his supervisor Dr. Anna Koltunow (CSIRO, Plant Industry, Adelaide) isolated a cDNA from *Hieracium piloselloides* whilst screening for genes that were expressed early in embryo development. One of the cDNAs isolated during this screen shared limited sequence identity with the yeast *FKS1* gene (24% identity). The cDNA was kindly donated to the Fincher laboratory at the University of Adelaide. It should be emphasised that at this time no plant DNA sequence that shared homology with the *FKS1* gene was present in any of the public DNA sequence databases. Ms. Jing Li, a fellow PhD student in the Fincher laboratory, used the cDNA as a probe and isolated an *FKS1* homologue from a barley cDNA library. The barley cDNA was subsequently used as a probe to isolate a *Lolium multiflorum* (ryegrass) *GSL* cDNA, as described below. In this chapter the various molecular biological techniques and methodologies employed to isolate the predicted full length cDNA are described. The cDNA was used as the basis for the functional analyses described in subsequent chapters.

2.2 MATERIALS AND METHODS

2.2.1 Materials

The λZAPII cDNA synthesis kit, ExAssist helper phage, pBluescript (SK^+), *E. coli* strains XL1-Blue MRF′, XL1-Blue, DH5α and SOLR were purchased from Stratagene (La Jolla, CA, USA). The Superscript II cDNA synthesis kit, Thermoscript cDNA synthesis kit, Trizol reagent, 5′ RACE kit and Elongase reagents were purchased from Invitrogen Corporation (Carlsbad, CA, USA). The Nucleospin Extract kit was supplied by Macherey-Nagel (Düren, Germany). Rockwool was from Rockwool International A/S (Hedehusene, Denmark). The Ultraclean DNA purification kit was supplied by Mo-Bio (Solana Beach, CA, USA). MicroSpin S-200 HR columns, Hybond N+ nylon membrane, [α-^{32}P]-dCTP and Megaprime DNA labelling kit were from Amersham Life Sciences (Buckinghamshire, UK). Custom oligonucleotides and NitroPure nitrocellulose filters were purchased from Geneworks (Adelaide, SA, Australia). Casein hydrolysate, yeast extract, agarose, agar and tryptone were purchased from Becton Dickinson (Sparks, MD, USA). Restriction enzymes and BSA were from New England Biolabs (Beverly, MA, USA). Ampicillin, ethidium bromide, Ficoll, PVP, glycerol, salmon sperm DNA, DTT, EDTA and reagents for both liquid nutrient and White's media were from Sigma-Aldrich (St. Louis, MD, USA). Gene-Pulser electroporation cuvettes were from Bio-Rad (Hercules, CA, USA). Plasmid pGEM T-Easy, dNTPs and *Taq* DNA polymerase were supplied by Promega (Madison, WI, USA). The RX X-ray film was from Fuji Photo Film Co. (Tokyo, Japan). The T4 RNA ligase and glycogen (molecular biology grade) were obtained from Boehringer Mannheim (Mannheim, Germany). Big-Dye 2, Big-Dye 3 reagents, SYBR Green PCR master mix and SYBR Green I dye were from Applied Biosystems (Foster City, CA, USA). The 3MM Chr chromatography paper was from Whatman International (Maidstone, UK). The Zorbax Eclipse dsDNA column was supplied by Agilent Technologies (Palo Alto, CA, USA). HPLC was performed using a series II 1090 liquid chromatograph purchased from Hewlett-Packard (Palo Alto, CA, USA).

2.2.2 *Cultivation of* Lolium multiflorum

Lolium multiflorum plants were grown in a growth room at 23°C with a 16 h light and an 8 h dark cycle, in aerated liquid hydroponic media (*Appendix A*) in baskets containing rockwool (Gibeaut *et al.*, 1997). Tissue samples of interest were harvested and immediately frozen in liquid nitrogen before being transferred to -80°C for longer-term storage.

Suspension cultures of *Lolium multiflorum* endosperm were obtained from Professor Bruce Stone, Department of Biochemistry, La Trobe University, Victoria, Australia. The suspension cultures were grown in modified White's media (*Appendix C*) in the dark at 23°C on an orbital shaker set to 1000 rpm. Subculturing was performed every three weeks by the transfer of 20 ml culture to 100 ml of fresh White's medium. Cells used for RNA extractions were pelleted by centrifugation for 5 min at 2300 g, the supernatant was discarded and RNA was either extracted immediately, or pellets were snap frozen in liquid N_2 and stored at -80°C until required.

2.2.3 *DNA extraction*

Genomic DNA was extracted from young leaf tissue of *Lolium multiflorum* using a hot CTAB method as described by Lassner *et al.* (1989). Leaf tissue, typically 50-500 mg, was crushed in 500 µl CTAB extraction buffer (0.22 M Tris-HCl buffer, pH 8.0, containing 0.14 M Sorbitol, 0.02 M EDTA, 0.8 M NaCl, 0.8% w/v CTAB and 1% w/v N-laurylsarcosine) pre-warmed to 65°C. Chloroform/ isoamyl alcohol (24:1 v/v) (300 µl) was added and a final volume of 1 ml was obtained by the addition of further extraction buffer. Samples were mixed by inversion and incubated for 30 min in a water bath at 65°C with lids open. Samples were briefly mixed by inversion and cellular debris was pelleted by centrifugation at 16,000 g for 5 min. The aqueous phase was gently mixed with 600 µl isopropanol and the DNA was pelleted by centrifugation for 5 min at 16,000 g. Supernatant was discarded and the pellet was washed with 70% ethanol and dried under vacuum. DNA was resuspended in 50 µl sterile water and the DNA concentration was determined by A_{260} measurement in a UV spectrophotometer (Varian, Walnut Creek, CA, USA) before samples were stored at -80°C.

2.2.4 RNA extraction

Frozen tissues were ground to a powder under liquid N_2 using a sterilised mortar and pestle. Ground tissue (approx. 100 mg) was mixed with 200 µl Trizol reagent (http://www.invitrogen.com/content/sfs/manuals/15596026.pdf) and further homogenised using a sterile, hand held plastic homogeniser. An additional 800 µl Trizol reagent was added and the sample was mixed vigorously. Cellular debris was pelleted by centrifugation at 12,000 g for 15 min at 4°C and the liquid layer was retained. Samples were left at room temperature for 5 min before 200 µl chloroform was added and the samples were shaken gently by hand for 15 sec. After incubation at room temperature for 3 min the samples were centrifuged at 12,000 g for 15 min at 4°C, the aqueous phase being retained. Isopropanol (500 µl) was added, the sample was mixed gently and left at room temperature for 10 min. Further centrifugation at 12,000 g for 10 min at 4°C pelleted the RNA and the supernatant was carefully removed. The RNA pellet was washed once with 1 ml 75% ethanol and left to air dry. RNA was redissolved in 50 µl sterile water and stored at -80°C.

Tissues containing high levels of polysaccharide were further processed by heating the redissolved RNA sample to 65°C for 5 min. After the samples had cooled to room temperature they were centrifuged at 16,000 g for 15 sec. The supernatant was collected and placed at –20°C for 5 min before the sample was again centrifuged at 16,000 g for 15 sec. The supernatant containing the RNA was retained and stored at -80°C. RNA levels were determined by A_{260} measurements in a UV spectrophotometer (Varian, Walnut Creek, CA, USA) and checked to ensure that no degradation had occurred, using agarose gels containing ethidium bromide.

2.2.5 First strand cDNA synthesis

Total RNA (5 µg) was combined with 5 pmol of oligo$(dT)_{17}$ adaptor or gene-specific oligonucleotide and the volume was adjusted to 10 µl using sterile Milli-Q water. The mixture was incubated at 65°C for 5 min in a water bath and immediately placed on ice. First strand reactions were undertaken using a Superscript II cDNA synthesis kit (http://www.invitrogen.com/content/sfs/manuals/superscriptIIpps.pdf), or a Thermoscript cDNA synthesis kit according to the manufacturer's recommended protocol.

cDNA synthesis reactions were performed for up to 60 min at 42°C for Superscript II or at 55°C for Thermoscript based reactions, after which 30 µl sterile Milli-Q water was added. The reaction was terminated by the addition of 1 µl 0.5 M EDTA, pH 8.0. The reaction mixture was gently mixed and pulse centrifuged, and 2 U RNase H was added before the mixture was heated at 37°C for 20 min to degrade the RNA. cDNA was purified from the reaction mix using an UltraClean kit and the purified cDNA was redissolved in 30 µl sterile Milli-Q water. cDNA was stored at -20°C or used directly in PCR.

2.2.6 Preparation of [^{32}P]-radiolabelled DNA probes

DNA probes were radiolabelled with [α-^{32}P]-dCTP, using a Megaprime DNA labelling kit (http://www4.amershambiosciences.com/aptrix/upp00919.nsf/(FileDownload)?OpenAgent&docid=0A78CB58DCE620A6C1256C94000DD326&file=RPN1604.pdf). Template DNA (20-50 ng) was mixed with 5 µl of random nonamers (supplied) and sterile Milli-Q water was added to a final volume of 33 µl. The DNA-primer mixture was boiled for 5 min and allowed to cool slowly to room temperature. After cooling, 10 µl labelling buffer (supplied), 5 µl [α-^{32}P]-dCTP and 2 µl Klenow DNA polymerase were added and the reaction mixture was incubated at 37°C for 30 min. Radiolabelled probes were separated from unincorporated radionucleotides using MicroSpin S-200 HR columns. The Sephacryl resin in the spin column was resuspended by briefly vortexing and the column was pre-spun at 830 g for 1 min. The entire 50 µl of the labelling reaction was loaded onto the centre of the resin and the column was centrifuged for 2 min at 830 g. Labelled probe was collected, whilst unincorporated label remained in the column. The purified probe was denatured by boiling for 5 min and was added directly to the hybridisation solution.

2.2.7 Screening a Lolium multiflorum *cDNA library*

A *Lolium multiflorum* endosperm suspension-cultured cell cDNA library constructed using a λZAPII cDNA synthesis kit (http://www.stratagene.com/manuals/200450.pdf) was kindly provided by Dr. Wojciech Grzemski (Department of Plant Science, University of Adelaide, SA, Australia). *E. coli* XL1-Blue MRF' cells were prepared in LB media (1% w/v NaCl, 1% w/v tryptone and 0.5% w/v yeast extract, pH 7.0)

containing 10 mM $MgSO_4$ and 0.2% (w/v) maltose, to an A_{600} of 0.5. The cells were centrifuged at 1000 g for 15 min and resuspended in 10 mM $MgSO_4$ at an A_{600} of 0.5. The cells were competent after 20 min incubation at 37°C.

The cDNA library was plated onto lawns of competent *E. coli* XL1-Blue MRF′ cells in 0.7% (w/v) agar in NZY-media (1% w/v casein hydrolysate, 0.5% w/v NaCl, 0.5% w/v yeast extract and 0.2% w/v $MgSO_4.7H_2O$, pH 7.0) over 1.5% (w/v) agar in NZY media, pH 7.5. Plates were incubated at 37°C for 8-12 h until plaques were clearly visible on the bacterial lawn. The plates were transferred to 4°C for approx. 4 h. Duplicate NitroPure nitrocellulose filters were overlaid on the bacterial lawn for 3 min. The DNA on the filters was denatured for 3 min in 0.5 M NaOH containing 1.5 M NaCl and neutralised for 3 min in 0.5 M Tris-HCl buffer, pH 7.5 containing 1.5 M NaCl. The DNA was fixed to the membranes by baking for 2 h under vacuum at 80°C. Filters were incubated at 65°C in 6x SSC (1x SSC is 150 mM NaCl, 15 mM sodium citrate, pH 7.0) containing 5x Denhardt's solution (0.1% w/v BSA, 0.1% w/v Ficoll and 0.1% PVP), 0.5% (w/v) SDS and 100 $\mu g.ml^{-1}$ salmon sperm DNA, for 2 h. The prehybridisation mix was discarded and replaced with 50 ml hybridisation solution, which had the same composition as the prehybridisation solution, except that 3x SSC replaced the 6x SSC.

A cDNA of approx. 2.1 kb encoding a barley *GSL* cDNA fragment was kindly donated in pBluescript (SK+) by Ms. Jing Li (Department of Plant Science, University of Adelaide, SA, Australia). A 2134 bp *Eco*RI/ *Xho*I DNA fragment was excised from the pBluescript (SK+) cloning vector and purified as described in section 2.2.5. This barley *GSL* DNA restriction fragment was randomly labelled with α-[^{32}P]-dCTP as described in section 2.2.6. The labelled DNA probe was added directly to the hybridisation solution and the filters were incubated for 16 h at 65°C with gentle rocking. The filters were washed sequentially for 20 min at 65°C in 2x SSC containing 0.1% (w/v) SDS, in 1x SSC/0.1% (w/v) SDS, in 0.5x SSC/0.1% (w/v) SDS and finally in 0.1x SSC/0.1% (w/v) SDS. The filters were blotted dry and overlayed with RX X-ray film at -80°C for approx. 24 h, using an intensifying screen. Autoradiographs were developed in an automated Curix system (Agfa, Greenville,

SC, USA). Positive clones were selected and were subjected to three rounds of plaque purification using the detection methods described above.

Following the identification of a *L. multiflorum GSL* gene fragment, another round of library screening was undertaken as described above using the newly identified 1206 bp ryegrass fragment as a probe.

2.2.8 Rescue of clones from λZAPII into pBluescript

Purified clones from the suspension-cultured endosperm library cloned into λZAPII were rescued directly into pBluescript (SK+) using the manufacturer's recommended protocol. Positive plaques were excised from 137 mm agar plates into 500 µl SM buffer (50 mM Tris-HCl buffer, pH 7.5 containing 10 mM NaCl, 8 mM $MgCl_2$ and 0.01% w/v gelatin) and 20 µl chloroform, and the samples were vortexed thoroughly before being stored overnight at 4°C. A 50 µl portion of the bacteriophage mixture was added to 200 µl competent *E. coli* XL1-Blue MRF' cells along with 1µl ExAssist helper phage, and the mixture was incubated for 15 min at 37°C. A volume of 3 ml LB media (1% w/v NaCl, 1% w/v tryptone and 0.5% w/v yeast extract, pH 7.0) was added and the mixture was incubated for a further 3 h at 37°C with shaking. The mixture was heated to 70°C for 20 min and centrifuged at 1000 g for 15 min and the supernatant recovered. The lysed bacteriophage mixture (10 µl) was added to 200 µl SOLR cells suspended in 10 mM $MgSO_4$ so that the A_{600} was 1.0, and incubated at 37°C for 15 min. The mixture was subsequently plated on LB agar plates (1% w/v NaCl, 1% w/v tryptone and 0.5% w/v yeast extract, pH 7.0 with 1.5% w/v Agar) containing 100 $\mu g.ml^{-1}$ ampicillin, and incubated for 16 h at 37°C. Colonies that grew after overnight incubation contained pBluescript (SK+) phagemids. The colonies were analysed for inserts by restriction digestion and clones of interest were sequenced as described in section 2.2.15.

2.2.9 Anchor-ligated RACE

For anchor-ligated RACE experiments, 3 µg total RNA was combined with 10 pmol of a gene-specific oligonucleotide and the volume was adjusted to 10 µl using sterile

Milli-Q water. The mixture was incubated at 65°C for 5 min and placed on ice. First strand reactions were undertaken using a Superscript II cDNA synthesis kit according to the manufacturer's recommended protocol. cDNA synthesis reactions were allowed to continue for 60 min at 42°C after which 30 µl sterile Milli-Q water was added. The reverse transcription reaction was terminated by the addition of 1 µl 0.5 M EDTA, pH 8.0. The cDNA was gently mixed and collected by centrifugation. RNA was destroyed by the addition of 2 µl 6 M NaOH and incubation at 65°C for 30 min. The reaction mixture was neutralised with 2 µl 6 M acetic acid. cDNA was purified using a Gene-Clean kit and the purified cDNA was eluted in approx. 30 µl sterile Milli-Q water. cDNA was precipitated by the addition of 20 µg glycogen (molecular biology grade), 4 µl 3 M sodium acetate and 100 µl cold 95% ethanol. The sample was gently inverted several times and placed at -20°C for 30 min before centrifugation at 16,000 g for 10 min at 4°C. The supernatant was carefully discarded and the remaining cDNA pellet was washed once with 40 µl 80% ethanol and left to air dry. cDNA was resuspended in 6 µl sterile Milli-Q water and stored at -20°C or used directly in an anchor ligation reaction.

Anchor sequences were ligated to cDNAs as follows. cDNA (1.5 µl) was mixed with 1.0 µl 10x T_4 RNA ligase buffer and 1.0 µl anchor oligonucleotide (6 pmol.µl^{-1}), and the reaction volume was brought to 10 µl by the addition of sterile Milli-Q water before 1.0 µl T_4 RNA ligase (20 U.µl^{-1}; Boehringer Mannheim) was added. Tubes were gently mixed, pulse centrifuged and incubated at 37°C for a minimum of 6 h. The anchor-ligated cDNA pool was stored at -80°C or used directly in PCR as described in section 2.2.10. 5′-End oligonucleotides, complementary to the ligated anchor were used in combination with the gene-specific primers lmcasyn2R and lmcasyn3R (*Appendix B*) in a two-round, nested PCR approach aimed at amplifying the missing 5′ cDNA sequence of the *L. multiflorum GSL* cDNA.

2.2.10 PCR using degenerate oligonucleotides

Putative *GSL* gene sequences were retrieved from the Genbank DNA database and compared for similarity and regions of sequence conservation in multiple peptide alignments (*Figure 2.4*). DNA sequence that corresponded to the most highly

conserved peptide sequence was used as the basis for the design of a degenerate primer for PCR. At sites where nucleotide sequence was not 100% conserved between the aligned sequences, alternative nucleotides were incorporated to maximise chances of amplification of *GSL* genes. PCR was performed in 25 µl reaction volumes using 1 µl cDNA as template, 300 nM primers, 200 µM each dNTP, 1 U *Taq* DNA polymerase, 1.5 mM $MgCl_2$ in a 10 mM Tris-HCl buffer, pH 8.3, containing 50 mM KCl. Cycling conditions were altered to suit oligonucleotide melting temperatures and the extension time was varied according to the length of desired product, but typically cycling was as follows: 94°C, 30 sec; 35 cycles of 94°C, 30 sec; 50-55°C, 30 sec; 72°C, 30 sec-2 min with a final extension step at 72°C for 3 min. PCR products were separated on agarose gels containing ethidium bromide. PCR bands were cut from the gel and the DNA was purified from the agarose using a Gene-Clean kit. Purified PCR fragments were cloned into the modified (T-tailed) *Eco*RV site of the pGEM T-Easy cloning vector using the manufacturer's recommended protocol.

2.2.11 5′RACE

5′ RACE was typically performed using 4 µg total RNA extracted as described in section 2.2.4, employing a 5′ RACE kit and following the manufacturer's directions. Briefly, total RNA was combined with 20 ng gene specific primer in a final volume of 15.5 µl, which was incubated for 10 min at 70°C to denature the RNA. The RNA mixture was cooled on ice for several minutes and collected at the bottom of the tube by a brief pulse spin in a bench top centrifuge. The sample was warmed to 42°C and PCR reagents were directly added to the tube giving the following final concentrations: 20 mM Tris-HCl buffer, pH 8.4, containing 50 mM KCl, 1.5 mM $MgCl_2$, 10 mM DTT, 100 nM lmcasyn7R primer (*Appendix B*), 4 µg total RNA, 400 µM each dNTP and 200 U Superscript II reverse transcriptase. The reaction mix was incubated at 50°C for 1 h and terminated by heating to 70°C for 15 min. The reaction was cooled on ice and reagents were again collected by brief centrifugation and were warmed to 37°C. RNase H (1 µl) was added and the reaction was incubated at 37°C for 30 min to destroy RNA. cDNAs were purified and washed using a Nucleospin Extract kit according to the manufacturer's protocol. The entire cDNA pool was used

in a TdT tailing reaction in a final volume of 25 µl with 10 mM Tris-HCl buffer, pH 8.4, containing 25 mM KCl, 1.5 mM $MgCl_2$, cDNA and 2.5 µl 2 mM dCTP. The mixture was heated for 3 min at 94°C, cooled and collected by pulse centrifugation before 1 µl terminal transferase (TdT) was added and the tailing reaction carried out for 10 min at 37°C. Heating to 65°C for 10 min terminated the tailing reaction. The tailed cDNAs were used directly in 25 µl PCRs under the following conditions: 20 mM Tris-HCl buffer, pH 8.4, containing 50 mM KCl, 1.5 mM $MgCl_2$, with a final concentration of 400 nM lmcasyn8R primer (*Appendix B*), 400 nM Abridged Anchor Primer, 200 µM each dNTP and 2.5 U *Taq* DNA polymerase. Cycling conditions were selected to suit oligonucleotide melting temperatures and the extension time was varied according to the length of desired product, but typical cycling was as follows: 94°C, 30 sec; 35 cycles of 94°C, 30 sec; 50-55°C, 30 sec; 72°C, 30 sec-2 min with a final extension step at 72°C for 3 min.

A single round of PCR was often insufficient to amplify sufficient DNA from low abundance cDNAs and in these instances a second round of nested PCR was undertaken. First round PCR products were diluted 50-fold with sterile water and 2 µl of the diluted reaction was used in a 25 µl second round reaction with the same reagent concentrations described above. Primer lmcasyn9R and universal anchor primer (UAP; *Appendix B*) at a final concentration of 400 nM were used in the second round PCR reactions.

2.2.12 PCR-based genomic walking

This technique was based on an article by Siebert *et al.* (1995). Adaptor mix consisting of 5 µmol adaptor 1- $^{5'}$ CTA ATA CGA CTC ACT ATA GGG CTC GAG CGG CCG CCC GGG CAG GT $_{3'}$ and 5 µmol adaptor 2- $^{5'}$ H_2N-CCC GTC CA-P $_{3'}$ in a total volume of 50 µl was heated at 90°C for 10 min and left to hybridise for 16 h at room temperature in 30 mM Tris-HCl buffer, pH 7.8, containing 10 mM $MgCl_2$, 10 mM DTT and 1 mM ATP.

Adaptor-ligated DNA was prepared from 2.5 µg *L. multiflorum* genomic DNA extracted as described in section 2.2.3. Genomic DNA was restriction digested in a

100 µl reaction volume with 80 U of the selected 6 bp blunt-end cutting restriction enzymes. The following restriction enzymes were used in conjunction with the recommended buffer supplied by the manufacturer; *Dra*I, *Eco*RV, *Msc*I, *Nae*I, *Nru*I, *Pml*I, *Pvu*II, *Sma*I, *Ssp*I and *Stu*I. Digests proceeded for 16 h at 37°C except that *Sma*I digestion was carried out at 25°C. The DNA was extracted once with phenol/chloroform/isoamyl alcohol (25:24:1 v/v), once with chloroform/isoamyl alcohol (24:1 v/v) and was precipitated by the addition of 0.1 vol 3 M NaOAc, 20 µg glycogen (molecular biology grade) and 2.5 vol 95% ethanol. Samples were mixed and centrifuged at 13,000 rpm in a bench top microcentrifuge at 4°C. DNA pellets were washed with 75% ethanol and dried in a Speed-Vac (Savant, Farmingdale NY, USA) under vacuum before being redissolved in 20 µl 10 mM Tris-HCl buffer, pH 7.5, containing 0.1 mM EDTA. Half of the purified DNA (10 µl) was ligated to an excess of adaptor mix for 16 h at 16°C under the following reaction conditions: 30 mM Tris-HCl buffer, pH 7.8, containing 10 mM $MgCl_2$, 10 mM DTT, 1 mM ATP, 5 µM adaptor mix and 6 U T_4 DNA ligase in a total volume of 20 µl. The ligation reaction was terminated by heating at 70°C for 5 min and reactions were diluted by the addition of 180 µl 10 mM Tris-HCl buffer, pH 7.5, containing 1 mM EDTA and were stored at -20°C.

Primary PCR amplification was performed in a volume of 50 µl using Elongase reagents. The ligated, diluted DNA (1 µl) was used as a template in PCR mixtures containing a final concentration of 200 µM each dNTP and 1 U (1 µl) Elongase enzyme mix in a mix of buffer A and B, which was combined to an optimal Mg^{2+} concentration of 1.6 mM in reaction buffer containing 20 mM Tris-HCl buffer, pH 8.4, with 50 mM KCl. Adaptor primer 1 (AP1; *Appendix B*), 10 pmol, was used in conjunction with various 3′ gene-specific primers. Thermal cycling conditions for the primary PCR amplification were as follows: initial denaturation at 94°C, 45 sec; 35 cycles of 94°C, 45 sec; 50°C, 45 sec; 68°C, 4 min; final extension 68°C, 7 min; 4°C hold (the melting temperature was dependent on the gene specific primer used in the reaction). Primary PCR products were diluted 25-fold in sterile water for use in a second round of PCR.

Second round PCR was conducted in 25 µl reaction volumes using 1.5 µl diluted primary PCR product as template in a reaction mix containing 300 µM each dNTP, 1 U *Taq* DNA polymerase, 1.5 mM $MgCl_2$ in a 10 mM Tris-HCl buffer, pH 8.3, containing 50 mM KCl. Adaptor primer 2 (AP2; *Appendix B*), 10 pmol, was used in conjunction with various 3′ gene-specific primers. Cycling conditions were altered slightly by reducing the extension time from 4 min to 3.5 min and only 30 cycles were conducted in the second round. The entire second round reaction mixture was separated in a 1.3% (w/v) agarose gel containing ethidium bromide. Bands of interest were excised from gels and DNA was purified from gel slices using an Ultra-Clean DNA purification kit, according to the manufacturers protocol.

2.2.13 Cloning PCR fragments into pGEM T-Easy

Purified PCR fragments were routinely cloned into the T-tailed cloning vector pGEM T-Easy for further manipulation and identification. Ligation reactions were set up in 10 µl volumes incorporating 10 ng pGEM T-Easy vector, 5 µl 2x rapid ligation buffer, 2-3.5 µl purified PCR product, 1.5 Weiss U T_4 DNA ligase and sterile Milli-Q water to 10 µl when needed. Reactions were incubated for 16 h at 16°C and ligated DNA was purified by butan-1-ol extraction. A volume of 40 µl water was added to the ligation reaction along with 500 µl butan-1-ol. The sample was mixed vigorously and centrifuged at 16,000 g for 30 min. The supernatant was discarded and the pellet was dried under vacuum before being resuspended in 3 µl sterile Milli-Q water. Ligations were stored at -20°C or were used in transformation reactions forthwith.

2.2.14 Transformation of E. coli *by electroporation*

A 500 ml culture of *E. coli* (strains DH5α or XL1 Blue) in LB media (1% w/v NaCl, 1% w/v tryptone and 0.5% w/v yeast extract, pH 7.0) was grown at 37°C with shaking until an A_{600} of 0.6 was reached. The cells were pelleted by centrifugation at 2300 g for 10 min. Supernatant was discarded and the cells were resuspended in 200 ml ice-cold sterile Milli-Q water. Centrifugation was repeated and the cells were resuspended in 40 ml ice-cold sterile Milli-Q water. The centrifugation step was repeated and the cells were resuspended in 10 ml of ice-cold sterile Milli-Q water.

Following another repeat of the centrifugation step the cells were resuspended in 10 ml ice-cold sterile 10% (v/v) glycerol. Finally the cells were resuspended in 4 ml ice-cold sterile 10% (v/v) glycerol and 40 µl aliquots were frozen in liquid N_2. Electrocompetent cells were stored at -80°C until required.

At least 1 h prior to transformation, Gene-Pulser electroporation cuvettes (1.0 mm) were placed on ice. Electrocompetent cells and ligation mixes (if frozen) were thawed on ice for 10 min. An aliquot of 1 µl of the cleaned ligation mix (section 2.2.14) was added to 40 µl electrocompetent cells and the mixture was transferred immediately to the chilled cuvette that was placed in the Gene pulser (Bio-Rad Hercules, CA, USA) set to 1.8 V, 25 µFD and 200 Ω. Transformed cells were resuspended in 300 µl of LB media (1% w/v NaCl, 1% w/v tryptone and 0.5% w/v yeast extract, pH 7.0) and were incubated at 37°C for 1 h. Cells were plated out on LB agar plates (1% w/v NaCl, 1% w/v tryptone and 0.5% w/v yeast extract, pH 7.0 with 1.5% w/v Agar) with the appropriate selective media, routinely 100 $\mu g.ml^{-1}$ ampicillin, and were incubated for 16 h at 37°C.

2.2.15 Plasmid DNA mini-preparations

Plasmids containing cDNAs and gene fragments of (1→3)-β-D-glucan synthases were grown for 16 h with shaking in 3 ml LB media containing 10 $\mu g.ml^{-1}$ ampicillin at 37°C. DNA was extracted from overnight cultures using an alkaline lysis protocol. The culture (2 ml) was centrifuged for 2 min at 16,000 g and the supernatant was discarded. The pellet was resuspended in 100 µl GTE buffer (25 mM Tris-HCl buffer, pH 8.0, containing 50 mM glucose and 10 mM EDTA) and placed on ice for 5 min. A freshly prepared mixture of 1% (w/v) SDS and 0.2 M NaOH (200 µl) was added and the sample was inverted several times. A volume of 3 M potassium acetate, pH 4.8 (150 µl), was added and the tubes were inverted several more times before being placed at -20°C for 20 min. Samples were centrifuged at 16,000 g for 15 min to pellet cellular debris and DNA was precipitated from the supernatant by the addition of 1 ml 100% ethanol for 10 min at –20°C. Plasmid DNA was pelleted by centrifugation at 16,000 g for 20 min and the pellet was washed once in 300 µl 75%

ethanol and dried. Plasmid DNA was redissolved in 30 µl sterile 25 mM Tris-HCl buffer, pH 7.5, containing 10 mM EDTA and 1 µl RNase H (20 $mg.ml^{-1}$).

2.2.16 Nucleotide sequence analysis

The Department of Molecular Pathology at the Institute of Medical and Veterinary Sciences, SA, Australia, performed nucleotide sequence analysis using an ABI 373 sequencer and 3700 capillary sequencer. Sequencing reactions were performed in 20 µl reaction volumes using Big-Dye 2 or Big-Dye 3 reagents. Template DNA (0.2-0.5 µg) was added with 3.2 pmol sequencing primer to 4 µl Big-Dye 3 reaction mix. Sterile Milli-Q water was used to bring the final reaction volume to 20 µl. PCR cycling conditions were as follows: an initial denaturation step at 96° for 30 sec was followed by 25 cycles of 96°C for 10 sec, 50°C for 5 sec and 60°C for 4 min. Freshly prepared 75% isopropanol (80 µl) was added and the sample was thoroughly mixed before being left at room temperature for 15 min. DNA was pelleted by centrifugation at 16,000 g for 20 min. The supernatant was discarded and DNA pellets were washed once in 150 µl 75% isopropanol. DNA pellets were dried under vacuum and submitted for sequencing.

2.2.17 Southern analysis

Genomic DNA (10 µg) extracted from leaf tissue of *L. multiflorum* as described in section 2.2.4 was digested for 6 h at 37°C with 100 U *Bam*HI, *Hin*dIII, *Eco*RI or *Xba*I. Digested DNA was separated on 1% (w/v) agarose gels at 25 V for approx. 16 h and the DNA fragments were transferred to a nylon membrane using the method of Southern (1975). A wick consisting of two layers of chromatography paper was draped over a sheet of glass and soaked with 0.4 M NaOH transfer buffer. Agarose gels were placed wells down on the wick and air bubbles were excluded before a Hybond N+ nylon membrane, moistened and cut to gel size, was placed over the gel. Three moistened pieces of chromatography paper and one dry piece of chromatography paper cut to gel size were overlaid on the nylon membrane. Interleaved paper towel was placed on top of the chromatography paper and the DNA was left to transfer to the membrane for at least 16 h at room temperature. The nylon

membrane was removed and neutralised in a solution of 2x SSC. Membranes were blotted dry and dried under vacuum at 80°C prior to probing. Prehybridisation of the membranes was conducted in a 20 ml solution of 6x SSC, 1x Denhardt's III solution (2% w/v BSA, 2% w/v Ficoll 400 and 2% PVP), 1% (w/v) SDS and 2.5 mg denatured salmon sperm DNA for a minimum of 4 h at 65°C. Hybridisation mixture (10 ml) containing 3x SSC, 1x Denhardt's III solution, 1% (w/v) SDS and 2.5 mg denatured salmon sperm DNA was used to replace the discarded prehybridisation mixture. Denatured, radiolabelled probe manufactured as described in section 2.2.6 was added directly to the hybridisation mixture and the probe was allowed to hybridise to the membranes for 16 h at 65°C. The membranes were washed sequentially for 20 min at 65°C in 2x SSC containing 0.1% (w/v) SDS, with 1x SSC/0.1% (w/v) SDS and with 0.5x SSC/0.1% (w/v) SDS. The membranes were blotted dry, sealed in plastic and RX X-ray film was exposed to the membrane at -80°C for approx. 24 h, using an intensifying screen.

2.2.18 RT-PCR

RT-PCR was conducted on cDNAs, produced as described in section 2.2.9 that were synthesised from various tissues of *L. multiflorum.* RT-PCR was used as an alternative to Northern analysis for semi-quantitative measures of gene expression where low levels of *LmGSL1* expression were observed. Following the synthesis of the cDNA, RNA was degraded by the addition of 2 U of RNase H to the reaction mixture and the mixture was incubated at 37°C for 20 min. The reaction mixture was diluted by the addition of 30 µl sterile milli-Q water and 1 µl cDNA was used directly in PCR. PCR was performed in 25 µl with a final concentration of 200 µM each dNTP, 1 U *Taq* DNA polymerase, 1.5 mM $MgCl_2$ in 10 mM Tris-HCl buffer, pH 8.3, containing 50 mM KCl, and 20 pmol of the gene-specific oligonucleotide combinations of lmcasyn1/lmcasyn1R or lmgapdhF/lmgapdhR (*Appendix B*). Cycling conditions were as follows: 94°C, 30 sec; 30 cycles of 94°C, 30 sec; 50°C, 30 sec; 72°C, 30 sec. PCR products were separated on 1.5% (w/v) agarose gels containing ethidium bromide and images of the gel illuminated with UV light were captured.

2.2.19 Quantitative (real-time) PCR

Quantitative (real-time) PCR experiments were performed using a Rotorgene 2000 Real-Time cycler, RG2072, followed by analysis with DNA sample analysis system v4.2 software from Corbett Research (Mortlake, NSW, Australia) in consultation with Dr. Neil Shirley (Department of Plant Science, University of Adelaide, SA, Australia). To prepare standards, three 25 µl PCRs were conducted for both of the primer combinations lmcasyn1/lmcasyn1R and lmgapdhF/lmgapdhR (*Appendix B*). PCR was performed with a dNTP concentration of 200 µM, 1 U *Taq* DNA polymerase, 1.5 mM $MgCl_2$ in 10 mM Tris-HCl buffer, pH 8.3, containing 50 mM KCl with 20 pmol of each oligonucleotide. Thermal cycling conditions were as follows: 94°C, 30 sec followed by 35 cycles of 94°C, 30 sec; 55°C, 30 sec; 72°C, 30 sec. PCR products were separated in 2% (w/v) agarose gels containing ethidium bromide and bands of the expected size were excised from the gel. DNA was purified from the agarose using a Nucleospin column. The PCR products were further purified by HPLC on a Zorbax Eclipse dsDNA column, 2.1 mm x 150 mm x 3.5 µM. The two elution solutions were 0.1 M TEAA, 0.1 M EDTA, pH 7.0 (solution A) and 0.1 M TEAA, 0.1 M EDTA, 25% MeCN, pH 7.0 (solution B). The gradient was set from 35% to 70% over a 30 min period and separation was conducted at 40°C. The flow rate was 0.2 $ml.min^{-1}$, and the column was equilibrated in solution A for at least 10 min prior to the purification on a Hewlett-Packard series II 1090 liquid chromatograph. Purified PCR products were sequenced as described in section 2.2.15 to confirm the identity of the product. A dilution series of the HPLC purified PCR products of *LmGSL1* and *LmGAPDH* were prepared, ranging from 1×10^1 to 1×10^7 $molecules.\mu l^{-1}$ and were used to generate standard curves of fluorescence levels for the given concentration of PCR product.

Total RNA was extracted from leaves of *L. multiflorum* at three stages of development, namely young, middle and mature aged, and at three time points from endosperm suspension-cultured cells, namely 4, 8 and 12 d post subculture, according to the protocol described in section 2.2.4. Two separate cDNA synthesis reactions were performed for each RNA sample (section 2.2.5) and the two cDNA populations of 50 µl were pooled. Quantitative PCR was conducted in 20 µl reaction volumes using 10 µl 2x SYBR Green PCR master mix, 0.3 µM of both the forward and reverse

oligonucleotides (lmcasyn1/lmcasyn1R and lmgapdhF/ lmgapdhR), 1 µl of the pooled cDNA population and 0.6 µl of a 100-fold dilution of SYBR Green I dye. Cycling parameters were as follows: 95°C, 600 sec followed by 55 cycles of 95°C, 20 sec; 55°C, 30 sec; 72°C, 30 sec. The presence of PCR products was confirmed by electrophoresis in agarose gels.

2.2.20 Genetic mapping of LmGSL1

A 419 bp PCR product generated from *L. multiflorum* cDNA using the oligonucleotides lmcasyn1/lmcasyn1R was cloned into pGEM T-Easy as described above (section 2.2.13). A 459 bp fragment was cut from the pGEM T-Easy vector using the restriction enzyme *Not*I. Restriction fragments were separated by electrophoresis on 2% (w/v) agarose gels and the 459 bp fragment was excised from the gel. The probe was purified from the agarose using a Nucleospin kit.

This DNA probe was sent to Dr. John Forster at the Cooperative Research Centre for Molecular Plant Breeding, La Trobe University, Victoria, Australia to be tested against a *Lolium perenne* mapping population. The probe was radiolabelled and initially hybridised to a filter with *L. perenne* DNA from a North African$_6$ x Aurora$_6$ F1 two-way pseudo-testcross mapping population, restriction digested with *Dra*I, *Eco*RI, *Eco*RV or *Hin*dIII. A filter with 56 North African$_6$ x Aurora$_6$ F1 accessions, all digested with *Eco*RV, was used to generate statistically meaningful mapping datapoints.

2.2.21 DNA sequence analysis and manipulation

Data from automated DNA sequencing were analysed using the Chromas program (Technelysium Pty Ltd, Helensvale, Queensland) and further alignment analyses and manipulations were performed using the University of Wisconsin, Genetics Computer Group software (Devereaux *et al.*, 1984) in the ANGIS suite of programs at the Australian National Genomic Information Service (http://www.angis.org.au). Deduced amino acid sequences were also analysed for motifs and other elements using this suite of programs. Database searches were performed using BLAST software (Altschul *et al.*, 1990) accessed via the National Centre for Biotechnology

Information's suite of programs (http://www.ncbi.nlm.nih.gov/BLAST/). PCR primers were chosen with the aid of Primer 3 software (Rozen and Skaletsky, 1996) in the BioManager suite of programs at the Australian National Genomic Information Service (http://www.angis.org.au) and were further analysed using NetPrimer software (http://www.premierbiosoft.com/netprimer/netprlaunch/netprlaunch.html) in the MolBiol.net suite of programs (http://www.molbiol.net/). Sequences for phylogenetic analysis were aligned using the ClustalW program (Thompson *et al.*, 1994) accessed via the ANGIS website (http://www.angis.org.au) and phylogenetic trees were generated using Treeview (http://taxonomy.zoology.gla.ac.uk/rod/rod.html). Genomic DNA sequence was scanned for intron/exon boundaries using GenSCAN software (Burge and Karlin, 1997) accessed via the Massachusetts Institute of Technology's website (http://genes.mit.edu/GENSCAN.html).

2.3 RESULTS AND DISCUSSION

2.3.1 Isolation of a GSL *cDNA fragment from a* Lolium multiflorum *cDNA library*

The isolation of a cDNA encoding a putative *GSL* from a *Lolium multiflorum* cDNA library required an appropriate probe. A 2134 bp *Eco*RI/ *Xho*I restriction fragment of a putative barley *GSL* was obtained from a plasmid donated by Ms. Jing Li (University of Adelaide) for this purpose (*Figure 2.1*). The randomly labelled probe was used to screen an amplified cDNA library generated from the RNA of suspension-cultured cells of *L. multiflorum* endosperm. Approximately 6 x 10^5 plaques were screened with the barley *GSL* cDNA probe. Five positive clones were purified to homogeneity through three rounds of screening and the cDNA inserts of the clones were rescued into pBluescript for characterisation. The plasmid DNA was purified and cDNAs were digested with *Xho*I and *Eco*RI, which indicated that four of the cDNAs had unique restriction patterns, whilst the fifth cDNA appeared to be a duplicate of one of the others (*Figure 2.2*).

To confirm these findings all five cDNAs were sequenced using T3 and T7 primers. The two cDNAs that shared similar restriction patterns, *lmcasyn2* and *lmcasyn4*, also shared sequence similarity and were identified as fragments of a putative *GSL* cDNA based upon their sequence similarity to the yeast *FKS1* gene. The 1224 bp *L. multiflorum* cDNA fragment included a putative stop codon, a 381 bp 3′ untranslated region and an 18 bp polyA tail. The other cDNAs shared sequence similarity to a predicted outer membrane protein and to a cysteine proteinase inhibitor, while one could not be identified.

Having identified a putative *L. multiflorum* specific *GSL* gene fragment of 1224 bp, a second screen of the cDNA library was undertaken, using the 1224 bp cDNA fragment to prepare a probe. It was hoped that a longer cDNA or, ideally the full-length cDNA, might be isolated from the library using the *L. multiflorum* probe.

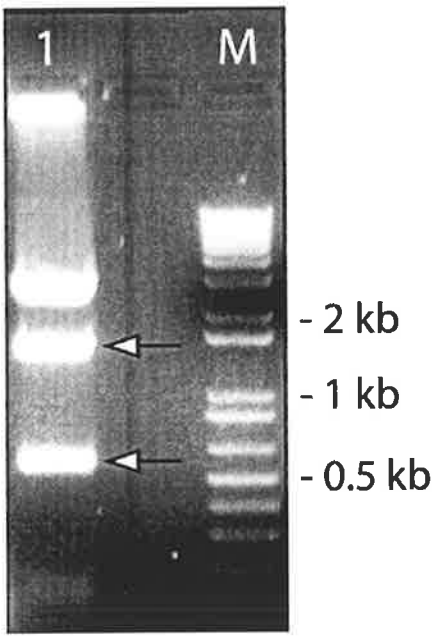

Figure 2.1 Isolation of the *HvGSL1* probe. **1** pBluescript plasmid DNA digested with *Eco*RI and *Xho*I. Restriction fragments of *HvGSL1* indicated with arrows were purified as probes. **M** DNA molecular size marker.

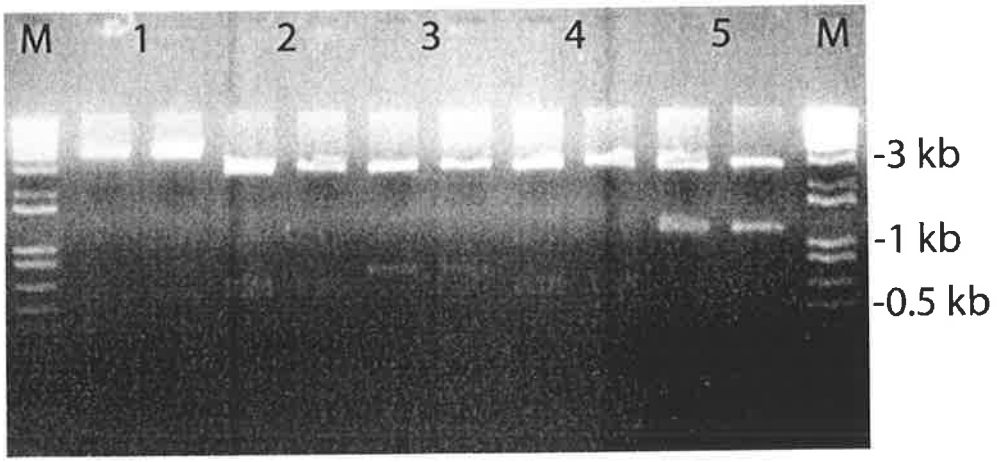

Figure 2.2 Restriction analyses of clones from ryegrass suspension culture cDNA library. pBluescript plasmid DNA containing putative (1→3)-β-D-glucan synthase cDNAs were digested with *Eco*RI and *Xho*I in duplicate. cDNA in lanes **2** and **4** (*lmcasyn2* and *lmcasyn4*) were identified as putative (1→3)-β-D-glucan synthases following sequencing with T3 and T7 primers. **M** DNA molecular size marker.

Four cDNA clones were purified as described previously and restriction analysis of the purified plasmid DNA revealed two unique banding patterns. The corresponding plasmid DNAs were sequenced and *lmcasyn7*, a 530 bp fragment, showed 100% sequence identity with the previously identified 1224 bp *L. multiflorum GSL* gene fragment and did not extend the sequence at the 5′ end. The other cDNA, *lmcasyn6,* was slightly larger in size at around 850 bp but had sequence identity to a prohibitin-like protein. Having exhausted the possibility of extracting a larger portion of the *L. multiflorum GSL* cDNA from the existing library, alternative methods for obtaining the full-length cDNA were sought.

2.3.2 GSL *cDNA sequence extension using PCR*

The first PCR method undertaken to extend the existing 1224 bp cDNA of the newly identified *L. multiflorum GSL* gene toward the 5′ end was anchor-ligated PCR. Anchor sequences were ligated onto the 5′ ends of a cDNA population and PCR was conducted using primers that were specific for the anchor sequence at the 5′ end and for the *L. multiflorum GSL* gene at the 3′ end. The *L. multiflorum GSL* nested primers, lmcasyn2R and lmcasyn3R (*Appendix B*), were positioned towards the 5′ end of the 1224 bp fragment obtained from the library to maximise the chance of obtaining novel 5′ end cDNA sequence. Thirty separate PCR reactions were set up from three 10 µl anchor ligation reactions and after two rounds of semi-nested PCR, two weak bands of approx. 380 bp and two of approx. 450 bp could be viewed on agarose gels (*Figure 2.3*).

These bands were purified and ligated into the pGEM T-Easy vector and the DNA was sequenced using T7 and SP6 primers. Sequencing results combined with nucleotide homology-based searches failed to identify the inserts as *GSL* gene fragments.

The deduced peptide sequence from the *Hieracium piloselloides GSL* cDNA (*HpGSL1*; donated by Nick Paech, CSIRO, Plant Industry) was aligned with four fungal *FKS1* genes found in the Genbank database. A small region of sequence conservation was identified in the alignment (*Figure 2.4*) and the coding bias for these

amino acids was examined in DNA sequence from *L. multiflorum*. A degenerate oligonucleotide, lmcasyn2 (*Appendix B*), was designed to this region and semi-nested PCR was undertaken with the gene-specific nested reverse primers lmcasyn1R and lmcasyn3R (*Appendix B*) on cDNA from *L. multiflorum* suspension-cultured endosperm cells harvested four days post-subculture. A strong band of approx. 3 kb could be viewed in an agarose gel following electrophoresis (*Figure 2.5*).

The approx. 3 kb band was ligated into pGEM T-Easy and the insert was sequenced from both ends with T7 and SP6 sequencing primers. Comparison of the DNA sequence obtained from the cDNA with DNA sequences present in the NCBI database using the BLAST local alignment program suggested the sequence may be that of a GSL. The full 3 kb of the cDNA was subsequently sequenced in a stepwise manner using gene specific oligonucleotides. An identical overlap of 250 bp between the 3′ end of the new 3 kb cDNA and the 5′ end of the cDNA obtained from the *L. multiflorum* cDNA library provided evidence that the PCR fragment was indeed part of the same cDNA.

No sites of DNA sequence conservation were identified in multiple sequence alignments in a position more towards the 5′ end of the cDNA than the existing primers (data not shown), limiting the possibility of further amplifying the 5′ end of the gene using techniques based on degenerate primers. Anchor-ligated RACE and 5′-RACE experiments failed to produce any *GSL* DNA sequence that extended the existing cDNA (data not shown), so an alternate method for obtaining the sequence of the *GSL* 5′ end was pursued.

Genomic walking, a PCR based method for obtaining 5′ sequence from genomic DNA, was employed. Adaptor 2, that is ligated onto the end of restriction digested genomic DNA has an amino group at the 5′ end and is phosphorylated at the 3′ end to limit the same adaptor being ligated onto fragments in both the forward and reverse orientation. The presence of restriction fragments having the same adaptor sequence

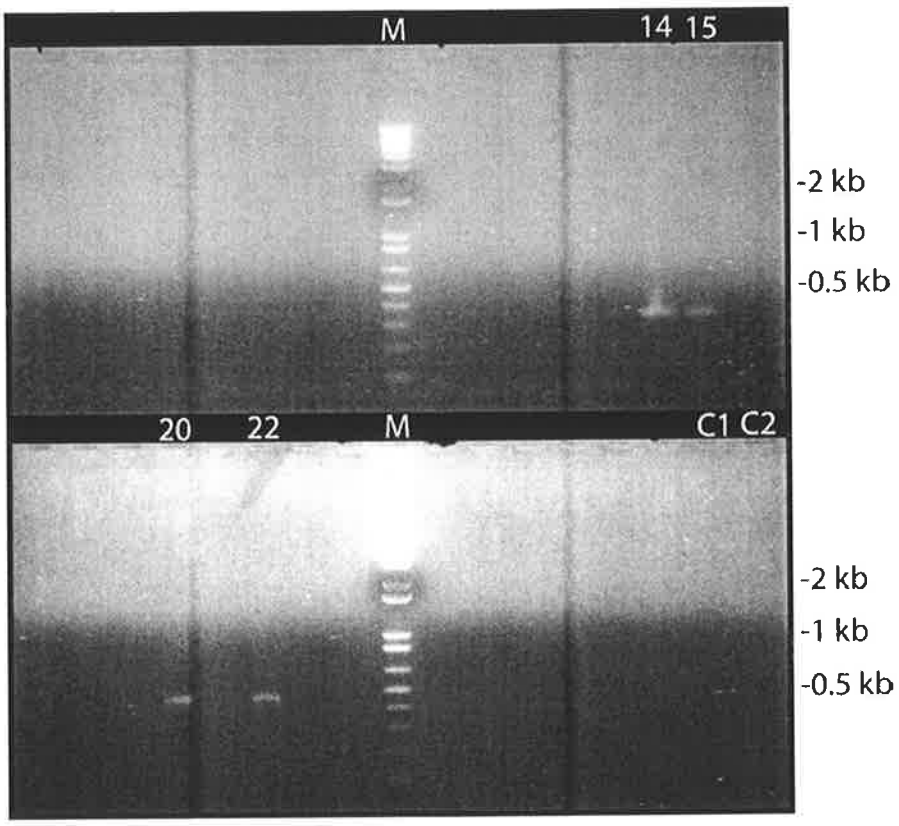

Figure 2.3 Agarose gel analysis of PCR products amplified from anchor-ligated cDNAs. Lanes **14** (380 bp), **15** (380 bp), **20** (450 bp) and **22** (450 bp), contain products generated by PCR. **C1** and **C2** no template PCR controls. **M** DNA molecular size marker.

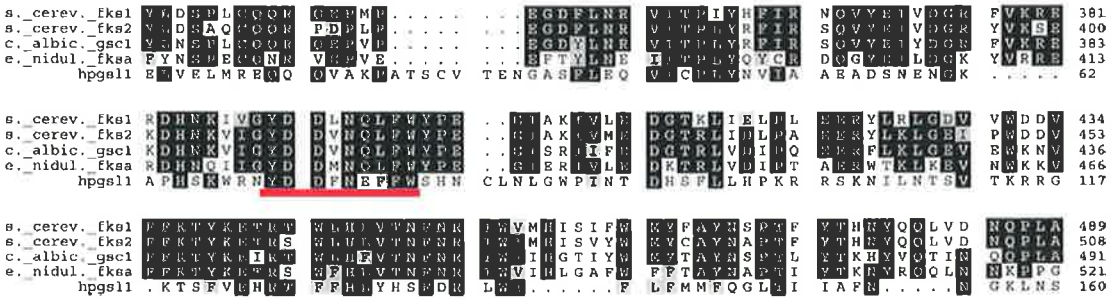

Figure 2.4 Multiple sequence alignment of deduced amino acids of putative (1→3)-β-D-glucan synthases. Sequences aligned are the *Saccharomyces cerevisiae* FKS1 and FKS2 proteins, *Candida albicans* GSC1, *Emericella nidulans* FKSA and *Hieracium pilloselloides* HpGSL1. The red bar indicates the region of sequence conservation used in the design of PCR primer lmcasyn2. The alignments were performed using the Pileup program and are graphically presented using the Prettybox program from the ANGIS suite of programs.

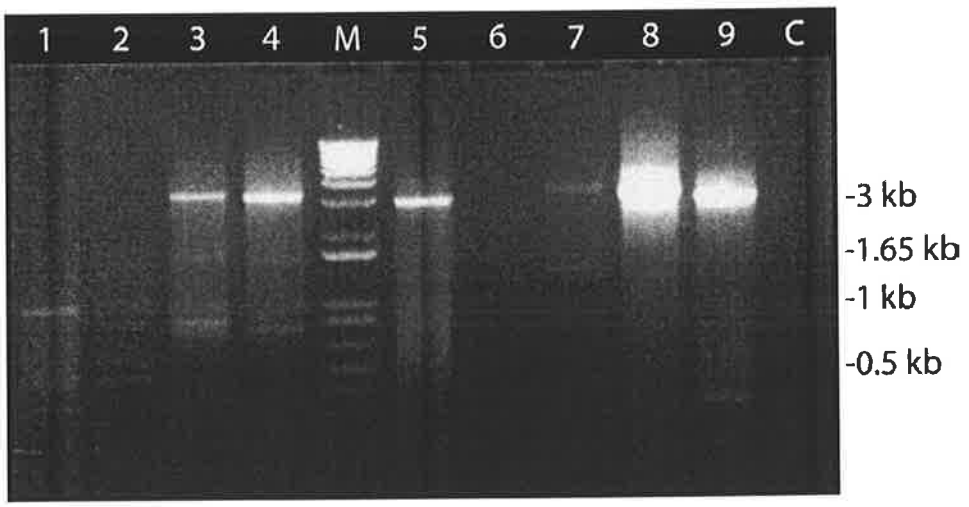

Figure 2.5 Agarose gel analysis of semi-nested PCR products amplified from ryegrass endosperm cDNA employing a degenerate 5′ primer. Lanes **1-5** oligo dT primed cDNAs, lanes **6-9** lmcasyn1R primed cDNAs. Lane **8** contains the approx. 3 kb PCR product that was identified as a putative (1→3)-β-D-glucan synthase following cloning into pGEM T-Easy and DNA sequencing. The primers lmcasyn2 and lmcasyn1R were used in the first round of PCR and lmcasyn2 and lmcasyn3R were employed in the second round. **M** DNA molecular size marker. **C** No template PCR control.

ligated at either end could lead to the amplification of non-specific products during PCR, when using primers designed to the adaptor sequence. However, the amplification of non-specific products is further reduced because the adaptor sequences have a tendency to preferentially bind to one another due to their complementary nature, and this leads to the formation of "panhandle" structures. These do not amplify and so suppress replication during subsequent rounds of PCR. This further reduces the occurrence of PCR products that are primed at each end with adaptor primers alone, such that products primed with a combination of a gene-specific primer and an adaptor primer are enriched. Two rounds of nested PCR were also employed to limit the number of false positives.

The results of the genomic walking experiments, in which a total of more than 5 kb of nucleotide sequence was obtained, are summarised in Table 2.1. Not all walks resulted in the identification of coding sequence and care was taken to ensure that sufficient overlap in sequence from different walks (usually about 100 bp) existed to enable a continuous DNA sequence (contig) to be generated.

Because the genomic DNA might be expected to include introns, computer software programs such as GenScan were used to predict intron-exon boundaries in the DNA sequences, but routinely failed to identify splice sites in the ryegrass genomic DNA sequences. During the course of the genomic walking experiments a cDNA predicted to encode a *GSL* gene from cotton was deposited in the Genbank database. This cDNA sequence (accession number AF085717), designated *GhGSL1*, along with the *Hieracium* and barley cDNAs, were used as a guide to identify the ryegrass coding regions present in the genomic DNA sequence that resulted from genomic walking experiments. A schematic diagram of the 5′ end of the genomic sequence of *LmGSL1* gene obtained from the genomic walking experiments is presented in Figure 2.6. This region of approx. 5 kb was dominated by introns, and contained only 1.3 kb of coding sequence, corresponding to 436 amino acid residues. Genomic walking experiments were halted after a putative start methionine was identified, in a position of agreement with other putative plant *GSL* genes recently deposited in the databases, at the 5′ end of the predicted cDNA sequence.

Genomic walk no.	*1st round gene specific primer*	*2nd round gene specific primer*	*Number of coding bases (bp)*	*Approx. amino acid position*
1	lmcasyn8R	lmcasyn9R	246	355-436
2	lmcasyn10R	lmcasyn11R	93	324-354
6	lmcasyn22R	lmcasyn23R	258	238-323
7	lmcasyn26R	lmcasyn27R	183	177-237
8	lmcasyn30R	lmcasyn31R	276	85-176
11	lmcasyn38R	lmcasyn39R	252	1-84

Table 2.1 Summary of genomic walking experiments. DNA sequence from preceding walk was used as the basis for the design of primers used to walk further into unknown 5′ end DNA sequence. Primer sequences are located in Appendix B.

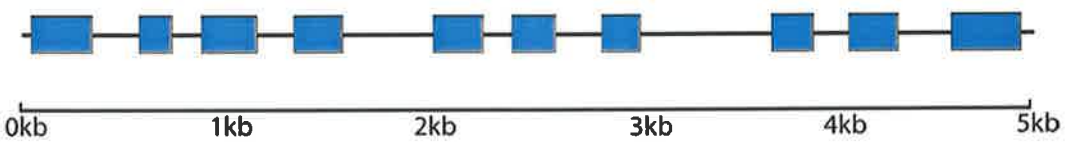

Figure 2.6 Schematic diagram of the 5′ end of the *LmGSL1* gene. Blue boxes represent predicted coding DNA sequence (exons).

Following the identification of the putative start methionine, a set of nested gene-specific primers, lmgsl15′-1 and lmgsl15′-2 (*Appendix B*), were designed to the 5′ end of the putative ryegrass *GSL* gene so that the sequence might be confirmed by the amplification and characterisation of a single cDNA sequence, hence negating the concerns about prediction of intron/exon boundaries. The nested PCR approach yielded a 1.3 kb fragment after two rounds of nested PCR (*Figure 2.7*) which, when ligated into pGEM T-Easy and sequenced with T7 and SP6, confirmed the results of the genomic walking experiments. The predicted full-length cDNA and deduced protein sequences of the *L. multiflorum GSL* gene, *LmGSL1*, compiled from three overlapping cDNA clones, are presented in *Figure 2.8*.

2.3.3 GSL *gene structure*

Analysis of the genomic structure of *Arabidopsis* and rice *GSL* genes has revealed the presence of two quite distinct groups of *GSL* genes, one possessing between none and two introns, and a second type that may possess as many as 48 introns (*Figure 2.9*). The presence of these multiple intron sequences makes the *GSL* genes some of the largest plant genes known, extending over 22 kb. Given that the *LmGSL1* gene contains nine introns in the predicted 1308 bp of coding sequence at the 5′ end it appears likely that *LmGSL1* falls into the second, multiple intron class of *GSL* genes identified by Richmond and Somerville (2000; http://cellwall.stanford.edu/).

The sequence of the *LmGSL1* cDNA is 6118 bp in length and contains an open reading frame of 5718 bp. There is a 3′ untranslated region of 379 bp and an 18 bp poly(A) tract but no obvious polyadenylation signal sequence (AATAAA) was identified in the 3′ sequence. Overall the nucleotide composition of the mature *LmGSL1* cDNA is slightly AT biased, with a GC content of 43%. Closer analysis of the sequence reveals that there is a preference for A or T in the wobble base position, with 56% of the codons ending in A or T overall. However, the 200 bp region at the 5′ end of the *LmGSL1* cDNA is very GC rich (74%). In yeast, highly expressed genes are biased towards G or C in the wobble base position (Konarska *et al.*, 1985) and in barley a (1→3; 1→4)-β-glucan endohydrolase (Slakeski *et al.*, 1990) and thaumatin-

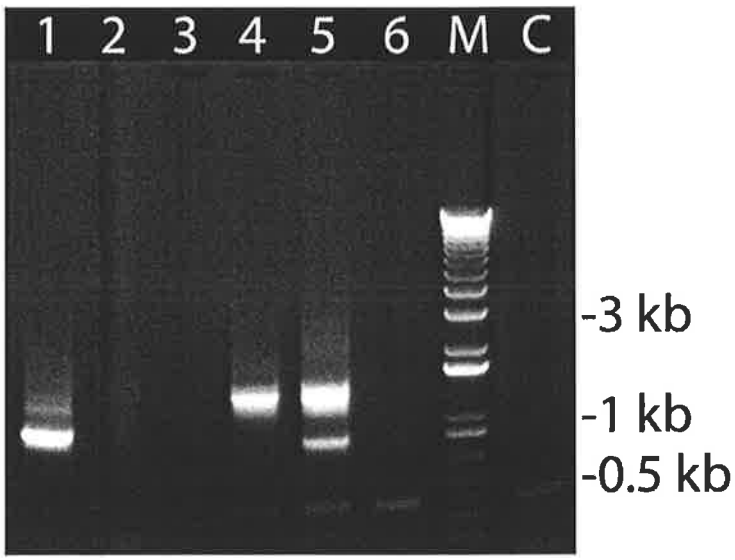

Figure 2.7 Agarose gel analysis of 2nd round PCR products resulting from amplification of the *LmGSL1* 5′ end. Various cDNAs: **1** young leaf, **2** mid leaf, **3** old leaf, **4** suspension cultured cells (SCC) 4 days post-subculture, **5** SCC 8 days post-subculture, **6** SCC 12 days post-subculture were used as templates. **M** DNA molecular size marker. **C** No template PCR control.

```
ATGGCGAGGGCGGAGGCCAACTGGGAGCGCCTGGTGCGGGCGGCGCTCCGCGGGGAGCGGATGGGCGGCGGCTACGGGGTCCCCGCCAGC    90
M  A  R  A  E  A  N  W  E  R  L  V  R  A  A  L  R  G  E  R  M  G  G  G  Y  G  V  P  A  S      30

GGCATCGCCGGGAACGTGCCCACCTCGCTCGGCAACAACACCCACATCGACGAGGTGCTGCGCGCCGCCGACGAGATCCAGGACGAGGAC    180
G  I  A  G  N  V  P  T  S  L  G  N  N  T  H  I  D  E  V  L  R  A  A  D  E  I  Q  D  E  D      60

CCCACCGTCGCCAGAATCCTGTGTGAGCATGCATATGCGCTAGCCCAAAATCTGGATCCCAATAGCGAAGGGAGAGGCGTCCTGCAGTTC    270
P  T  V  A  R  I  L  C  E  H  A  Y  A  L  A  Q  N  L  D  P  N  S  E  G  R  G  V  L  Q  F      90

AAAACCGGTTTAATGTCAGTAATCAGGCAAAAACTAGCAAAGAGGGAAGGCGGTGCTATAGACCGGAGTCAGGATATTGCTAAACTGCAG    360
K  T  G  L  M  S  V  I  R  Q  K  L  A  K  R  E  G  G  A  I  D  R  S  Q  D  I  A  K  L  Q      120

GAGTTTTATAAGCTATACAGAGAAAAGCATAAAGTTGATGAGTTGTGTGAAGATGAAATGAAGCTTAGGGAATCTGCTGTGTTTAGTGGT    450
E  F  Y  K  L  Y  R  E  K  H  K  V  D  E  L  C  E  D  E  M  K  L  R  E  S  A  V  F  S  G      150

AACCTTGGAGAGCTGGAACGCAAAACTCTGAAGCGCAAAAAAGTACTTGCCACTCTCAAGGTCTTATGGTCAGTAATAGAGGATATAACA    540
N  L  G  E  L  E  R  K  T  L  K  R  K  K  V  L  A  T  L  K  V  L  W  S  V  I  E  D  I  T      180

AAGGAAATTTCCCCTGAGGATGCAGATAAATTGATTTCTGAACAGATGAAAAAAGTCATGCAAAAGGATGCGGCAAGGACAGAGGATGTT    630
K  E  I  S  P  E  D  A  D  K  L  I  S  E  Q  M  K  K  V  M  Q  K  D  A  A  R  T  E  D  V      210

GTGGCGTATAATATCATTCCTCTAGATGCCGTGTCTACAACTAATGCAATTGTCACTTTTCCAGAGGTGAGGGCAGCAATATCAGCTTTG    720
V  A  Y  N  I  I  P  L  D  A  V  S  T  T  N  A  I  V  T  F  P  E  V  R  A  A  I  S  A  L      240

CAGTACCATAGGGATCTGCCCAGGCTTCCTGGAACCATTTCAGTTCCTGATGCTAGGAATTCAGATATGCTGGACTTGTTGCACTGCGTG    810
Q  Y  H  R  D  L  P  R  L  P  G  T  I  S  V  P  D  A  R  N  S  D  M  L  D  L  L  H  C  V      270

TTTGGTTTTCAGAAAGGCAATGTGAGCAATCAACGGGAGCACATTGTTCACCTGTTGGCAAATGAGCAGTCTCGATTAGGCAAACTATCA    900
F  G  F  Q  K  G  N  V  S  N  Q  R  E  H  I  V  H  L  L  A  N  E  Q  S  R  L  G  K  L  S      300

GGGAATGAACCGAAAATTGACGAAGGTGCAGTACATGTCGTGTTCTCCAAGTCTCTAGATAACTACATGAAATGGTGCAGCTATTTGCCA    990
G  N  E  P  K  I  D  E  G  A  V  H  V  V  F  S  K  S  L  D  N  Y  M  K  W  C  S  Y  L  P      330

CTACGTCCTGTCTGGCTTAGCGCTGAATCGTTGACCAAAGAGAAAAAGTTGCTATATGTGTGTTTATACTACCTGATCTGGGGAGAGGCT    1080
L  R  P  V  W  L  S  A  E  S  L  T  K  E  K  K  L  L  Y  V  C  L  Y  Y  L  I  W  G  E  A      360

GGCAACATACGATTTCTTCCAGAATGCTTATGCTACATTTTTCATCATCTGGCAAGGGAACCAGAGGAAACTATGCGGAAACAGATTGCA    1170
G  N  I  R  F  L  P  E  C  L  C  Y  I  F  H  H  L  A  R  E  P  E  E  T  M  R  K  Q  I  A      390

TACCCAGCTGAAAGTTGTATTTCTAACGATGGTGTATCATTTCTTGACCAAGTCATTTCCCCTCTATATGAAATCACCGCAGCTGAAGCA    1260
Y  P  A  E  S  C  I  S  N  D  G  V  S  F  L  D  Q  V  I  S  P  L  Y  E  I  T  A  A  E  A      420

GGCAACAATGACAATGGGCGGGCAGCACATTCTGCATGGAGAAACTACGATGACTTTAACGAGTTTTTTTGGTCTTTGAAATGTTTTCAG    1350
G  N  N  D  N  G  R  A  A  H  S  A  W  R  N  Y  D  D  F  N  E  F  F  W  S  L  K  C  F  Q      450

TTGGGTTGGCCACGGAAACTGAGCATTCCACTTTTCTCGAAGCCTACTACGAAGGAGGGTTCGCTCCATCGGCCGCATCATTATGGAAAG    1440
L  G  W  P  R  K  L  S  I  P  L  F  S  K  P  T  T  K  E  G  S  L  H  R  P  H  H  Y  G  K      480

ACATCTTTTGTGGAACACAGAACTTTTCTCCATCTTTACCACAGCTTTCACCGCTTTTGGATGTTCCTAATTATGATGTTTCAGGGACTT    1530
T  S  F  V  E  H  R  T  F  L  H  L  Y  H  S  F  H  R  F  W  M  F  L  I  M  M  F  Q  G  L      510

ACTATCATTGCTTTCAACAAAGGTAGTTTTAAAGACAAGACTGTATTGGAACTTCTTAGCTTGGGCCCAACTTATGTCGTAATGAAATTC    1620
T  I  I  A  F  N  K  G  S  F  K  D  K  T  V  L  E  L  L  S  L  G  P  T  Y  V  V  M  K  F      540

ATTGAGAGTGTATTGGACATTCTGATGATGTATGGTGCATATTCAACATCTCGTCGATCTGCCATTACTAGAGTGATCTGGCGATTCTGT    1710
I  E  S  V  L  D  I  L  M  M  Y  G  A  Y  S  T  S  R  R  S  A  I  T  R  V  I  W  R  F  C      570

TGGTTTACCATGGCTTCATTGGTCATCTGTTACCTATATATCAAAGCACTTCAAGATGGAGCGCAGTCTGCACCTTTCAAGATATATGTT    1800
W  F  T  M  A  S  L  V  I  C  Y  L  Y  I  K  A  L  Q  D  G  A  Q  S  A  P  F  K  I  Y  V      600

GTTGTAATCAGTGCATATGCGGGTTTCAAGATAATCGTCAGCCTTCTCATGAGTGTTCCTTGTTGCCGTGGTGTTACCAATGCTTGCTAC    1890
V  V  I  S  A  Y  A  G  F  K  I  I  V  S  L  L  M  S  V  P  C  C  R  G  V  T  N  A  C  Y      630

AGCTGGTCTTTTATACGCCTTATTCAGTGGATGCATCAGGAGCACAATTACGTTGGAAGAGGCATGCATGAAAGGCCTCTAGACTATATC    1980
S  W  S  F  I  R  L  I  Q  W  M  H  Q  E  H  N  Y  V  G  R  G  M  H  E  R  P  L  D  Y  I      660

CAATATGTGGCTTTCTGGCTTGTTATTCTTGCAGCAAAATTTTCGTTTACCTATTTTCTCCAGATTAAACCTCTTGTAGAACCAACACAA    2070
Q  Y  V  A  F  W  L  V  I  L  A  A  K  F  S  F  T  Y  F  L  Q  I  K  P  L  V  E  P  T  Q      690

CTGATCATCAGTTTCAGAGACTTGCAGTATCAATGGCATGACTTTTTTTCAAAGAATAACCATAATGCCTTCACAATTCTTTCTTTATGG    2160
L  I  I  S  F  R  D  L  Q  Y  Q  W  H  D  F  F  S  K  N  N  H  N  A  F  T  I  L  S  L  W      720

GCTCCAGTGGTCTCAATTTATCTTTTGGACATCCATGTATTTTACACCATCATGTCTGCTATTGTCGGATTCCTTCTTGGTGCACGTGAA    2250
A  P  V  V  S  I  Y  L  L  D  I  H  V  F  Y  T  I  M  S  A  I  V  G  F  L  L  G  A  R  E      750
```

```
CGACTGGGAGAGATTAGGTCTGTTGAAGCAGTTCACCGATTCTTTGAGAAGTTCCCTGAAGCATTCATGGATAAACTTCATGTTCCTGTT   2340
R  L  G  E  I  R  S  V  E  A  V  H  R  F  F  E  K  F  P  E  A  F  M  D  K  L  H  V  P  V     780

CCAAAAAGGAAACAACTGCTATCATCTGGTCAGCTTCCAGAGTTAAATAAGTTTGACGCATCTAGATTCGCTCCTTTCTGGAATGAAATT   2430
P  K  R  K  Q  L  L  S  S  G  Q  L  P  E  L  N  K  F  D  A  S  R  F  A  P  F  W  N  E  I     810

GTGAAGAATTTGCGGGAAGAAGATTACATTAACAACACCGAACTGGAGTTACTCTTGATGCCCAAGAATAAAGGTGGTCTTCCAATTGTG   2520
V  K  N  L  R  E  E  D  Y  I  N  N  T  E  L  E  L  L  L  M  P  K  N  K  G  G  L  P  I  V     840

CAGTGGCCTCTTTTCTTGCTTGCTAGCAAGGTTTTCTTGGCGAAAGATATTGCAGTTGATTGCAAAGACTCGCAAGACTCACAAGATGAA   2610
Q  W  P  L  F  L  L  A  S  K  V  F  L  A  K  D  I  A  V  D  C  K  D  S  Q  D  S  Q  D  E     870

CTCTGGCTAAGGATTTCAAAGGACGAATACATGCAATATGCTGTCGAGGAGTGCTTTCATACCATTTATCATATCCTGACCTCTATACTA   2700
L  W  L  R  I  S  K  D  E  Y  M  Q  Y  A  V  E  E  C  F  H  T  I  Y  H  I  L  T  S  I  L     900

GATAAAGAAGGCCATCTCTGGGTGCAAAGGATTTATGGTGGTATTCAAGAAAGCATTGCAAAGAAGAATATCCAGAGTGATATCCATTTC   2790
D  K  E  G  H  L  W  V  Q  R  I  Y  G  G  I  Q  E  S  I  A  K  K  N  I  Q  S  D  I  H  F     930

AGCAAATTGCCTAATGTCATTGCCAAGCTCGTTGCTGTAGCAGGAATACTGAAAGAAGCAGAGTCTGCTGATATGAAGAAGGGGGCAGTT   2880
S  K  L  P  N  V  I  A  K  L  V  A  V  A  G  I  L  K  E  A  E  S  A  D  M  K  K  G  A  V     960

AATGCGATTCAGGACCTATATGAAGTTGTTCATCACGAAGTGCTATCTGTTGATATGAGTGGCAACATTGATGATTGGAGTCAGATAAAT   2970
N  A  I  Q  D  L  Y  E  V  V  H  H  E  V  L  S  V  D  M  S  G  N  I  D  D  W  S  Q  I  N     990

AGAGCAAGAGCCGAAGGCCGCCTCTTCAGTAATCTCAAGTGGCCAAATGATCCTGGATTGAAGGACCTCATCAAACGATTGCATTC.CTT   3060
R  A  R  A  E  G  R  L  F  S  N  L  K  W  P  N  D  P  G  L  K  D  L  I  K  R  L  H  X  L    1020

CTGACCATCAAGGAATCAGCTGCGAATGTTCCTAAAAACCTGGAAGCCTGTCGGAGACTGGAGTTCTTCACGAACTCTCTGTTCATGCGA   3150
L  T  I  K  E  S  A  A  N  V  P  K  N  L  E  A  C  R  R  L  E  F  F  T  N  S  L  F  M  R    1050

ATGCCTCTCGCAAGGCCTGTTTCAGAAATGCTTTCCTTTAGCGTGTTCACTCCATATTACTCGGAGACTGTGCTTTATAGTATCGCTGAA   3240
M  P  L  A  R  P  V  S  E  M  L  S  F  S  V  F  T  P  Y  Y  S  E  T  V  L  Y  S  I  A  E    1080

CTCCAGAAAAGAAATGAAGATGGTATAAGTACACTATTTTATCTTCAGAAGATATATCCAGATGAATGGAAGAACTTCCTTACTCGCATC   3330
L  Q  K  R  N  E  D  G  I  S  T  L  F  Y  L  Q  K  I  Y  P  D  E  W  K  N  F  L  T  R  I    1110

AACAGGGATGAAAATGCAGCAGAGTCTGAACTTTTTAGCAGTGCAAATGACATACTAGAACTGCGCCTTTGGGCATCTTACCGTGGGCAG   3420
N  R  D  E  N  A  A  E  S  E  L  F  S  S  A  N  D  I  L  E  L  R  L  W  A  S  Y  R  G  Q    1140

ACCTTAGCGCGAACAGTTCGTGGGATGATGTATTACCGGAAGGCCCTTATGTTGCAAAGTTATCTGGAGAGAATGCATTCTGAAGACCTT   3510
T  L  A  R  T  V  R  G  M  M  Y  Y  R  K  A  L  M  L  Q  S  Y  L  E  R  M  H  S  E  D  L    1170

GAATCTGCATTTGATATGGCTGGTCTGGCTGACACACATTTTGAGTACTCCCCTGAAGCACGCGCACAGGCTGATTTGAAGTTTACATAC   3600
E  S  A  F  D  M  A  G  L  A  D  T  H  F  E  Y  S  P  E  A  R  A  Q  A  D  L  K  F  T  Y    1200

GTGGTAACCTGCCAAATTTATGGATTACAGAAAGGAGAAGGGAAACAAGAAGCTGCCGATATAGCCCTTCTAATGCAAAGAAACGAAGCT   3690
V  V  T  C  Q  I  Y  G  L  Q  K  G  E  G  K  Q  E  A  A  D  I  A  L  L  M  Q  R  N  E  A    1230

CTCAGAATTGCTTACATTGATGTTGTCGAGAGCATTAAGAATGGAAAGCCTAGCACTGAGTATTACTCGAAGCTTGTTAAAGCTGACATC   3780
L  R  I  A  Y  I  D  V  V  E  S  I  K  N  G  K  P  S  T  E  Y  Y  S  K  L  V  K  A  D  I    1260

CATGGAAAAGACAAGGAAATTTATTCAGTTAAGTTGCCTGGCAATCCAAAGCTTGGGGAGGGTAAACCTGAAAACCAAAATCATGCCGTA   3870
H  G  K  D  K  E  I  Y  S  V  K  L  P  G  N  P  K  L  G  E  G  K  P  E  N  Q  N  H  A  V    1290

ATATTCACTCGTGGAAATGCTGTACAGACTATTGATATGAATCAGGACAACTATTTCGAGGAGGCACTCAAGATGAGAAACCTGCTTGAG   3960
I  F  T  R  G  N  A  V  Q  T  I  D  M  N  Q  D  N  Y  F  E  E  A  L  K  M  R  N  L  L  E    1320

GAGTTCTCTCAAGATCATGGCAAGTTCAAGCCTTCAATTCTTGGTGTTAGGGAACATGTCTTCACAGGAAGTGTTTCCTCCCTGGCCTCA   4050
E  F  S  Q  D  H  G  K  F  K  P  S  I  L  G  V  R  E  H  V  F  T  G  S  V  S  S  L  A  S    1350

TTTATGTCGAGTCAGGAAACTAGCTTTGTAACATCAGGACAGCGTGTTCTTTCTAATCCACTAAAAGTGAGAATGCATTATGGTCACCCA   4140
F  M  S  S  Q  E  T  S  F  V  T  S  G  Q  R  V  L  S  N  P  L  K  V  R  M  H  Y  G  H  P    1380

GATGTTTTTGATAGAATTTTTCATATTACGAGGGGGGGCATCAGTAAGGCATCCCGTATCATCAATATCAGTGAGGATATATTCGCAGGG   4230
D  V  F  D  R  I  F  H  I  T  R  G  G  I  S  K  A  S  R  I  I  N  I  S  E  D  I  F  A  G    1410

TTCAACTCGACGTTGCGTCAAGGGAACATAACTCATCATGAGTATATTCAGGTTGGGAAAGGAACAGATGTTGGGCTTAACCAGATTGCA   4320
F  N  S  T  L  R  Q  G  N  I  T  H  H  E  Y  I  Q  V  G  K  G  T  D  V  G  L  N  Q  I  A    1440

CTATTTGAAGGAAAAGTTGCTGGAGGAAACGGTGAACAAGTGCTTAGTCGAGATATATACCGACTTGGACAGCTCTTTGACTgTTTCAGG   4410
L  F  E  G  K  V  A  G  G  N  G  E  Q  V  L  S  R  D  I  Y  R  L  G  Q  L  F  D  C  F  R    1470

ATGCTATCTTCTACTGTGACCACTATTGGATTCTATTTCTGTACTATGCTAACTGTACTGACTGTGTACATATTTCTATATGGAGAAACC   4500
M  L  S  S  T  V  T  T  I  G  F  Y  F  C  T  M  L  T  V  L  T  V  Y  I  F  L  Y  G  E  T    1500
```

```
TATCTGGCTTTATCTGGTGTTGGAGAATCAATTCAAAATAGAGCGGATATTATGCAGAATATAGCCCTGACCGTGTTTCTGAACACACAA  4590
Y  L  A  L  S  G  V  G  E  S  I  Q  N  R  A  D  I  M  Q  N  I  A  L  T  V  F  L  N  T  Q    1530

TTTCTTTTCCAGAATGGTGTGTTTACTGCTATTCCCATGATTGTAGGTCTCATCCTGGAAGCTGGTGTCTTGACGGCTTTTGTCAACTTC  4680
F  L  F  Q  N  G  V  F  T  A  I  P  M  I  V  G  L  I  L  E  A  G  V  L  T  A  F  V  N  F    1560

ATTACAATGCAGTTCCAGCTATGTTCTGTGTTTTTCACTTTCTCTCTTGGAACAAGGACTCACTACTTCGGTCGCACAATACTACATGGG  4770
I  T  M  Q  F  Q  L  C  S  V  F  F  T  F  S  L  G  T  R  T  H  Y  F  G  R  T  I  L  H  G    1590

GGCGCAAAGTATAGGGCAACTGGTAGGGGTTTCGTGGTGCGGCATATTAAGTTTGCTGAGAATTACCGTCTTTATTCCAGAAGCCATTTC  4860
G  A  K  Y  R  A  T  G  R  G  F  V  V  R  H  I  K  F  A  E  N  Y  R  L  Y  S  R  S  H  F    1620

GTGAAAGGGTTGGAGGTTGCACTCTTGTTGGTGATCTTTCTAGCTTATGGGTTTAATGATGGTGGTGCGATTGGCTATATTTTACTATCC  4950
V  K  G  L  E  V  A  L  L  L  V  I  F  L  A  Y  G  F  N  D  G  G  A  I  G  Y  I  L  L  S    1650

ATAAGTAGCTGGTTTATGGCGCTTTCGTGGCTTTTTGCTCCGTATGTTTTCAACCCATCTGGATTTGAATGGCAGAAGGTTGTTGAGGAT  5040
I  S  S  W  F  M  A  L  S  W  L  F  A  P  Y  V  F  N  P  S  G  F  E  W  Q  K  V  V  E  D    1680

TTCAGAGACTGGACAAACTGGCTATTTTACCGGGGTGGTTTTGGAGTTAAAGGAGAGGAAAGCTGGGAAGCCTGGTGGGATGAAGAACTG  5130
F  R  D  W  T  N  W  L  F  Y  R  G  G  F  G  V  K  G  E  E  S  W  E  A  W  W  D  E  E  L    1710

GGACATATCCAAACTTTTCGTGGGAGGATACTGGAGACTATACTTAGTTTAAGATTTTTCATTTTCCAGTATGGAGTTGTTTACCATATG  5220
G  H  I  Q  T  F  R  G  R  I  L  E  T  I  L  S  L  R  F  F  I  F  Q  Y  G  V  V  Y  H  M    1740

GATGCAAGCGAACCAAGTACAGCATTATTGGTATATTGGGTATCCTGGGCTGTGCTTGGAGGGCTTTTTGTCCTCCTCATGGTATTCAGT  5310
D  A  S  E  P  S  T  A  L  L  V  Y  W  V  S  W  A  V  L  G  G  L  F  V  L  L  M  V  F  S    1770

TTAAACCCCAAGGCCATGGTTCATTTCCAACTGCTACTGCGTCTTGTCAAAAGTATTGCCCTATTAGTGGTTTTGGCAGGTTTGATTGTG  5400
L  N  P  K  A  M  V  H  F  Q  L  L  L  R  L  V  K  S  I  A  L  L  V  V  L  A  G  L  I  V    1800

GCAATTGTGTCAACACGCCTTAGTTTTACAGATGTACTTGCTTCCATTCTGGCATATGTGCCTACTGGATGGGGAATTCTTTCGATTGCT  5490
A  I  V  S  T  R  L  S  F  T  D  V  L  A  S  I  L  A  Y  V  P  T  G  W  G  I  L  S  I  A    1830

GTGGCATGGAAACCCATAGTGAAAAGGCTAGGTTTGTGGAAAACAGTGCGCTCTCTTGGTCGACTGTATGATGCCGGCATGGGAATGATC  5580
V  A  W  K  P  I  V  K  R  L  G  L  W  K  T  V  R  S  L  G  R  L  Y  D  A  G  M  G  M  I    1860

ATCTTTGTACCCATAGCCATTTGCTCGTGGTTTCCCTTCATTTCCACCTTCCAGACGCGACTATTGTTTAACCAGGCTTTTAGCAGAGGT  5670
I  F  V  P  I  A  I  C  S  W  F  P  F  I  S  T  F  Q  T  R  L  L  F  N  Q  A  F  S  R  G    1890

TTGGAGATTTCTCTCATCCTTGCTGGCCAGGATCAGAATACAGGTGCATGATGGCAGCCTTACAGAACTTTTGAATCTTCAGCCAGATCA  5760
L  E  I  S  L  I  L  A  G  Q  D  Q  N  T  G  A  *                                            1906

TGCTTCTCTGTGGCTCGATCGATCCTGGGTTCTCAGTTTAGCTGTAAATGTGTATATCTTGATGTTGAGAAGCAGTTATCTGCTATGGTT  5850

GTAGCCTGTAGGTGGTGGTGTACACTAAGGACTGGGTACTGATTCATTGTAAAAAGAACTTGTCGAGTGTTTATGTTAATTTAGACATTG  5940

TAGATTTTGGATCTGGTAGTGAGAAGTTTGATATTGAGAAATTGATGAGCTAAGTTACTAAGAGAACACCATGGCCTTGGAAATGGAACG  6030

AATTCATGTAATTAGCCACTTGATGTAGATTGAATAGCAGTACTGATTTATGGATAACCAGGATAGCCTGAAAAAAAAAAAAAAAAAA    6118
```

Figure 2.8 ***LmGSL1*** **nucleotide and deduced amino acid sequence (Accession number AY286332).**

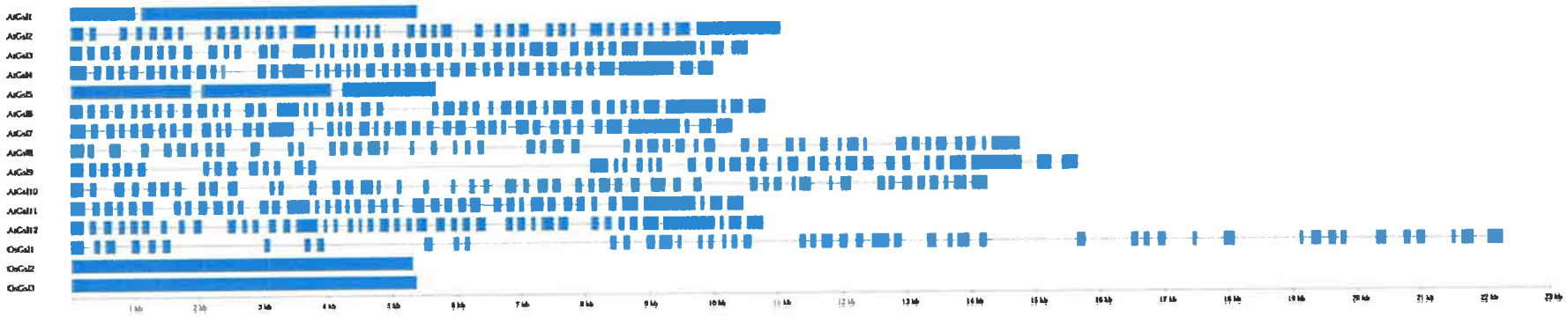

Figure 2.9 Schematic diagram of putative plant (1→3)-β-D-glucan synthase genes. *AtGSLs* from *Arabidopsis thaliana*, *OsGSLs* from *Oryza sativa*. Blue boxes represent predicted coding DNA sequences. Diagram taken from http://cellwall.stanford.edu/

like protein (Osmond, 2000) that are both highly expressed also possess a marked preference for G or C in the wobble base position.

Although introns are ubiquitous and share a high degree of structural and sequence similarity across species, the signals that specifically define splice sites are not completely understood, especially in plants. Some conserved short terminal sequences within introns function in intron splicing and virtually all introns begin with the dinucleotide GT and end with AG (Green *et al.*, 1991; Moore and Sharp, 1993; Lal *et al.*, 1999). This is true in the case of *L. multiflorum* where all 10 intron sequences began with GT and ended with AG. All 10 introns were AT rich and therefore no evidence for GC rich introns that are often evident in monocot species (Goodall and Filipowicz, 1989, 1991) was found.

2.3.4 Amino acid sequence analysis

The deduced LmGSL1 mature protein of 1906 amino acid residues has a predicted molecular weight of 217,097 Da and a pI of 7.7. No obvious ER targeting signal peptide sequence was detected in the LmGSL1 sequence and it is unclear where the NH_2-terminal amino acid residue for the mature enzyme is located.

The amino acid sequence of the putative LmGSL1 protein was analysed for transmembrane helices using TopPredII software (von Heijne, 1992) and the mature protein was predicted to contain 14 transmembrane spanning domains (*Figure 2.10*) with several other notable features. Firstly, there are two larger regions that are predicted to be cytoplasmic, one at the NH_2-terminal end and the other a large loop more centrally located. Secondly, comparisons of peptide sequences predicted from recently identified plant *GSL* genes with the LmGSL1 sequence reveals a region of amino acid sequence between the 1300-1530 residues that appears to be highly conserved across all species examined. This region of sequence conservation lies within the large centrally located, predicted cytoplasmic loop and it is tempting to speculate that this region of the protein may contain the catalytic site of the (1→3)-β-D-glucan synthase enzyme. As a result of this finding some of the proof-of-function experiments described in later chapters have focussed specifically on this region of conserved sequence.

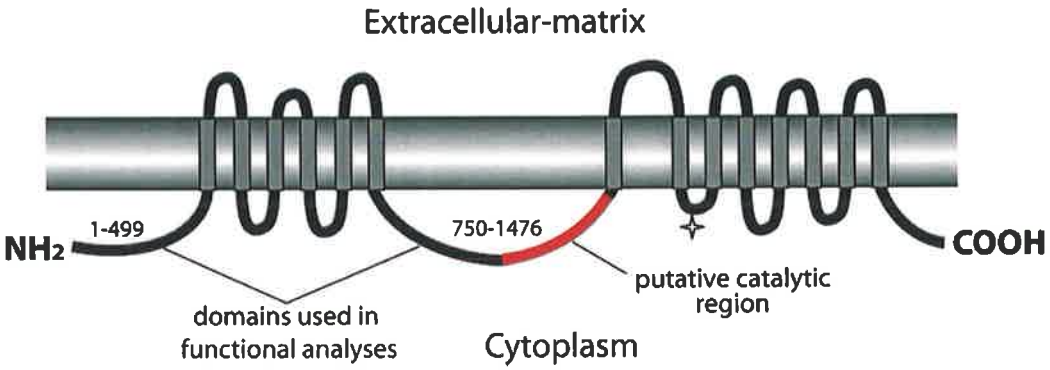

Figure 2.10 Predicted topological profile of LmGSL1. Predicted cytoplasmic domains indicated with amino acid residue numbers were used in later studies of function. Putative catalytic region indicated in red. Topology prediction made using TopPredII software. ✧ Denotes site of RXTG motif, putative UDP-glucose binding site.

An RXTG motif, which has been implicated in UDP-glucose binding (Inoue *et al.*, 1996), is found in a small loop between transmembrane helices 8 and 9 (*Figure 2.10*). A similar motif is found in other higher plant callose synthases (Østergaard *et al.*, 2002). Comparisons of amino acid sequence from higher plant (1→3)-β-D-glucan synthases in the area corresponding to the large centrally located loop revealed a number of absolutely conserved motifs. These included SET, DEW, PGxPxxGxGKP, IDxNQDxxxEE and SED, motifs that are positioned on loop, helix, loop, helix/loop/helix, and loop structural elements, respectively, which were recently identified by Li *et al.* (2003) and proposed as residues involved in catalysis. The LmGSL1 protein does not contain the D,D,D,Q,xx,R,W motif found in the processive β-glycosyl transferases of bacteria (Saxena *et al.*, 1990) and the cellulose synthases of *Arabidopsis* and barley (Arioli *et al.*, 1998; Burton *et al.*, 2001). Motif searches conducted on the deduced LmGSL1 amino acid sequence using the ScanProsite program at the Prosite web site (http://www.expasy.ch/cgi-bin/scanprosite) revealed the presence of seven possible N-glycosylation sites, three tyrosine sulphation sites, a single cAMP or cGMP-dependent protein kinase phosphorylation site and multiple protein kinase C, Casein kinase II and tyrosine kinase phosphorylation sites (data not shown). Multiple N-myristoylation sites and a possible leucine zipper were also detected in the deduced peptide sequence. It should be noted however that all of these motifs have a high probability of occurrence and may not necessarily mean that phosphorylation, myristoylation, etc. occurs at these sites

The deduced amino acid sequence of LmGSL1 was aligned with other predicted full length GSL proteins from *Arabidopsis*, rice, barley, cotton, tobacco and yeast to establish the phylogenetic relationships between various GSL proteins (*Figure 2.11*). The ryegrass GSL1 protein is grouped closely with the barley HvGSL1 protein, the rice OsGSL8 protein, the cotton GhGSL1 protein and the AtGSL10 protein of *Arabidopsis*. The *GSL* genes, *AtGSL1*, *AtGSL5*, *OsGSL2* and *OsGSL3*, which are predicted to have two or less introns in their genomic sequence, group together on a separate branch of the phylogenetic tree when the deduced amino acid sequences for these genes are compared. The yeast FKS1 protein is only distantly related to the plant GSLs as evidenced by its isolated position on the unrooted phylogenetic tree (*Figure 2.11*).

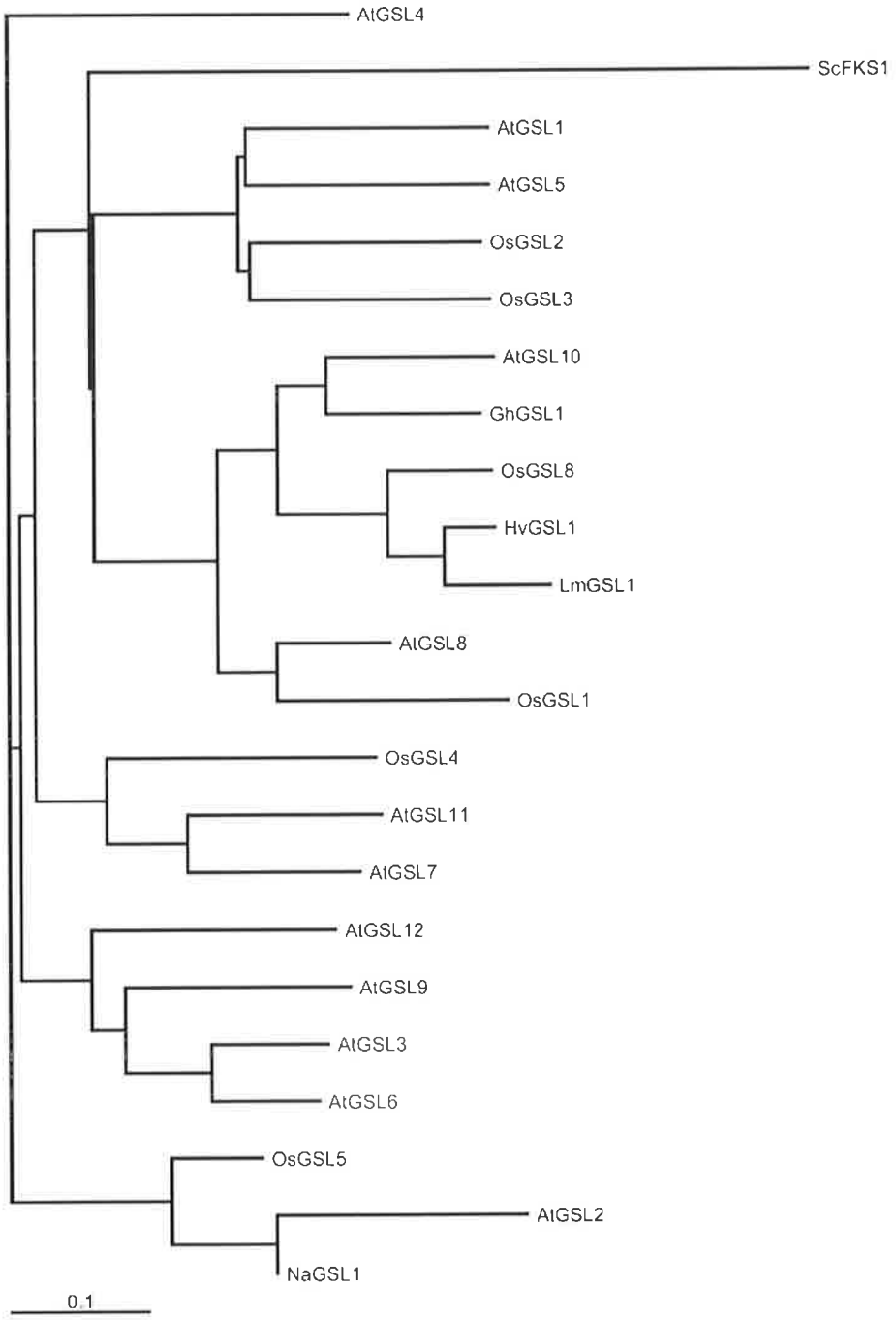

Figure 2.11 Unrooted phylogenetic tree of deduced peptide sequences of putative (1→3)-β-D-glucan synthases. Deduced peptide sequences used in alignment are ScFKS1 *Saccharomyces cerevisiae* FKS1 (Accession number U12893), OsGSL1 *Oryza sativa* GSL1 (Accession number AP001389), *Oryza sativa* GSL2 (Accession number AP003223), *Oryza sativa* GSL3 (Accession number AP003268), *Oryza sativa* GSL4 (Accession number AP003447), *Oryza sativa* GSL5 (Accession number AP003454), *Oryza sativa* GSL8 (Accession number BE040137), *Arabidopsis thaliana* GSL1 (Accession number AF162444), *Arabidopsis thaliana* GSL2 (Accession number AC006436), *Arabidopsis thaliana* GSL3 (Accession number AC006223), *Arabidopsis thaliana* GSL4 (Accession number AB023038), *Arabidopsis thaliana* GSL5 (Accession number AC005142), *Arabidopsis thaliana* GSL6 (Accession number AF237733), *Arabidopsis thaliana* GSL7 (Accession number AC007592), *Arabidopsis thaliana* GSL8 (Accession number AC006922), *Arabidopsis thaliana* GSL9 (Accession number AB025605), *Arabidopsis thaliana* GSL10 (Accession number AC012395), *Arabidopsis thaliana* GSL11 (Accession number AL163527), *Arabidopsis thaliana* GSL12 (Accession number AL353013), *Nicotiana alata* GSL1 (Accession number AF304372), *Gossypium hirsutum* GSL1 (Accession number AF085717), *Hordeum vulgare* GSL1 (Accession number AY177665) and *Lolium multiflorum* GSL1 (Accession number AY286332).

2.3.5 *The* GSL *gene family*

Southern analyses of *L. multiflorum* genomic DNA probed with the *LmGSL1* cDNA suggests the *GSL* gene, *LmGSL1*, is a single gene or part of a small gene family, based upon the number of hybridising bands detected on the probed blot (*Figure 2.12*). However, the presence of 12 and 13 *GSL* genes in *Arabidopsis* and rice, respectively, would indicate plants contain a moderately sized family of *GSL* genes. Alignment of the *LmGSL1* cDNA sequence with sequences in barley EST libraries has revealed that there are at least seven individual genes in the barley genome homologous to the putative callose synthase gene. The Southern blot (*Figure 2.12*) was washed at high stringency (0.1x SSC at 65°C) and the probe used has homology with the 3′ end of the ryegrass cDNA where there is often sequence divergence in homologous genes. This may explain the low number of bands observed on the Southern blot. Other *L. multiflorum GSL* genes might not be detected under these conditions and it can be concluded that the Southern analysis (*Figure 2.12*) has probably underestimated the number of *GSL* genes in ryegrass.

2.3.6 *Expression of the* LmGSL1 *gene in* Lolium multiflorum

Given the likelihood that multiple *GSL* genes exist in the *L. multiflorum* genome, *LmGSL1* gene-specific primers were designed for the analysis of mRNA levels of the *LmGSL1* gene, utilising two PCR based techniques. Quantitative (real-time) PCR was used in a comparative study of *LmGSL1* mRNA levels in young leaf, mid leaf, old leaf, and in endosperm suspension cultures four, eight and twelve days post-subculture. *LmGSL1* mRNA was detected in all the leaf tissues examined but expression was greatest in the young leaf tissue, lowest in the mid leaf tissue and was elevated slightly in the older leaf tissue. The younger suspension cultures had maximal *LmGSL1* mRNA levels, which declined with age (*Figure 2.13*). Younger plant tissues would be expected to contain more cells that are undergoing division and rapid cell growth per gram of fresh weight than their more mature counterparts and if the *LmGSL1* gene were involved in the formation of callose at the cell plate or in

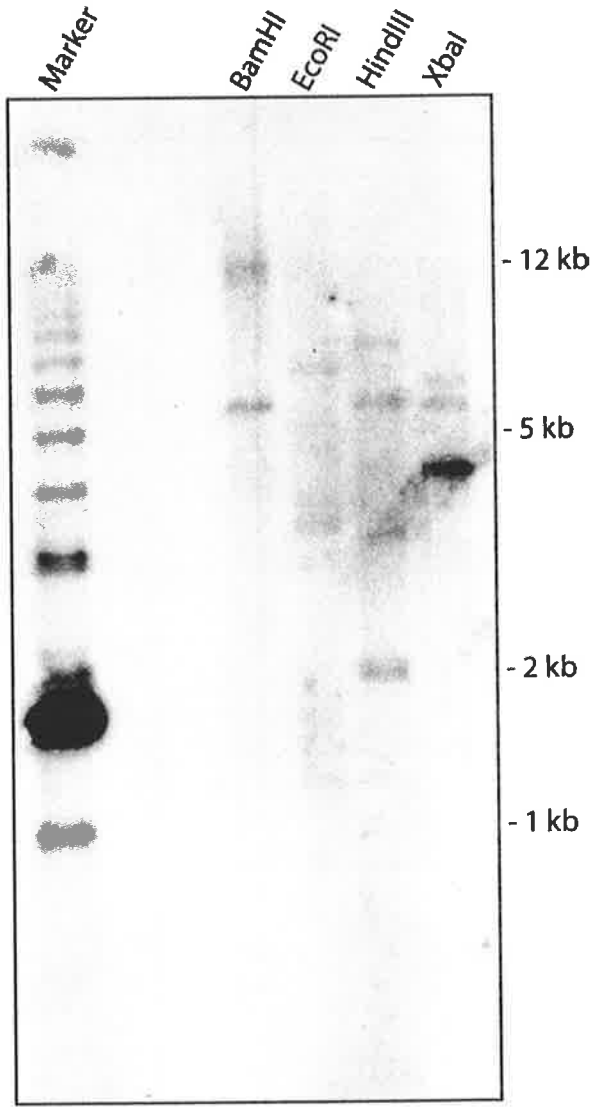

Figure 2.12 Southern hybridisation of *LmGSL1* probe with ryegrass genomic DNA. A 400 bp restriction fragment of *LmGSL1* was randomly labelled with [α-^{32}P]dCTP and hybridised to L. multiflorum genomic DNA that was digested with the indicated restriction enzymes.

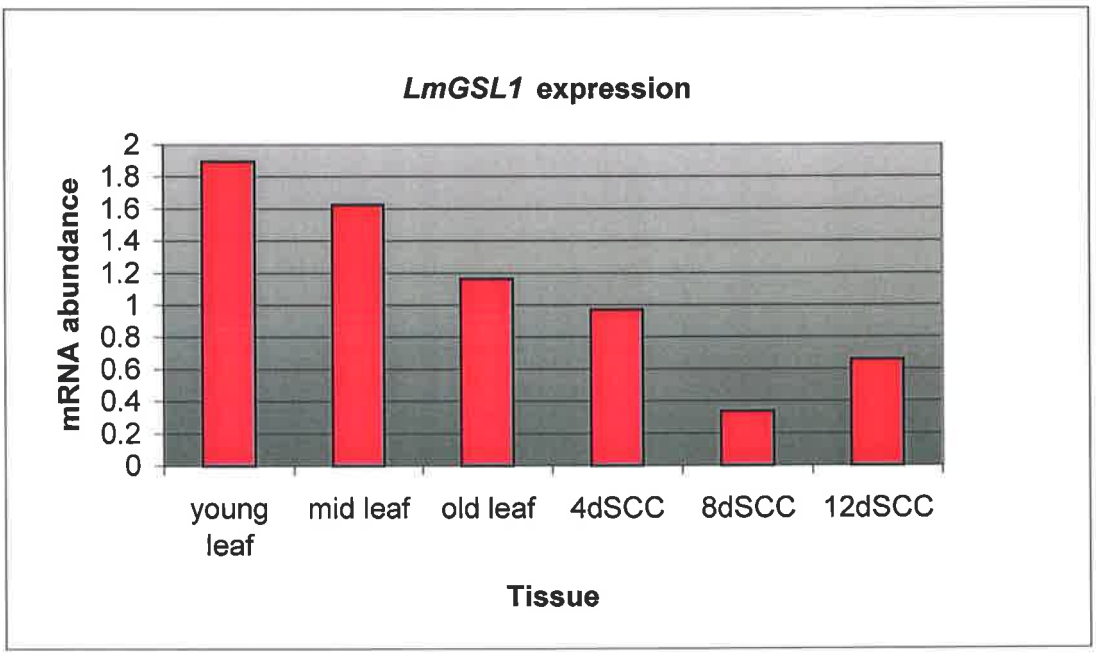

Figure 2.13 *LmGSL1* mRNA levels in ryegrass tissues. *LmGSL1* mRNA levels decline with age in leaf tissue and are higher in suspension cultured endosperm cells 4 days post-subculture compared with older cultures when normalised as a ratio of *LmGAPDH* expression.

other specialised cell types, one might expect *LmGSL1* expression to be greater in these tissues.

RT-PCR was used to measure *LmGSL1* transcription in a semi-quantitative fashion in various tissues of *L. multiflorum*. Two control genes, *LmGAPDH* and *Lm5SRNA*, were also amplified in these experiments for comparison of expression levels of housekeeping genes that are reported to be relatively uniform in most tissues (Edwards and Denhardt, 1985; Vandesompele *et al.*, 2002). *LmGSL1* mRNA was detectable at low levels in nearly all the tissues examined (*Figure 2.14*). The RNA from older leaves and roots appears to be present at a lower level than the other tissues examined, based upon the intensity of bands observed in the two control panels. This may be related, in part, to the fact that high quality RNA was routinely more difficult to extract from these tissues.

2.3.7 *Mapping of* LmGSL1

L multiflorum and *L. perenne* are very closely related in evolutionary terms and both possess 14 chromosomes. Mapping experiments were undertaken by Dr. John Forster at the Cooperative Research Centre for Molecular Plant Breeding, La Trobe University, Victoria, Australia using a *L. perenne* population, as access to a *L. multiflorum* mapping population could not be obtained. Initial results obtained from mapping experiments in perennial ryegrass failed to map the *LmGSL1* gene to a specific chromosomal location in the *Lolium* genome even though a clear segregation pattern of a restriction length polymorphism (RFLP) was observed in the *Eco*RV digested DNA of the heterozygous North African$_6$ x Aurora$_6$ mapping lines (*Figure 2.15*) and the North African$_6$ x Aurora$_6$ F1 two-way pseudo-testcross mapping populations (*Figure 2.16*). Although at least two polymorphisms were detected in the Aurora$_6$ parental line a lack of RFLP markers located in a position more distal to where the *LmGSL1* probe hybridised meant that a final position could not be accurately determined. Later, as more markers were placed on the genetic map, the *LmGSL1* RFLP locus could be integrated, and was located on the long arm of chromosome LG4. This is in agreement with findings in barley, where the *HvGSL1* gene is located in a syntenous position on the long arm of the homeologous chromosome 4H (Ms. Jing Li, University of Adelaide, personal communication).

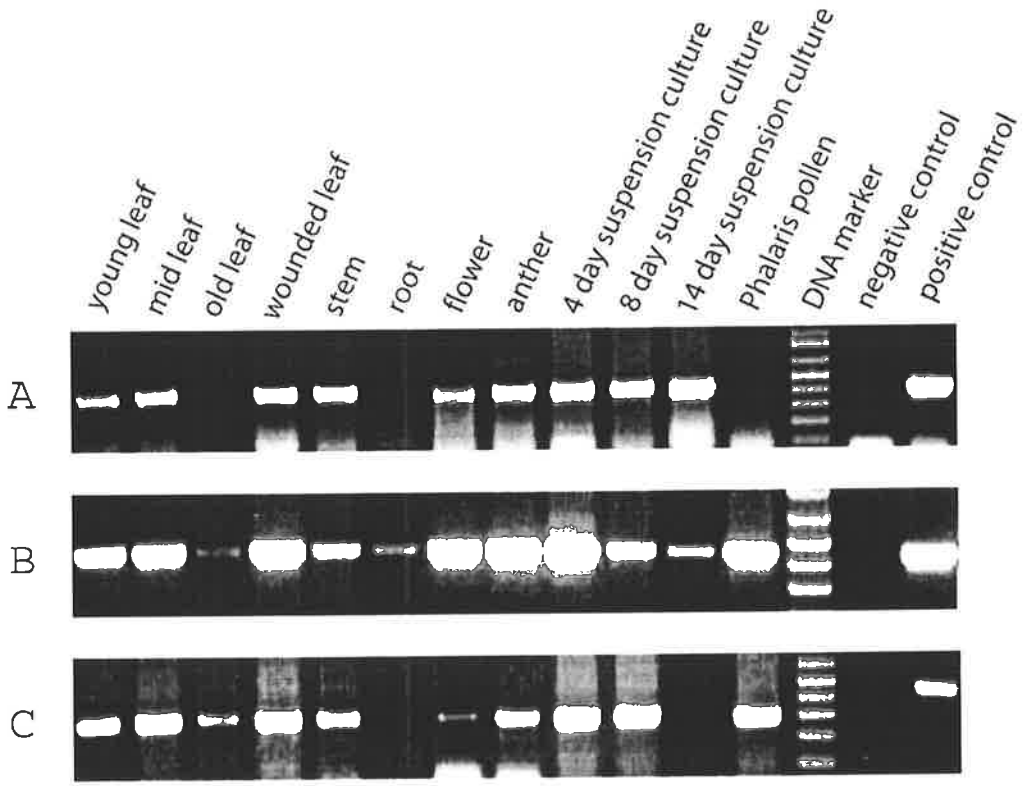

Figure 2.14 Semi-quantitative analysis of *LmGSL1* mRNA levels. RT-PCR products were subject to agarose gel electrophoresis after 30 cycles of PCR. Panel **A** *LmGSL1* mRNA levels, **B** *LmGAPDH* mRNA levels, **C** *Lm5SRNA* mRNA levels. Note that relative intensities of bands provide only a semi-quantitative indication of relative mRNA levels.

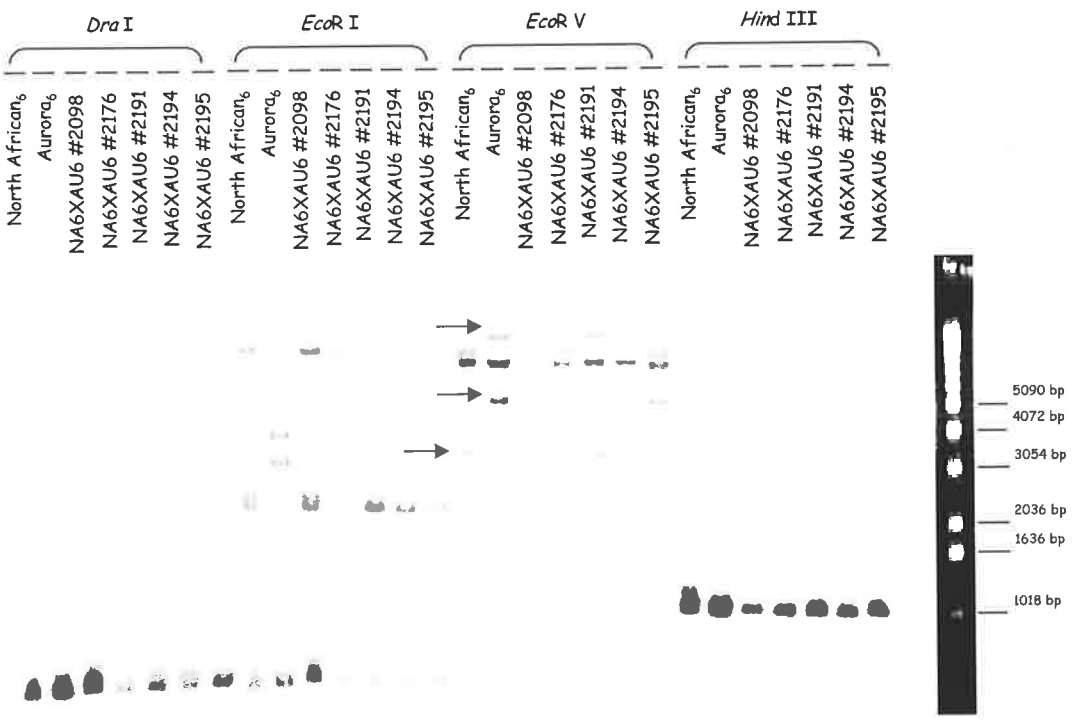

Figure 2.15 Perennial ryegrass mapping lines hybridised with the *LmGSL1* probe. DNA from North African$_6$ x Aurora$_6$ mapping lines was digested with the restriction enzymes *Dra*I, *Eco*RI, *Eco*RV and *Hin*dIII. A clear polymorphism was detectable in *Eco*RV digested DNA, as indicated with arrows. Image courtesy of Dr. John Forster.

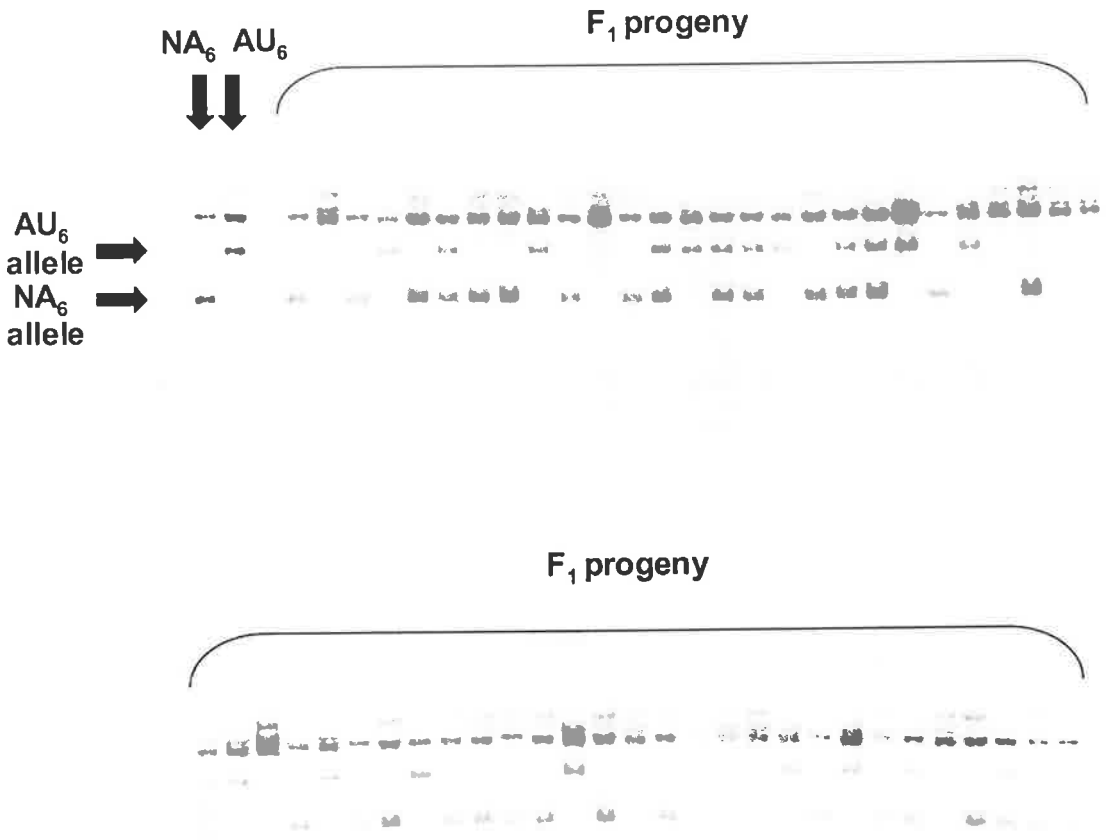

Figure 2.16 North African$_6$ x Aurora$_6$ F1 two-way pseudo-testcross mapping populations hybridised to the *LmGSL1* probe. Genomic DNA from 57 F1 progeny of a North African$_6$ x Aurora$_6$ cross were digested with EcoRV electrophoresed and blotted onto nylon membrane. The [α-^{32}P]dCTP labelled *LmGSL1* probe was hybridised to the membranes which were washed to high stringency. Image courtesy of Dr. John Forster.

2.4 SUMMARY AND CONCLUSIONS

A near full-length cDNA sequence, designated *LmGSL1*, was determined from three overlapping cDNA clones after the 5′ end of the *LmGSL1* gene was located by walking stepwise through genomic DNA. The cDNA, found in a wide range of *L. multiflorum* tissues, was identified as a putative *GSL* gene based upon DNA sequence homology to the yeast *FKS1* gene and other recently identified plant *GSL* genes. The *LmGSL1* cDNA has an AT bias although the 5′ end is quite GC rich. The genomic sequence contains a large number of introns. The cDNA encodes a large, 217 kDa, integral membrane protein that possesses two comparatively large, predicted cytoplasmic domains. *LmGSL1* appears to be part of a medium sized gene family based on genome sequencing results from *Arabidopsis* and rice, which contain 12 and 13 *GSL* genes respectively. Genome sequencing of *L. multiflorum* would provide a definitive answer to the question of gene copy number. The *LmGSL1* gene lies on the long arm of chromosome LG4, which is consistent with the finding that the homologous *HvGSL1* gene of barley lays in a syntenous position on the long arm of the barley homeologous chromosome 4H. The sequencing of genomic DNA from the 5′ end of the *LmGSL1* gene revealed the presence of multiple introns in this region of the gene and indicates that the gene, like many of the *GSL* genes identified in *Arabidopsis* and rice, may contain as many as 48 introns. The *LmGSL1* gene is transcribed at low levels in all tissues examined, but expression appears to be slightly greater in tissues such as young leaf and recently subcultured endosperm cells, where cells are rapidly dividing.

The mature LmGSL1 protein of 1906 amino acid residues does not contain the D,D,D,QxxR,W motif found in the processive β-glycosyl transferases of bacteria (Saxena *et al.*, 1990) and the cellulose synthases of *Arabidopsis* and barley (Arioli *et al.*, 1998; Burton *et al.*, 2001). Like the FKS1 and AtGSL5 proteins, the LmGSL1 protein encodes a putative UDP-glucose binding site that is located in the fifth cytoplasmic domain of the deduced protein (amino acid residues 1595-1598, RXTG; Inoue *et al.*, 1996; Cui *et al.*, 2001). No evidence of a calmodulin-binding domain reported to be present in the cotton GhGSL1 protein (Cui *et al.*, 2001) could be detected in the LmGSL1 protein. LmGSL1 shares a number of absolutely conserved

motifs with the barley HvGSL1 sequence; these have been proposed as catalytic residues. These include SET, DEW, PGxPxxGxGKP, IDxNQDxxxEE and SED, motifs that are positioned on loop, helix, loop, helix/loop/helix, and loop structural elements, respectively (Li *et al.*, 2003). Other frequently occurring motifs were also identified in the LmGSL1 protein. In evolutionary terms the ryegrass GSL1 protein appears to be most closely related to the barley HvGSL1 protein and the rice OsGSL8 protein when compared with peptide sequences currently available in public databases. The LmGSL1 deduced protein shares 91% identity with the barley HvGSL1 deduced protein but there are regions including amino acid residues 1300-1530 where there is 100% identity and accordingly other regions where the sequence is less conserved. Two large cytoplasmic domains were predicted at the amino terminal and at the centre of the LmGSL1 protein and tracts of sequence conservation were found to coincide with the more centrally located cytoplasmic domain. Consequently, these domains were the focus of further study into the function of the *GSL* genes in plants by attempts to demonstrate callose synthase activity when these two large cytoplasmic domains were expressed in heterologous expression systems. The *GSL* cDNA described here was isolated from *L. multiflorum* but the availability of systems for the analysis of gene function are poor in this species when compared with barley and *Arabidopsis* so functional analyses were conducted in these species where greater resources for this type of work were available. Experiments in which the two large cytoplasmic domains of the homologous barley *HvGSL1* gene were studied using heterologous expression systems are described in the next chapter.

CHAPTER 3

HETEROLOGOUS EXPRESSION OF A BARLEY (1→3)-β-D-GLUCAN SYNTHASE

3.1 INTRODUCTION

Heterologous expression systems can be used as a means to produce recombinant proteins in relatively high abundance and purity, provided a cDNA encoding the protein has been isolated. Thus, heterologous expression may negate the need for lengthy purification processes when an enzyme of interest is extracted from the tissue in which it normally resides. Various expression systems have been developed, including systems based upon bacterial, yeast, insect, plant and animal cells (Frommer and Ninnemann, 1995; Dreyer *et al.*, 1999). *E. coli* based systems offer the advantages that they are relatively rapid and straightforward to culture and that they often express recombinant proteins at a high level. The disadvantages of this system are that the expressed protein may be misfolded, resulting in the loss of or an alteration in its activity. Furthermore, essential amino acid modifications may not be effected in the heterologous host cell, and this could also lead to reduced activity or incorrect folding. Misfolded proteins often aggregate and precipitate from solution as "inclusion bodies". Despite the availability of procedures for the dissolution of insoluble proteins in inclusion bodies, including the use of powerful chaotropic agents, activity is seldom recovered. Membrane bound plant proteins have been expressed successfully in *E. coli* but they have generally been small in size, possess only a single transmembrane helix and have mostly been transporter proteins (Dreyer *et al.*, 1999; Sauer *et al.*, 1990). Mammalian systems, whilst not expressing recombinant proteins to the same level and being technically more demanding in terms of culture, do offer the advantage that expressed proteins are subjected to post-translational modifications typical of eukaryotic systems (Barnes *et al.*, 1994; Rossmann *et al.*, 1996; Kammerloher *et al.*, 1994; Geisse *et al.*, 1996; Daniel and Carling, 2002) and this increases the chance of producing a functional plant recombinant protein.

The (1→3)-β-D-glucan synthase of the human pathogenic mold *Aspergillus fumigatus*, AfFKS1p, has been the focus of heterologous expression experiments. However, the recombinant proteins were not assayed for activity but rather were used for antibody production (Beauvais *et al.*, 2001). Attempts to produce the entire *A. fumigatus* FKS1p protein using the baculovirus expression system failed because

transcription in the insect cell resulted in the production of a truncated mRNA (Beauvais *et al.,* 2001). The conserved hydrophilic internal fragment (amino acid residues 841 to 1265) of the *A. fumigatus* FKS1p amino acid sequence was expressed in *E. coli.* A GST fusion protein with a molecular size of 74 kDa was produced, this released a polypeptide of 48 kDa after human thrombin digestion, corresponding to the expected molecular size of the AfFKS1p fragment (Beauvais *et al.,* 2001). The NH_2-terminal fragment of AfFKS1p (amino acid residues 1 to 387) was also be expressed in *E. coli*, but in contrast, expression of the COOH-terminus was unsuccessful (amino acid residues 1441 to 1904; Beauvais *et al.,* 2001).

The generation of a tagged protein in which a protein of interest is synthesised with a short affinity tag attached at either the NH_2- or COOH-terminus provides a convenient method for the purification of heterologously expressed proteins. For example, poly-histidine tags allow efficient purification of an expressed protein via immobilized metal affinity chromatography (Janknecht and Nordheim, 1991). The fusion of the protein of interest to another protein, often permits the synthesis of otherwise poorly translated polypeptides. Fusions that increase the solubility of a protein have also been used with some success in heterologous expression systems (Guan *et al.,* 1998; Maina *et al.,* 1988). The main disadvantages of tagged or fusion-protein technologies are that liberation of the passenger proteins following purification, if attempted, often requires protease treatment (e.g. Factor Xa or enterokinase). Cleavage is rarely complete, yields are therefore reduced and additional steps may be required to obtain an active product.

In the previous chapter, analysis of aligned multiple peptide sequences of putative (1→3)-β-D-glucan synthases revealed regions that were highly conserved. One might speculate that these regions form part of the catalytic site in these large membrane-bound proteins, although it must be remembered that no group has yet demonstrated that purified callose synthase enzyme can actually synthesise (1→3)-β-D-glucan *in vitro*. Li *et al.* (2003) identified a number of absolutely conserved motifs in the barley HvGSL1 protein including SET, DEW, PGxPxxGxGKP, IDxNQDxxxEE and SED. All are positioned on a large centrally located loop, which Li *et al.* (2003) propose as the catalytic site of the barley (1→3)-β-D-glucan synthase. To assess the hypothesis

that the catalytic site of the (1→3)-β-D-glucan synthase enzyme is located in this region, peptides from the two larger predicted cytoplasmic regions of the barley HvGSL1 protein (*Figure 3.3*) were expressed in *E. coli* and in the human embryonic kidney cell line, 293T, and (1→3)-β-D-glucan synthase activity was subsequently measured in cell homogenates. The expression of the full-length barley HvGSL1 protein, which is 1906 amino acid residues long, could not be undertaken because the cDNA encoding the HvGSL1 protein was not available as a single molecule but rather as six, separate overlapping clones. The results of the heterologous expression of barley *HvGSL1* cDNA fragments are described below.

3.2 MATERIALS AND METHODS

3.2.1 Materials

Plasmids containing fragments of the barley *HvGSL1* cDNA were kindly provided by Ms. Jing Li (Department of Plant Science, University of Adelaide, Australia). Dr. Tim Adams (CSIRO, Division of Health Sciences and Nutrition, Parkville, Australia) generously donated the mammalian cell expression vector pME18S and performed the transient transfection and subsequent expression experiments in the human embryonic kidney cell line, 293T. Mr. Michael Schober (Department of Plant Science, University of Adelaide, Australia) kindly donated a microsomal membrane preparation extracted from endosperm cultures of *Lolium multiflorum*.

Restriction enzymes and BSA were from New England Biolabs (Beverly, MA, USA). NucleoSpin Extract kit was purchased from Macherey-Nagel (Duran, Germany). Expand DNA polymerase and Complete protease inhibitor was supplied by Roche-Diagnostics (Basel, Switzerland). Plasmids pDONR201, pDEST17, custom oligonucleotides, mouse Anti-His-HRP Antibody, Novex precast 4-20% Tris-glycine gradient gels, SeeBlue Plus 2 molecular weight standard, Gateway clonase enzymes, Dulbecco's Modified Eagle Medium, Nutrient Mixture F-12 (DMEM/F-12) and Lipofectamine 2000 were from Invitrogen (Carlsbad, CA, USA). *E. coli* strains DH5α and BL-21 were from Stratagene (La Jolla, CA, USA). DEAE Sepharose CL-6B resin was from Pharmacia (Peapack, NJ, USA). Tryptone and yeast extract were obtained from Becton-Dickinson (Sparks, MD, USA). RNase H, glucose, EGTA, SDS, kanamycin, ampicillin, chloramphenicol, Trizma-base, IPTG, imidazole, mercaptoethanol, bromophenol blue, polyacrylamide, Coomassie Brilliant Blue R, urea, BSA, cellobiose, $NaPO_4$, KH_2PO_4, K_2HPO_4 and UDP-glucose were from Sigma-Aldrich (St. Louis, MD, USA). Glycerol, glycine, Tween 20, Triton X-100, $CaCl_2$ and NaCl were obtained from Merck (Whitehouse Station, NJ, USA). LMW SDS Marker kit and UDP-D-[U-^{14}C]-glucose were purchased from Amersham Biosciences (Piscataway, NJ, USA). Ni-NTA affinity columns were from Qiagen (Valencia, CA, USA). NitroBind nitrocellulose membranes were purchased from Osmonics Inc. (Minnetonka, MN, USA). Goat Anti-Mouse IgG-HRP conjugate, luminol and p-coumaric acid was purchased from Biorad (Hercules, CA, USA). RX

X-ray film was from Fuji Photo Film Co. (Tokyo, Japan). Plasmid pGEM T-Easy was obtained from Promega (Madison, WI, USA). Ecolume scintillation fluid was from ICN (Costa Mesa, CA, USA). Foetal calf serum was from JRH Biosciences (Lennexa, KS, USA). Six-well tissue culture plates were from Nunclon (Rochester, NY, USA). Enhanced green fluorescent protein expression plasmid pCMS-EGFP was from Clontech (Palo Alto, CA, USA).

3.2.2 Restriction enzyme digestion of plasmid DNA

Plasmid DNA (5 μg) containing *HvGSL1* cDNA fragments was digested in 20 μl containing 0.5 μl restriction enzyme and 1x reaction buffer (supplied) at 37°C (unless specified otherwise) for 2-4 h. Where double digests were performed, 0.5 μl of each enzyme was added and the manufacturer's buffer recommendation was followed. Restriction enzyme combinations that could not be used in double digests due to incompatible buffer conditions were digested sequentially and purified in between using a NucleoSpin Extract kit. Restriction fragments were routinely isolated by 1.2% (w/v) agarose gel electrophoresis, gel excision and purification using a NucleoSpin Extract kit.

3.2.3 PCR amplification of HvGSL1 *cDNA fragments incorporating recombination signal sequences*

Two PCR primer sets were designed, incorporating overhanging "Gateway" recombination signal sequences and *HvGSL1* cDNA sequence. Primers, Y1F and Y1R (*Appendix B*), were used to amplify an approx. 1 kb portion of the *HvGSL1* cDNA (nucleotide position 54-1003 bp; Region A, *Figure 3.3*) from two overlapping *HvGSL1* restriction fragments, employing an end-fill PCR approach. Similarly, primers Y2F and Y2R (*Appendix B*) were used to amplify an approx. 2 kb fragment of the *HvGSL1* cDNA (nucleotide position 2253-4396 bp; Region B, *Figure 3.3*) from a plasmid containing a larger *HvGSL1* cDNA.

HvGSL1 DNA restriction fragments or plasmid DNA (0.5 μg) were used as PCR templates in 25 μl reaction volumes using a final concentration of 300 nM primers, 200 μM each dNTP, 0.1 U Expand DNA polymerase and 1x Expand buffer with 1.5

mM $MgCl_2$ (supplied). Reactions were conducted in a DNA Engine Tetrad thermal cycler (MJ Research, Reno, MV, USA) under the following conditions: 94°C for 30 sec followed by 35 cycles of 94°C for 30 sec, an annealing temperature of 65°C for 30 sec and an extension time of 1 or 2 min at 72°C (depending upon length of expected product). For end-filling reactions five cycles of PCR were conducted in the absence of primers. Primers were added to the reaction mix and the cycling conditions described above were followed. PCR products were isolated by 1.2% (w/v) agarose gel electrophoresis, gel excision and purification using a NucleoSpin Extract kit.

3.2.4 Donor vector recombination reactions

Purified PCR products (100-200 ng) incorporating "Gateway" recombination signal sequences were recombined into the pDONR201 vector (100-200 ng; *Figure 3.1*) via the Gateway cloning BP reaction in a 10 µl reaction volume with 2 µl BP reaction buffer (supplied) and 1 µl BP clonase enzyme mix. The recombination reaction was left for 16 h at 25°C and was stopped by heating to 94°C for 5 min.

3.2.5 Transformation of E. coli *by electroporation*

E. coli were prepared and transformed as described in section 2.2.14, except that cultures contained kanamycin at a concentration of 50 $\mu g.ml^{-1}$ instead of ampicillin.

3.2.6 Plasmid DNA mini-preparations

Plasmid DNA was extracted from overnight cultures as described in section 2.2.15.

3.2.7 DNA sequencing and sequence analysis

DNA sequences were determined by the Max-Planck-Institut für Züchtungsforschung (MPIZ) DNA core facility on Applied Biosystems (Weiterstadt, Germany) ABI Prism 377 and 3700 sequencers using BigDye-terminator chemistry. Premixed reagents

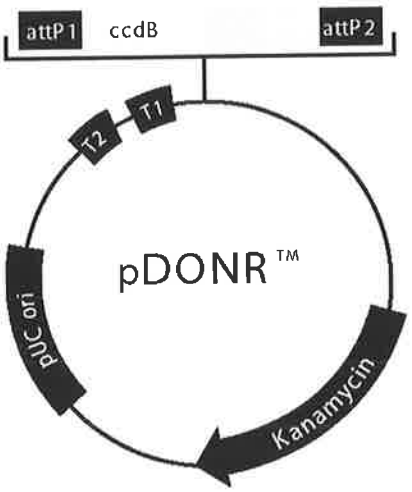

Comments for:	pDONR™201 4470 nucleotides
rrnB T2 transcription termination sequence (c):	73-100
rrnB T1 transcription termination sequence (c):	232-275
Recommended forward priming site:	300-324
attP1:	332-563
ccdB gene (c):	959-1264
Chloramphenicol resistance gene (c):	1606-2265
attP2 (c):	2513-2744
Recommended reverse priming site:	2769-2792
Kanamycin resistance gene:	2868-3677
Gentamicin resistance gene (c):	---
pUC origin:	3794-4467

(c) = complementary strand

Invitrogen

Figure 3.1 pDONR201 cloning vector. The *HvGSL1* cDNA fragments with their incorporated recombination signal sequences replace the *ccdB* gene and the chloramphenicol resistance gene, Cm^R between the *att*P1 and *att*P2 sequences during the BP recombination reaction.

were from Applied Biosystems. Oligonucleotides were purchased from Invitrogen. Cloned inserts in pDONR201 were sequenced with ENT5 and ENT3 primers (*Appendix B*). Data from automated sequencing was analysed as described in section 2.2.21.

3.2.8 *Generation of* E. coli *expression constructs by recombination*

Both *HvGSL1* cDNA fragments were transferred from the pDONR201 cloning vector into the *E. coli* expression vector, pDEST17 (*Figure 3.2*). Purified pDONR201 plasmid DNA containing the *HvGSL1* cDNA fragments (100-200 ng) was recombined into the pDEST17 destination vector (100-200 ng) via the gateway cloning LR reaction in a 10 µl reaction volume with 2 µl LR reaction buffer (supplied) and 1 µl LR clonase enzyme mix. The recombination reaction was left for 16 h at 25°C and was stopped by heating to 94°C for 5 min. The newly recombined expression construct (1 µl) was used to transform *E. coli* DH5α electrocompetent cells as described in section 2.2.14 and DNA was purified as described in section 2.2.15. Restriction mapping was used to confirm that recombination reactions were successful.

3.2.9 *Expression of barley peptides in* E. coli

Purified plasmid DNA (1 µg) verified by restriction mapping was used to transform *E. coli* BL-21 electrocompetent cells as described in section 2.2.14. Isolated colonies were cultured for 16 h in 3 ml Terrific broth (100 ml 0.17 M KH_2P0_4, 0.72 M K_2HPO_4 was added to 900 ml base broth; 1.33% w/v tryptone, 2.66% w/v yeast extract, 0.44% v/v glycerol) containing 100 $\mu g.ml^{-1}$ of ampicillin and 50 $\mu g.ml^{-1}$ chloramphenicol at 37°C with shaking. Overnight culture (1 ml) was used to seed a larger 40 ml culture for expression of the recombinant proteins. The culture media and selection parameters were as described above. Cultures were grown at 37°C with shaking until an A_{600} of 0.6 was reached, at which point, a glycerol stock of the culture was prepared and 750 µl of the culture was stored as a control. Cultures were placed on a platform shaker at 24°C and 6 µl 1 M IPTG was added to induce expression

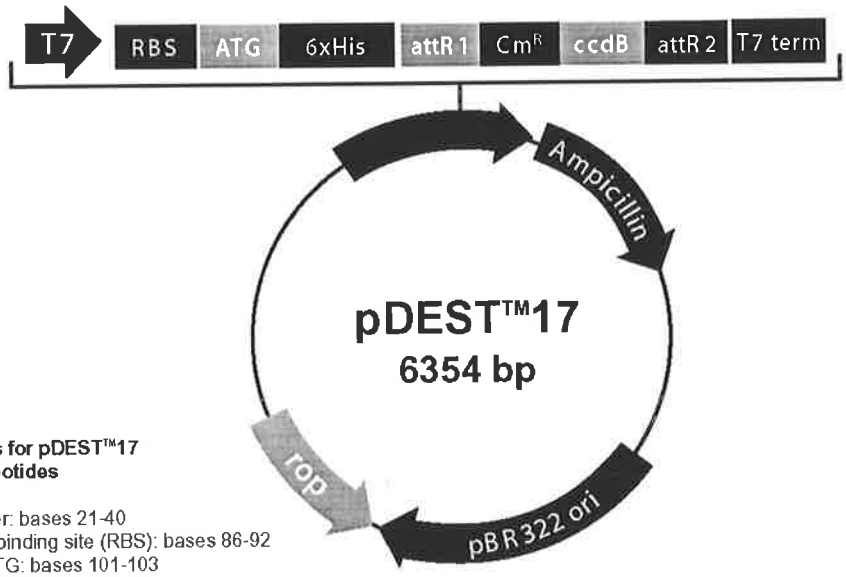

Figure 3.2 pDEST17 *E. coli* expression vector. The *HvGSL1* cDNA fragments from the pDONR201 vector replace the *ccdB* gene and the chloramphenicol resistance gene, Cm^R between the *att*R1 and *att*R2 sequences during the LR recombination reaction. The recombination reaction creates a construct that when expressed contains an ATG start codon, an NH_2-terminal 6xHis tag and an in frame HvGSL1 peptide with the T7 terminator sequence.

of the recombinant proteins. Cultures were incubated at 24°C for 4 h and 500 µl culture was stored at –20°C. *E coli* were pelleted by brief centrifugation and the supernatant was discarded.

3.2.10 Purification of His-tagged barley peptides

All purification steps were carried out at 4°C and the recombinant His-tagged proteins were purified using Ni-NTA affinity columns. IPTG induced culture (15 ml) was briefly centrifuged in a bench top centrifuge to separate the soluble fraction from the pellet containing the insoluble fraction. The pellet was resuspended in 1 ml sodium phosphate buffer, 50 mM Na_2HPO_4/50 mM NaH_2PO_4, pH 7.0, containing 300 mM NaCl and was kept on ice. Buffer containing imidazole at 10 mM, 5 mM and 1 mM was prepared. Resuspended pellets were sonicated twice for 20 sec to lyse the cells. Cellular debris was pelleted by centrifugation at 16,000 g for 30 min and supernatant was transferred to a chilled eppendorf tube. Ni-NTA columns were equilibrated by the addition of 600 µl 50mM sodium phosphate buffer, pH 7.0, containing 300 mM NaCl and imidazole, and the column was centrifuged for 1 min at 800 g according to the manufacturer's instructions. Cell lysate (600 µl) was added to the column and the column was centrifuged for 1 min at 800 g. The column was washed three times by the addition of 600 µl 50mM sodium phosphate buffer, pH 7.0, containing 300 mM NaCl and imidazole, and washes were kept on ice. Protein was eluted from the column with 2x 200 µl 50mM sodium phosphate buffer, pH 7.0, containing 300 mM NaCl and 250 mM imidazole. To check protein solubility and recovery from columns, the pellet of cellular debris was resuspended in 500 µl 8 M urea. After centrifugation for 15 min at 16,000 g the supernatant containing the solubilized protein fraction was removed.

3.2.11 Polyacrylamide gel electrophoresis

Proteins were prepared for electrophoresis by boiling for 10 min in 3 mM Tris-HCl buffer, pH 6.8, containing 20% (v/v) glycerol, 4% (w/v) SDS, 5% (v/v) mercaptoethanol and 0.0005% (w/v) bromophenol blue. Expression of the recombinant proteins was assessed by polyacrylamide gel electrophoresis (Laemmli,

1970) with a 5% (w/v) polyacrylamide stacking gel and 12.5% (w/v) polyacrylamide resolving gel. Proteins were separated at 30-60 mA in 25 mM Tris-HCl buffer, pH 8.3, containing 250 mM glycine and 0.1% (w/v) SDS in a Hoefer SE 250 protein electrophoresis system (Hoefer Scientific Instruments, San Francisco, CA, USA). In some instances proteins were separated in Novex 4-20% Tris–glycine precast gradient gels using the same current and buffer conditions described above in a Novex XCell II minicell electrophoresis system (Novex Electrophoresis, Tokyo, Japan). Gels were stained for 16 h in Coomassie Brilliant Blue R in 25% (v/v) methanol and 7% (v/v) acetic acid and destained in the same methanol/acetic acid solvent. A LMW SDS Marker kit containing the proteins phosphorylase (M_r 97000), albumin (M_r 66000), ovalbumin (M_r 45000), carbonic anhydrase (M_r 30000), trypsin inhibitor (M_r 20100) and α-lactalbumin (M_r 14400) was used to estimate protein molecular weights. Alternatively, a SeeBlue Plus 2 pre-stained protein standard was used to estimate protein molecular weights and contained the following proteins; myosin (M_r 250000), phosphorylase B (M_r 148000), BSA (M_r 98000), glutamic dehydrogenase (M_r 64000), alcohol dehydrogenase (M_r 50000), carbonic anhydrase (M_r 36000), myoglobin red (M_r 22000), lysozyme (M_r 16000), aprotinin (M_r 6000) and insulin β chain (M_r 4000).

3.2.12 Western analysis of tagged barley peptides

Tagged proteins were transferred from polyacrylamide gels (section 3.2.11) to NitroBind nitrocellulose membranes and were detected with a monoclonal antibody raised against a His-tag or c-Myc tag. Proteins were transferred from polyacrylamide gels using a semi-dry blotting system (CBS Scientific, Del Mar, CA, USA) under a constant voltage (100 V) for 1 h. Filters carrying the proteins were blocked with 1x TBS, (0.05 M Tris-HCl buffer, pH 7.4, containing 0.15 M NaCl) containing 4% (w/v) BSA and 2% (v/v) Tween 20. The filters were incubated with mouse Anti-His-HRP Antibody or Anti-c-Myc-HRP Antibody 9B11 diluted 1:10000 in 1x TBS containing 0.05% (v/v) Tween 20 and 1% (w/v) BSA for 16 h at 4°C with gentle rocking. Filters were rinsed three times in 1x TBS for 3 min. The filters were incubated with Goat Anti-Mouse IgG-HRP conjugate diluted 1:2000 in 1x TBS containing 0.05% (v/v) Tween 20 and 1% (w/v) BSA for 2 h at room temperature with gentle rocking. Finally, the filters were washed 3x in 1x TBS for 3 mins and blotted dry. Filters were incubated with approx. 15 ml of luminol stock mix (0.1 M Tris-HCl buffer, pH 8.6,

containing 22.5% w/v luminol and 7 mmol p-coumaric acid) for 1 min. The filters were blotted dry and overlayed with RX X-ray film at room temperature for approx. 30 sec using an intensifying screen. Autoradiographs were developed using an automated Curix system (Agfa, Greenville, SC, USA).

3.2.13 Activity of barley peptides expressed in E. coli

Crude cellular extracts containing partially purified proteins were assayed in duplicate for callose synthase activity using a radiolabelled substrate assay (Bulone *et al.*, 1995). Radiolabelled substrate, 0.5 μCi UDP-D-[U-^{14}C]-glucose was dried under N_2 and a master mix of reaction buffer was used to resolvate the pellet. Purified proteins (10 or 100 μl) along with an extract purified from untransformed BL-21 cells were assayed in 1 ml of reaction buffer containing 5.2 mM $CaCl_2$, 20 mM cellobiose and 10 mM UDP-glucose. Reactions were incubated at room temperature for 1 h on a rotating incubator before 3 ml 100% ethanol was added and samples were heated to 95°C for 5 min, terminating the reaction. The samples were left to cool to room temperature and were centrifuged at 5000 rpm for 5 min. Supernatant was discarded and another 3 ml 100% ethanol was added. This process of washing was repeated twice more and the pellets were resuspended in 4 ml scintillation fluid. Incorporated radioactivity was quantified by liquid scintillation counting and activity expressed as pmol glucose incorporated into ethanol-insoluble material per μl of extract per min.

3.2.14 PCR amplification of HvGSL1 *cDNA fragments*

A second set of PCR primers were designed to amplify and introduce several unique restriction enzyme sites for cloning, a Kozac's consensus start sequence, a translation stop codon and a c-Myc tag into the two predicted cytoplasmic domains of the *HvGSL1* cDNA described in section 3.2.3. The primers, hvgsl1xho1 and hvgsl1Reag1 (*Appendix B*), were used to amplify the approx. 1 kb portion of the *HvGSL1* cDNA (nucleotide position 54-1003 bp; Region A, *Figure 3.3*) from the pDONR201 vector described in section 3.2.4. The primers, hvgsl2xho1 and hvgs2R1eag1 (*Appendix B*), were used to amplify an approx. 2 kb fragment of the *HvGSL1* cDNA (nucleotide position 2253-4396 bp; Region B, *Figure 3.3*) from a plasmid containing this region of the *HvGSL1* cDNA.

PCR was conducted as described in section 3.2.3 except the annealing temperature was reduced to 55°C. Purified PCR products were initially ligated into pGEM T-Easy as described in section 2.2.13 and inserts were sequenced as described in section 2.2.16 using SP6 and T7 sequencing primers (*Appendix B*).

3.2.15 Construction of mammalian cell expression constructs

HvGSL1 cDNA fragments were excised from pGEM T-Easy with *Xho*I and *Eag*I restriction endonucleases under the conditions described in section 3.2.2. The 423 bp stuffer fragment of the pME18S expression vector was removed with *Xho*I and *Eag*I restriction endonucleases and the corresponding *HvGSL1* cDNA fragments from the pGEM T-Easy vector were ligated into these sites using the ligation conditions described in section 2.2.13. Both expression constructs were checked by restriction mapping experiments to confirm the presence of the inserts and the plasmids were used to transform DH5α electrocompetent cells as described in section 2.2.14. Plasmid DNA was purified as described section 2.2.15 and the DNA was sent to Dr. Tim Adams at CSIRO, Division of Health Sciences and Nutrition.

3.2.16 Expression of barley peptides in mammalian cells

Transient transfection experiments in the human embryonic kidney cell line, 293T, were conducted by Dr. Tim Adams (CSIRO, Division of Health Sciences and Nutrition). Briefly, the human embryonic kidney cell line, 293T, was maintained in Dulbecco's Modified Eagle Medium: Nutrient Mixture F-12 (DMEM/F-12) supplemented with 10% (v/v) foetal calf serum at 37°C under CO_2.

The day prior to transfection, adherent cells were detached using trypsin-versene, and were seeded out at 8 x 10^5 cells per well in 6-well tissue culture plates in a final volume of 2 ml medium per well. Plasmid DNA (4 μg) in 200 μl serum-free DMEM/F-12 was mixed with 12 μl Lipofectamine 2000 in 200 μl serum-free DMEM/F-12 and was left for 20 min at room temperature. The DNA:lipid mixture (400 μl) was added drop wise to a single well of a 6-well plate and left for 4-6 h at 37°C under CO_2. The supernatant was aspirated and replaced with complete growth medium (2 ml). Transfection efficiency was monitored by transfecting a plasmid

expression vector encoding an enhanced green fluorescent protein (EGFP) and examining cell cultures 24-48 h later by fluorescent microscopy.

Culture supernatants were aspirated 48-72 h post-transfection, the cells washed once with phosphate-buffered saline (1 mM KH_2PO_4, 0.15 M NaCl and 3 mM Na_2HPO_4, pH 7.2), and cell lysates prepared by solubilizing the cell monolayer with 1 ml of lysis buffer supplemented with protease inhibitors (20mM HEPES, pH 7.5, containing 150 mM NaCl, 1% (v/v) Triton X-100, 1.5 mM $MgCl_2$, 1.0 mM EGTA, Complete protease inhibitor and 10% (v/v) glycerol). After 30 min incubation on ice, the lysate was collected, centrifuged for 10 min at 16,000 g to pellet nuclear debris, and frozen at -70°C prior to analysis.

3.2.17 Activity of barley peptides expressed in mammalian cells

Protein levels from crude mammalian cell lysates were assessed by polyacrylamide gel electrophoresis as described in section 3.2.11. Aliquots of 100 µl of the crude cell lysates from both expression constructs and an empty vector control were assayed for callose synthase activity as described in section 3.2.13.

3.3 RESULTS AND DISCUSSION

3.3.1 Expression of barley peptides in E. coli

The larger cytoplasmic region of the barley HvGSL1 protein indicated as region B in Figure 3.3 contained an area of sequence conservation when compared with other plant (1→3)-β-D-glucan synthases and might therefore contain the catalytic site of the (1→3)-β-D-glucan synthase enzyme. Fragments of the cDNA from this region and the other large cytoplasmic region at the NH_2-terminus, indicated as region A in Figure 3.3, were amplified by PCR and recombined into an *E. coli* expression vector to determine whether the expression of these fragments could lead to the production of callose.

For the first fragment, which corresponded to a large part of the NH_2-terminal coding region of *HvGSL1* (nucleotide position 54-1003, Region A, *Figure 3.3*), two overlapping cDNA fragments were combined as a template in end-fill PCR because a single clone that covered this region was not available. The two overlapping *HvGSL1* cDNA fragments (overlap by approx. 100 bp) were excised from their respective cloning vectors with restriction endonucleases. An approx. 500 bp *HvGSL1* fragment was liberated from pGEM T-Easy with *Not*I and an approx. 600 bp *HvGSL1* fragment was excised from pGEM T-Easy with *Not*I (*Figure 3.4*). The fragments were purified and combined. End-fill PCR yielded a single *HvGSL1* cDNA fragment of 1006 bp (*Figure 3.5*), which included the recombination signal sequences required for later experiments and was engineered for expression of the *HvGSL1* fragment in *E. coli*.

For the second fragment, which corresponded to a large part of the centrally located cytoplasmic loop of *HvGSL1* (nucleotide position 2253-4396, Region B, *Figure 3.3*), a pBluescript plasmid containing an approx. 2.6 kb *HvGSL1* cDNA insert was used as a template in PCR. PCR produced a 2197 bp fragment (*Figure 3.6*) that also possessed the recombination signal sequences and was engineered for expression in *E. coli*.

The two PCR amplified *HvGSL1* cDNA fragments were separately recombined into the pDONR201 cloning vector (BP reaction) and vector DNA was sequenced.

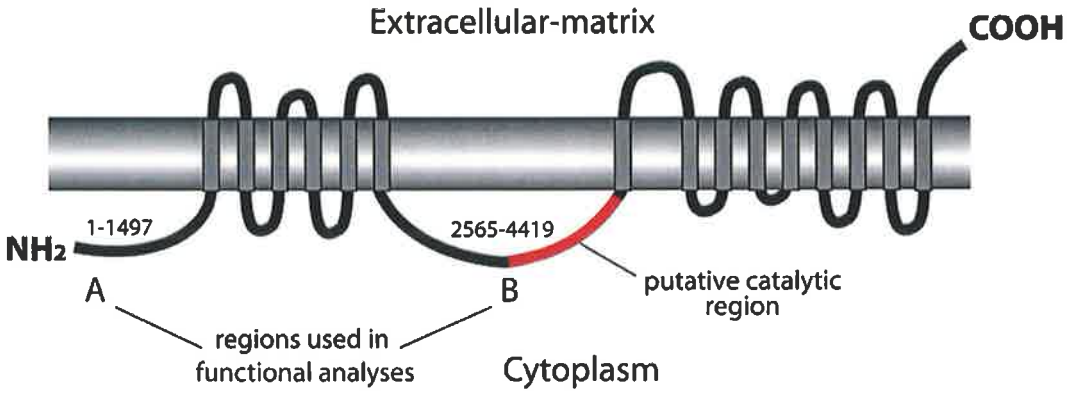

Figure 3.3 Topological profile of the barley HvGSL1 protein. Parts of the predicted cytoplasmic regions designated **A** and **B** were expressed in *E. coli* and in mammalian cells. The nucleotide positions encoding the major cytoplasmic regions are indicated on the diagram and the putative catalytic region is indicated in red. The topology prediction was made using TopPredII software.

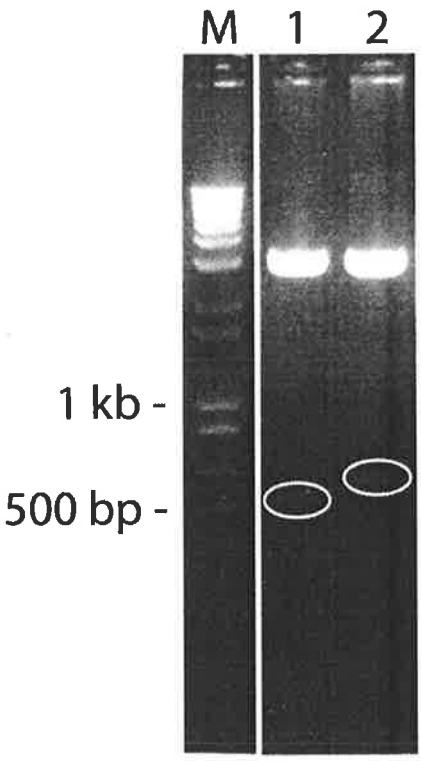

Figure 3.4 Agarose gel containing *HvGSL1* restriction fragments purified for use as templates in PCR. Faint bands in Lane **1**, 500 bp fragment and Lane **2**, 600 bp fragment indicated by ellipses were purified.

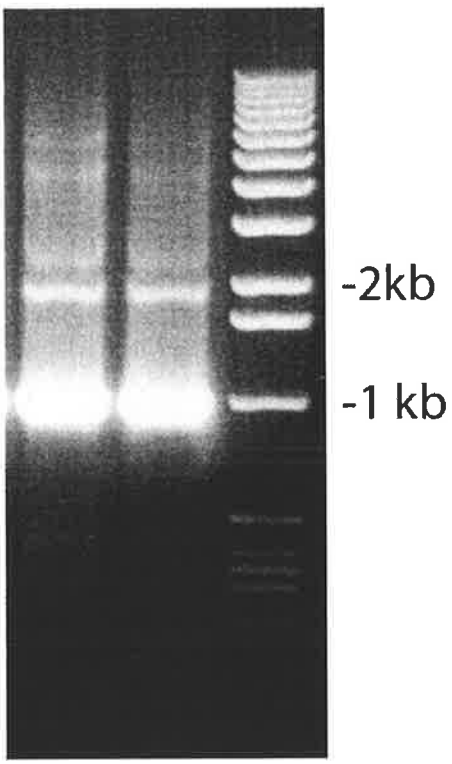

Figure 3.5 Agarose gel containing PCR amplified *HvGSL1* fragments incorporating recombination signal sequences. Primers incorporating recombination signal sequences and *HvGSL1* specific sequence were used to amplify an approx. 1 kb fragment from two *HvGSL1* restriction fragments for expression in *E. coli* using end-fill PCR.

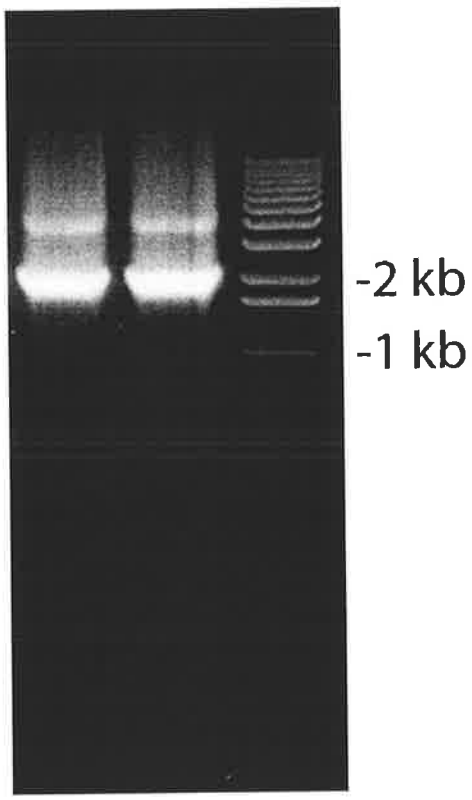

Figure 3.6 PCR amplification of a *HvGSL1* fragment incorporating recombination signal sequences. Primers incorporating recombination signal sequences and *HvGSL1* specific sequences were used to amplify an approx. 2 kb fragment from a *HvGSL1* restriction fragment for expression in *E. coli.*

Sequencing results indicated that the recombination reactions were successful, introducing the *HvGSL1* cDNA fragments into the pDONR201 vector in the expected orientation and that both fragments were in the correct frame for expression.

Both of the *HvGSL1* fragments were transferred from the pDONR201 cloning vector to the *E. coli* expression vector, pDEST17, in a second recombination (LR) reaction. Recombination into the pDEST17 vector produced two HvGSL1 expression plasmids, pAJ11 and pAJ12. Transcription of these plasmids produced HvGSL1 peptides with NH_2-terminal histidine tags. Plasmid pAJ11 encodes the approx. 1kb NH_2-terminal cytoplasmic domain of HvGSL1 (Region A, *Figure 3.3*) whilst pAJ12 encodes the approx. 2kb central cytoplasmic loop of HvGSL1 (Region B, *Figure 3.3*). The presence of the *HvGSL1* fragments in the expression vector was confirmed following the second recombination reaction by restriction mapping.

Expression of the recombinant proteins was induced in *E. coli* cultures by the addition of IPTG, a lactose analogue, which leads to expression of the highly processive T7 RNA polymerase and subsequent high-level expression of the downstream, tagged protein.

Proteins from the expression cultures were viewed on polyacrylamide gels, which confirmed that both the *HvGSL1* cDNA fragments in the pDEST17 vector were expressed (*Figure 3.7*). A band of approx. 41 kDa, corresponding to pAJ11, the 1006 bp *HvGSL1* fragment and attached pDEST17 vector sequence (an additional 52 amino acid residues), was visible in the induced sample on the polyacrylamide gel (red ellipse, lane 2). The pAJ12 construct containing the 2197 bp *HvGSL1* fragment and attached pDEST17 vector sequence was detected as an approx. 84 kDa band, in the induced sample on the same polyacrylamide gel (red ellipse, lane 4). Thus, in both cases the sizes of the major IPTG-induced, expressed peptides were approximately as expected based upon estimations from the sizes of the cDNA fragments used to create the expression vectors. The next requirement was to purify the expressed His-tagged proteins from the *E. coli* homogenate by affinity chromatography so that assays for callose synthase could be undertaken on the purified proteins.

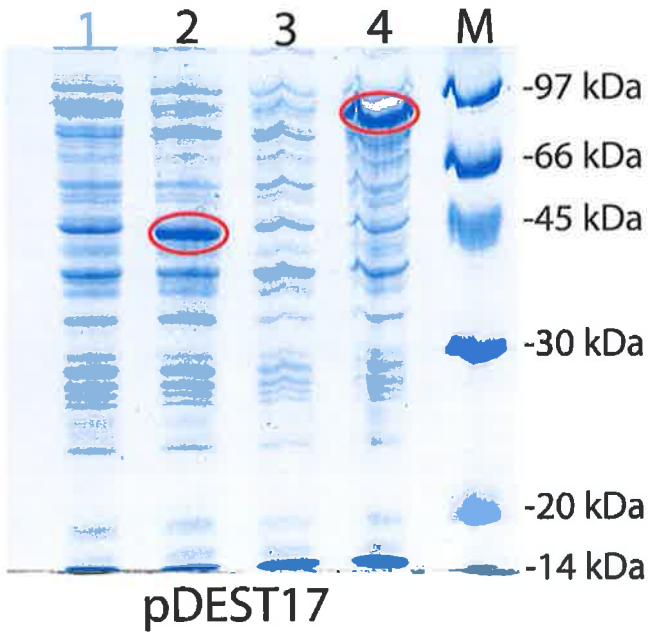

Figure 3.7 Polyacrylamide gel analysis of HvGSL1 peptides expressed in *E. coli*. Two *HvGSL1* cDNA fragments predicted to be cytoplasmic, corresponding to nucleotide position. 54-1003 bp and nucleotide position. 2253-4396 bp were expressed in pDEST17. Lane **1**; proteins from uninduced culture of AJ11 (54-1003 bp) and Lane **2**; proteins from induced culture of pAJ11 (54-1003 bp). Lane **3**; proteins from uninduced culture of pAJ12 (2253-4396 bp) and Lane **4**; proteins from induced culture of pAJ12 (2253-4396 bp). **M** molecular weight size standards. In lanes 2 & 4 prominent bands of the expected size for the recombinant HvGSL1 peptides are evident, red ellipses.

3.3.2 Purification of barley peptides expressed in E.coli

Purification of the histidine-tagged HvGSL1 proteins was attempted using affinity columns in which the six histidine residues present in the recombinant fusion protein are bound to a chelating nickel resin (Janknecht and Nordheim, 1991). The soluble fractions in which the recombinant proteins were detected (section 3.3.1) were applied to Ni-NTA columns with low concentrations of imidazole (10 mM, 5 mM and 1 mM). The binding strength of the proteins to the affinity column is reduced with the higher concentrations of imidazole. A balance between the level of protein purity and protein recovery can be achieved using the different concentrations of imidazole. Unbound proteins were washed through the column and the bound histidine-tagged recombinant protein was eluted from the column by applying a high concentration of imidazole (250 mM). Proteins eluted from the column were separated on polyacrylamide gels. A number of weak protein bands were visible in the gel (lanes 3 & 6; *Figure 3.8*) but the expected HvGSL1 polypeptides of 41 and 84 kDa were not visibly enriched. Following this poor purification result, a sample from the insoluble protein fraction was dissolved in 8 M urea so that the insoluble proteins might be analysed by SDS-PAGE. Proteins in retained washes from the purification process and urea-solubilized proteins were separated on a polyacrylamide gel, which revealed that most of the His-tagged HvGSL1 proteins were present in the insoluble fraction (data not shown). The aggregation of recombinant proteins into insoluble inclusion bodies has been well documented in *E. coli* (Wingfield *et al.*, 1999; Dreyer *et al.*, 1999; Zhang *et al.*, 1998). In attempts to overcome this problem, the expression experiments were repeated with the induction temperature lowered from 24°C to 16°C, because this has been reported to aid in solubilization of expressed proteins in *E. coli* (Han *et al.*, 1999; Huang *et al.*, 1998; Weickert *et al.*, 1997). However, no difference was observed using this modification of the procedure.

The detection of bands of the expected size, corresponding to the HvGSL1 fragments, in the purified fractions would provide evidence that purification enriched the expressed proteins even though the HvGSL1 proteins were largely insoluble. A western blot of the fractions from the purification procedure was therefore prepared and an Anti-His tag monoclonal antibody was used to probe the blot for proteins containing multiple histidine residues (data not shown). Faint bands of 41 and 84 kDa

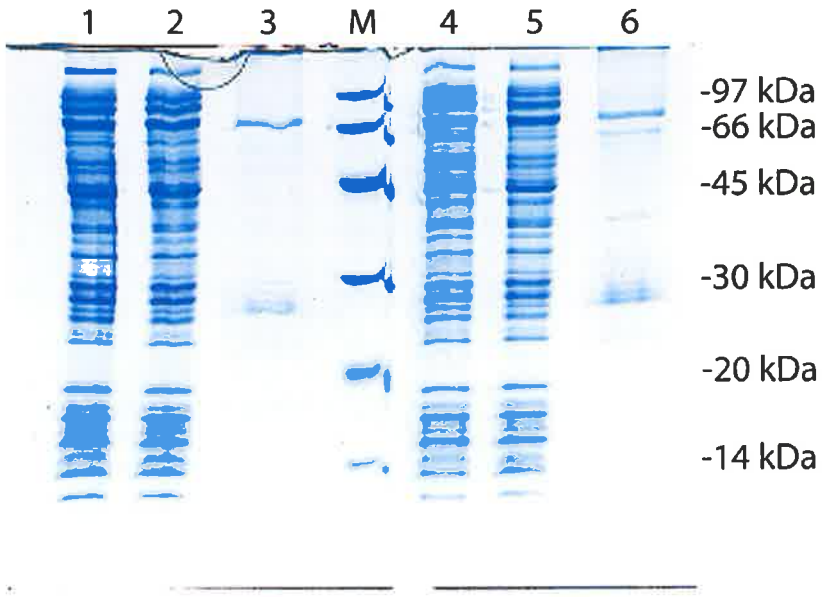

Figure 3.8 Polyacrylamide gel analysis of partially purified HvGSL1 peptides expressed in *E. coli*. Two *HvGSL1* cDNA fragments predicted to be cytoplasmic, corresponding to nucleotide posn. 54-1003 bp, pAJ11 and nucleotide posn. 2253-4396 bp, pAJ12, were expressed and purified using Ni-NTA affinity chromatography. Lane **1**; proteins from soluble fraction of culture expressing pAJ11 (54-1003 bp). Lane **2**; proteins from unbound column fraction of culture expressing pAJ11 (54-1003 bp). Lane **3**; proteins purified from soluble fraction of culture expressing pAJ11 (54-1003 bp). Lane **4**; proteins from soluble fraction of culture expressing pAJ12 (2253-4396 bp). Lane **5**; proteins from unbound column fraction of culture expressing pAJ12 (2253-4396 bp). Lane **6**; proteins purified from soluble fraction of culture expressing pAJ12 (2253-4396 bp). **M** molecular weight size standards. Lanes 3 & 6 contain the purified fractions and indicate that purification of the HvGSL1 His-tagged proteins, of 41 and 84 kDa respectfully, was limited.

were detected in the purified fractions but much of the antibody signal was detected in the soluble and unbound fractions, probably as a result of the greater abundance of proteins that were present in these fractions. Antibody also bound to the marker track, which suggested that the antibody was binding non-specifically. Western analyses did not clearly indicate that purification procedures were successful but the non-specific binding of the Anti-His monoclonal antibody may have masked any purification by obscuring detection of the anticipated HvGSL1 peptides on the blot. As a result, activity assays were performed on the partially purified extracts.

3.3.3 Activity of barley peptides expressed in E. coli

Partially purified proteins from the pAJ11 and pAJ12 induced cultures were eluted from NiNTA columns and assayed for callose synthase activity using a radiolabelled substrate assay. In this assay radiolabelled ^{14}C-glucose is incorporated into newly synthesised (1→3)-β-D-glucan, which is ethanol-insoluble, from the radiolabelled substrate, UDP-[U-^{14}C]-D-glucose. The reaction can be summarised as follows:

$$(G)_n + \text{UDPGlc} \rightleftharpoons (G)_{n+1} + \text{UDP}$$

where G is a glycosyl residue and n in the degree of polymerisation of the (1→3)-β-D-glucan chain. A *Lolium multiflorum* microsomal membrane preparation was obtained for use as a positive control in the assays (Mr. Michael Schober, Department of Plant Science, University of Adelaide) and an aliquot of this preparation was boiled as a negative control. The results of the assays are presented graphically in Figure 3.9. No significant callose synthase activity was detected in either of the purified extracts containing the HvGSL1 recombinant peptides. The unboiled positive control exhibited activity typical of *L. multiflorum* microsomal preparations (Mr. Michael Schober, personal communication).

The catalytic region of plant callose synthase enzymes has not yet been identified. Some predictions regarding the catalytic residues in the barley callose synthase enzyme have been made using computer aided modelling and from amino acid sequence comparisons to other glycosyl transferases (Li *et al.*, 2003). The models suggest that the barley callose synthase enzyme is more closely related to the family

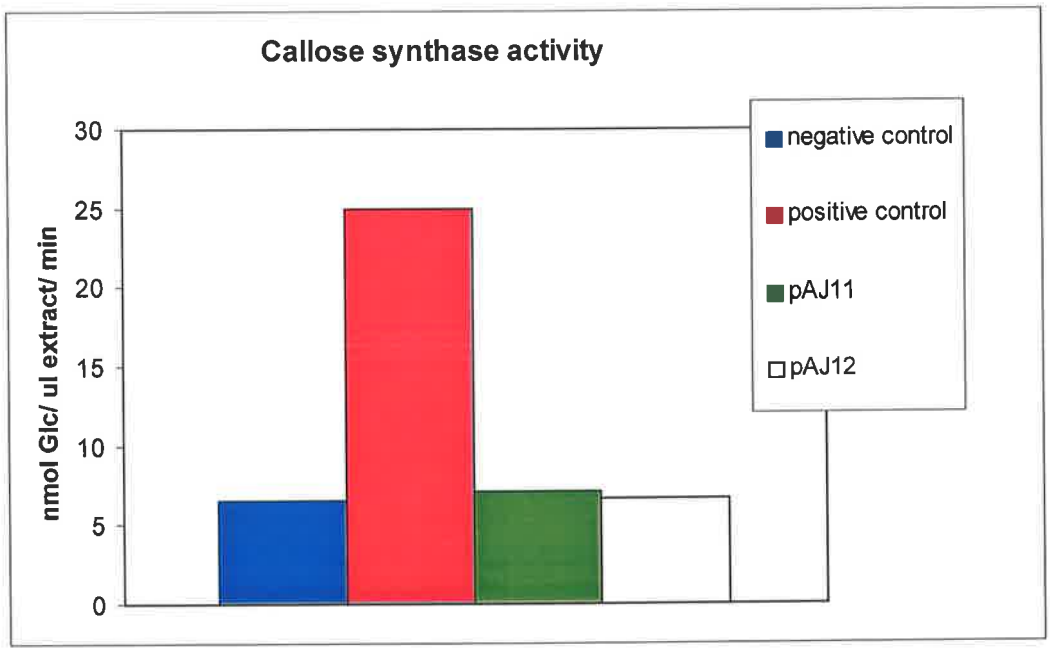

Figure 3.9 Callose synthase enzyme assays conducted on partially purified HvGSL1 recombinant peptides expressed in *E. coli*. The positive control is a microsomal membrane preparation extracted from *Hordeum vulgare* endosperm suspension cultures. Plasmid pAJ11 corresponds to approx. 1 kb NH_2-terminal region of *HvGSL1* and pAJ12 corresponds to approx. 2 kb, more centrally located, predicted cytoplasmic region.

GT2 enzymes than the family GT28 enzymes. The family GT2 enzymes contain highly conserved MDDN, TDDN, IDH and GDA motifs that are positioned on sheet, sheet, loop and helix structural elements, respectively and are predicted to form a GT-A fold (Charnock and Davies, 1999). The experimental work presented here suggests that more than a single region is required for activity if one assumes that the expressed barley peptides have adopted the correct fold. It may be that a number of regions of the plant callose synthase protein are required for (1→3)-β-D-glucan biosynthesis or that ancillary proteins participate in activity.

In summary, purification of the expressed HvGSL1 peptides was not successful and the data obtained from activity assays on the barley peptides expressed in *E. coli* indicated that the peptides had no callose synthase activity. However, it is possible that the expressed peptides lacked an essential amino acid modification. To address this issue the same HvGSL1 peptides were expressed in mammalian cells, which are capable of most of the amino acid modifications that are found in plant proteins.

3.3.4 Expression of barley peptides in mammalian cells

Transient transfection of mammalian cells has been used for various cloning and structure-function studies of plant transporter proteins (Kammerloher *et al.*, 1994; Kristoffersen *et al.*, 1996; Chang and Bush, 1997). The approx. 1 kb *HvGSL1* cDNA fragment corresponding to the NH_2-terminal cytoplasmic region or nucleotide position 54-1003 bp (Region A, *Figure 3.3*) was ligated into the expression plasmid pME18S, to form the pAJ15 expression construct and the approx. 2 kb more centrally located cytoplasmic region of the *HvGSL1* cDNA corresponding to nucleotide position 2253-4396 bp (Region B, *Figure 3.3*) was ligated into pME18S to form the pAJ16 expression construct.

The pAJ15 and pAJ16 plasmids were transiently expressed in transfected human embryonic kidney cells, line 293T, by Dr. Tim Adams (CSIRO, Division of Health Sciences and Nutrition). Transfection efficiency was measured by detection of EGFP fluorescence in cells transfected with an EGFP expression plasmid. Routinely, more than 50% of cells were positive for EGFP (data not shown). Protein levels in crude cell lysates were assessed in polyacrylamide gels (*Figure 3.10*). No differences were

detected between the protein composition of culture in which the HvGSL1 peptides were expressed and those containing the empty expression vector alone (*Figure 3.10*). Expression of the pAJ15 construct should yield a protein of approx. 36 kDa whilst expression of pAJ16 is expected to yield a protein of approx. 80 kDa. These bands could not be detected, so more sensitive Western analyses employing an antibody raised against the c-Myc protein present in the pME18S vector were used to confirm that the HvGSL1/c-Myc proteins were expressed in the mammalian cell cultures (*Figure 3.11*). The presence of a discrete band of the expected size for the NH_2-terminal region (Region A, *Figure 3.3*) of HvGSL1 (37 kDa) in the Western blot confirmed the expression of HvGSL1/c-Myc tagged protein, so (1→3)-β-D-glucan synthase activity assays were undertaken. The central cytoplasmic loop of HvGSL1 (Region B, *Figure 3.3*) should produce an 80 kDa protein when expressed in mammalian cells but no 80 kDa band was detected in Western blots probed with the c-Myc antibody (data not shown). It may be that this recombinant protein is not present in the detergent solubilized fraction that was used in the Western blot. The absence of this protein might also be explained by an error during transcription of the expression plasmid such that a truncated protein is produced or that an error was made during the construction of the expression plasmid. DNA sequencing of the plasmid was conducted prior to expression experiments so plasmid error is probably unlikely. Immunoprecipitating the protein from lysates might enable the detection of this recalcitrant protein.

3.3.5 Activity of barley peptides expressed in mammalian cells

Crude mammalian cell extracts from cultures expressing the pAJ15 and pAJ16 constructs were assayed for callose synthase activity, alone and combined, and the results of these experiments are presented graphically in Figure 3.12. Ethanol-insoluble radiolabelled product was detected at similar levels after assays of all the mammalian cell lysates, including the sample from the empty pME18S expression vector. Mammalian cells do not normally synthesise callose (Stone and Clarke, 1992) so the detection of activity would represent a gain-of-function. However, the UDP-glucose substrate can be incorporated into other glucose-based polymers, such as glycogen, in mammalian cells (Stone and Clarke, 1992). It seems likely that the incorporation of the radiolabel measured in this assay, specifically the levels

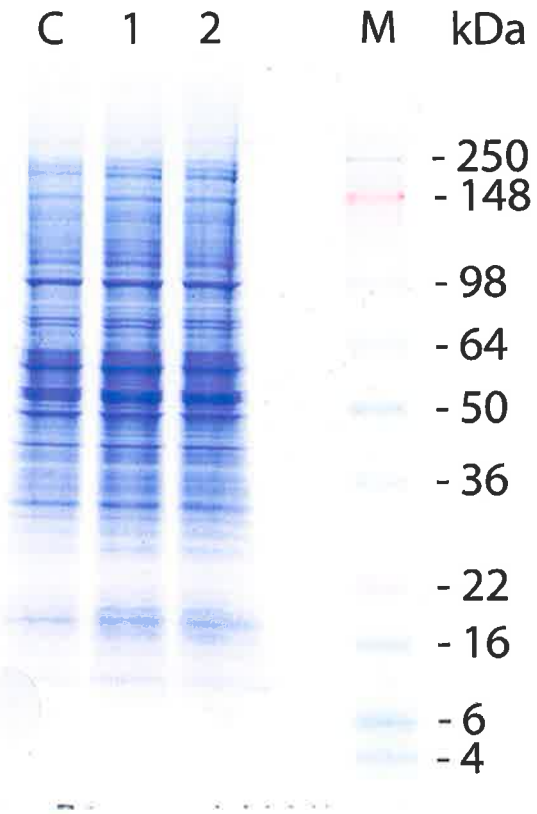

Figure 3.10 SDS-PAGE of crude mammalian cell extracts from expression cultures. C control, proteins from untransformed cell cultures. Lane **1**; proteins from cultures expressing pAJ15 construct. Lane **2**; proteins from cultures expressing pAJ16 construct. **M** molecular weight markers. The HvGSL1 recombinant peptides of 37 and 80 kDa were not prominent in extracts from cultures expressing pAJ15 or pAJ16, lanes 1 & 2.

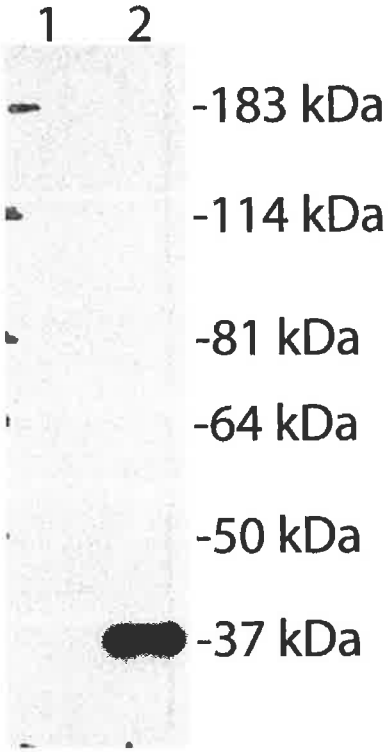

Figure 3.11 Western analyses of c-Myc /HvGSL1 proteins expressed in mammalian cells using c-Myc monoclonal antibody. Lane **1**; proteins from cultures expressing empty pME18S expression vector. Lane **2**; proteins from cultures expressing pAJ15. A 37 kDa band corresponding to the HvGSL1 NH_2-terminal domain was evident in lane **2**. Image courtesy of Dr. Tim Adams.

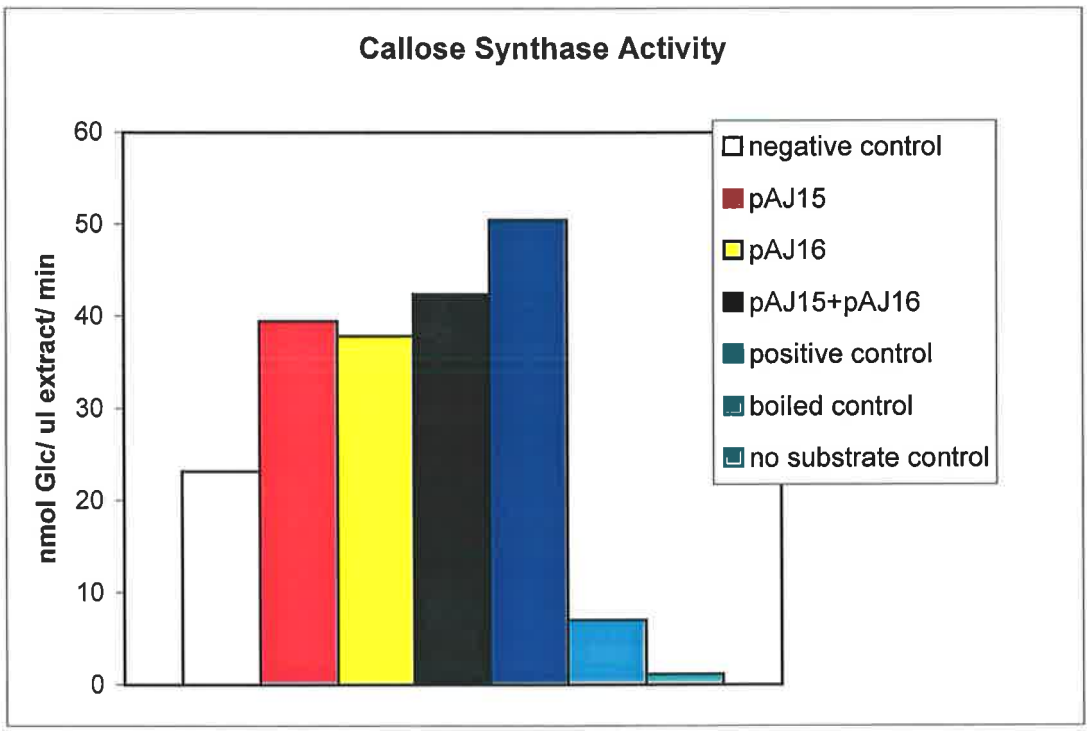

Figure 3.12 Results of callose synthase enzyme assays conducted on crude cell extracts of mammalian cell cultures expressing HvGSL1 recombinant peptides.

detected in the extracts from cells expressing the empty pME18S vector alone, must be due to the formation of polymers other than (1→3)-β-D-glucan. Crude extracts from both of the HvGSL1 expression cultures were combined to determine if there was any cooperative interaction between the two *HvGSL1* predicted cytoplasmic peptides but no change in the levels of callose synthase activity was found. From these results it was concluded that the selected HvGSL1 peptides alone were not able to synthesise (1→3)-β-D-glucan in mammalian cell systems. Again, this assumption is based on the premise that the HvGSL1 peptides were expressed in a correctly folded form and possessed post-translational modifications necessary for activity in the native GSL protein.

3.4 SUMMARY AND CONCLUSIONS

The two largest cytoplasmic regions of the barley *HvGSL1* cDNA were expressed in *E. coli* and in the human embryonic kidney cell line, 293T. Crude cellular extracts and partially purified proteins from the expression cultures were assayed for callose synthase activity. The expressed regions were not capable of synthesizing (1→3)-β-D-glucan alone or when combined. The centrally located region contained a number of conserved amino acid residues when compared with other callose synthase peptide sequences and this region has been proposed as the site of catalysis (Li *et al.*, 2003). However, data presented here indicates that whilst the site of catalysis may be contained within this region, other regions or ancillary proteins are required for (1→3)-β-D-glucan synthesis.

Recombinant proteins were clearly evident in protein extracts from bacterial cultures expressing the HvGSL1 peptides and although the proteins included a His-tag, purification on Ni-NTA columns was not achieved. The purification procedures employed here were conducted on the assumption that the expressed proteins were soluble. Later it was noted that the bulk of the recombinant proteins were in the insoluble fraction when 8 M urea was used to denature cellular proteins. In this instance it may have been better to purify the HvGSL1 peptides in a denatured form using Ni-NTA resin rather than a column and then attempt to refold the peptide before assaying for activity. With the power of hindsight and the luxury of more time, the purification of the fusion proteins from the *E. coli* system might be achievable.

Alternatively, one might address the issue of solubility. Various techniques for increasing the solubility of heterologously expressed proteins have been reported (Maina *et al.*, 1988; Guan *et al.*, 1988) often by creating a fusion protein that contains a highly soluble protein, such as maltose binding protein. This approach would require a new expression construct to be produced and would ideally contain a cleavage site so that the solubility enhancing protein and His-tag could be removed prior to activity studies. This approach might maximise the chance of purifying soluble, native HvGSL1 peptides from the *E. coli* expression system.

Extracts from the mammalian cell cultures contained no detectable recombinant HvGSL1 proteins on Coomassie stained gels, but Western analysis employing a monoclonal antibody raised against a c-Myc tag enabled a protein of 37 kDa, corresponding to the NH_2-terminal region of *HvGSL1* to be detected on protein blots. Expression of the central loop region of HvGSL1 would produce a polypeptide of 80 kDa but this protein was not detected in protein blots. The NH_2-terminal HvGSL1 peptide was expressed at a low level and enzyme activity in the culture was comparable to levels in culture expressing the empty vector alone, indicating that ^{14}C-glucose was incorporated into polymers other than (1→3)-β-D-glucan. The presence of the c-Myc tag in the *HvGSL1* expression constructs could be used to purify the recombinant proteins by immunoaffinity approaches. A culture of human embryonic kidney cells stably transformed with the expression constructs could be produced and used for the expression of the HvGSL1 peptides in large-scale cultures to increase the abundance of HvGSL1 peptides for purification.

During the course of the expression studies described in this chapter, evidence that multiple proteins might be required for (1→3)-β-D-glucan synthesis was published (Hong *et al.*, 2001a, 2001b). The possibility that proteins other than HvGSL1 protein are required for the synthesis of (1→3)-β-D-glucan clearly diminished our chances of detecting activity in expressed fragments of the *HvGSL1* gene. Thus, heterologous expression of HvGSL1 peptides was abandoned at this stage in favour of the gene silencing experiments described in Chapter 5. However, possible interactions of the barley HvGSL1 protein with ancillary proteins necessary for activity were first investigated using the yeast two-hybrid system. These experiments are described in the next chapter.

CHAPTER 4

YEAST TWO-HYBRID ANALYSIS OF POSSIBLE PROTEIN-PROTEIN INTERACTIONS OF A BARLEY (1→3)-β-D-GLUCAN SYNTHASE

4.1 INTRODUCTION

The failure to detect any catalytic activity associated with the HvGSL1 polypeptides expressed in the heterologous systems, as discussed in the previous chapter, may well relate to the absence of ancillary or regulatory proteins. The presence of multiple polypeptides found in preparations capable of producing callose supports this hypothesis and it may be that the active callose synthase enzyme forms a complex with a group of proteins. The concept of a (1→3)-β-D-glucan synthase complex has gained significant support over recent years (Bulone *et al.*, 1995; Cui *et al.*, 2001; Hong *et al.*, 2001a, 2001b; Verma, 2001).

Previous studies of (1→3)-β-D-glucan synthesis have implicated a range of proteins in the production of callose. In yeast, (1→3)-β-D-glucan synthesis is dependent upon a guanosine triphosphate (GTP) binding protein, Rho1p (Mol *et al.*, 1994; Qadota *et al.*, 1996; Drgonova *et al.*, 1996; Mazur and Baginsky, 1996). Plants contain a unique subfamily of Rho GTPases that include the *Rop* and *Rac* gene families, which are vital components of cellular signalling networks. One might therefore anticipate that the barley HvGSL1 protein could interact with a Rho GTPase, given the observations in yeast and the coincident detection of the various Rop and Rac proteins at the sites of known (1→3)-β-D-glucan synthesis in plants. In *Arabidopsis*, the Rop4 and Rop6 proteins have been located in root meristems at the cross walls and cell plate (Molendijk *et al.*, 2001). Furthermore, *Arabidopsis Rop1* and *Rac2* mRNA is specifically expressed in pollen (Delmer *et al.*, 1995; Li *et al.*, 1999). The interaction of the plant (1→3)-β-D-glucan synthase and the Rho GTPase may however be mediated via another protein, UDP-glucose transferase (UGT), as highlighted by the work of Hong *et al.* (2001b) in which UGT1 was found to interact with Rop1. Hong *et al.* (2001a) also demonstrated that the *Arabidopsis* AtGSL6 protein interacts with phragmoplastin and the UDP-glucose transferase, both in a yeast two-hybrid system and *in vitro*.

A calmodulin-binding domain has been identified in the deduced peptide sequence of a putative cotton (1→3)-β-D-glucan synthase gene (*CFL1*) and calmodulin binding was confirmed using a calmodulin gel overlay assay (Cui *et al.*, 2001). A possible

calmodulin-binding domain was also identified in the HvGSL1 protein in a similar position, between amino acid residues 232-248, and also in the AtGSL5 protein (unpublished data). A purified plasma membrane fraction from cotton fibres, in which polypeptides of annexins were detected, bound to and inhibited the activity of a partially purified cotton (1→3)-β-D-glucan synthase (Andrawis *et al.*, 1993) and immunolocalisation studies have shown that sucrose synthase co-localises at sites of callose synthesis in cotton fibres (Amor *et al.*, 1995). These collective data add to the concept of a (1→3)-β-D-glucan synthase multi-protein complex.

The putative barley callose synthase protein HvGSL1 has a predicted topological profile with a large centrally located cytoplasmic loop and an NH_2-terminal region that is also predicted to be cytoplasmic (Li *et al.*, 2003). These large predicted cytoplasmic regions of HvGSL1 were chosen to assess any protein-protein interactions that may occur between the barley callose synthase protein and other proteins, using a yeast two-hybrid approach to screen several plant cDNA libraries. Selected regions rather than the full length HvGSL1 protein were chosen to analyse protein-protein interactions because of the increased likelihood of errors occurring during the transcription of a large 6 kb cDNA, the fact that the *HvGSL1* cDNA was comprised of a number of overlapping cDNA clones and concerns about the correct folding of a membrane bound protein with up to 14 transmembrane spanning domains.

The development of the yeast two-hybrid system over the last 10 years has provided a convenient tool to study protein-protein interactions and allows the rapid identification of the corresponding cDNAs (Fields and Song, 1989). In this technique, a cDNA encoding a protein of interest can be screened directly against another expressed cDNA or against a library of expressed cDNAs for an interaction that is detected by the transcriptional activation of a reporter gene. The reporter gene becomes active when the reporter activation domain (AD) of the yeast *Gal4* gene fused to one protein is bought into close proximity of the reporter-binding domain (BD) of the yeast *Gal4* gene by the interacting protein (*Figure 4.1*). This technology can also be used to study interactions between DNA and protein in a one-hybrid system (Bush *et al.*, 1996) or between RNA and protein in a three-hybrid system (Sen

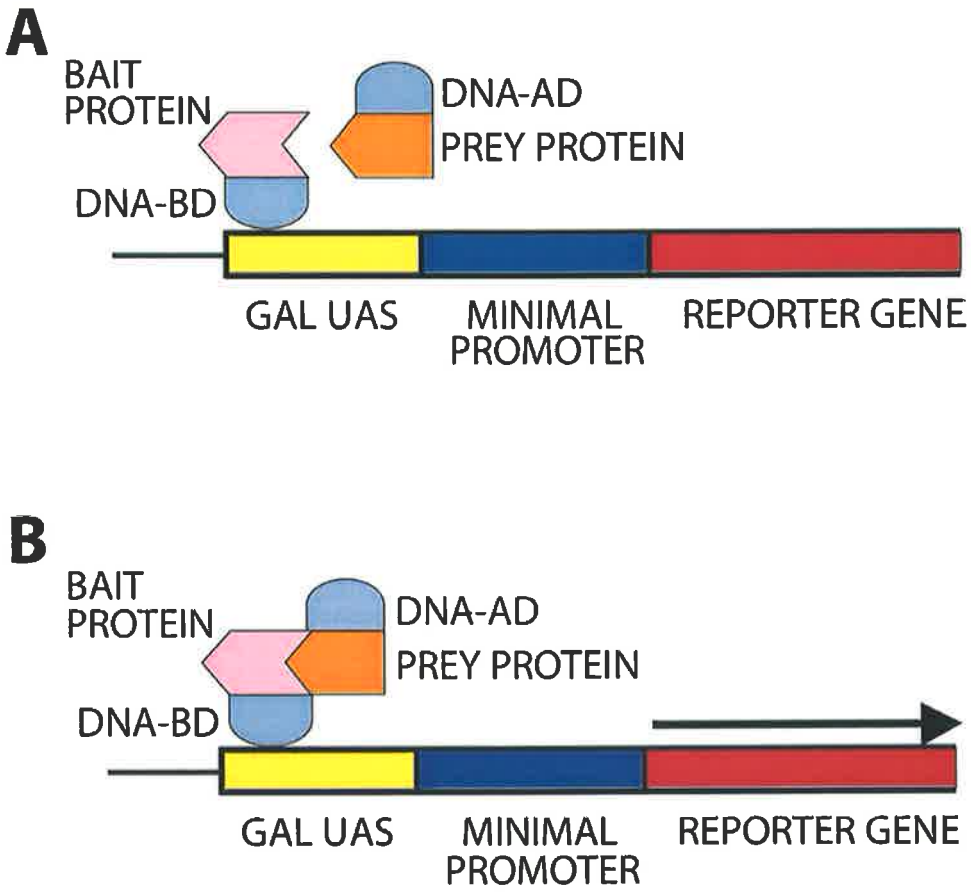

Figure 4.1 Schematic representation of the yeast two-hybrid system. In panel **A** a gene fusion is generated that encodes the protein of interest (bait protein) as a hybrid with the DNA binding domain (DNA-BD) of the yeast *Gal4* gene. This domain enables the hybrid protein to localise to the nucleus and bind DNA in a site-specific fashion. A second gene or library of sequences is expressed (prey protein) as a hybrid with the DNA activation domain (DNA-AD) of the yeast *Gal4* gene. This hybrid protein also enters the nucleus. The bait and prey proteins do not interact and binding of the bait hybrid protein to the *Gal4* upstream activation sequence (GAL-UAS) fails to activate transcription of the reporter gene that is under the control of the minimal promoter. In panel **B** the bait and prey proteins interact which brings the two domains of the *Gal4* promoter into close proximity reconstituting the transcriptional activation of the promoter and leading to transcription of the reporter gene.

Gupta *et al.,* 1996). An automated yeast two-hybrid system has been developed (Walhout and Vidal, 2001) and when used to screen 96 different cDNAs thought to be involved in Huntington's disease in a pair wise manner, revealed nearly 2000 protein-protein interactions (http://www.molgen.mpg.de/~agwanker/). In plants the yeast two-hybrid system has been used to study a number of different protein groups for interactions with other proteins including phytochromes, cryptochromes and auxin regulated transcription factors (Quail, 2000; Jarillo *et al.,* 2001; Ouellet *et al.,* 2001; Immink *et al.,* 2002). One of the three *Arabidopsis* genes that are the focus of gene silencing assays in the following chapter has been analysed using the two-hybrid system. The *Arabidopsis* callose synthase cDNA, *AtGSL6*, was shown to interact with phragmoplastin and a UDP-glucose transferase (*UGT-1*) when expressed in yeast (Hong *et al.,* 2001a). Furthermore, UGT1 was shown to interact with Rop1, a Rho-like protein in another yeast two-hybrid screen conducted by Hong *et al.* (2001b).

Here, two fragments of the barley *HvGSL1* gene are used to investigate potential protein-protein interactions between callose synthase and other proteins, through yeast two-hybrid screening of an *Arabidopsis* whole plant cDNA library, a barley inflorescence cDNA library and a developing wheat endosperm cDNA library.

4.2 MATERIALS AND METHODS

4.2.1 Materials

A modified pAS2-1 shuttle vector was obtained from Dr. Joachim Uhrig and Dr. Tim Soellick (Max Planck Institute for Plant Breeding Research, Cologne, Germany). A wheat early developing endosperm cDNA library in pGADT7-Rec, a Gal4 activation domain (AD) vector, was generously donated by Dr. Sergei Lopato (Department of Plant Science, University of Adelaide, Australia).

The *Saccharomyces cerevisiae* yeast strains AH109 [MATa, trp1-901, leu2-3, 112, ura3-52, his3-200, gal4Δ, gal80Δ, LYS2::GAL1$_{UAS}$-GAL1$_{TATA}$-HIS3, GAL2$_{UAS}$-GAL2$_{TATA}$-ADE2, URA3::MEL1$_{UAS}$-MEL1$_{TATA}$-lacZ] and Y187 [MATα, ura3-52, his3-200, ade2-101, trp1-901, leu2-3, 112, gal4Δ, met–, gal80Δ, URA3::GAL1$_{UAS}$-GAL1$_{TATA}$-lacZ], Herring testes DNA, pGBKT7, pGADT7-Rec, X-α-Gal and synthetic drop out media (-2 {-leu, -trp} and –4 {-ade, -his, -leu, -trp}) were from Clontech (Palo Alto, CA, USA). Custom oligonucleotides were from Invitrogen Corporation (Carlsbad, CA, USA) or Geneworks (Adelaide, SA, Australia). Agar, yeast extract and peptone were from Becton-Dickinson (Sparks, MD, USA). Trizma base, EDTA, kanamycin, yeast nitrogen base, glucose, LiAc, PEG 3500, DMSO, adenine hemi-sulphate, NaCl, glass beads (212-300 μM) and SDS were from Sigma-Aldrich (St. Louis, MD, USA). Restriction enzymes were from New England Biolabs (Beverly, MA, USA). NucleoSpin Extract kit was from Macherey-Nagel (Düren, Germany). Plasmid pGEM T-Easy was from Promega (Madison, WI, USA).

4.2.2 Generation of HvGSL1 *bait constructs by recombination*

The two *HvGSL1* PCR fragments recombined into the pDONR201 cloning vector described in Chapter 3 were passed on to Dr. Joachim Uhrig and Dr. Tim Soellick at the Max Planck Institute for Plant Breeding Research, Cologne, who undertook screening for protein-protein interactions against this group's existing cDNA libraries using their established protocols (Soellick *et al.*, 2000). Briefly, the pAS2-1 vector was modified by the addition of "Gateway" recombination signal sequences and the *HvGSL1* fragments were recombined into the modified pAS2-1 vector as described in

section 3.2.8. The recombination reactions created two *HvGSL1:Gal4* binding-domain (BD) fusion constructs or bait constructs, designated pAJ3 (nucleotide position 58-1110 bp in *HvGSL1, region A*; *Figure 4.2*) and pAJ4 (nucleotide position 2253-4396 bp in *HvGSL1, region B*; *Figure 4.2*). The two bait constructs were used to transform DH5α electrocompetent *E. coli* as described in section 2.2.14, except that 50 $\mu g.ml^{-1}$ kanamycin replaced the ampicillin, and DNA was extracted from clones as described in section 2.2.15. DNA sequencing of the expression constructs was conducted using ENT5 and ENT3 primers (*Appendix B*) as described in section 2.2.16 to check that inserts were in the correct frame for expression. The resultant bait constructs were used to transform the yeast strain Y187 and were screened against a barley flower cDNA library and an *Arabidopsis* whole plant cDNA library both of which were ligated to Gal4 activation domain vectors. Transformation and screening protocols for these constructs were essentially conducted as described below.

4.2.3 Yeast transformation

Saccharomyces cerevisiae strains Y187 and AH109 were streaked from frozen glycerol stocks onto SD 0.6% (w/v) agar plates (0.6% w/v yeast nitrogen base, 2% w/v glucose, 0.083% w/v drop out media {supplied}, pH 5.6) and were incubated at 30°C for 3-5 days. Isolated colonies (2-3) were used to inoculate 1 ml SD media (0.6% w/v yeast nitrogen base, 2% w/v glucose, 0.083% w/v drop out media {supplied}, pH 5.6) and clumps were dispersed by vortexing. The yeast mixture was transferred to 50 ml SD media in a flask and incubated at 30°C for 16 h with shaking or until an A_{600} greater than 1.5 was reached. Overnight culture (50 ml) was transferred into 300 ml SD media and incubated at 30°C for 3 h with shaking. Cells were pelleted by centrifugation at 1000 g for 5 min at room temperature. Supernatant was discarded and cells were resuspended in 50 ml 10 mM Tris-HCl buffer, pH 8.0, containing 1 mM EDTA. Cells were pelleted by centrifugation at 1000 g for 5 min at room temperature. Cells were resuspended in 1.5 ml of 10 mM Tris-HCl buffer, pH 8.0, containing 1 mM EDTA and 100 mM LiAc, and 100 µl was added to HvGSL1:Gal4 binding domain (BD) bait constructs (1-2 µg) along with 0.1 mg Herring testes carrier DNA in a final volume of 0.6 ml. The mixture was vortexed vigorously. Sterile 100 mM LiAc containing 66% (w/v) PEG 3500 (0.6 ml) was

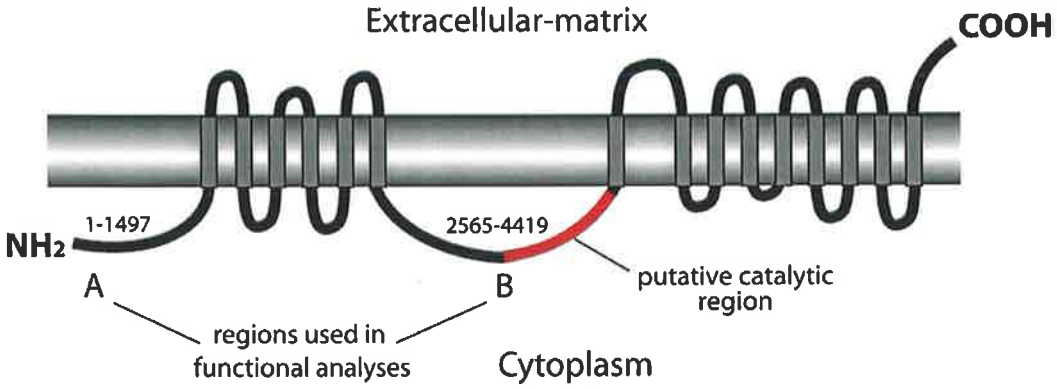

Figure 4.2 Topological profile of the barley HvGSL1 protein. Predicted cytoplasmic regions designated **A** and **B** were expressed in yeast for analysis of possible protein-protein interactions. Nucleotide positions of the major cytoplasmic regions are indicated. The putative catalytic region is indicated in red. The topology prediction was made using TopPredII software.

added and the mixture was again vortexed vigorously. Cells were incubated at 30°C for 30 min with gentle shaking and 70 µl of DMSO was added. Cells were mixed gently by swirling and were placed at 42°C for 15 min with occasional swirling. The mixture was chilled on ice for 1-2 min and transformed cells were collected by centrifugation at 1000 g for 5 min. Cells were resuspended in 0.5 ml 10 mM Tris-HCl buffer, pH 8.0, containing 1 mM EDTA and were plated onto SD 0.6% (w/v) agar plates with appropriate selection.

4.2.4 *PCR amplification of* HvGSL1 *cDNA fragments incorporating restriction enzyme sites*

Four PCR primer sets were used to amplify predicted cytoplasmic regions of the HvGSL1 protein and to incorporate unique restriction enzyme sites for cloning into the pGBKT7 Gal4 binding-domain (BD) vector (*Figure 4.3*). The primers, hvgsl1 and hvgsl1R (*Appendix B*), were used to amplify a cDNA fragment corresponding to amino acid residues 20-370 in the HvGSL1 protein (*Region A*; *Figure 4.2*) and incorporated an *Nco*I site at the 5′ end and an *Xma*I site at the 3′ end. The primers, hvgsl2 and hvgsl2R (*Appendix B*), were used to amplify a cDNA fragment corresponding to amino acid residues 751-1465 in HvGSL1 (*Region B*; *Figure 4.2*) and incorporated an *Nde*I site at the 5′ end and a *Bam*HI site at the 3′ end. Similarly, hvgsl3 and hvgsl2R (*Appendix B*) were used to amplify a cDNA fragment corresponding to amino acid residues 992-1465 in HvGSL1 (*Region B*; *Figure 4.2*) and incorporated an *Nde*I site at the 5′ end and a *Bam*HI site at the 3′ end. Finally, hvgsl2 and hvgsl3R (*Appendix B*) were used to amplify a cDNA fragment corresponding to amino acid residues 751-1108 in HvGSL1 (*Region B*; *Figure 4.2*) and incorporated an *Nde*I site at the 5′ end and a *Bam*HI site at the 3′ end.

Plasmids containing *HvGSL1* cDNA fragments described in Chapter 3 were used as templates and PCR was conducted using Elongase reagents as previously described in section 2.2.12, except that the Mg^{2+} concentration was reduced from 1.6 mM to 1.5 mM and reactions were conducted in a total volume of 25 µl. Cycling parameters were adjusted according to the length of expected products and the T_m of the primers used, but typically conditions were; 94°C for 30 sec followed by 35 cycles of 94°C for 30 sec, an annealing temperature of 50°C for 30 sec and an extension time of 1 min at

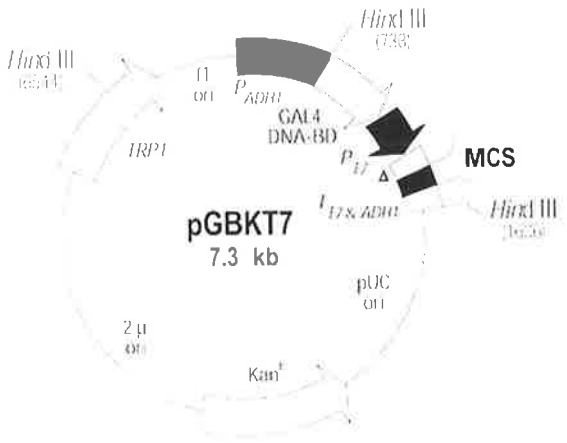

Figure 4.3 Gal4 binding domain (BD) plasmid, pGBKT7. The pGBKT7 plasmid expresses proteins fused to amino acids 1–147 of the GAL4 DNA binding domain (BD). In yeast, fusion proteins are expressed at high levels from the constitutive ADH1 promoter (P_{ADH1}); transcription is terminated by the T7 and ADH1 transcription termination signals ($T_{T7\ \&\ ADH1}$). Plasmid pGBKT7 also contains the T7 promoter, a c-Myc epitope tag, and a multiple cloning site (MCS). Plasmid pGBKT7 replicates autonomously in both *E. coli* and *S. cerevisiae* from the pUC and 2 μ ori, respectively. The plasmid carries the Kan^r for selection in *E. coli* and the TRP1 nutritional marker for selection in yeast. The barley *HvGSL1* cDNA fragments were ligated into the multiple cloning site of the plasmid.

72°C. PCR products were isolated by 1.2% (w/v) agarose gel electrophoresis, gel excision and purification using a NucleoSpin Extract kit. Purified PCR products were initially ligated into pGEM T-Easy as described in section 2.2.13 and inserts were sequenced as described in section 2.2.16 using SP6 and T7 sequencing primers (*Appendix B*).

4.2.5 Generation of HvGSL1 *bait constructs by ligation*

The four *HvGSL1* PCR fragments were individually excised from the pGEM T-Easy cloning vector using the restriction enzyme sites engineered into the primers as described in section 3.2.2. Restriction fragments were isolated by 1.2% (w/v) agarose gel electrophoresis, gel excision and purification using a NucleoSpin Extract kit, and ligated into the corresponding sites of the pGBKT7 vector as described in section 2.2.13. These four ligations created HvGSL1:Gal4 binding-domain (BD) fusion constructs or the bait constructs, pAJ11 (amino acid residues 20-335), pAJ12 (amino acid residues 1000-1465), pAJ13 (amino acid residues 753-1117) and pAJ14 (amino acid residues 753-1465). The four bait constructs were used to transform electrocompetent *E. coli*, strain DH5α, as described in section 2.2.14, except that 25 $\mu g.ml^{-1}$ kanamycin replaced the 100 $\mu g.ml^{-1}$ ampicillin, and DNA was extracted from clones as described in section 2.2.15. DNA sequencing of the bait constructs was conducted as described in section 2.2.16 to check that inserts were in the correct frame for expression. The bait constructs along with the empty activation domain (AD) vector, pGADT7-Rec (*Figure 4.4*), were used to co-transform the yeast strain AH109 as described in section 4.2.3 so that any self-activation and non-specific protein binding properties could be identified.

4.2.6 Investigation of hybrid protein interactions

Self-activation and non-specific protein binding properties were tested by plating the yeast strain AH109 co-transformed with HvGSL1:Gal4 (BD) bait constructs and the empty pGADT7-Rec (AD) vector on selective SD 0.6% (w/v) agar plates (0.6 % w/v yeast nitrogen base, 2% w/v glucose, 0.083% w/v drop out media, pH 5.6), lacking tryptophan and leucine, and plates were incubated up side down for 3-5 days at 30°C. Individual colonies were streaked on SD 0.6% (w/v) agar plates containing X-α-Gal

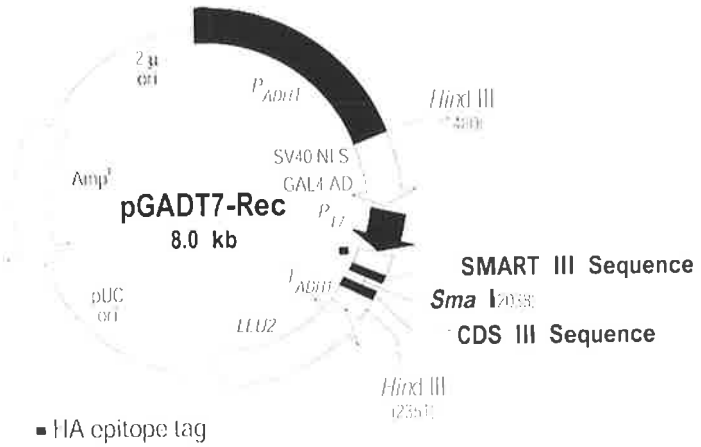

Figure 4.4 Gal4 activation domain (AD) plasmid, pGADT7-Rec. In yeast, pGADT7-Rec expresses a protein of interest as a GAL4 activation domain (AD) fusion. Transcription starts with the constitutive ADH1 promoter (P_{ADH1}) and ends with the ADH1 termination signal (T_{ADH1}). The GAL4 AD sequence includes the SV40 nuclear localization signal (SV40 NLS) so that fusions translocate to the yeast nucleus. GAL4 AD fusions also contain a hemagglutinin (HA) epitope tag. The T7 promoter in pGADT7-Rec is for *in vitro* transcription and translation of the hemagglutinin (HA)-tagged fusion protein. In its circular form, pGADT7-Rec replicates autonomously in both *E. coli* and *S. cerevisiae* from the pUC and 2 μ ori, respectively. The plasmid carries Amp^r for selection in *E. coli* and the LEU2 nutritional marker for selection in yeast. cDNA fragments were recombined into the linearised vector between the SMARTIII and CDSIII primer sequences.

(20 mg.L^{-1}) and lacking adenine, histidine, tryptophan and leucine for 18 h at 30°C. Bait constructs that were not self-activating, as determined by assaying for α-galactosidase activity, were subsequently screened against a wheat early endosperm cDNA library that was generously donated by Dr. Sergei Lopato (University of Adelaide, Department of Plant Science). The expression of the bait proteins could not be confirmed due to the lack of an appropriate antibody.

Bait constructs were used to transform the Y187 yeast strain as described in section 4.2.3 and cells were plated onto SD 0.6% (w/v) agar plates lacking tryptophan and were incubated for 3 days at 30°C. An individual colony was transferred to 50 ml SD liquid media lacking tryptophan and the cells were cultured for 16 h at 30°C with shaking. Cells were pelleted by centrifugation at 800 g for 5 min and were resuspended in 50 ml YPD media (1% w/v yeast extract, 2% w/v peptone, 2% w/v glucose) containing filter sterilised 0.01% (w/v) adenine hemi-sulphate and kanamycin (25 μg.ml^{-1}). The cells were transferred to a 50 ml culture vessel. A stored aliquot of wheat early endosperm cDNA library:Gal4 (AD) prey construct in strain AH109 (approx. 1x 10^7 cells) was thawed and added directly to the culture vessel. The strains were left to mate for 16 h at 30°C with very gentle swirling. Cells were pelleted by centrifugation at 800 g for 5 min and were washed twice in 0.5x YPD media containing filter sterilised 0.01% (w/v) adenine hemi-sulphate and kanamycin (25 μg.ml^{-1}). Cells were pelleted in between washes and after the second wash by centrifugation at 800 g for 5 min. Cells were resuspended in 7.5 ml of YPD media containing filter sterilised 0.01% (w/v) adenine hemi-sulphate and kanamycin (25 μg.ml^{-1}) by vortexing and 200 μl aliquots were plated onto 150 mm diameter SD 0.6% (w/v) agar plates lacking adenine, histidine, tryptophan and leucine and plates were sealed and incubated upside down for 5-10 days at 30°C. Isolated, large colonies were streaked onto SD 0.6% (w/v) agar plates containing X-α-Gal (20 mg. L^{-1}) and lacking adenine, histidine, tryptophan and leucine and plates were incubated for 1-2 days at 30°C to screen for putative protein-protein interactions. Blue colonies were transferred to 5 ml YPD media and were incubated for 16 h at 30°C with shaking. Background levels of α-galactosidase activity were assessed in controls co-transformed with the empty prey construct.

4.2.7 Yeast DNA extraction

Cells from overnight cultures (2 ml) were pelleted by centrifugation at 16,000 g for 15 sec and supernatant was discarded. Extraction buffer (200 µl), 50 mM Tris-HCl buffer containing 130 mM NaCl, 5 mM EDTA and 5% (w/v) SDS, pH 7.4, was added along with approx. 30 glass beads (212-300 µM) and 200 µl phenol/chloroform (1:1; v/v). The cells were resuspended by three 2 min mixes in a platform shaker set to 3,000 rpm and tubes were placed on ice. Cellular debris was pelleted by centrifugation at 16,000 g for 15 min at 4°C and supernatant was transferred to a clean eppendorf tube. Ethanol (1 ml) was added along with 100 µl 3 M sodium acetate, pH 5.0, and the samples were mixed by inversion and left at -20°C for 1 h. DNA was pelleted by centrifugation at 13,000 rpm in a desktop centrifuge for 15 min at 4°C and supernatant was discarded before the pellet was washed twice with 300 µl of 70% ethanol. DNA was dried under vacuum and resuspended in 20 µl sterile water.

4.2.8 PCR amplification of inserts from interacting prey constructs

Inserts from putative interacting prey constructs were amplified by PCR to ensure inserts were present and that duplicates were not further characterised. DNA (1 µl) extracted as described in section 4.2.7 was used as a template in PCR using the primers T7 and 2HRev (*Appendix B*) and the conditions described in section 2.2.10. Cycling conditions were 94°C for 30 sec followed by 35 cycles of 94°C for 30 sec, 50°C for 30 sec and 72°C for 2.5 min. Half of the total volume of the PCR products was separated by 1.2% (w/v) agarose gel electrophoresis. PCR products that appeared to be duplicates, as determined by the size of products in agarose gels, were digested with the restriction enzyme *Hae*III to identify duplicates, as described in section 3.2.2 and the restriction fragments were separated by 1.2% (w/v) agarose gel electrophoresis.

4.2.9 Co-transformation of bait and prey constructs to confirm interactions

DNA from a single interacting prey construct identified as described in section 4.2.8 was used to transform electrocompetent *E. coli*, strain DH5α, as described in section

2.2.14 and DNA was prepared as described in section 2.2.15. The yeast strain AH109 was co-transformed with bait and prey constructs to confirm the interactions, and with the empty pGBKT7 (BD) vector and prey constructs to check for false positives, as described in section 4.2.3. Transformed cells were plated on SD 0.6% (w/v) agar plates lacking tryptophan and leucine and were incubated at 30°C for 3 days. Individual colonies were streaked onto the same media and were incubated for 16 h at 30°C. Lifts were prepared from the streaks and were replica plated onto SD 0.6% (w/v) agar plates lacking tryptophan and leucine and onto SD 0.6% (w/v) agar plates containing X-α-Gal (20 $mg.L^{-1}$) and lacking adenine, histidine, tryptophan and leucine. The plates were incubated at 30°C for 1-2 days. Streaks that grew on the SD 0.6% (w/v) agar plates lacking adenine, histidine, tryptophan and leucine corresponding to bait and prey co-transformations that appeared blue, due to α-galactosidase activity, were identified as positive interactors only if the streaks co-transformed with the empty pGBKT7 (BD) vector and prey construct failed to grow on the same media.

4.2.10 Identification of cDNAs from interacting proteins

The cDNAs from interacting prey constructs were identified by DNA sequencing the pGADT7-Rec based cDNA:Gal4 (AD) prey constructs with T7 and 2HRev primers as described in section 2.2.16. DNA sequences were analysed and identified as described in section 2.2.21.

4.3 RESULTS AND DISCUSSION

4.3.1 Generation and screening of HvGSL1 *bait constructs in barley and* Arabidopsis

Some of the early problems associated with false positives and false negatives in the yeast two-hybrid system (Fashena *et al.,* 2000) have been overcome by the use of vectors and yeast strains that allow for stringent selection of interactions by simultaneous and coordinated activation of several growth and activity reporter genes. However, there are a number of factors to be considered when using the yeast two-hybrid system. Firstly, in some instances hybrid proteins may not be stably expressed in yeast or located at the yeast nucleus where these protein-protein interactions are detected. Secondly, the DNA-BD or AD fusion moiety may occlude the normal site of interaction, or may impair the proper folding of the hybrid protein, and thus interfere with the ability of the two hybrid proteins to interact. Thirdly, conditions in yeast cells may not allow the proper folding or post-translational modifications (such as glycosylation) required for interaction of some plant proteins. Finally, it is possible that the expressed polypeptides are in some way toxic to the cell in which they are translated. Conversely, the detection of a specific interaction between plant proteins in a yeast system does not necessarily indicate that there is a corresponding interaction in the proteins' native environment, a point noted in work on expressed mammalian proteins (Fields and Sternglanz, 1994).

With these factors in mind the two barley *HvGSL1* cDNA fragments corresponding to the larger predicted cytoplasmic regions of the HvGSL1 protein (A & B, *Figure 4.2*) were recombined from the pDONR201 cloning vector, described in Chapter 3, into a modified pAS2-1 shuttle vector with high efficiency. Recombination created two HvGSL1:Gal4 binding domain (BD) fusions or baits, designated pAJ3 and pAJ4, that correspond to the NH_2-terminal cytoplasmic region and the larger more centrally located cytoplasmic region of the HvGSL1 protein, respectively. The bait constructs were initially used to transform *E. coli* and plasmid recombinations were confirmed by DNA sequencing. The yield and quality of DNA extracted from yeast was often lower than that from bacteria, and the extraction protocols and culture of yeast is more time consuming and complicated, so *E. coli* was used as a tool for DNA plasmid manipulations prior to their use in yeast.

Dr. Tim Soellick and Dr. Joachim Uhrig at the Max Planck Institute for Plant Breeding Research, Cologne, Germany conducted the library screening work, including testing for self-activation for the pAJ3 and pAJ4 constructs. Tests for non-specific DNA binding and transcriptional activation were negative so the bait constructs were screened against two existing cDNA libraries from which protein interactions had been previously identified and protein expression had been verified by Western analysis. The cDNA libraries screened by Dr. Tim Soellick and Dr. Joachim Uhlrig were from barley inflorescences and *Arabidopsis* whole plants.

No protein interactions were detected when screening the pAJ3 or pAJ4 bait constructs against yeast expressing the cDNA library generated from barley inflorescences nor were any interactions evident when the pAJ4 bait was screened against yeast expressing the cDNA library from *Arabidopsis*. Histidine autotrophy and β-galactosidase activity were detected in five instances when the pAJ3 bait construct was screened against the *Arabidopsis* library. PCR was performed on the interacting clones identified in the screen to determine the number of unique clones based on the size of their inserts. Two unique clones were identified during this process (*Figure 4.5*) and the inserts of these plasmids were sequenced and compared to DNA sequence databases, which identified one clone as a ribosomal protein and the other clone as a tryptophan synthase α-subunit-like protein. The cDNA insert from the interacting prey construct had 97% identity over 850 bases to the *Arabidopsis* tryptophan synthase α-subunit-like protein and therefore was unlikely to represent an error in sequencing or gene identification. Ribosomal proteins are common false positives in yeast two-hybrid screens (Dr. Joachim Uhrig; personal communication) and are unlikely to represent a true protein interaction attributable to the barley HvGSL1 sequence. The identification of an interaction between the barley HvGSL1 NH_2-terminus and an *Arabidopsis* tryptophan synthase α-subunit-like protein (Accession number U18993) was unexpected and has not been reported previously. Callose synthase has not been implicated in amino acid biosynthesis in plants and it is hard to imagine that the production of callose and amino acids are linked, it seems likely therefore that this result represents a false positive interaction. However, in plants, the tryptophan synthase α-subunit catalyses the conversion of indole-3-glycerol phosphate to indole and glyceraldehyde-3-phosphate whilst the β-subunit

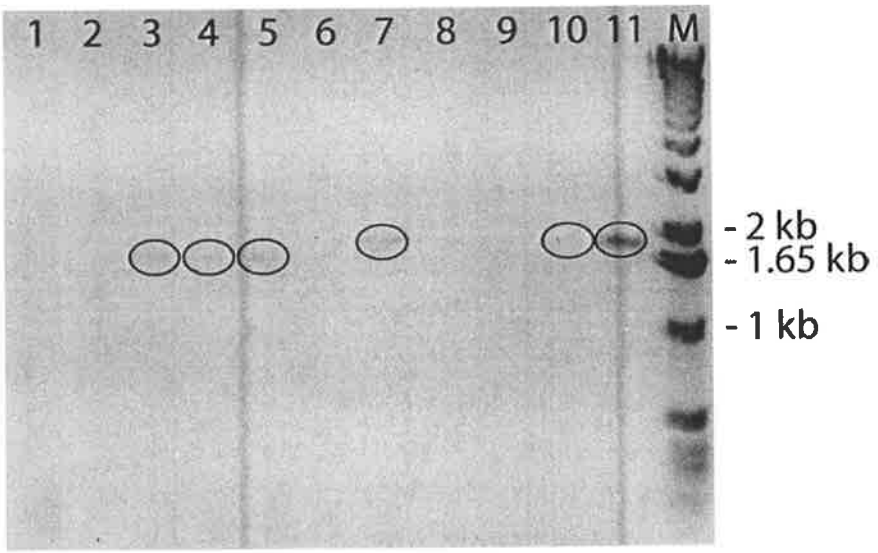

Figure 4.5 Agarose gel analysis of PCR amplified inserts from prey constructs of *Arabidopsis* whole plant cDNA library that interacted with the pAJ3 bait construct. Lanes **3**, **4** and **5** contain an approx. faint 1.8 kb product, indicated by ellipse, identified as a ribosomal protein. Lanes **7**, **10** and **11** contain an approx faint 1.9 kb product, indicated by ellipse, identified as a tryptophan synthase α-subunit-like protein. **M** DNA molecular size marker. Image courtesy of Dr. Tim Soellick.

catalyses the conversion of indole and L-serine to L-tryptophan and water (Radwanski *et al.*, 1996). Indole is a precursor of the auxin, indoleacetic acid (IAA), which is a plant growth regulator (Meir *et al.*, 1984) and IAA treatment induces the deposition of callose at the cell plate (Kapoor and Bhatla, 1998), probably as a result of an increase cell divisions as part of the growth response. It may be that there is an interaction or signalling between IAA, tryptophan synthase and (1→3)-β-D-glucan synthase. Further experimentation will be required to explain this finding. Domain swapping experiments would also be useful for the validation of this result.

4.3.2 Generation and screening of HvGSL1 *bait constructs in wheat*

Having screened a barley inflorescence library and conducted a heterologous screen against an *Arabidopsis* whole plant library with limited success, the possibility that the HvGSL1 protein was involved in early endosperm development (Stone and Clarke, 1992) was investigated by screening a cDNA library generated from early developing endosperm from grains of wheat. In barley, mRNA of the *HvGSL1* gene is detected in early developing grains at relatively high levels in comparison with most other barley tissues (Ms. Jing Li, personal communication).

Four *HvGSL1* cDNA fragments corresponding to the two largest predicted cytoplasmic regions were again amplified by PCR. The NH_2-terminal cytoplasmic region was amplified as a single, approx. 950 bp fragment. The larger more centrally located cytoplasmic domain was amplified as an approx. 2.1 kb fragment and also as two smaller overlapping fragments of approx. 1 kb and approx. 1.4 kb. The overlapping fragments were produced to address concerns over the possibility of errors occurring during the translation of the larger 2.1 kb fragment (Dr. Sergei Lopato, personal communication).

Bands of the expected size were generated by PCR using the four primer sets targeted to the *HvGSL1* cDNA sequence (*Figure 4.6*). The four indicated cDNA fragments were successfully ligated into the pGEM T-Easy vector. Inserts were sequenced and corresponded to the expected *HvGSL1* cDNA sequences, with the engineered restriction enzyme sites. The *HvGSL1* cDNA fragments were excised from pGEM T-Easy by cutting at the primer encoded restriction enzyme sites (*Figure 4.7*) and the

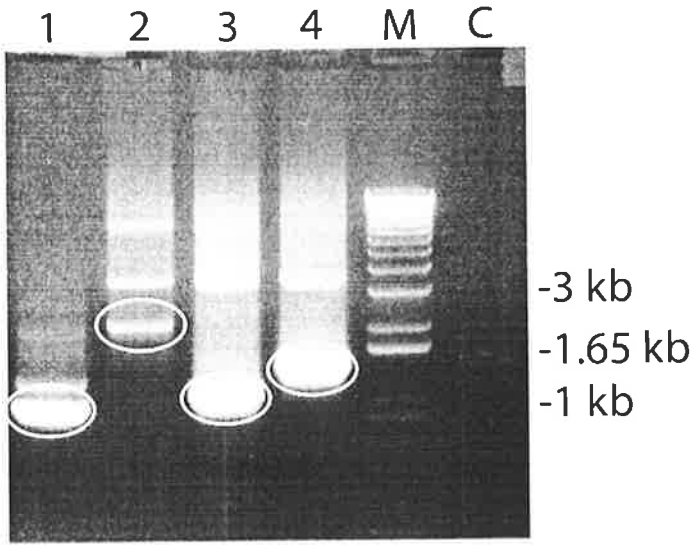

Figure 4.6 Agarose gel analysis of PCR amplified *HvGSL1* cDNA fragments. Lane **1** contains a 985 bp *HvGSL1* fragment amplified using the primers, hvgsl1 and hvgsl1R. Lane **2** contains a 2142 bp *HvGSL1* fragment amplified using the primers, hvgsl2 and hvgsl2R. Lane **3** contains a 1071 bp *HvGSL1* fragment amplified using the primers, hvgsl3 and hvgsl2R. Lane **4** contains a 1420 bp *HvGSL1* fragment amplified using the primers, hvgsl2 and hvgsl3R. **M** molecular size markers. **C** no template PCR control.

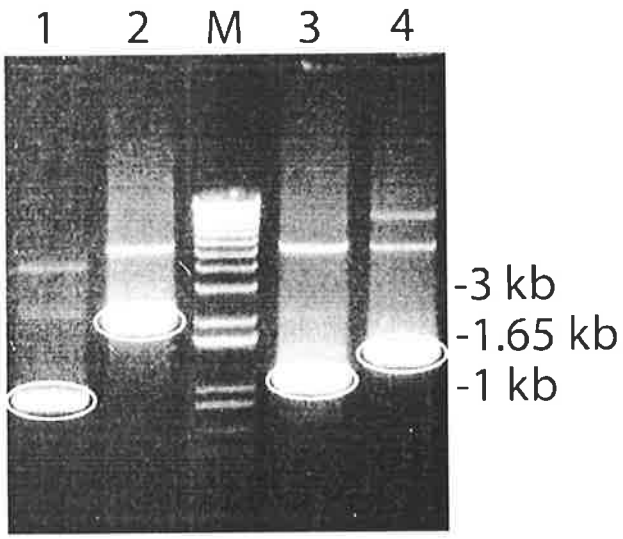

Figure 4.7 Agarose gel analysis of *HvGSL1* restriction fragments used to construct bait vectors. Lane **1** 985 bp *HvGSL1* fragment ligated into pGBKT7 to create pAJ11. Lane **2** 2142 bp *HvGSL1* fragment ligated into pGBKT7 to create pAJ14. **M** molecular size markers. Lane **3** 1071 bp *HvGSL1* fragment ligated into pGBKT7 to create pAJ13. Lane **4** 1420 bp *HvGSL1* fragment ligated into pGBKT7 to create pAJ12. Bands used in the ligations are circled.

purified fragments were ligated into the corresponding sites of the pGBKT7 (BD) vector. The integrity of the bait vectors was confirmed by sequencing the inserts.

Three of the bait constructs, namely pAJ12, pAJ13 and pAJ14, failed to identify any protein-protein interactions from the wheat early developing endosperm cDNA library following three rounds of selection. All three of these bait constructs express polypeptides from the larger more centrally located cytoplasmic region of HvGSL1 that has been proposed as the catalytic site of the barley (1→3)-β-D-glucan synthase (Li *et al.*, 2003). If this region of the HvGSL1 protein is indeed involved in the catalysis of (1→3)-β-D-glucan in barley then one might expect that other proteins would be unlikely to interact with this region. The results of the yeast two-hybrid screens with these three bait constructs would support this hypothesis.

The pAJ11 bait construct expresses a polypeptide from the NH_2-terminal cytoplasmic region of the HvGSL1 protein and this region was previously found to interact with an *Arabidopsis* tryptophan synthase α-subunit-like protein, as discussed in the previous section. The pAJ11 bait construct was initially found to interact at the protein level in 19 instances with proteins from the wheat early developing endosperm cDNA library. Only five of 19 interacting clones were found to contain unique inserts, based on the size of PCR amplified inserts, (*Figure 4.8*) and these five clones along with the pAJ11 bait construct were used to co-transform the AH109 yeast strain to check for false positive interactions. Three of the five clones were found to be false positives due to their capacity for tryptophan autotrophy in the presence of the empty pGBKT7 (BD) vector (*Figure 4.9*). The other two clones appeared to represent true protein-protein interactions because no tryptophan autotrophy or α-galactosidase activity in the presence of the empty pGBKT7 (BD) vector were observed. The clones were analysed by restriction digestion of the inserts (*Figure 4.10*) before the two pGADT7-Rec (AD) prey constructs, each expressing a unique cDNA from the wheat early developing endosperm library, were sequenced. The sequence of clone 7 shared weak identity (41%) with an *Arabidopsis* putative protein (Accession number AL391222) whilst the sequence of clone 17 shared 87% identity with an unknown rice protein (Accession number AL607005).

The identification of the interaction between the NH_2-terminal cytoplasmic domain of the HvGSL1 polypeptides and the wheat cDNA that shares sequence identity with the unknown rice protein was an interesting but frustrating finding in the sense that little can be inferred from the interaction without knowledge or clues as to the function of the interacting partner.

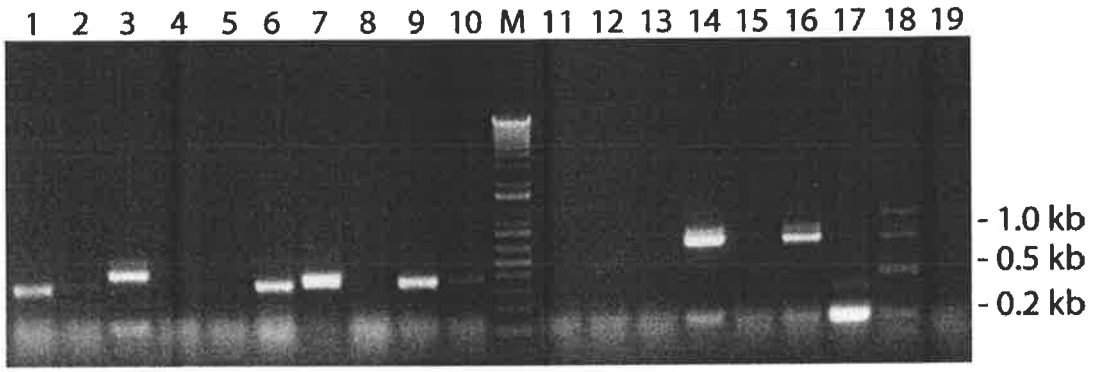

Figure 4.8 Agarose gel analysis of PCR amplified inserts from prey constructs of wheat early developing endosperm cDNA library that interacted with the pAJ11 bait construct. Clones corresponding to PCR products from lanes **3, 7, 9, 14** and **17** were chosen as representatives of unique products and were characterised further. **M** molecular size markers.

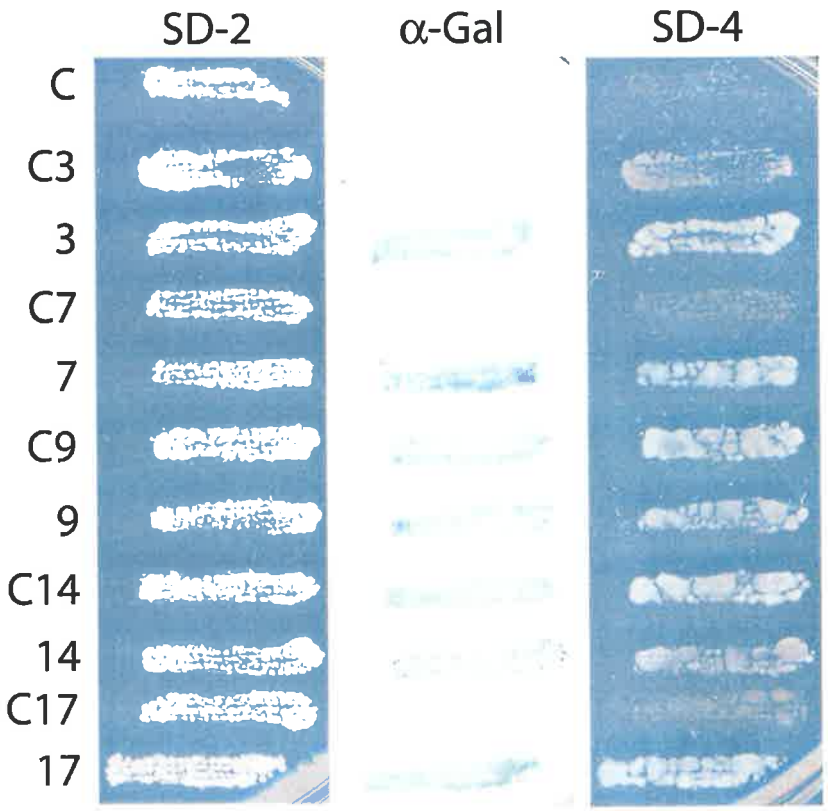

Figure 4.9 Replica plated yeast colonies from the wheat early developing endosperm cDNA library that interacted with the pAJ11 bait construct. Yeast strain AH109 was co-transformed with pAJ11 and the various prey constructs or as a control (C) with empty pGBKT7 BD vector and the various prey constructs. Colonies were plated onto **SD-2**, media lacking tryptophan and leucine, onto **SD-4** media lacking adenine, histidine, tryptophan and leucine and onto nitrocellulose on SD-4 media containing X-**α-Gal** to assay for α-galactosidase activity. Two of the clones, **7** and **17**, showed a positive interaction because they were capable of adenine, histidine, tryptophan and leucine autotrophy and α-galactosidase activity in the presence of the pAJ11 bait construct but not in the presence of the empty pGBKT7 BD vector. The other clones were identified as false positives due to α-galactosidase activity and tryptophan autotrophy in the absence of an insert in the pGBKT7 vector.

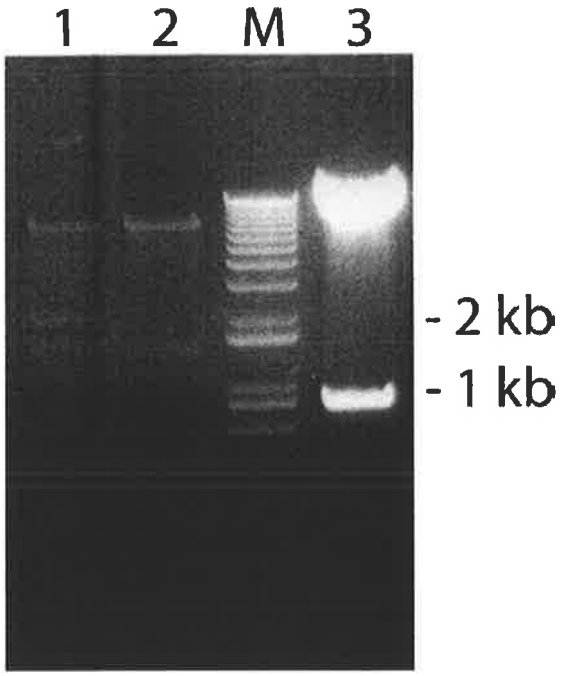

Figure 4.10 Agarose gel analysis of restriction fragments from prey construct that interacted with the pAJ11 bait construct. DNA was extracted from yeast cultures and insert integrity and size of the prey constructs were checked by restriction analysis prior to DNA sequencing. Lane **1** contains restriction fragments corresponding to insert and plasmid from clone 7. Lane **2** contains restriction fragments corresponding to insert and plasmid from clone 17. **M** molecular size markers. Lane **3** contains linearised empty pGADT7-Rec AD plasmid.

4.4 SUMMARY AND CONCLUSIONS

The NH_2-terminal region of the HvGSL1 protein was found to interact with an *Arabidopsis* tryptophan synthase α-subunit-like protein in a heterologous yeast two-hybrid screen and with an unknown protein from a wheat early developing endosperm cDNA library. This indicates that this region of the protein is probably involved in protein interactions. A putative calmodulin-binding domain was identified in the HvGSL1 protein (unpublished data) and is present in the pAJ11 bait construct but no HvGSL1-calmodulin interactions were detected in any of the screens conducted.

Similarly, interactions with Rho-like GTPases, phragmoplastin or UGT that have been identified previously (Mol *et al.*, 1994; Hong *et al.*, 2001a, 2001b) were not found for the HvGSL1 polypeptides used in this study. Nor was there any interaction between HvGSL1 and other proteins that have been found to co-locate with (1→3)-β-D-glucan synthesis, such as sucrose synthase (Amor *et al.*, 1995) or annexins (Andrawis *et al.*, 1993). These findings can be interpreted in several ways. Firstly, it may be that the domains selected for the construction of the bait vectors in this study are not specifically involved in these anticipated protein-protein interactions. Secondly, only a small portion of the entire HvGSL1 protein has been expressed in the bait constructs and it may be that other domains are required for the correct folding of the HvGSL1 protein or that the other domains are crucial in positioning or supporting an interacting protein. However, the general lack of proteins interacting with the central cytoplasmic region of HvGSL1 might also be taken as evidence that other proteins are not required for callose synthase activity.

Bait constructs that interact with proteins encoded by unknown cDNAs in the yeast two-hybrid system represent a major limitation with the type of investigative screen described here. However, many of the proteins that were anticipated to be involved in callose synthesis have been previously identified in yeast and many homologues have been found in plants. This would have enabled their identification using homology-based searches. Further investigation of protein interactions with HvGSL1 polypeptides from regions other than those selected in this study are likely to uncover some of the possible interactions described above.

The gain of function experiments involving heterologous expression systems, described in Chapter 3, did not provide any evidence that the barley *HvGSL1* gene was involved in the production of callose and the data presented in this chapter involving regions of the HvGSL1 protein did not highlight any interactions with proteins that have been previously linked with callose synthesis. In the following chapter the function of the barley *GSL1* gene is further investigated, this time in loss-of-function experiments utilising transient gene silencing assays in single cells of the barley leaf.

CHAPTER 5

TRANSIENT GENE SILENCING OF (1→3)-β-D-GLUCAN SYNTHASES IN BARLEY AND *ARABIDOPSIS THALIANA*

5.1 INTRODUCTION

Callose is deposited between the plasma membrane and the cell wall following exposure of plants to a range of abiotic and biotic stresses, including wounding, desiccation, metal toxicity and microbial attack (Stone and Clarke, 1992). Particular attention has been focused on callose formation in plant-microbe interactions, during which plant host cells respond to microbial attack by rapidly synthesising and depositing callose as plugs, drops or plates in close proximity to the invading pathogen (Ryals *et al.*, 1996; Donofrio and Delaney, 2001). These callosic deposits are commonly referred to as papillae and may contain, in addition to (1→3)-β-D-glucan, minor amounts of other polysaccharides, proteins or phenolic compounds (Smart *et al.*, 1986a, 1986b; Bolwell, 1993). While the precise function of callosic papillae during microbial attack has not been demonstrated unequivocally, it is generally believed that the papillae act as a physical barrier to impede microbial penetration (Cahill and Weste, 1983; Stone and Clarke, 1992). By slowing or immobilizing the invading microorganisms, the host plant could focus upon them a number of anti-microbial compounds, such as wall-degrading enzymes, phytoalexins and active oxygen species, or initiate cascade responses involving specific resistance genes (Brown *et al.*, 1998).

In this chapter, experiments aimed at analysing functions of putative callose synthase genes through transient gene silencing in barley and *Arabidopsis* are described. Biolistic transient expression, where micro particles of gold are coated with DNA and projected at high speed into single cells, is a convenient and relatively straightforward way to study the effects a gene may have *in vivo*. This technique can be used to express a novel protein in a cell or to silence an endogenous gene by inducing the mechanisms of post-transcriptional gene silencing. Biolistic transient expression has been used in barley to complement *mlo* mutants (Shirasu *et al.*, 1999), to interfere with co-bombarded GUS and GFP constructs and to silence the dihydroflavanol-4-reductase gene, *Ant18* (Schweizer *et al.*, 2000), to complement a *rar1* mutant (Zhou *et al.*, 2001) and to silence the *MLO* and *Gα* genes of barley (Kim *et al.*, 2002). The technique of transient gene silencing by bombardment has become routine in barley

and is applicable to other species, provided the appropriate promoter and other transcriptional elements are used in silencing vectors.

Twelve *GSL* genes have been identified in *Arabidopsis thaliana* (Richmond and Somerville, 2000; Verma and Hong, 2001; http://cellwall.stanford.edu/), where individual members of the family presumably mediate the synthesis of callose in different tissues or under different environmental conditions. One or more of these genes are probably involved in the formation of papillae in *Arabidopsis*. Access to DNA sequence for these 12 genes facilitates the design of gene-specific primers, which might enable the mRNA levels of the 12 genes to be examined in leaves before and after powdery mildew infection. *GSL* genes that are upregulated in response to fungal challenge might then be targeted for silencing by engineering double stranded RNA interference (dsRNAi) vectors (Wesley *et al.,* 2001) that encode gene-specific inverted repeats.

Less DNA sequence information is available for barley, but currently one can discriminate at least six or seven independent EST sequences in the public databases. It is apparent that within all plant *GSL* genes some regions of sequence are conserved and other regions are quite divergent (*Figures 5.6 and 5.7*). By targeting the sequence from a conserved region of the barley *HvGSL1* gene for the construction of a gene-silencing vector one might be able to interfere with the expression of multiple barley *GSL* genes. The individual *HvGSL1* gene alone could be targeted by incorporating the sequence from a divergent region of the gene into a second construct.

If the barley *HvGSL1* gene or selected *Arabidopsis GSL* genes are involved in the formation of papillae that result from fungal challenge, silencing the genes through transient gene silencing might abolish the formation of papillae and this could be detected by histochemical staining for callose. This loss-of-function would link the *GSL* gene to papillae formation by reference to the phenotype produced. Plasmids encoding double stranded RNA (dsRNAi) molecules with homology to *GSL* genes could be introduced using the biolistic approach (Shirasu *et al.*, 1999), which would result in the degradation of endogenous *GSL* mRNA by induction of sequence-specific degradation (Baulcombe, 1996).

The data presented in this chapter detail investigations into the possibility that the barley *HvGSL* genes and the *Arabidopsis AtGSL* genes are involved in the formation of callose that is easily detected in leaves at the sites of attempted fungal penetration (Stone *et al.,* 1985). This hypothesis was investigated by use of single cell transient gene-silencing assays in barley and *Arabidopsis* (Shirasu *et al.,* 1999). I conducted the work in Prof. Paul Schulze-Lefert's laboratory in the Department of Plant Microbe Interactions at the Max-Planck-Institute for Plant Breeding Research, Cologne, Germany.

5.2 MATERIALS AND METHODS

5.2.1 Materials

Plasmids pUbi-Nos and pUbi-GUS-Nos were kindly donated by Dr. Ralph Panstruga (Max-Planck-Institute for Plant Breeding Research, Cologne, Germany). Plasmid pamPAT-35SxGUS was donated by Dr. Judith Mueller (Max-Planck-Institute for Plant Breeding Research, Cologne, Germany). Plasmid pJawohl3 was generously donated by Dr. Bekir Uelker (Max-Planck-Institute for Plant Breeding Research, Cologne, Germany). Plasmids containing fragments of the barley *HvGSL1* gene were kindly provided by Ms. Jing Li (Department of Plant Science, University of Adelaide, Australia).

Trizol reagent, EDTA, $K_4[Fe(CN)_6]$, $K_3[Fe(CN)_6]$, X-Glu, Triton X-100, MS media, ampicillin and benzimidazole was obtained from Sigma-Aldrich (Taufkirchen, Germany). NucleoSpin Extract kit was from Macherey-Nagel (Düren, Germany). Restriction enzymes, BSA, T_4 DNA ligase and 10x ligase buffer were supplied by New England Biolabs (Frankfurt, Germany). Coomassie brilliant blue R-250 was obtained from Serva Fine Biochemicals (Heidelberg, Germany). Aniline blue fluorochrome was from Biosupplies (Parkville, Australia). Expand DNA polymerase, 10x Expand buffer with $MgCl_2$ and spermidine were from Roche Diagnostics GmbH (Mannheim, Germany). Gold microcarriers (1µm) and macrocarrier rupture discs were from Bio-Rad (München, Germany). Custom oligonucleotides and Superscript II cDNA synthesis kit were from Invitrogen Corporation (Karlsruhe, Germany). *E. coli* strain DH5α was from Stratagene (Jolla, CA, USA). pGEM T-Easy was from Promega (Mannhein, Germany). Agar, tryptone, yeast extract and agarose were from Becton-Dickinson (Heidelberg, Germany).

5.2.2 Plant and fungal material

Hordeum vulgare cvs. Ingrid and Ingrid *mlo-3* used in transient knockout experiments were grown in growth chambers under 16 h light and 8 h darkness in soil at 18°C. Primary leaves from 6-8 d old seedlings were cut into 50 mm sections and incubated

on 80 mm Petri dishes containing fresh 1.5% (w/v) agar and 10% (w/v) sucrose media in a growth chamber for 4 h prior to bombardment.

Arabidopsis thaliana glA (glaborous) plants used in transient knockout experiments were grown under sterile conditions in a growth chamber cycling between 16 h light and 8 h darkness in glass culture vessels containing 0.5x MS media, pH 5.7, with 1% (w/v) agarose at 22°C. Each culture vessel contained seven *A. thaliana glA* plants evenly arranged in a hexagonal shape with a single plant at the centre. *A. thaliana* plants cultivated for RNA extraction were grown in growth rooms under 16 h light and 8 h darkness in soil at 22°C.

Blumeria graminis f. sp. *hordei* strain K1 was cultivated on *H. vulgare* cv. Ingrid at 22°C (16 h light, 8 h darkness). Spores from host plants 7-9 days post-inoculation were used to heavily inoculate plants and detached leaves via a 65 cm tall infection tower (Schweizer *et al.*, 2000). Heavily infected barley plants were shaken over the tower. After 5 min. inoculated plant material was returned to a growth room at 22°C (16 h light, 8 h darkness) for 48 h.

5.2.3 RNA extraction

RNA was extracted from various tissues with Trizol reagent using the protocol described in section 2.2.4.

5.2.4 First strand cDNA synthesis

cDNA was synthesised from total RNA as described in section 2.2.5

5.2.5 PCR amplification of GSL *cDNAs*

Plasmid DNA (approx. 0.5 µg) or cDNA (1-2 µg) was used as a template in 25 µl reaction volumes using a final concentration of 300 nM primers, 200 µM each dNTP, 0.1 U Expand DNA polymerase and 1x Expand buffer with 1.5 mM $MgCl_2$ (supplied). Reactions were conducted in a DNA Engine Tetrad thermal cycler (MJ Research, Reno, MV, USA) under the following conditions: 94°C for 30 sec followed

by 35 cycles of 94°C for 30 sec, an annealing temperature of 50-65°C for 30 sec (dependent upon primer T_m) and an extension time of 15-60 sec at 72°C (dependent upon length of expected product). PCR products were routinely isolated by 1.2% (w/v) agarose gel electrophoresis, gel excision and purification using a NucleoSpin Extract kit.

5.2.6 Cloning of cDNAs and restriction fragments

Plasmid DNA and PCR fragments or restriction fragments were ligated together as described in section 2.2.13. *E. coli* cells were transformed with plasmid constructs as described in section 2.2.14 and DNA was extracted from overnight cultures of selected clones as described in section 2.2.15.

5.2.7 Restriction enzyme digestion of PCR amplified cDNAs and plasmid DNA

Purified PCR products and plasmid DNAs were restriction digested as described in section 3.2.2.

5.2.8 DNA sequencing and sequence analysis

DNA sequences were determined as described in section 3.2.7.

5.2.9 Construction of pUbi-Mla13I-Nos; A dsRNAi vector for transient gene silencing in **Hordeum vulgare**

A barley dsRNAi vector was constructed based on the backbone of an existing plasmid containing the barley ubiquitin promoter and nopaline synthase terminator, pUbi-Nos, that was kindly donated by Dr. Ralph Panstruga (Max-Planck-Institute for Plant Breeding Research). Two complementary oligonucleotides, pUbi-Nos MCSF and pUbi-Nos MCSR (*Appendix B*), were designed to incorporate a larger multiple cloning site into the *Hin*dIII/*Eco*RV cut pUbi-Nos vector. The oligonucleotides (1 µmol of each) were heated to 95°C for 2 min in a 10 µl volume and cooled slowly to room temperature. This synthetic dsDNA fragment was ligated into the *Hin*dIII/*Eco*RV cut pUbi-Nos vector to form pUbi-MCS-NOS. pUbi-MCS-NOS plasmid DNA was restriction mapped to check for the presence of the unique

restriction sites located in the newly added multiple cloning site. DNA sequencing was also conducted to confirm the new multiple cloning site (MCS) was in the correct orientation and location.

Two primers, mla1F and mla1R, (*Appendix B*) incorporating the same terminal restriction sites as those of the newly introduced MCS of pUbi-MCS-NOS as well as sequence homology to the barley *Mla1* third intron were synthesised. A plasmid containing the barley *Mla1* third intron, generously provided by Dr. Ralph Panstruga (Max-Planck-Institute for Plant Breeding Research), was used as a template in PCR. The purified PCR product was digested with *Pst*I/*Mlu*I and was ligated into the *Pst*I/*Mlu*I sites of the pUbi-MCS-NOS plasmid to generate pUbi-Mla13I-NOS. Plasmid DNA was submitted for sequencing to ensure vector integrity.

5.2.10 Construction HvGSL *dsRNAi silencing constructs*

Plasmid pAJ2 was constructed by introducing 148 bp of *HvGSL1* DNA sequence on either side of the *Mla1* third intron as an inverted repeat in the pUbi-Mla13I-NOS vector. The primer pair dsRNAi1 and dsRNAi1R (*Appendix B*) and the alternate primer combination of dsRNAi2 and dsRNAi2R (*Appendix B*) were used in PCR with DNA from a pBluescript plasmid containing 2560 bp of the *HvGSL1* cDNA (donated by Ms. Jing Li, University of Adelaide) as a template. The resultant PCR fragments were separately ligated into pGEM T-Easy. Ligations were confirmed by DNA sequencing and *HvGSL1* fragments were cut from the vector with *Pst*I/*Asc*I for the dsRNAi1-1R product and *Bam*HI/*Eco*RV for the dsRNAi2-2R product. These fragments were separately ligated into the corresponding sites of the digested pUbi-Mla13I-NOS vector. The *Pst*I/*Asc*I, dsRNAi1-1R product was ligated into pUbi-Mla13I-NOS in the antisense orientation and the *Bam*HI/*Eco*RV, dsRNAi2-2R product was ligated into pUbi-Mla13I-NOS in the sense orientation. The pUbi-Mla13I-NOS vectors containing *HvGSL1* fragments were sequenced and both were digested with *Asc*I and *Eco*RV. The *Mla1* third intron/dsRNAi2-2R fragment was ligated into the *Asc*I/*Eco*RV sites of the pUbi-Mla13I-NOS vector containing the *HvGSL1* dsRNAi1-1R fragment to produce the pAJ2 dsRNAi plasmid (summarised in *Figure 5.1*).

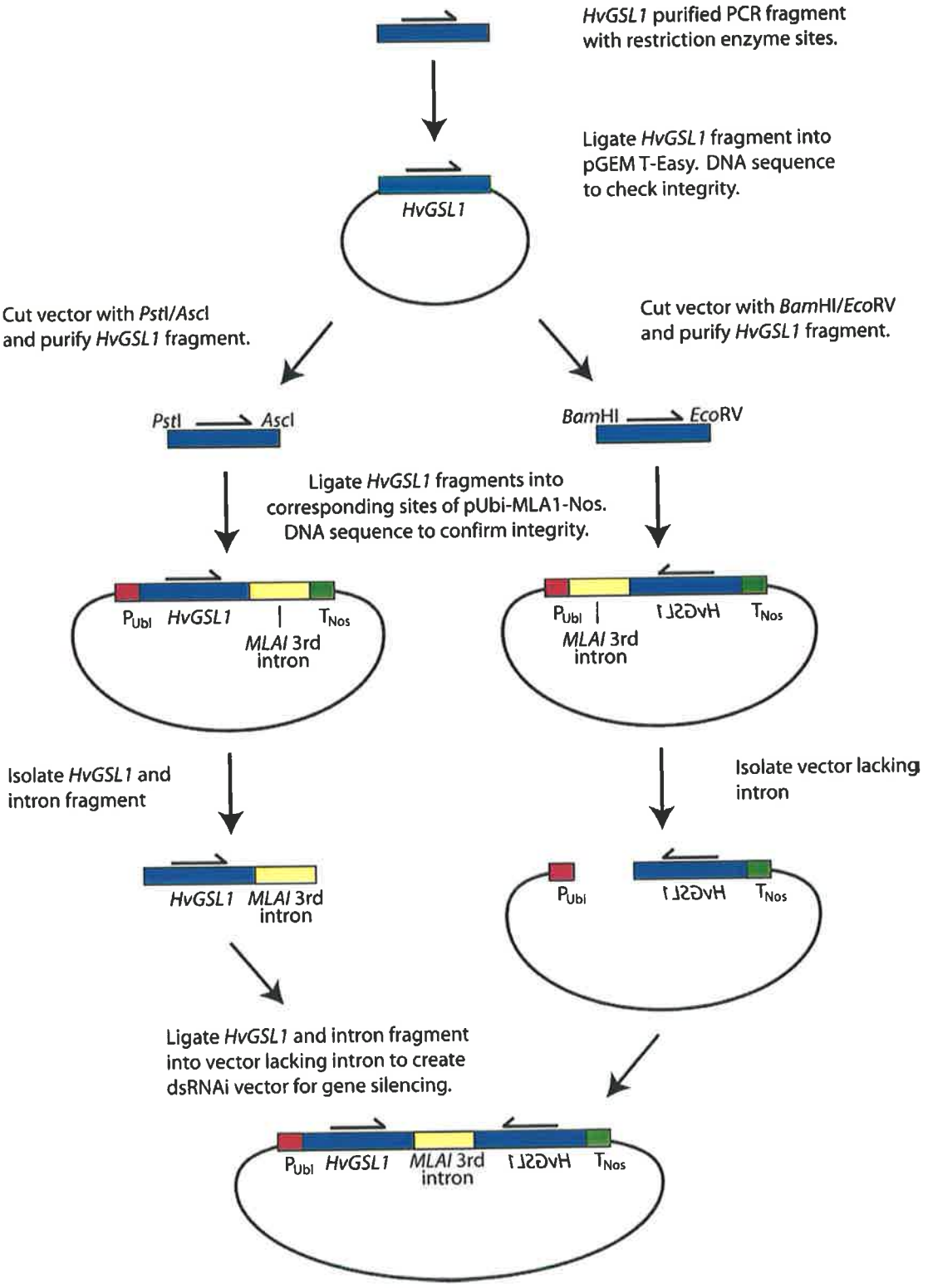

Figure 5.1 Schematic representation of the steps involved in creating dsRNAi silencing vectors. Plasmid pUbi-Mla1-Nos contains the barley ubiquitin promoter for expression in barley, the 1 kb 3rd intron from the *Mla1* gene and the barley nopaline synthase terminator. The *HvGSL1* fragment is inserted as shown.

pAJ4 was constructed in the same manner. The primers, dsRNAi3 and dsRNAi3R2 (*Appendix B*) and a second primer combination of dsRNAi4 and dsRNAi4R (*Appendix B*) were used in PCR along with DNA from a pBluescript plasmid containing approx. 1000 bp of the *HvGSL1* cDNA (donated by Ms. Jing Li, University of Adelaide) as a template. The fragments were ligated into pGEM T-Easy for the purpose of identification and were then introduced into the corresponding restriction sites of pUbi-Mla13I-NOS in the same manner described above, leading to the formation of the pAJ4 dsRNAi plasmid.

5.2.11 *RT-PCR analysis of* GSL *expression following powdery mildew infection in* Arabidopsis thaliana

Four-week-old *A. thaliana glA* (glaborous) mutants were inoculated with *Blumeria graminis* spores as described in section 5.2.2 and inoculated leaves were harvested and frozen in liquid N_2 after 24 h. RNA was extracted from the leaves as described in section 5.2.3 and 10 µg of total RNA was used in cDNA synthesis reactions as described in section 5.2.4. Duplicate cDNA reactions were performed for the control and infected leaf samples and the duplicate populations were pooled prior to PCR. The DNA sequences of the 12 *Arabidopsis* putative *GSL* genes were retrieved from the Genbank database and gene specific primers were designed to each of the genes (*Table 5.1*; *Appendix B*). Semi-quantitative RT-PCR was performed using the conditions described in section 5.2.5 at an annealing temperature of 50°C and using an extension time of 1 min. PCR was performed in triplicate and stopped after 20, 25 and 30 cycles respectively for semi-quantitative comparisons based on the relative abundance of PCR products in 1.2% (w/v) agarose gels. Polymerase chain reactions were repeated to assess the reproducibility of initial experiments.

5.2.12 *Construction of* AtGSL *dsRNAi silencing constructs*

The dsRNAi vectors designed to alter *AtGSL* expression contained gene-specific inverted repeats separated by an intron and were based on the pJawohl3 DNA plasmid generously donated by Dr. Bekir Uelker (Max-Planck-Institute for Plant Breeding Research). Primers used in RT-PCR were modified to include unique restriction enzyme sites for directional cloning. PCR primer combinations and restriction

fragment details used to produce the pAJ5(*AtGSL6*), pAJ6(*AtGSL11*) and pAJ7(*AtGSL5*) dsRNAi plasmids are summarised in Table 5.2.

The six *AtGSL* PCR fragments were ligated into pGEM T-Easy, ligations were confirmed by DNA sequencing and the *AtGSL* cDNA fragments were cut from the pGEM T-Easy vector using the restriction enzyme combinations listed in Table 5.2. The purified fragments were ligated into the corresponding sites in pJawohl3 (*Figure 5.2*). The *WRKY33* intron and sense *AtGSL* fragments were cut from pJawohl3 with *Eco*RI/*Xho*I and were ligated into the corresponding sites of the pJawohl3 plasmid containing the complementary sense *AtGSL* fragment to create the pAJ5, pAJ6 and pAJ7 dsRNAi plasmids (process summarised in *Figure 5.1*).

5.2.13 Particle bombardment of leaves with dsRNAi constructs

Gold microcarriers (1 μm) were weighed out (30 mg) and were coated with plasmid DNA after repeated washing. Gold microcarriers were initially resuspended in 1 ml 70% ethanol and placed in a platform vortexer for 5 min. Microcarriers were left to soak at room temperature for 15 min and were pelleted by a 5 sec pulse in a bench top centrifuge. Supernatant was discarded and the microcarriers were resuspended in 1 ml sterile Milli-Q water by vortexing vigorously for 1 min. The microcarriers were left to settle for 1 min and were pelleted by centrifugation as before. This washing process was repeated a further two times. The supernatant was discarded and the microcarriers were resuspended in 500 μl sterile glycerol:water 1:1 (v/v) to a final concentration of 60 $mg.ml^{-1}$. Microcarriers were resuspended by vortexing for 5 min in a platform vortexer prior to coating with plasmid DNA. Whilst maintaining the vortexing 50 μl of resuspended microcarrier was removed to a clean 1.5 ml eppendorf tube placed in the vortexer and 5 μl DNA plasmid (1 $\mu g.\mu l^{-1}$) or plasmid combinations of the dsRNAi constructs and marker constructs were added along with 20 μl 0.1 M spermidine and 50 μl 2.5 M $CaCl_2$. The mixture was vortexed for 3 min and the microcarriers were allowed to settle for 1 min and were pelleted by a 5 sec pulse in a bench top centrifuge. Supernatant was discarded and the microcarriers were washed once in 140 μl 70% ethanol, the microcarriers were resuspended by gentle

Target gene	*3' Primer*	*5' Primer*	*Expected size (bp)*
AtGSL1	RiCS11	RiCS11R	300
AtGSL2	RiCS5	RiCS5R	253
AtGSL3	RiCS2	RiCSR	262
AtGSL4	RiCS8	RiCS8R	260
AtGSL5	RiCS12	RiCS12R	276
AtGSL6	AtdsRNAi1	AtdsRNAi1R	644
AtGSL7	RiCS7	RiCS7R	282
AtGSL8	RiCS10	RiCS10R	299
AtGSL9	RiCS4	RiCS4R	293
AtGSL10	RiCS9	RiCS9R	255
AtGSL11	RiCS6	RiCS6R	298
AtGSL12	RiCS3	RiCS3R	257
AtGAPDH	GAPF	GAPR	1000

Table 5.1 Primer combinations used in semi-quantitative RT-PCR experiments for analysis of AtGSL expression. For nucleotide sequence of the primers employed see Appendix B.

Gene amplified	*Size of PCR product*	*Primers used for antisense fragment*	*pJawohl3 sites used for cloning*	*Primers used for sense fragment*	*pJawohl3 sites used for cloning*
AtGSL5	230bp	rics12r/rics12	*Bam*HI/*Hin*dIII	cs12xma/cs12rspe	*Xma*I/*Spe*I
AtGSL6	640bp	rics1r/rics1b	*Bam*HI/*Nco*I	rics1b/cals1rb	*Xma*I/*Spe*I
AtGSL11	280bp	cs6hind/cs6rbam	*Bam*HI/*Hin*dIII	rics6/rics6r	*Eco*RI/*Spe*I

Table 5.2 PCR Primers and restriction enzyme combinations used to create *AtGSL* dsRNAi constructs. For nucleotide sequence of the primers employed see Appendix B.

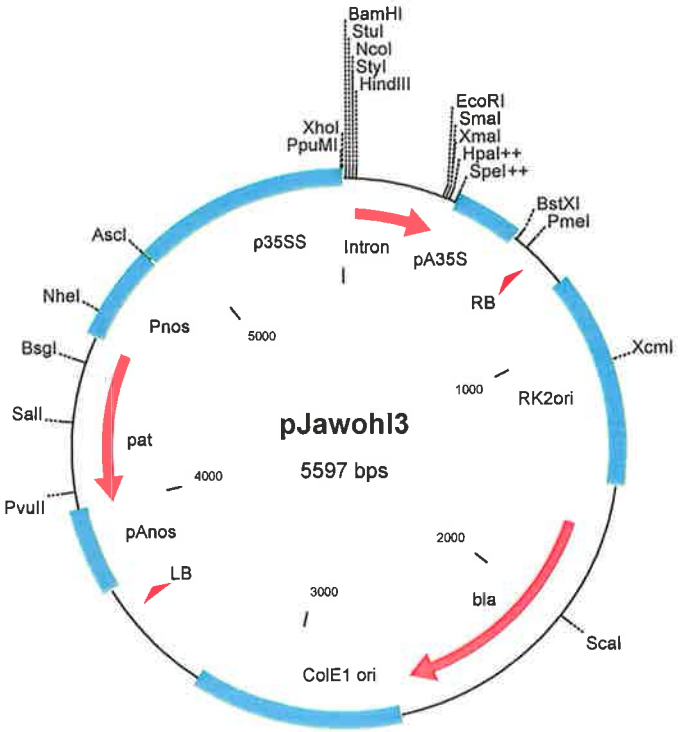

Figure 5.2 Map of pJawohl3 *Arabidopsis* dsRNAi silencing vector. The pJawohl3 plasmid used to carry the *AtGSL* dsRNAi inserts contained tandem CaMV 35S promoters for strong constitutive expression of the dsRNAi inverted repeat, the small *Arabidopsis WRKY33* intron, the *Bar* gene, and the nopaline synthase terminator. *AtGSL* fragments were ligated into the multiple cloning sites on either side of the *WRKY33* intron in the sense and antisense direction.

vortexing and pelleted as described above. Supernatant was discarded and the microcarriers were gently washed as previously described in 140 µl 100% ethanol. The DNA coated microcarriers were finally resuspended in 48 µl 100% ethanol and kept on ice until bombardment.

Plasmid pUbi-GUS-NOS (donated by Dr. Ralph Panstruga, Max-Planck-Institute for Plant Breeding Research) was used as a reporter construct in barley bombardments. In *Arabidopsis* bombardments the pamPAT-35SxGUS reporter construct (*Figure 5.3*; donated by Dr. Judith Mueller, Max-Planck-Institute for Plant Breeding Research) was employed. The empty dsRNAi vectors pUbi-Mla13I-NOS (for barley) and pJawohl3 (for *Arabidopsis*) were used as controls.

A Biolistic PD-1000/He particle delivery gun (Biorad, München, Germany) with a Hepta adapter, which provided the use of seven macrocarrier discs per bombardment, was used to deliver the microcarriers and the dsRNAi plasmids and marker plasmid to the leaves. The seven macrocarriers were placed in the Hepta adapter and were evenly coated with the vortexed, DNA-coated, microcarriers and left to dry. The loaded adapter was placed in the bombardment chamber with a Petri dish of barley leaf blades or tissue cultured *Arabidopsis* plants (section 5.2.2.). A 900 psi rupture disc was utilised and pressurised helium was used to shoot the DNA-coated microcarriers into the leaf epidermal cells. Bombarded barley leaf blades were transferred to 1.5% (w/v) agar plates containing 85 µM benzimidazole after 24 h to inhibit senescence. The plates were returned to the growth cabinet for a further 72 h before being heavily inoculated with fresh spores of the barley powdery mildew fungus *Blumeria graminis* strain K1 as described in section 5.2.2. *Arabidopsis* plants remained in the growth cabinet for 120 h post bombardment prior to inoculation with the barley powdery mildew fungus.

5.2.14 Staining and microscopic analysis of bombarded plant material

Arabidopsis leaves were removed from inoculated plants. The inoculated barley leaf blades or *Arabidopsis* leaves were placed into a GUS staining solution, which was vacuum infiltrated for 1 h at 25 mm Hg. The GUS staining solution was based on a

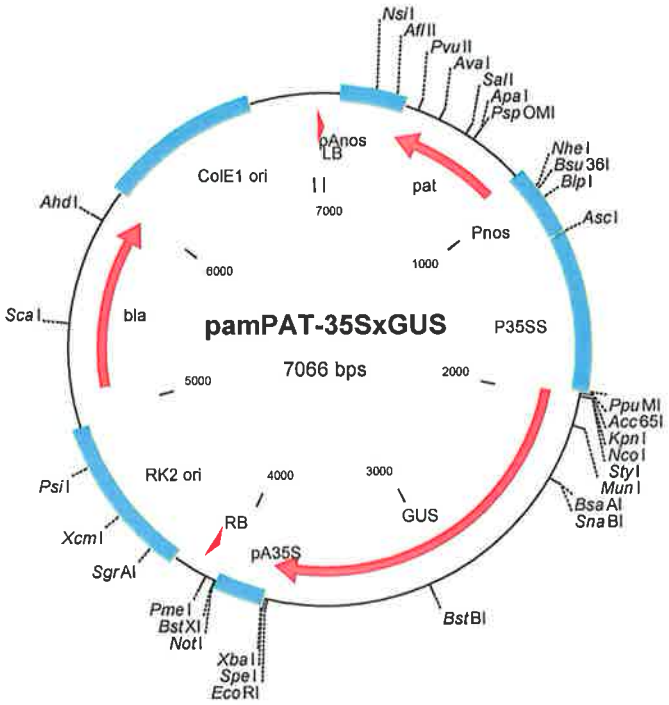

Figure 5.3 Map of pamPAT-35SxGUS marker construct. The pamPAT-35SxGUS reporter construct used as a marker in transient gene silencing assays contained tandem CaMV 35S promoters for strong constitutive expression of the bacterial β-glucuronidase (*GUS*) gene and the CaMV 35S terminator. Other elements of the vector were not used in transient gene silencing assays.

0.1 M Na_2HPO_4/0.1 M NaH_2PO_4 buffer, pH 7.0, containing 10 mM EDTA, 5 mM $K_4[Fe(CN)_6]$, 5 mM $K_3[Fe(CN)_6]$, 1 mg.ml^{-1} X-Glu, 0.1% Triton X-100 and 20% methanol. Leaves were incubated in the GUS staining solution for 16 h at 37°C and were destained in a solution of 2:1 (v/v) ethanol: (1 lactic acid: 2 glycerol: 1 water). Leaves were destained for a minimum of 48 h at room temperature, individual leaves were removed from the destaining solution and fungal structures were stained in a solution of 0.6% Coomassie brilliant blue R-250 in methanol for about 30 sec. Leaves were rinsed in water and in 10 mM Na_2HPO_4/10 mM NaH_2PO_4 buffer, pH 9.0. Excess phosphate buffer was drained from the leaves before overlaying with 0.02% aniline blue fluorochrome in 10 mM Na_2HPO_4/10 mM NaH_2PO_4 buffer, pH 9.0, for 20 min at room temperature. Leaves were rinsed in water and mounted on glass slides in sterile 1:1 (v/v) glycerol: water under glass cover slips.

Leaf material stained as described above was analysed using a Zeiss Axiovert 135TV microscope (Carl Zeiss, Oberkochen, Germany) equipped with a Super Pressure HBO 100 W mercury vapour lamp for fluorescence studies. Epi-illumination was used with an excitation filter having a cut off limit at 365 nm, a chromatic beam splitter FT395 and a barrier filter LP420. Images were captured with a DXM1200 digital camera (Nikon, Tokyo, Japan) that was connected to an IBM compatible PC (programmes: ACT-1 v1.00 (Nikon, Tokyo, Japan) and Image Tool v2.00 (UTHSCSA, San Antonio, USA). Digital images of GUS stained and mildew infected epidermal cells were captured using identical exposure and lighting settings for each bombardment. Images were converted to greyscale and a histogram of the fungal associated callose deposits were taken and the data recorded using the software described above. In barley a minimum of 50 papillae from individual GUS stained and mildew infected cells were examined using this technique.

5.3 RESULTS AND DISCUSSION

5.3.1 Construction of pUbi-MLA13I-Nos

Hybridisation of the complementary oligonucleotides, pUbi-Nos MCSF and pUbi-Nos MCSR, led to the formation of a new dsDNA molecule containing multiple restriction enzyme sites and *Hin*dIII/*Eco*RV compatible ends (*Figure 5.4*). This dsDNA fragment was ligated into the *Hin*dIII/*Eco*RV-cut pUbi-Nos vector, to create the pUbi-MCS-Nos vector. DNA sequencing and restriction mapping of the new pUbi-MCS-Nos vector confirmed the presence of the multiple cloning site. The incorporation of the new multiple cloning sites greatly extended the cloning options of the pUbi-Nos vector.

The barley *MLA1* third intron was amplified by PCR. This 1 kb PCR fragment was initially ligated into pGEM T-Easy and DNA sequencing confirmed its identity. The barley *MLA1* third intron was cut from pGEM T-Easy with *Pst*I/*Mlu*I restriction enzymes and ligated into the corresponding sites of the pUbi-MCS-Nos plasmid to generate pUbi-Mla13I-Nos (*Figure 5.5*). DNA sequencing and restriction mapping of the pUbi-Mla13I-Nos confirmed vector integrity. The *MLA1* third intron was introduced into the vector such that the two *HvGSL1* cDNA fragments that would be introduced later as an inverted repeat would be physically separated. However, following transcription the intron is spliced out, leaving the inverted repeat. There is evidence to suggest that vectors of this nature are more efficient at inducing the mechanisms of post-transcriptional gene silencing than those lacking an intron (Smith *et al.*, 2000; Wesley *et al.*, 2001).

5.3.2 Construction of barley GSL *dsRNAi constructs*

Comparisons of putative plant *GSL* genes with the barley *HvGSL1* gene revealed a region of DNA sequence that appeared to be highly conserved (4700-4900 bp in the *HvGSL1* cDNA sequence; *Figure 5.6*). Other regions that shared little to no DNA sequence homology (e.g. 520-750 bp region of *HvGSL1*) were also identified in the comparisons (*Figure 5.7*). These observations guided the design of two dsRNAi constructs, one that would be specific for the *HvGSL1* gene, pAJ2, and the second a

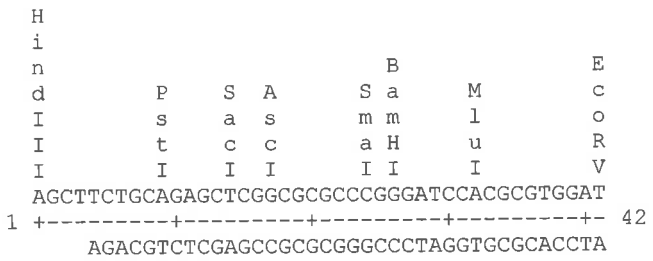

Figure 5.4 Multiple cloning site introduced into pUbi-Nos. The dsDNA molecule was produced from the hybridisation of two oligonucleotides and was ligated into the *Hin*dIII/*Eco*RV sites of the pUbi-Nos plasmid, greatly extending the cloning options of the vector.

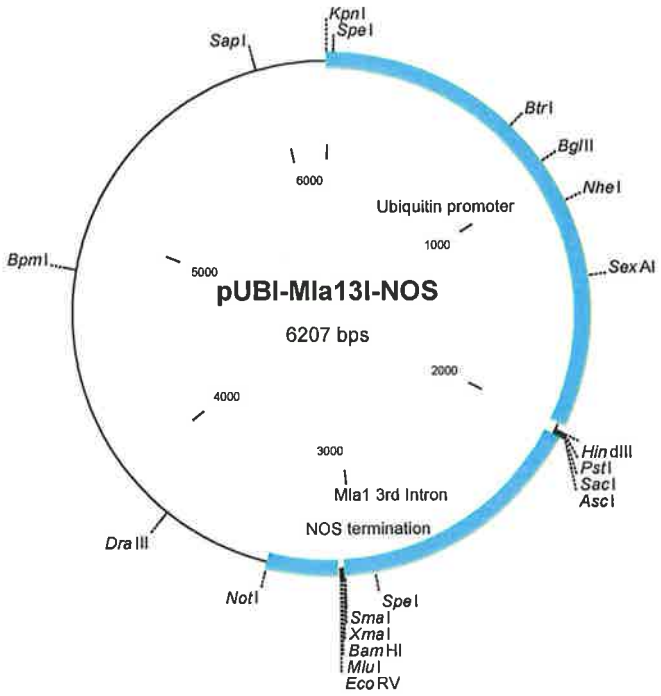

Figure 5.5 Map of pUbi-Mla13I-Nos dsRNAi silencing vector. The pUbi-Mla13I-Nos plasmid used to carry the dsRNAi inserts contained the barley ubiquitin promoter for constitutive expression of the dsRNAi inverted repeat, the barley *MLA1* 3rd intron and the barley nopaline synthase terminator (NOS). *HvGSL* fragments were ligated into the multiple cloning sites of the vector on either side of the *MLA1* 3rd intron in the sense and antisense direction, forming an inverted repeat.

dsRNAi construct, pAJ4, that could potentially interfere with the expression of multiple barley *GSL* genes, based upon regions of DNA sequence homology in plant *GSL* genes in the databases. A PCR fragment corresponding to a poorly conserved region of plant *GSL* genes was amplified from *HvGSL1* using two separate primer combinations. Separate primer combinations allowed the introduction of unique restriction enzyme sites that could be used for the directional cloning of the resultant PCR products into pUbi-Mla13I-Nos, as described in section 5.2.10. The DNA sequence of the *HvGSL1* fragments used to create pAJ2 is presented in Figure 5.8.

The two *HvGSL1* 201 bp PCR fragments amplified from the poorly conserved region of the *HvGSL1* gene were initially ligated into pGEM T-Easy. This provided a means to characterise the PCR products *via* DNA sequencing and ensured that the restriction enzymes used to generate the fragments for subsequent cloning steps had a sufficient stretch of DNA to bind, thus enhancing digestion efficiency of endonuclease enzymes that cut poorly or do not cut close to an end. Clones could also be stored for the longer term as glycerol stocks. Both PCR fragments were subsequently cut from pGEM T-Easy and separately ligated into pUbi-Mla13I-Nos. DNA sequencing confirmed that ligations were successful. The antisense *HvGSL1* fragment and *Mla1* third intron were cut from the pUbi-Mla13I-Nos vector as one and were ligated into the pUbi-Mla13I-Nos vector containing the sense *HvGSL1* fragment, thereby forming the pAJ2 plasmid (summarised in *Figure 5.1*). This somewhat convoluted cloning approach was undertaken because of the inherently difficult task of working with inverted repeat structures, which interfere with DNA sequencing reactions and other techniques by the formation of hairpin loop structures.

The second barley dsRNAi construct, pAJ4, was produced in an identical manner. Briefly, a 195 bp fragment of the *HvGSL1* gene (*Figure 5.9*) was amplified by PCR using two separate primer combinations, the resultant PCR products were ligated into pGEM T-Easy and the inserts were characterised by DNA sequencing, which identified them as *HvGSL1* fragments. The *HvGSL1* fragments were cut from pGEM T-Easy and ligated into the pUbi-Mla13I-Nos vector. DNA sequencing was conducted to confirm the presence of the *HvGSL1* fragments in the vector. The antisense *HvGSL1* fragment and *Mla1* third intron were cut from one vector and

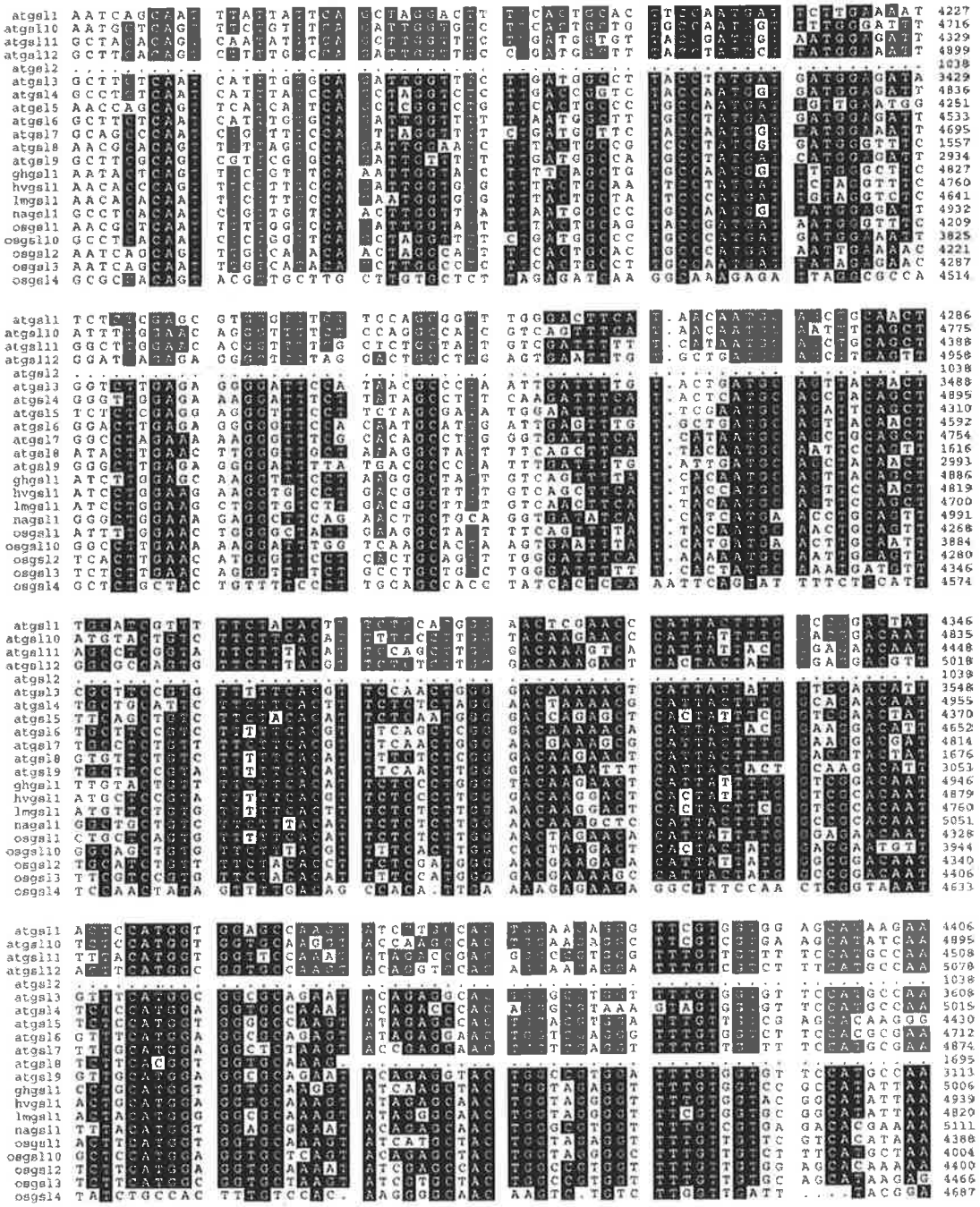

Figure 5.6 Multiple DNA sequence alignment of putative plant *GSL* genes highlighting conserved nature of sequence from the cytoplasmic region thought to contain the catalytic site. Sequence from this region was engineered into dsRNAi vectors. DNA sequences were aligned using the EclustalW program and are graphically presented using the Prettybox program from the ANGIS suite of programs. Numbers on the right correspond to nucleotide positions. Sequences aligned are *Oryza sativa GSL1* (Accession number AP001389), *Oryza sativa GSL2* (Accession number AP003223), *Oryza sativa GSL3* (Accession number AP003268), *Oryza sativa GSL4* (Accession number AP003447), *Oryza sativa GSL10* (Accession number AC104427), *Arabidopsis thaliana GSL1* (Accession number AF162444), *Arabidopsis thaliana GSL2* (Accession number AC006436), *Arabidopsis thaliana GSL3* (Accession number AC006223), *Arabidopsis thaliana GSL4* (Accession number AB023038), *Arabidopsis thaliana GSL5* (Accession number AC005142), *Arabidopsis thaliana GSL6* (Accession number AF237733), *Arabidopsis thaliana GSL7* (Accession number AC007592), *Arabidopsis thaliana GSL8* (Accession number AC006922), *Arabidopsis thaliana GSL9* (Accession number AB025605), *Arabidopsis thaliana GSL10* (Accession number AC012395), *Arabidopsis thaliana GSL11* (Accession number AL163527), *Arabidopsis thaliana GSL12* (Accession number AL353013), *Nicotiana alata GSL1* (Accession number AF304372), *Gossypium hirsutum GSL1* (Accession number AF085717), *Hordeum vulgare GSL1* (Accession number AY177665) and *Lolium multiflorum GSL1* (Accession number AY286332).

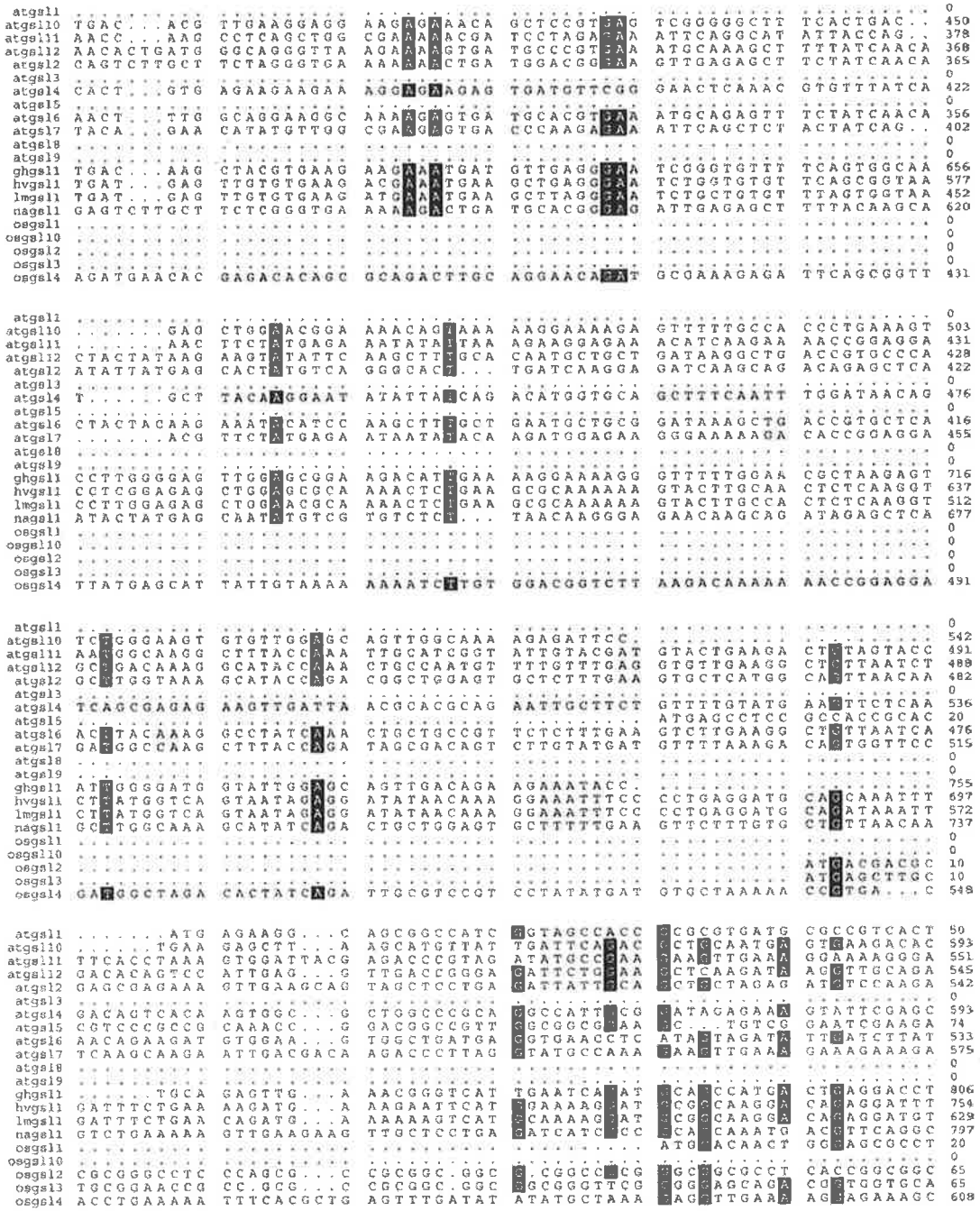

Figure 5.7 Multiple DNA sequence alignment of putative plant *GSL* genes highlighting divergent nature of sequence from the NH_2-terminal cytoplasmic region. Sequence from this region was engineered into dsRNAi vectors. DNA sequences were aligned using the EclustalW program and are graphically presented using the Prettybox program from the ANGIS suite of programs. Numbers on the right correspond to nucleotide positions. Sequences aligned are *Oryza sativa GSL1* (Accession number AP001389), *Oryza sativa GSL2* (Accession number AP003223), *Oryza sativa GSL3* (Accession number AP003268), *Oryza sativa GSL4* (Accession number AP003447), *Oryza sativa GSL10* (Accession number AC104427), *Arabidopsis thaliana GSL1* (Accession number AF162444), *Arabidopsis thaliana GSL2* (Accession number AC006436), *Arabidopsis thaliana GSL3* (Accession number AC006223), *Arabidopsis thaliana GSL4* (Accession number AB023038), *Arabidopsis thaliana GSL5* (Accession number AC005142), *Arabidopsis thaliana GSL6* (Accession number AF237733), *Arabidopsis thaliana GSL7* (Accession number AC007592), *Arabidopsis thaliana GSL8* (Accession number AC006922), *Arabidopsis thaliana GSL9* (Accession number AB025605), *Arabidopsis thaliana GSL10* (Accession number AC012395), *Arabidopsis thaliana GSL11* (Accession number AL163527), *Arabidopsis thaliana GSL12* (Accession number AL353013), *Nicotiana alata GSL1* (Accession number AF304372), *Gossypium hirsutum GSL1* (Accession number AF085717), *Hordeum vulgare GSL1* (Accession number AY177665) and *Lolium multiflorum GSL1* (Accession number AY286332).

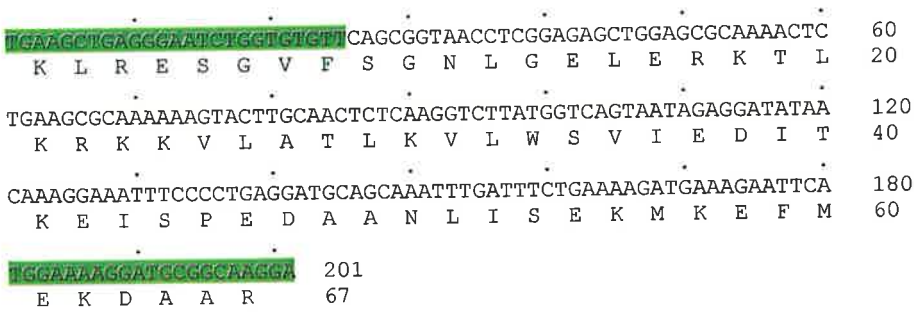

Figure 5.8 DNA sequence and deduced peptide sequence of the gene-specific region of *HvGSL1* amplified by PCR and used in the dsRNAi silencing construct pAJ2. Sequences highlighted in green were used as the basis for primer design.

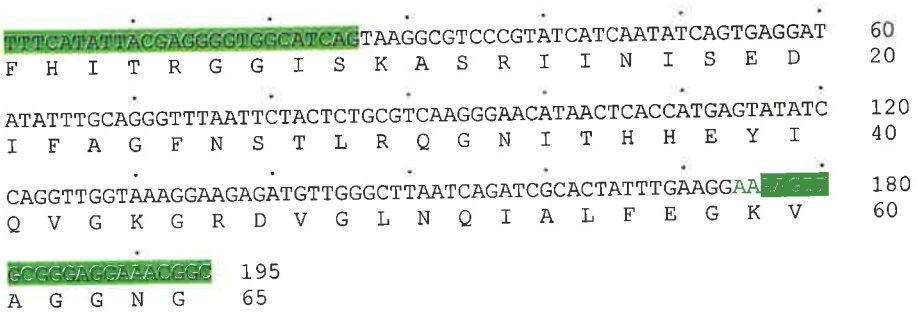

Figure 5.9 DNA sequence and deduced peptide sequence of the more conserved region of *HvGSL1* amplified by PCR and used in the dsRNAi silencing construct pAJ4. Sequences highlighted in green were used as the basis for primer design.

ligated into the other pUbi-Mla13I-Nos vector containing the sense *HvGSL1* fragment, thereby forming the pAJ4 plasmid.

5.3.3 *Bombardment of barley leaf blades with dsRNAi constructs*

The barley dsRNAi silencing constructs, pAJ2 and pAJ4, were co-bombarded into barley leaf epidermal cells with a marker plasmid expressing the bacterial β-glucuronidase (*GUS*) gene. The dsRNAi constructs and the marker plasmid were carried on the same microcarriers so that staining for GUS activity could be used as a marker for cells that had potentially altered levels of *GSL* expression. Heavy inoculations of powdery mildew spores were required to maximise the chances of finding GUS stained cells that had also been challenged by the fungus. A staining technique was developed whereby GUS expression, fungal structures and callose deposits could be analysed in a single field of view. Initial observations of GUS stained and mildew infected epidermal cells suggested that the dsRNAi constructs, pAJ2 and pAJ4, used together, failed to completely abolish callose deposits in papillae (*Figure 5.10*).

To determine whether a more subtle alteration in callose deposition had resulted from expression of the dsRNAi constructs images of visibly infected, GUS stained cells were analysed more closely using a CCD camera. The camera was connected to the analytical microscope, set at conserved illumination and exposure levels, and around 60 images per bombardment experiment corresponding to a minimum of 50 individual transformed and infected cells were captured.. Captured images were converted to grey scale before papillae area and papillae fluorescence were measured using ImageTool software (http://ddsdx.uthscsa .edu/dig/). Data from two separate bombardment experiments are presented graphically in Figures 5.11 A and B.

These data suggest that the silencing constructs pAJ2 and pAJ4, which contain two 180 bp pieces of the *HvGSL1* gene, fail to alter the formation of papillae that result from fungal challenge. Experiments in which the dsRNAi constructs were used alone also failed to effect papillae formation (data not shown). It is evident, based on the error bars produced from measurements of the papillae area (*Figure 5.11 A*), that there

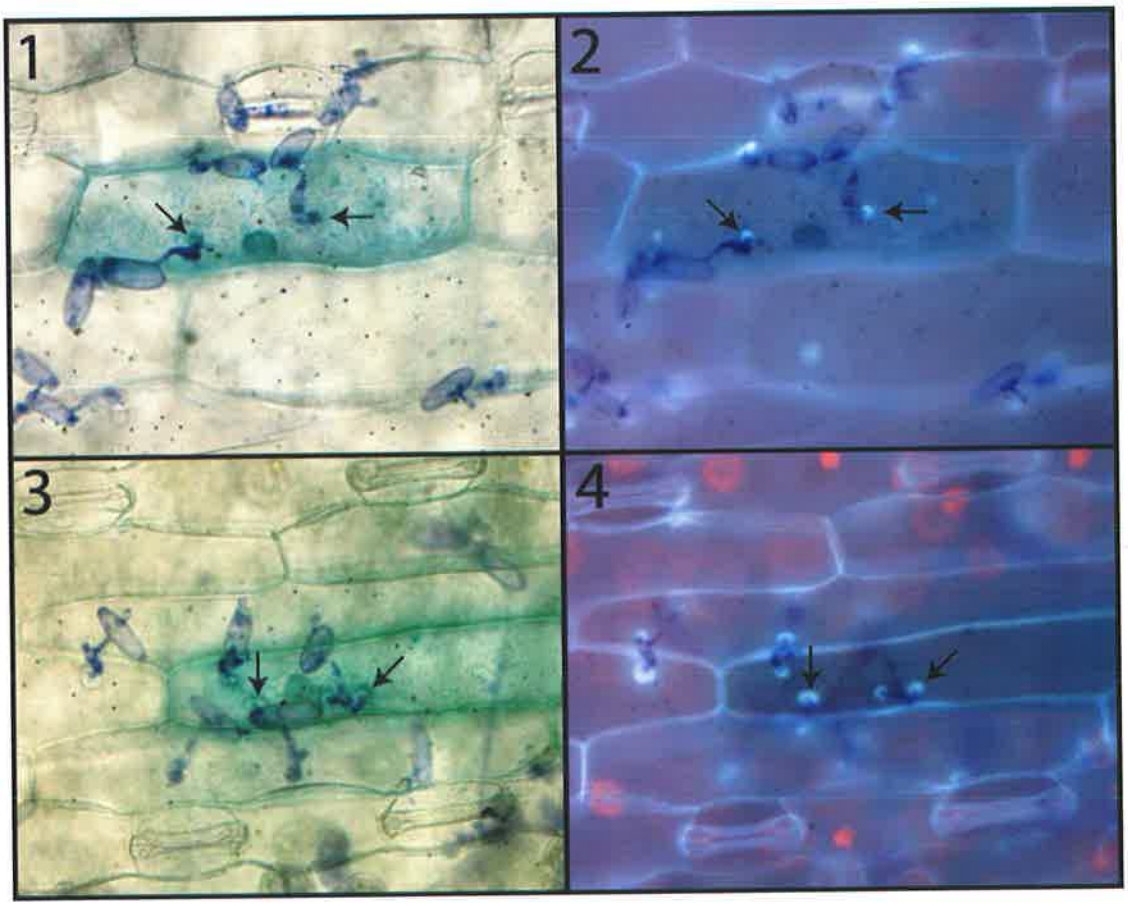

Figure 5.10 Two images of GUS stained epidermal cells of barley infected with powdery mildew. Bright field images (40x) (**1**) control and (**3**) dsRNAi bombarded wild-type Ingrid barley leaves. Arrows denote papillae, purple structures are fungal spores and hyphae stained with Coomassie blue, green coloration due to GUS activity. Panels (**2**) and (**4**) are UV illuminated images of bright field, callose deposits fluoresce white under UV light after staining with aniline blue fluorochrome showing control (**2**) and dsRNAi (**4**) material, respectively. Leaf blades were bombarded with both pUbi-Mla13I-Nos and pUbi-GUS-Nos in controls and the dsRNAi silencing constructs, pAJ2, pAJ4 and the marker plasmid pUbi-GUS-Nos for silencing assays.

was a large variation in the size of papillae and it may therefore be a poor measure of changes in callose deposition. The large variation in papillae area is likely to relate to the biological variation in timing of fungal spore germination and hyphal infection. Fungal spores of a similar developmental stage were used to inoculate detached barley leaf blades but there is undoubtedly some variation in the time before spores germinate on the leaf surface and secondly, there will also be some variation in the time a hyphae grows before attempting to penetrate the epidermal cell layer (Skou *et al.*, 1984; Heitefuss and Ebrahim-Nesbat, 1986). The development of secondary hyphae also adds to the variation in the size of observed papillae as they develop at a later stage. Measurements of papillae fluorescence levels appeared to be uniform in all infected cells examined and failed to highlight any differences in leaves bombarded with control or dsRNAi vectors (*Figure 5.11 B*). No alteration in the frequency of papillae formation was evident in tissues bombarded with the pAJ2 and pAJ4 dsRNAi silencing constructs, which suggested that the *HvGSL1* gene does not have a direct role in the formation of callose at sites of fungal penetration. However, it may be that post-transcriptional silencing of the *HvGSL1* gene through the dsRNAi constructs has little effect on HvGSL1 activity, particularly if the HvGSL1 protein is very stable. This possibility is further addressed in transgenic plants stably transformed with dsRNAi constructs (Chapter 6).

5.3.4 Arabidopsis thaliana GSL *expression following fungal challenge.*

Twelve *GSL* genes have been identified in *Arabidopsis thaliana* (Richmond and Somerville, 2000; Verma and Hong, 2001; http://cellwall.stanford.edu/). The availability of DNA sequence for these 12 genes enabled gene specific primers to be designed for the comparison of *GSL* mRNA levels in leaf tissue before and after powdery mildew infection utilising a semi-quantitative RT-PCR approach.

Six week old *Arabidopsis thaliana* plants were heavily inoculated with the powdery mildew fungus *Blumeria graminis* and leaves were harvested after 24 hours. RNA was extracted from control and inoculated leaves and two cDNA populations were synthesised from each of the RNA samples. Duplicate cDNA populations were pooled and RT-PCR was conducted to determine if any of the 12 *GSL* genes of *Arabidopsis* were upregulated in response to fungal challenge. Primers were designed

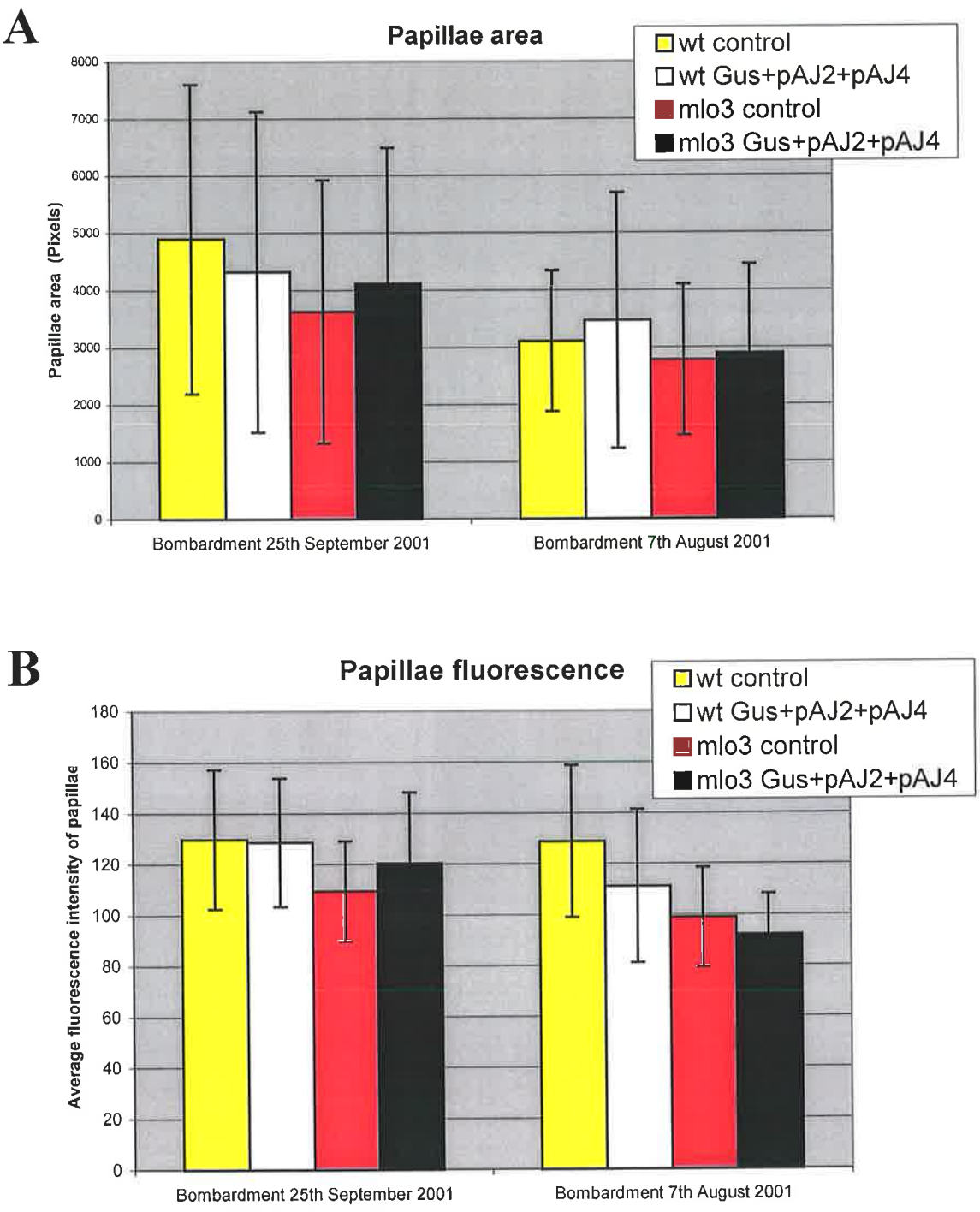

Figure 5.11 Results of single cell transient silencing assays in barley. **A)** The area of papillae and **B)** the average fluorescence intensity of callose deposits induced by fungal challenge were measured in a minimum of 50 independent GUS stained epidermal cells of barley using image analysis software and the data is presented graphically for two individual experiments. Wild type, Ingrid and *mlo3* mutant barley leaf blades were bombarded with pUbi-GUS-Nos and pUbi-Mla13I-Nos in the controls and with pUbi-GUS-Nos, pAJ2 and pAJ4 in dsRNAi silencing assays. Error bars indicate standard deviations.

to amplify portions of all 12 *Arabidopsis GSL* genes (*Table 5.1*). Results of the RT-PCR experiment after 30 cycles indicated that mRNA levels of *AtGSL5, AtGSL6* and *AtGSL11* were slightly elevated 24 h after fungal challenge (*Figure 5.12*). Transcript levels were also analysed after 25 and 35 cycles of PCR but the intensity of bands on agarose gels at these stages suggested amplification was outside the linear range and a comparison of levels at these stages would therefore not be truly representative. None of the 12 genes assayed were strongly upregulated, using the semi-quantitative RT-PCR method, and this suggested that proteins involved in the production of callose deposits might well be present prior to fungal attack. If this were the case then lowering mRNA levels by transient post-transcriptional gene silencing may not greatly affect the actual synthesis of callose, as postulated in section 5.3.3. The RT-PCR was repeated to ensure the results were not merely due to PCR conditions. The three genes that appeared to be upregulated (*AtGSL5*, *6* and *11*) were then targeted for silencing, using the single cell transient silencing assay that had been modified to suit *Arabidopsis* plants.

5.3.5 Construction of Arabidopsis GSL dsRNAi constructs.

The pJawohl3 binary plasmid used in the transient silencing assays in *Arabidopsis* contains tandem CaMV 35S promoters for constitutive strong expression of the dsRNAi inverted repeat, the small *Arabidopsis WRKY33* intron and the nopaline synthase terminator (*Figure 5.2*). Other important features of the pJawohl3 plasmid are the presence of left and right borders that allow the plasmid to insert in the *Arabidopsis* genome following *Agrobacterium* infection and a gene conferring resistance to the herbicide bialaphos (Thompson *et al.,* 1987). These features are redundant in transient silencing assays but very useful for stable transgenic studies that are explored in detail in Chapter 6.

The PCR primers listed in Table 5.2 were used to amplify fragments of the *AtGSL5*, *6* and *11* genes and the sequences of these cDNA fragments are provided in Figure 5.13 (*AtGSL5*), Figure 5.14 (*AtGSL6*) and Figure 5.15 (*AtGSL11*). The six PCR fragments were cloned into pGEM T-Easy and plasmid DNA was sequenced to confirm the identity of the PCR products. The *AtGSL* PCR fragments were cut from the pGEM T-Easy plasmid using the restriction endonucleases listed in Table 5.2 and ligated into

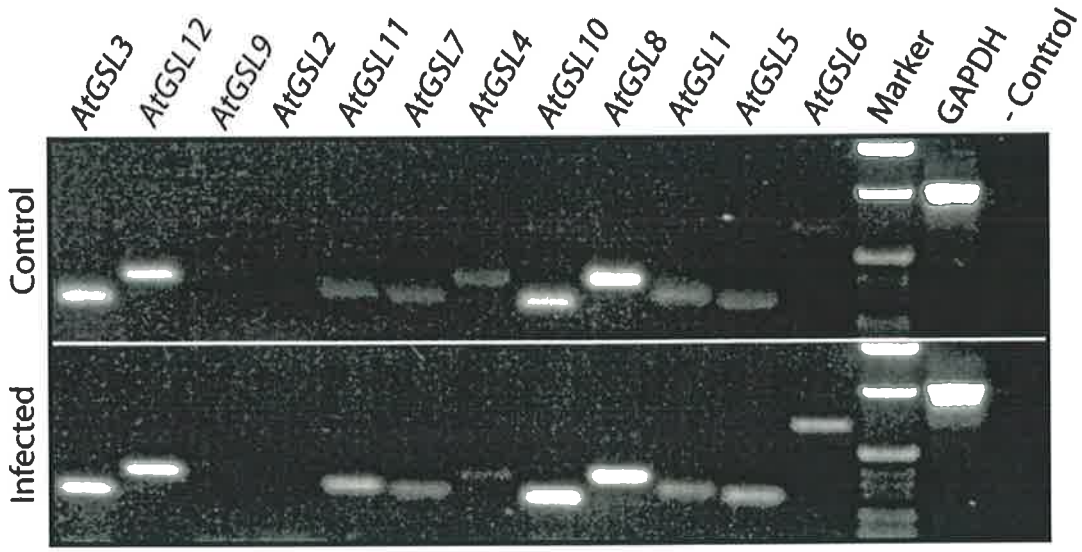

Figure 5.12 Semi-quantitative RT-PCR analysis of *Arabidopsis GSL* mRNA levels. Gene specific primers were used in 30 cycles of PCR to analyse the expression of 12 *AtGSL* genes in cDNA from infected and non-infected leaf tissue. *GAPDH* was used as a positive PCR control to ensure cDNA levels were comparable in both control and infected populations. Transcripts which appared to increase slightly in abundance following infection were *AtGSL5*, *AtGSL6* and *AtGSL11*.

```
CGAAGCGACGGGATGTTCGATTGAATCAGATATCAATGTTTGAGGCTAAGGTAGCCAGTG   60
  K  G  R  D  V  G  L  N  Q  I  S  M  F  E  A  K  V  A  S  G   20

GGAACGGAGAGCAGGTTCTCAGCCGAGATGTGTACCGGCTCGGGCACAGGCTTGATTTCT  120
  N  G  E  Q  V  L  S  R  D  V  Y  R  L  G  H  R  L  D  F  F   40

TCAGAATGTTATCATTTTTCTACACAACTGTAGGGTTTTTCTTCAACACAATGATGGTCA  180
  R  M  L  S  F  F  Y  T  T  V  G  F  F  F  N  T  M  M  V  I   60

TTCTTACTGTTTACGCTTTCCTCTGGGGACGGGTTTATCTGGCTCTCAGCGGGGTTGAGA  240
  L  T  V  Y  A  F  L  W  G  R  V  Y  L  A  L  S  G  V  E  K   80

AGTCCGCTCTAGCAGACAGTACGGACACCAACGCCG                           276
  S  A  L  A  D  S  T  D  T  N  A                               92
```

Figure 5.13 DNA sequence and deduced peptide sequence of the *AtGSL5* gene amplified by PCR and used in the dsRNAi silencing construct pAJ7. Sequences highlighted in green were used as the basis for primer design.

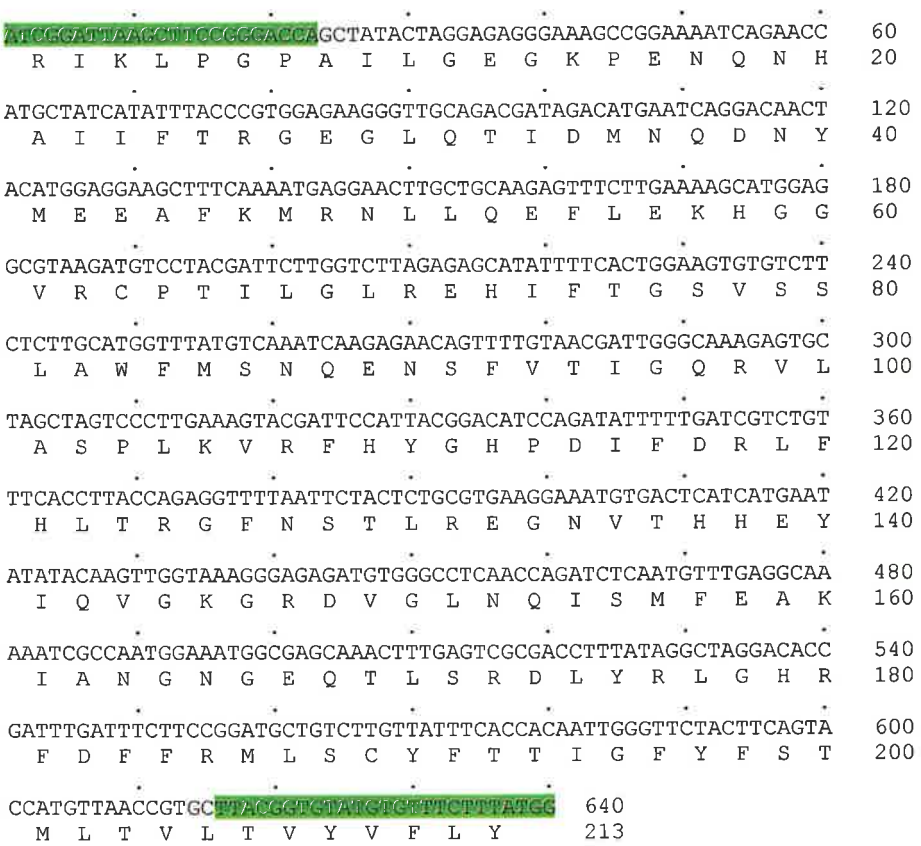

Figure 5.14 DNA sequence and deduced peptide sequence of the *AtGSL6* gene amplified by PCR and used in the dsRNAi silencing construct pAJ5. Sequences highlighted in green were used as the basis for primer design.

Figure 5.15 DNA sequence and deduced peptide sequence of the *AtGSL11* gene amplified by PCR and used in the dsRNAi silencing construct pAJ6. Sequences highlighted in green were used as the basis for primer design.

the corresponding sites of pJawohl3. The six pJawohl3 based plasmids were sequenced to verify that ligation experiments were successful. The *Arabidopsis* dsRNAi vectors were produced in the same manner as the barley dsRNAi vectors (summarised in *Figure 5.1*). The antisense strand and intron were cut from one vector and ligated into the vector containing no intron and the sense strand of the same gene to produce the three dsRNAi silencing constructs, pAJ5, pAJ6 and pAJ7.

5.3.6 *Bombardment of* Arabidopsis thaliana *with dsRNAi constructs.*

A. thaliana glA (glaborous) mutants were cultured in glass tissue culture vessels in an organised manner such that the seven plants within the culture vessel were directly aligned with the macrocarrier discs present in the Hepta Adapter of the bombardment chamber. *A. thaliana glA* mutants were used in this study for two reasons. Firstly, they lack trichomes, which limit the number of spores that reach the leaf surface, and, secondly, trichomes fluoresce under UV light and complicate the interpretation of results. *A. thaliana glA* mutants respond to fungal challenge in the same manner as wild-type *Arabidopsis* (Dr. Volker Lipka, personal communication).

Each of the *AtGSL* silencing constructs were used individually and the three constructs were also co-bombarded, along with the pamPAT-35SxGUS reporter construct (*Figure 5.2*), so that transiently transformed epidermal cells could be identified after staining for GUS. The staining protocol used for the analysis of callose deposits in bombarded barley leaf blades was adopted for the analysis of callose deposits in *Arabidopsis*, but the incubation time post-bombardment was extended to maximise the *AtGSL* silencing effect. This time extension was possible because the *Arabidopsis* plants were intact and were able to obtain water and nutrients from the tissue culture media as opposed to the detached leaf blades of barley, which deteriorated quite rapidly after 96 hours on agar plates.

Arabidopsis thaliana epidermal cells are smaller in size than those of barley. They also exhibit a more random shape than the rectangular shape of barley epidermal cells and are analogous to pieces of a jigsaw puzzle. As a result of these factors, the occurrence of GUS-stained cells that were challenged by the powdery mildew fungus was less frequent when compared with barley. Gold particles used as the carrier for

the marker and silencing constructs could be identified in GUS stained cells of *Arabidopsis*, thus providing an alternative means of identifying transiently transformed cells (*Figure 5.16 C*).

Results from transient silencing assays in *Arabidopsis* plants confirmed that the staining techniques employed enabled the detection of fungal structures, callose deposits and GUS activity, although GUS staining was often less intense than in barley cells. Papillae were detectable in the bulk of images captured from leaves bombarded with the empty pJawohl3 vector and many leaves bombarded with the dsRNAi silencing constructs (*Figure 5.15*). In some instances fungal hyphae that appeared to penetrate the epidermal layer of the *Arabidopsis* leaves were not associated with the presence of papillae. This was observed in both control and dsRNAi bombarded tissues and may merely be an issue of timing, because callose formation may not be instantaneous and the deposits may not be abundant enough to detect immediately following the breach of the cell wall. However, it may be that the dsRNAi constructs do effect the formation of callose in transformed cells.

Due to time constraints a large data set relating to the presence or absence of callose deposits in transiently transformed and infected cells of *Arabidopsis* could not be obtained and hence statistically based data will not be presented for this section of work. A more comprehensive analysis of the effects of these silencing constructs has been conducted in stably transformed plants of *Arabidopsis* and the results from this work are presented in Chapter 6.

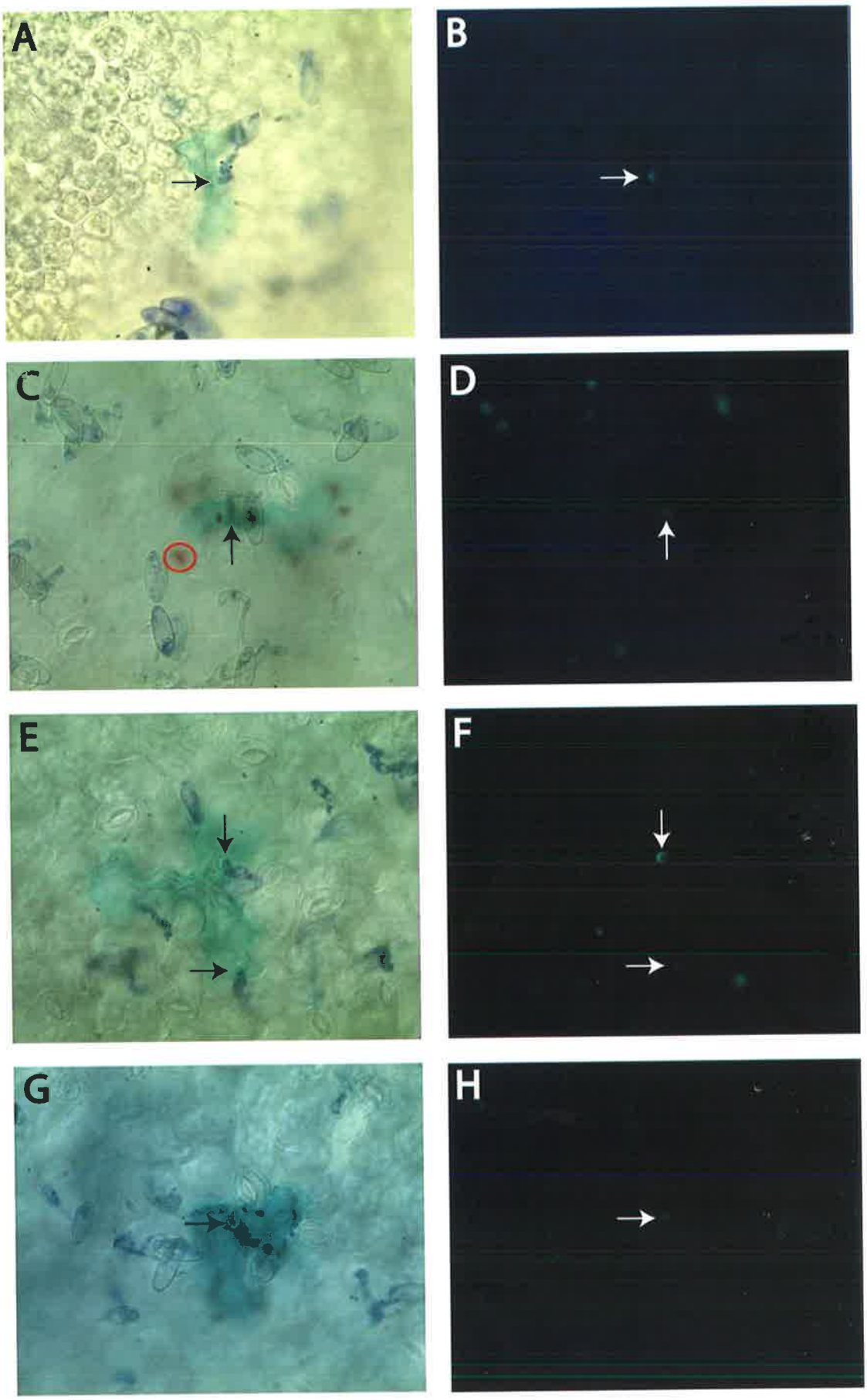

Figure 5.16 Bright field and fluorescence micrographs of transient silencing assays in leaves of *Arabidopsis thaliana*.

Figure 5.16 Bright field and fluorescence micrographs of transient silencing assays in leaves of *Arabidopsis thaliana* (40x). Bombarded plants were inoculated with spores of powdery mildew five days post bombardment. After 48 hours leaves were cleared and stained for 1) GUS activity which appears dark blue-green in transformed cells under bright field illumination 2) Fungal structures which appear purple under bright field illumination and 3) Callose deposits which fluoresce light blue-white under UV illumination. Arrows denote sites of hyphal penetration and resultant papillae. **A/B** Bright field and fluorescence image respectively, of leaf bombarded with empty pJawohl3 vector and marker plasmid. **C/D** Bright field and fluorescence image respectively, of leaf bombarded with pAJ7 (targeting *AtGSL5*), **red ellipse** encapsulates a gold particle used as the carrier in bombardments. **E/F** Bright field and fluorescence image respectively, of leaf bombarded with pAJ5 (targeting *AtGSL6*) vector and marker plasmid. **G/H** Bright field and fluorescence image respectively, of leaf bombarded with pAJ6 (targeting *AtGSL11*) vector and marker plasmid.

5.4 SUMMARY AND CONCLUSIONS

An existing vector was improved by the addition of a multiple cloning site and was further modified by the introduction of the third intron from the barley *MLA1* gene. This vector is functional and has been used to silence *CesA* genes of barley (Dr. Rachel Burton, personal communication).

Fragments of a barley *GSL* gene, designated *HvGSL1*, were ligated into the pUbi-MLA13I-Nos vector as an inverted repeat, the two HvGSL1 fragments being physically separated by the intron. The vector was introduced into the epidermal cells of detached barley leaves *via* particle bombardment. The barley dsRNAi constructs had no discernable impact upon the development or appearance of papillae that form as a result of the perturbation of the cell wall by fungal hyphae. No wounding was evident as a result of the bombardment protocol employed. Staining techniques were developed such that GUS activity, fungal architecture and callose deposits could be viewed in a single field of view. Results suggest that the barley gene, *HvGSL1*, is not involved in the formation of papillae at sites of attempted fungal penetration, although the possibility that HvGSL1 is a stable protein and that post-transcription silencing of the corresponding gene has little to no effect on HvGSL1 protein levels in the cell can not be discounted. It may be that a *GSL* gene other than *HvGSL1* plays a role in the formation of papillae and this will require further examination as new *GSL* genes are identified in barley. Attempts to disrupt the function of *HvGSL1* in tissues other than leaf using the existing dsRNAi constructs could not be undertaken because most other tissues are not easily amenable to microprojectile bombardment.

The expression of 12 *Arabidopsis GSL* genes were surveyed following challenge with the powdery mildew fungus *Blumeria graminis* and mRNA levels for three of the genes *AtGSL5*, *AtGSL6* and *AtGSL11* appeared to be mildly upregulated according to results obtained from semi-quantitative RT-PCR experiments. These genes were therefore targeted for silencing by engineering three dsRNAi vectors that would each potentially shut down the expression of one gene by inducing the mechanisms of post-transcriptional gene silencing (Chuang and Meyerowitz, 2000). *Arabidopsis thaliana glA* mutants were cultured in a manner that allowed intact plants to be bombarded and

extended the time tissues could be left after bombardment to maximise the potential for gene silencing. Results from bombardment experiments were inconclusive and large numbers of transiently transformed cells coincident with fungal challenge were not obtained, in part because of the small size of *Arabidopsis* epidermal cells but also because of the potential stability of the proteins.

Although the transient gene silencing experiments described in this chapter provided no conclusive evidence for the participation of *GSL* genes in papillae formation in either barley or *Arabidopsis*, one interpretation of the observations would be that the callose synthase enzyme itself is already present in the cell and is sufficiently stable to ensure that post-transcriptional degradation of newly transcribed callose synthase mRNA does not greatly diminish levels of active enzyme in the short term, transient assays. Balanced against this apparently negative result was the observation that three of the 12 *Arabidopsis GSL* genes were slightly up regulated following fungal infection. To investigate the effects of silencing these three genes (*AtGSL5*, *6* and *11*) on papillae formation in the longer term, where the effects of low enzyme turnover rates would be reduced or abolished, the dsRNAi gene silencing constructs were introduced into *Arabidopsis* by the floral dip method. The formation of callosic papillae could thereby be examined in segregating populations of transgenic *Arabidopsis* plants. The results of these experiments are described in the next Chapter.

CHAPTER 6

SILENCING OF (1→3)-β-D-GLUCAN SYNTHASE GENES IN TRANSGENIC *ARABIDOPSIS THALIANA*

6.1 INTRODUCTION

The work described here follows on from the transient gene silencing assays outlined in the previous chapter and was initiated in an attempt to identify members of the *Arabidopsis GSL* family that might be involved in the formation of callosic papillae that form in plant cells at sites of fungal penetration. Individual members of the family were presumed to mediate the synthesis of callose in different tissues and/or under different environmental conditions, but very limited information was available on biological functions of individual AtGSL family members. The GSL6 protein is located at the growing cell plate and interacts with two cell plate-associated proteins, phragmoplastin and a UDP-glucose transferase (Hong *et al.*, 2001a, 2001b). The three proteins are likely to form part of a larger complex that assembles at the cell plate (Hong *et al.*, 2001b). Transgenic tobacco lines over-expressing a *GFP-AtGSL6* gene construct showed increased callose deposition at the cell plate but this gene failed to complement a yeast *fks1* mutant (Hong *et al.*, 2001a). The *AtGSL5* gene has been shown to partially complement the yeast *fks1* mutant and is inducible by salicylic acid (Østergaard *et al.*, 2002). Despite these observations, direct genetic evidence linking *GSL* genes to callose biosynthesis in plants generally, or genetic evidence linking individual *AtGSL* family members to specific sites of callose deposition in *Arabidopsis*, has yet to be found. Semi-quantitative RT-PCR indicated that, of the 12 *Arabidopsis GSL* genes, mRNA transcript levels for *AtGSL5*, *AtGSL6* and *AtGSL11* increased slightly following powdery mildew challenge (*Figure 5.11*), and on this basis were chosen for further examination.

Transient gene silencing assays with double-stranded RNA interference (dsRNAi) constructs failed to provide convincing evidence that the three *AtGSL* genes were involved in the formation of papillae during fungal attack (Chapter 5). However, if the turnover rate of the callose synthase enzyme were low, lowering mRNA levels by transient post-transcriptional gene silencing might not have greatly affected the actual amount of enzyme activity in the cell, or the synthesis of callose. Stable transgenic lines of *Arabidopsis* were therefore generated, using the same dsRNAi constructs, in an alternative "loss-of-function" approach aimed at linking *GSL* gene expression and callose deposition. Analysis of gene silencing experiments was expected to be

simpler in stable transgenic plants because all cells in the transgenic plant should show lower expression of the targeted *GSL* gene and consequently any infected cells could be screened for the presence or absence of callosic papillae. Furthermore, silencing should be effective from the earliest stages of the transgenic plant's development and the *GSL* mRNAs targeted by dsRNAi constructs should remain very low throughout, so that active GSL proteins should not accumulate.

Deposition of callosic plugs, or papillae, at sites of fungal penetration is a widely recognised early response of host plants to microbial attack. It has been proposed that the papillae physically block fungal growth (Aist *et al.,* 1980; Inoue *et al.,* 1994; Israel *et al.,* 1980) and thereby provide valuable time for the host plant to mount its defensive strategies, although this is not universally accepted (reviewed in Stone and Clarke, 1992). Here, stable transgenic lines of *Arabidopsis* were generated using dsRNAi constructs specific for the *AtGSL5*, *AtGSL6* and *AtGSL11* genes. Transgenic lines were challenged with the fungal pathogen *Sphaerotheca fusca* and the resultant papillae were examined. Callose deposits found in germinating pollen and at the cell plate of dividing cells were also examined in the transgenic lines. A mutant line carrying a T-DNA insertion in the *AtGSL5* gene and the powdery mildew resistant line *pmr4-1* previously described by Vogel and Somerville (2000) were compared with the *AtGSL5*-dsRNAi line in assays with various plant pathogens, and following wounding.

It should be re-stated that no data from colleagues at the Max Planck Institute of Plant Breeding Research, Cologne are presented in this Chapter without due acknowledgement. Collaborative data from Dr. Volker Lipka, which are presented to support the findings described here are limited to Figure 6.8. In addition, the published manuscript, in which data from both groups are included, is presented as Appendix D.

6.2 MATERIALS AND METHODS

6.2.1 Materials

Quanti-Tect SYBR Green PCR mix was from Qiagen (Valencia, CA, USA). Sodium hypochlorite, NaOH, NaCl, rifampacin, carbenicillin, gentamycin, kanamycin, sucrose, dNTPs, Tween 20, TEAA, EDTA, MeCN, Na_2HPO_4, NaH_2PO_4, $MgCl_2$, Trizma base, KCl, MS media and reagents for liquid hydroponic media were from Sigma-Aldrich (St. Louis, MD, USA). Rockwool was from Rockwool International A/S (Hedehusene, Denmark). Gene-Pulser 1 mm electroporation cuvettes were supplied by Promega (Madison, WI, USA). Tryptone, yeast extract, agar and agarose was from Becton-Dickinson (Sparks, MD, USA). Superscript II cDNA synthesis kit was from Invitrogen Corporation (Carlsbad, CA, USA). *Taq* DNA polymerase, restriction enzymes and BSA were from New England Biolabs (Beverly, MA, USA). SYBR Green I dye was from Applied Biosystems (Foster City, CA, USA). Coomassie brilliant blue R-250 was from Serva Fine Biochemicals (Heidelberg, Germany). Aniline blue fluorochrome was from Biosupplies (Parkville, Australia). DNA-free kit was from Ambion (Austin, TX, USA). The Zorbax Eclipse dsDNA column was supplied by Agilent Technologies (Palo Alto, CA, USA). HPLC was performed using a series II 1090 liquid chromatograph purchased from Hewlett-Packard (Palo Alto, CA, USA).

6.2.2 Cultivation of plant and fungal material

The sequence-tagged *Arabidopsis thaliana* (Columbia) T-DNA insertion line GABI-KAT 089H05 segregating for T-DNA insertion in *AtGSL5* (http://www.mpiz-koeln.mpg.de/~GABI-Kat/GABI-Kat_homepage.html) was from the Max-Planck-Institute for Plant Breeeding Research (Cologne, Germany). The powdery mildew resistant *Arabidopsis* line *pmr4-1* was obtained from John Vogel and Shauna Somerville (Carnegie Institution of Washington, Stanford, CA, USA).

Arabidopsis thaliana plants used in stable transformation experiments and transgenic plants used for RNA isolation were grown in soil in growth rooms under 16 h light and 8 h dark in soil at 22°C. The majority of plants were cultivated in aerated liquid

hydroponic media (*Appendix A*) in baskets containing rockwool under the same conditions. Plants for transformation were grown for 5-6 weeks until floral shoots and many immature flowers were beginning to appear. In some cases the initial flowering stems were cut off to encourage a greater proliferation of flowers for transformation. Leaf tissue taken for RNA isolation was placed in liquid N_2 immediately following harvest and was stored at -80°C until needed.

In some instances *Arabidopsis thaliana* (Col-0) seed was germinated on 1% (w/v) agar plates containing MS media. Seed was surface-sterilised for 1 min in a solution containing 4.2% sodium hypochlorite, 0.9% sodium hydroxide and 0.1% Tween 20 and was rinsed 4x in sterile water before being placed onto the surface of the MS agar. Plates were incubated on an incline at 22°C with a 14 h photoperiod in a growth cabinet. Seedlings were transferred to rockwool cubes after 3-4 weeks and grown under the conditions described below.

The *Arabidopsis* powdery mildew fungus, *Sphaerotheca fusca*, was cultivated on zucchini vines in a glasshouse at approx. 24°C. Uninfected zucchini plants were introduced into the glasshouse every 4 weeks and an infected leaf was used to inoculate uninfected plants to maintain a stock of fresh spores.

6.2.3 Agrobacterium *mediated transformation of* Arabidopsis thaliana

The dsRNAi silencing constructs pAJ5, pAJ6 and pAJ7 described in section 5.2.12 were used for the stable transformation of *Arabidopsis*. *Arabidopsis* plants were grown as described in section 6.2.2 for approx. 6 weeks or until there were many immature inflorescence clusters and limited fertilised siliques. Plants at this stage of development were transformed using a floral dip method (Clough and Bent, 1998). *Agrobacterium tumafaciens* strain GV3101 carrying the helper plasmid pMP90RK were transformed separately with the binary vectors pAJ5, pAJ6 and pAJ7 by electroporation in a 1 mm cuvette under the following conditions; 2.5 V, 25 μF, 400 Ω. Transformed *A. tumafaciens* colonies were selected on LB agar plates (1% w/v NaCl, 1% w/v tryptone and 0.5% w/v yeast extract, pH 7.0 with 1% w/v agar) containing the antibiotics rifampacin 100 $\mu g.ml^{-1}$, carbenicillin 50 $\mu g.ml^{-1}$,

gentamycin 50 $\mu g.ml^{-1}$ and kanamycin 25 $\mu g.ml^{-1}$ for 3 days at 28°C. Isolated colonies were used to inoculate 10 ml LB media containing carbenicillin 50 $\mu g.ml^{-1}$ and kanamycin 25 $\mu g.ml^{-1}$, and were cultured for 2 days at 28°C with shaking. These starter cultures were used to seed 300 ml LB cultures that were grown under the same conditions and selection criteria as described above for 24 h. Bacteria were pelleted by centrifugation at 5000 rpm for 10 min and resuspended in 300 ml 5% (w/v) sucrose. Silwet L-77 (Lehle seeds, Round Rock, USA) was added to a final concentration of 0.05% (v/v) and *Arabidopsis* plants were inverted in the solution for approx. 10 sec whilst being gently agitated. Plants were covered with plastic for 24 h following dipping to maintain high humidity and were returned to the growth room. When seeds became mature the plant was no longer watered and a seed collection bag was placed over the plant. Dry seed was harvested and planted out in soil. Seed trays were placed at 4°C for two days to encourage even germination of the seeds before they were placed in a growth chamber as described in section 6.2.2. Transformants were selected after 6-8 d by three applications of the herbicide Basta 100 $mg.L^{-1}$ (AgrEvo, Düsseldorf, Germany) every second day in one week.

6.2.4 DNA extraction

Genomic DNA was extracted from young leaves of *Arabidopsis* as described in section 2.2.3.

6.2.5 RNA extraction

Total RNA was extracted from *Arabidopsis* young leaves and inflorescences as described in section 2.2.4.

6.2.6 First strand cDNA synthesis reactions

The RNA preparations destined for use in cDNA synthesis reactions was treated with DNase I, using a DNA-free kit according to the manufacturer's directions to remove any DNA that might act as a template in PCR reactions. Total RNA (2 µg) was combined with 1 µl of a 50 µmol stock oligo $(dT)_{21}$ adaptor primer, 1 µl dNTPs (10mM) and the volume was adjusted to 10 µl using sterile Milli-Q water. The

mixture was incubated at 65°C for 5 min in a water bath and immediately placed on ice. First strand reactions were undertaken using a Superscript II cDNA synthesis kit as described in section 2.2.5. The cDNA synthesis reactions were continued for 60 min at 42°C. Heating to 70°C for 15 min terminated the reactions and the cDNAs were diluted by the addition of 30 µl sterile Milli-Q water. The cDNAs were stored at -20°C or used directly in PCR.

6.2.7 Preparation of [^{32}P]- radiolabelled DNA probes

Radiolabelled DNA probes for Southern analyses were prepared as described in section 2.2.6.

6.2.8 Southern analysis

Genomic DNA was extracted from young leaves of *Arabidopsis* T_3 transgenic lines as described in section 2.2.3. DNA (5 µg) was digested with *Pvu*II and separately with *Bam*HI in 50 µl reaction volumes containing 1x reaction buffer (supplied). Restriction digests continued for at least 6 h at 37°C. Fragmented DNA was separated on agarose gels and transferred to nylon membranes as described in section 2.2.17.

6.2.9 Quantitative PCR analysis of AtGSL *mRNA levels in transgenic* Arabidopsis

Quantitative (real-time) PCR experiments were performed using a Rotorgene 2000 Real-Time cycler, RG2072, followed by analysis with DNA sample analysis system v4.2 software from Corbett Research (Mortlake, NSW, Australia) in consultation with Dr. Neil Shirley (Department of Plant Science, University of Adelaide, SA, Australia). To prepare the standards, three 25 µl PCR was conducted for all of the primer combinations; atcycloF/ atcycloR, atgapdhF/ atgapdhR, atgsl5F/ atgsl5R, atgsl6F/ atgsl6R and atgsl11F/ atgsl11R (*Appendix B*). PCR was performed with dNTP concentrations of 200 µM, 1 U *Taq* DNA polymerase, 1.5 mM $MgCl_2$ in a 10 mM Tris-HCl buffer, pH 8.3, containing 50 mM KCl with 3 µl primer stock (4 µM) and 1 µl cDNA. Thermal cycling conditions were as follows: 94°C, 30 sec followed

by 35 cycles of 94°C, 30 sec; 55°C, 30 sec; 72°C, 20 sec. PCR products were purified by HPLC on a Zorbax Eclipse dsDNA column, 2.1 mm x 150 mm x 3.5 μM. The two elution solutions were 0.1 M TEAA, 0.1 M EDTA, pH 7.0 (solution A) and 0.1 M TEAA, 0.1 M EDTA, 25% MeCN, pH 7.0 (solution B). The gradient was set from 35% to 70% over a 30 min time period and separation was conducted at 40°C. The flow rate was 0.2 $ml.min^{-1}$, and the column was equilibrated in solution A for at least 10 min prior to purification using a Hewlett-Packard series II 1090 liquid chromatograph. Purified PCR products were sequenced as described in section 2.2.16 to confirm the identity of the products. Dilution series' of the HPLC purified PCR products were prepared ranging from 1 x 10^1 to 1 x 10^7 $molecules.\mu l^{-1}$ and were used to generate standard curves of fluorescence levels for the given concentration of PCR product.

Quantitative PCR was conducted on cDNAs produced as described in section 6.2.6 in 20 μl reaction volumes using 10 μl 2x Quanti-Tect PCR master mix, 0.3 μM gene specific primers and 0.6 μl of a 100-fold dilution of SYBR Green I dye. Cycling parameters were as follows: 95°C, 10 min followed by 55 cycles of 95°C, 20 sec; 55°C, 30 sec; 72°C, 30 sec. PCR products were checked by electrophoresis in agarose gels.

6.2.10 Staining and microscopic analysis of plant material

Arabidopsis tissues and infected leaves were removed from plants and cleared in 95% ethanol for 48 h. The solution was replaced with 75% ethanol and the tissues were left for a minimum of 24 h. Infected leaf material was transferred to a solution of 0.6% Coomassie brilliant blue R-250 in methanol for 10-20 sec to stain fungal structures. Tissues were rinsed in water and in 10 mM sodium phosphate buffer, pH 9.0. Excess phosphate buffer was drained from the tissues before staining with 0.02% aniline blue fluorochrome in 10 mM sodium phosphate buffer, pH 9.0 for 20 min at room temperature. Tissues were rinsed in water and mounted on glass slides in sterile 1:1 (v/v) glycerol:water for bright field microscopic analyses and in sterile water under glass cover slips for confocal studies.

Tissues were analysed using a Zeiss Axioplan 20 fluorescence microscope (Carl Zeiss, Oberkochen, Germany) equipped with a HBO 50 W mercury vapour lamp for fluorescence studies. Epi-illumination was used with an excitation filter of 365 nm and a KP620 emission filter. Images were captured with a DC300F digital camera (Leica Microsystems AG, Heerbrugg, Switzerland) that was connected to an IBM compatible PC (program: IM1000 Image Manager v1.10; Leica Microsystems AG, Heerbrugg, Switzerland).

Various tissues were analysed using a MRC-1000UV Confocal Laser Scanning Microscope (Bio-Rad, Hercules, CA, USA). The microscope was equipped with a Diaphot 300 inverted microscope (Nikon Instech Co., Ltd., Kanagawa, Japan) and two lasers, Krypton/Argon and UV-Argon with excitation filters of 351 and 363 nm and an epi-detection 460 LP emission filter. Captured images were analysed and collated using Confocal Assistant v 4.02 software (Todd Clark Brelje).

6.2.11 Pathogenicity assays

In initial experiments on the transgenic *AtGSL5* lines carrying the dsRNAi construct, the formation of callosic plugs was examined in four to six week old plants 48 h after inoculating leaves with spores from the powdery mildew fungus *Sphaerotheca fusca*. Subsequently, infection severity was quantitated using several other fungal pathogens.

Seed collected from *Arabidopsis* T_3 plants that were shown to be transgenic by Southern analysis were sent to Professor Paul Schulze-Lefert's laboratory at the Max-Planck-Institute for Plant Breeding Research, Cologne, Germany to be assayed for resistance/susceptibility against a range of fungal pathogens including *Blumeria graminis*, *Golovinomyces orontii* and *Peronospora parasitica*. The T-DNA insertion mutant GABI-KAT 089H05 and the *pmr4-1* mutant were also challenged in parallel with the same pathogens. Dr. Volker Lipka conducted the assays with these pathogens.

Spores from the fungi, *Blumeria graminis* and *Golovinomyces orontii* were applied to *gsl5* mutants via a 65 cm infection tower by gently shaking heavily infected host plants over the tower. After 5 min the inoculated plants were returned to the growth

chamber at 22°C (16 h light, 8 h darkness). *Sphaerotheca fusca* infections were established by the transfer of fresh spores to *Arabidopsis* leaves using a small paintbrush. Infected leaf material was harvested from inoculated *Arabidopsis* plants after 48 h and was prepared for microscopic analysis as described in section 4.2.9. Infection phenotypes were monitored macroscopically by visible mycelial growth or microscopically where the frequency of sporulating bodies and degree of hyphal growth and infection were determined. *Peronospora parasitica* pv *Cala2* infections were established by applying aqueous suspensions of conidiosporangia at an approx. concentration of $1x10^5$ ml^{-1}. Plant material was harvested 3 days post inoculation.

6.2.12 Wounding

The leaves of 4-6 week old plants were mechanically wounded by pushing a small pipette through the leaf. After 24 h, the leaves were detached, cleared and stained for callose deposits as described in section 6.2.10.

6.2.13 Sequence analysis of pmr4-1 *mutant*

Dr. Volker Lipka isolated genomic DNA from the powdery mildew resistant *Arabidopsis* line *pmr4-1*. The three exons of *GSL5* (1870 bp, 2022 bp, 1448 bp) were PCR amplified under the following conditions; 40 cycles of 94°C 30 sec, 55°C 30 sec, 72°C 5 min using the following flanking oligonucleotide primers, atgl5e1/atgsl5e1r, atgsl5e2/atgsl5e2r and. atgsl5e3/atgsle3r (*Appendix B*) respectively. PCR products were purified using a Nucleospin extract kit and directly sequenced as described in section 3.2.7 using the additional primers atgsl5e1s/atgsl5e1rs for exon 1 and atgsl5e2s/atgsl5e2rs for exon 2 (*Appendix B*).

6.2.14 Segregation of callose deficiency in T-DNA insertion lines

Segregation analyses were performed on 95 independent T_2 generation GABI-KAT 089H05 T-DNA insertion lines by Dr. Volker Lipka. The presence of T-DNA was monitored through the resistance of seedlings to sulfadiazine (www.mpiz-koeln.mpg.de/GABI-KAT/). Callose formation was examined in 18 lines 48 h after inoculation of four to six week old seedlings with *Blumeria graminis*, and genomic

DNA was isolated from the same 18 lines for PCR analysis of T-DNA insertions specifically within the *AtGSL5* gene. The *AtGSL5*-specific primers were AtGSL5-ex2F and AtGSL5-ex2R (*Appendix B*), and the primer for the left border region of the T-DNA insert was GABI T-DNA LB (*Appendix B*). The precise position of the T-DNA insertion was determined by PCR-based sequencing from the left border of the T-DNA into exon 2 of the *AtGSL5* gene.

6.3 RESULTS

6.3.1 Plant growth and development

Three plants were used for each floral dip transformation, and the groups of three were transformed with the empty pJawohl3 vector and the three dsRNAi silencing constructs pAJ5 (*AtGSL6*), pAJ6 (*AtGSL11*) and pAJ7 (*AtGSL5*). The bulk of the T_0 seed from the 12 transformed plants was planted out to produce a green lawn of T_1 *Arabidopsis* seedlings covering the planter trays. The application of a glyphosinate-based herbicide enabled the identification of putative transgenics (Thompson *et al.*, 1987), which in turn were left to mature and set seed. This process of planting and selection was repeated until the seed from T_2 plants had been isolated. Four lines for each of the transformation constructs were chosen on the basis of their herbicide resistance segregation pattern being close to 3:1, and these lines were further characterised. Four lines were pursued for reasons of manageability and it was predicted that there would be a high probability of finding any plants possessing an altered callose phenotype from this number.

Transgenic plants carrying the *AtGSL5*-dsRNAi construct had mildly epinastic leaves, were slower to grow and consequently remained smaller in size when setting seed compared with wild type plants and plants transformed with the empty pJawohl3 vector, the *AtGSL6*-dsRNAi or the *AtGSL11*-dsRNAi constructs (*Figure 6.1*). The *AtGSL6*-, *AtGSL11*-dsRNAi lines and empty vector control lines exhibited normal phenotypes and no obvious morphological abnormalities were detected in leaves, stems, flowers, siliques or roots of T_3 plants.

6.3.2 Southern analysis of AtGSL *dsRNAi transgenics*

Genomic DNA was extracted from putative transgenic plants used in microscopic analyses for callose, and was analysed for the presence of multiple copies of the *AtGSL* gene fragment used in the respective dsRNAi transformation constructs. Thus, transgenic lines transformed with the *AtGSL5*-dsRNAi construct were probed with the *AtGSL5* fragment used to create the construct (*Figure 5.13*). The pattern of hybridising bands on the Southern blot indicated that both the independent lines, 7.11

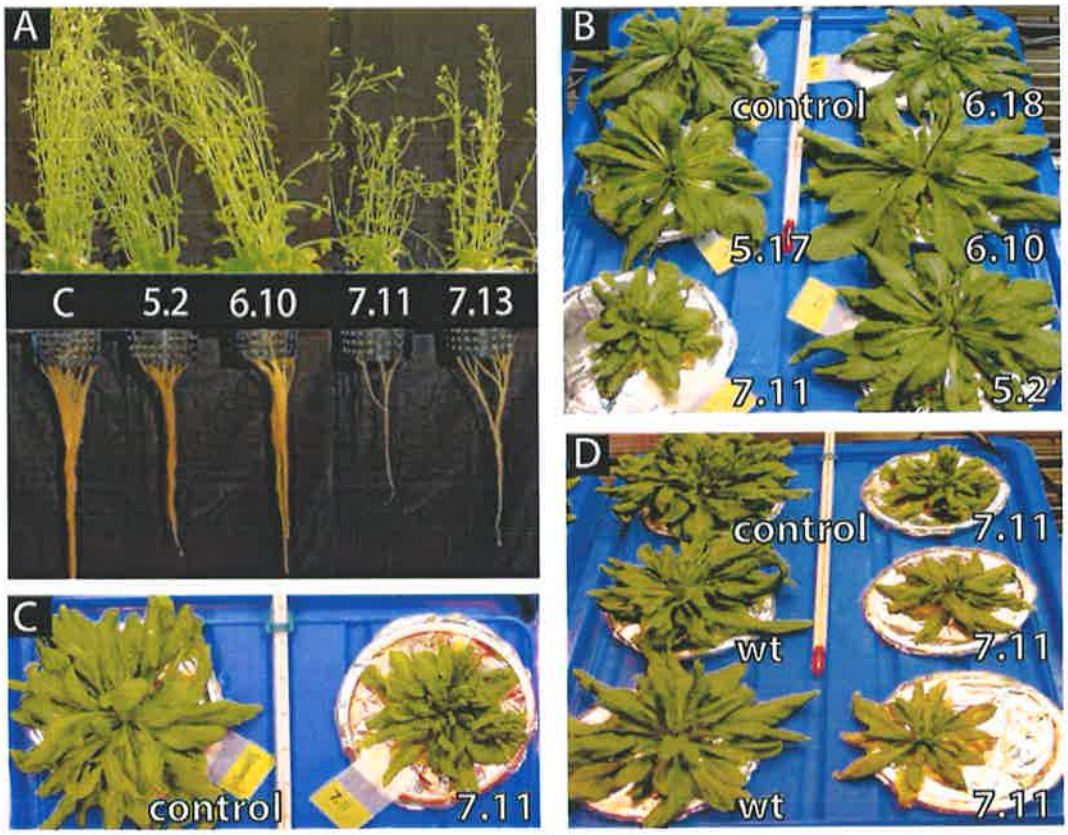

Figure 6.1 Phenotypes of *AtGSL*-dsRNAi transgenic lines of *Arabidopsis*. In Panel **A**, the reduced height and root development of the *AtGSL5* lines (7.11 & 7.13) are compared with the *AtGSL6* (5.2), *AtGSL11* (6.10) and empty vector control (C) plants. In Panel **B**, the *AtGSL5* line (7.11) is compared with two independent *AtGSL6* lines (5.2 & 5.17), two independent *AtGSL11* lines (6.10 & 6.18) and with an empty vector control plant at an earlier stage of development. No alterations in phenotype were detected in either of the *AtGSL6* or *AtGSL11* dsRNAi lines. In Panel **C**, the slower growth of the *AtGSL5* line (7.11) is again evident. In Panel **D**, empty vector control, wildtype and three *AtGSL5* plants are compared, note epinastic leaves on *AtGSL5* (7.11) lines.

and 7.13, contained extra copies of the *AtGSL5* gene when compared with wild type and transgenics transformed with the empty transformation vector alone (*Figure 6.2a*). Duplicate plants from the same independent lines contained the silencing construct at the same site within the genome, as expected, and the site of insertion was different between different lines.

Similarly, transgenic lines transformed with the *AtGSL6*-dsRNAi construct were probed with the *AtGSL6* fragment used to create the vector (*Figure 5.14*) and the Southern blot probed with this fragment is presented in Figure 6.2b. The pattern of hybridising bands on this blot indicated that the independent lines 5.16, 5.17 and 5.20 contained extra copies of the *AtGSL6* gene when compared with wild type and transgenics transformed with the empty transformation vector. Furthermore, lines 5.2 and 5.16 appear to have the *AtGSL6*-dsRNAi construct inserted at the same site within the genome and are unlikely to represent true independent lines. Line 5.17 appears to have the *AtGSL6*-dsRNAi construct inserted at multiple sites within the genome as indicated by the number of hybridising bands.

Transgenic lines transformed with the *AtGSL11*-dsRNAi construct were probed with the *AtGSL11* fragment used in the dsRNAi vector (*Figure 5.14*) and the Southern blot probed with this fragment is presented in Figure 6.2b. The pattern of hybridising bands on this blot indicated that the independent lines 6.10, 6.13 and 6.18 contained extra copies of the *AtGSL6* gene when compared with wild type and transgenics transformed with the empty transformation vector. Furthermore, lines 6.13 and 6.18 appear to have the *AtGSL6*-dsRNAi construct inserted at the same site within the genome and are unlikely to represent true independent lines. Lines 6.13 and 6.18 may also have the *AtGSL6*-dsRNAi construct inserted at multiple sites within the genome as indicated by the number of hybridising bands.

6.3.3 Quantitative PCR analysis of AtGSL *mRNA levels*

To determine whether the dsRNAi vectors in transgenic plants had altered endogenous *GSL* mRNA levels, total RNA was extracted from leaves and inflorescences of transgenic dsRNAi lines. The mRNA levels of the *AtGSL* genes were measured using quantitative PCR (Heid *et al.*, 1996) and data was normalised

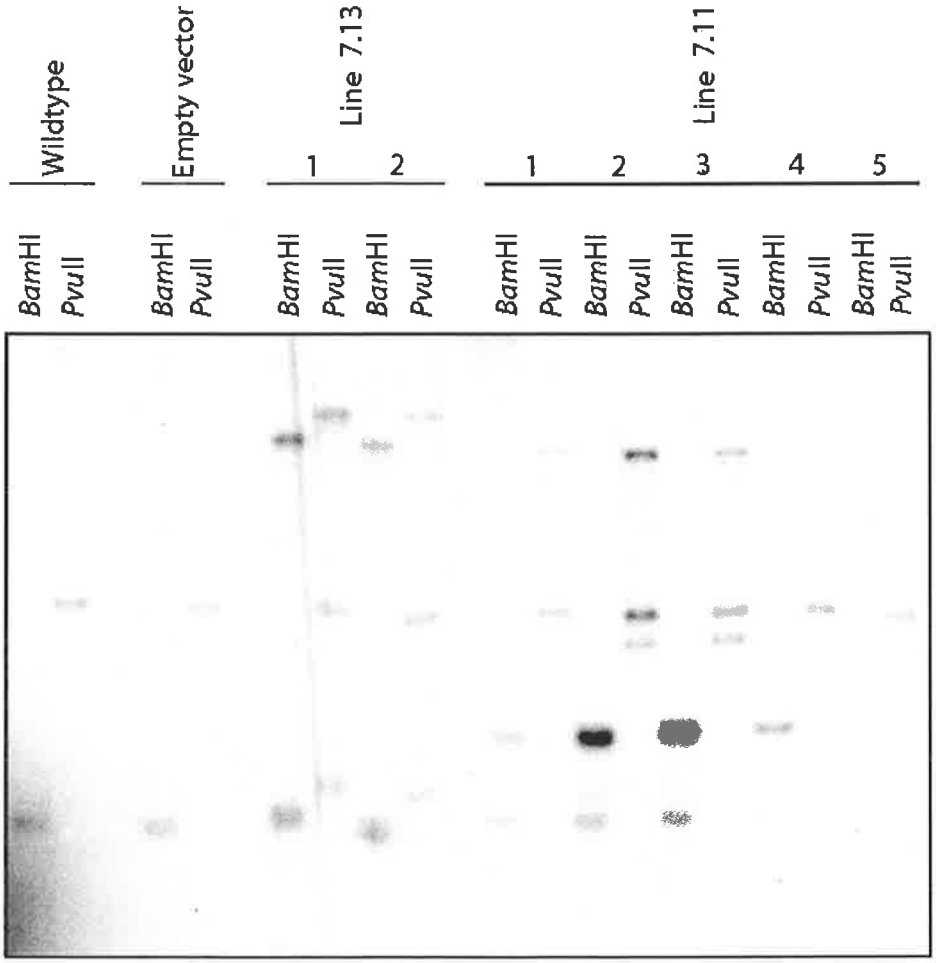

Figure 6.2a Southern analysis of *Arabidopsis* plants transformed with the *AtGSL5*-dsRNAi construct. Genomic DNA was separated by electrophoresis and a gel blot was probed with a radiolabelled *AtGSL5* fragment of 260 bp (*Figure 5.13*). Line 7.13 and 7.11 are independent lines carrying extra copies of *AtGSL5* in comparison to wild type and plants transformed with empty vector, as shown by the number of hybridising bands on the blot.

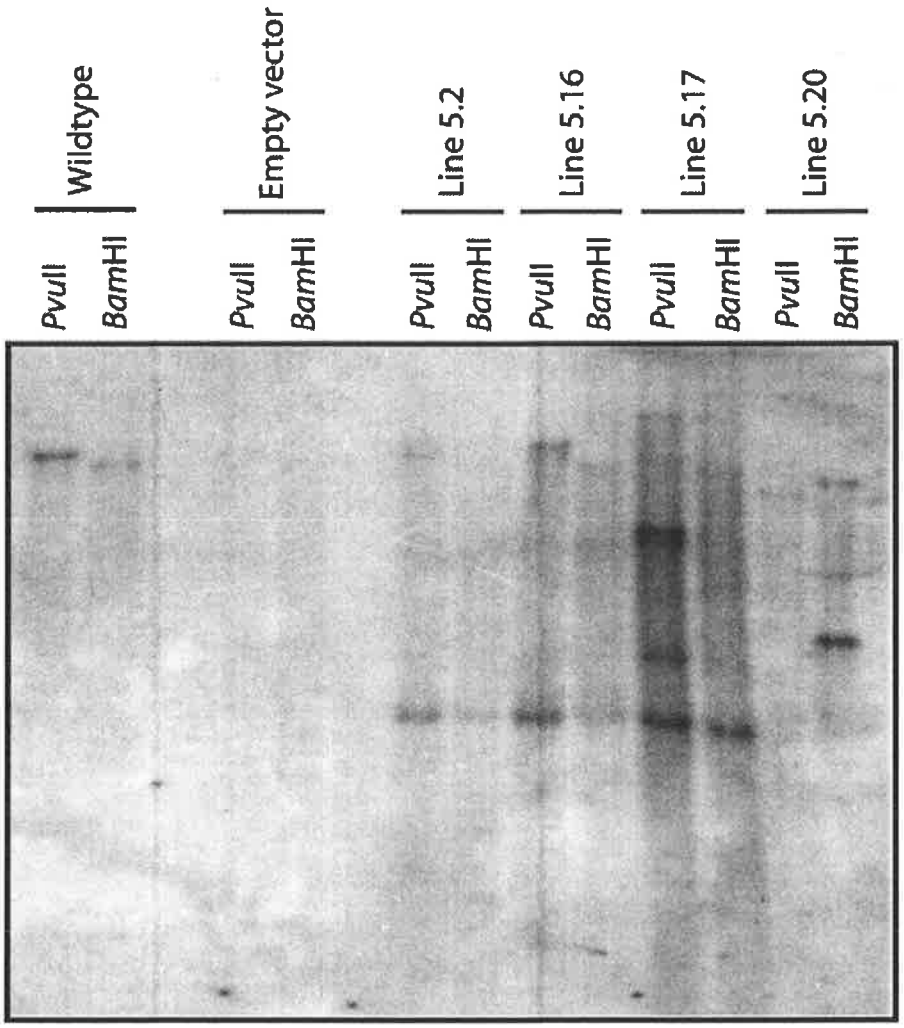

Figure 6.2b Southern analysis of *Arabidopsis* plants transformed with the *AtGSL6*-dsRNAi construct. Genomic DNA was separated by electrophoresis and a gel blot was probed with a radiolabelled *AtGSL6* fragment of 620 bp (*Figure 5.14*). Lines 5.2, 5.16, 5.17 and 5.20 are independent lines carrying extra copies of *AtGSL6* in comparison to wild type and plants transformed with empty vector (faint bands), as shown by the number of hybridising bands on the blot.

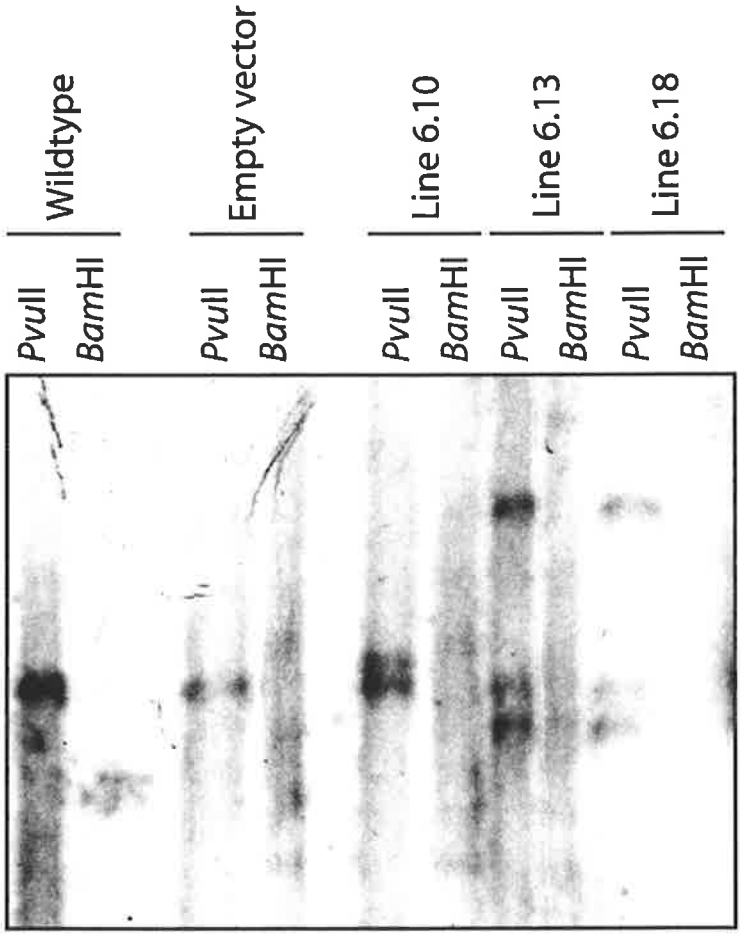

Figure 6.2c Southern analysis of *Arabidopsis* plants transformed with the *AtGSL11*-dsRNAi construct. Genomic DNA was separated by electrophoresis and a gel blot was probed with a radiolabelled *AtGSL11* fragment of 280 bp (*Figure 5.13*). Lines 6.10, 6.13 and 6.18 are independent lines carrying extra copies of *AtGSL11* in comparison to wild type and plants transformed with empty vector, as shown by the number of hybridising bands on the blot.

against the mRNA levels of two internal control genes, glyceraldehyde phosphate dehydrogenase (*GAPDH*) and cyclophilin (*cyclo*), because these genes are reported to have relatively uniform, cellular mRNA levels (Vandesompele *et al.*, 2002).

Quantitative PCR experiments indicated that mRNA levels for the three target *AtGSL* genes were generally 3- to 10-fold less abundant in dsRNAi lines than in the empty vector controls and wild type lines (*Figure 6.3*). In transgenic plants carrying the *AtGSL5*-dsRNAi construct, *AtGSL5* mRNA levels were found to be as much as 80% lower than the level in wild type and transgenics carrying the empty transformation vector. The mRNA levels for the *AtGSL6* and *AtGSL11* genes were also significantly less abundant in dsRNAi transgenic plants in which these genes were targeted, than the empty vector controls and wild type lines (*Figure 6.3*). The mRNA levels of the two *AtGSL* genes not targeted by the dsRNAi vectors were also assayed in all transgenics to determine whether there was any compensatory upregulation of these *GSL* genes in response to the reduced mRNA levels of target genes, but no evidence for this was found (data not shown). The transcript levels of the *AtGSL* genes most closely related to the *AtGSL* genes targeted in the dsRNAi constructs, namely *AtGSL1*, *AtGSL3* and *AtGSL7* were also examined by quantitative PCR, which indicated there may be some down-regulation of these genes (data not shown). The other six members of the *Arabidopsis GSL* gene family were not examined.

6.3.4 Microscopic analysis of callose deposits in transgenic dsRNAi lines

The formation of callosic papillae was examined in transgenic *AtGSL* lines carrying the dsRNAi constructs after inoculating leaves with spores from the virulent powdery mildew fungus, *Sphaerotheca fusca*. Hyphal growth was observed on leaves in all cases, and the rate of hyphal growth did not differ substantially between the lines after 48 h. Callosic papillae that stained brightly with the aniline blue fluorochrome were clearly evident in all *AtGSL6*, *AtGSL11* and control lines (*Figure 6.4a*). In contrast, in all *AtGSL5* transgenic lines, callosic papillae were completely absent, despite the fact that hyphal growth was occurring (*Figure 6.4a G&H and 6.4b*). Papillary callose was completely absent in all leaves from both of the *AtGSL5* independent dsRNAi lines for which at least 15 plants were examined for each line. Further, careful examination of the infection zones revealed no indication that the callosic papillae were

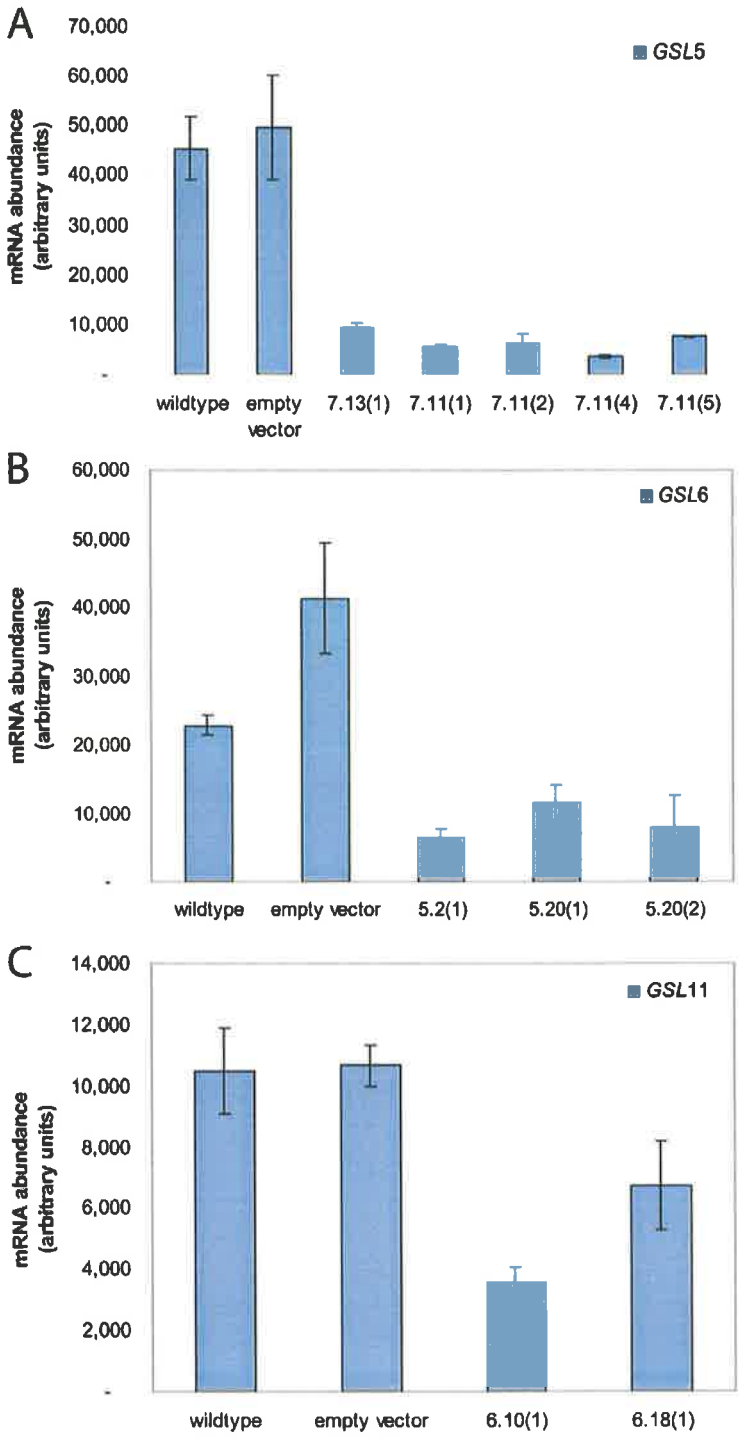

Figure 6.3 *AtGSL* mRNA transcript levels in dsRNAi transgenic lines. Quantitative PCR was used to measure mRNA levels, normalised against the two internal control genes *GAPDH* and *cyclophilin*, and to compare these with mRNA levels in wildtype and empty vector control plants. (**A**) Reduced *AtGSL5* mRNA levels in two independent transgenic *AtGSL5* lines. (**B**) Reduced *AtGSL6* mRNA levels in two independent transgenic *AtGSL6* lines. (**C**) Reduced *AtGSL11* mRNA levels in two independent transgenic *AtGSL11* lines.

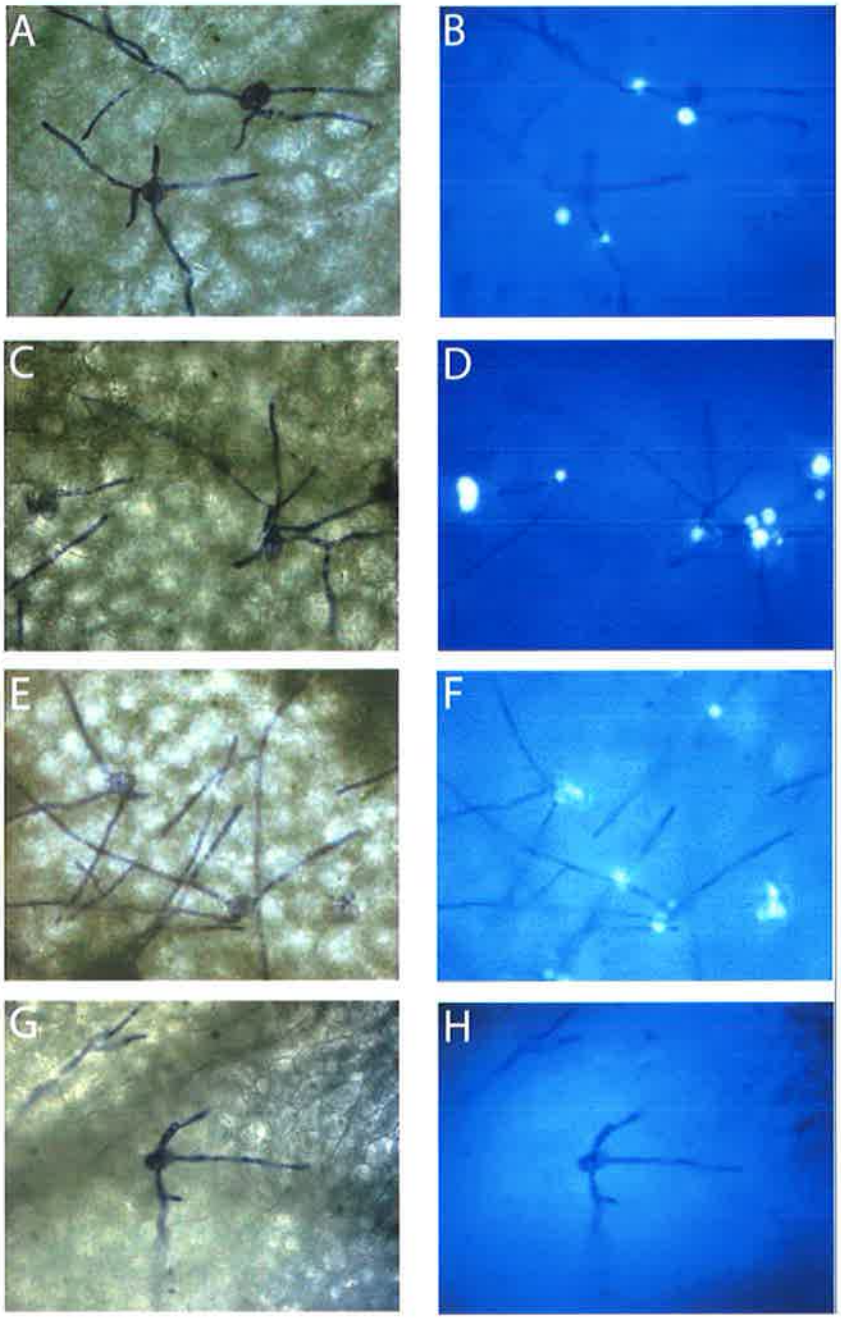

Figure 6.4a Microscopic analysis of leaves of *AtGSL*-dsRNAi transgenic lines of *Arabidopsis* infected with the normally compatible fungus *Sphaerotheca fusca*. Paired images in the left and right hand columns show bright field, Coomassie blue-stained leaf surfaces in parallel with fluorescence images of exactly the same regions of the leaves after staining with the aniline blue fluorochrome, respectively. **(A/B)** Empty vector control. **(C/D)** An *AtGSL6*-dsRNAi transgenic line. **(E/F)** An *AtGSL11*-dsRNAi transgenic line. **(G/H)** An *AtGSL5*-dsRNAi transgenic line. Brightly fluorescing callose deposits can be seen in the empty vector control and the *AtGSL6*- and *AtGSL11*-dsRNAi lines, but is absent in the *AtGSL5*-dsRNAi line.

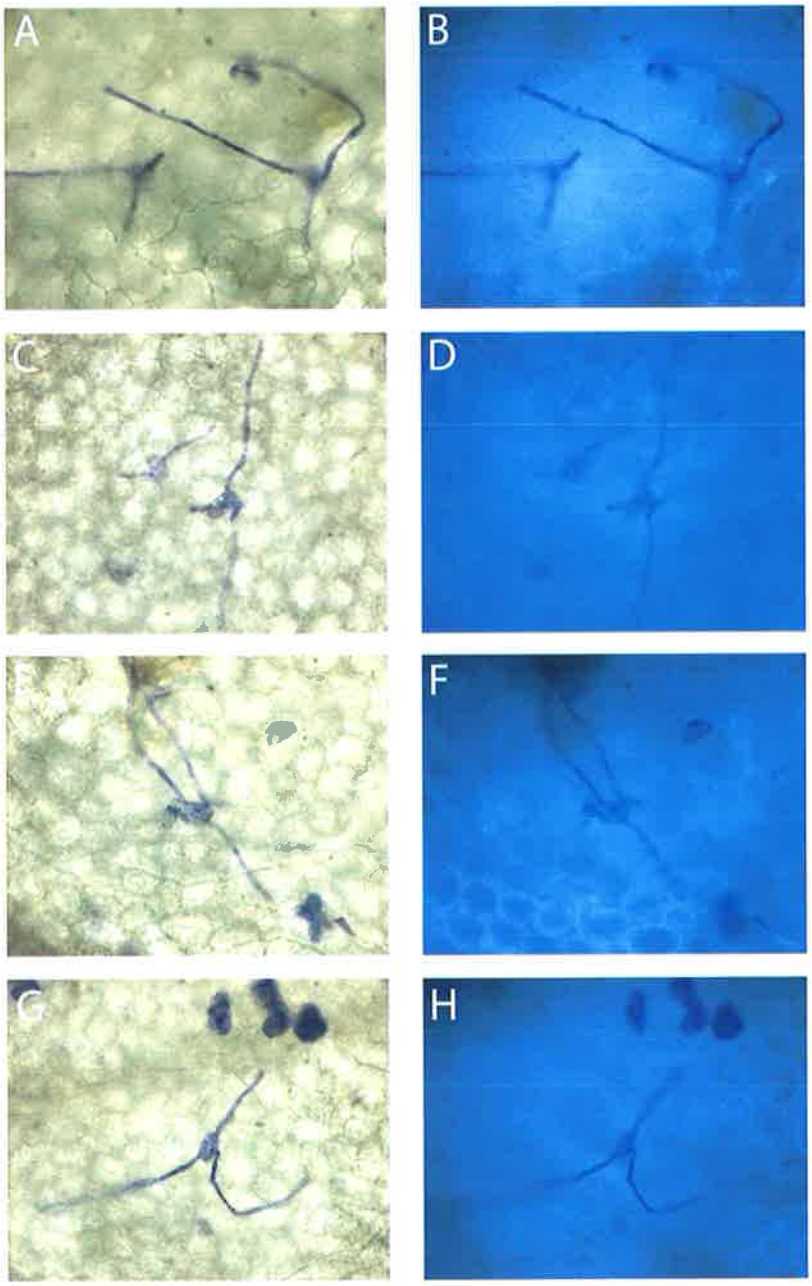

Figure 6.4b Microscopic analysis of leaves of *AtGSL5*-dsRNAi transgenic lines of *Arabidopsis* infected with the normally compatible fungus *Sphaerotheca fusca*. Paired images in the left and right hand columns show bright field, Coomassie blue-stained leaf surfaces in parallel with fluorescence images of exactly the same regions of the leaves after staining with the aniline blue fluorochrome, respectively. **(A/B, C/D, E/F, G/H)** *AtGSL5*-dsRNAi transgenic lines. The brightly fluorescing callose deposits seen in the empty vector control and the *AtGSL6*- and *AtGSL11*-dsRNAi lines (*Figure 6.4a*) are absent in the *AtGSL5*-dsRNAi line.

present in a less compact form. Although papillary callose was not detectable in *AtGSL5* dsRNAi lines, the typical round wall appositions that form beneath fungal appressoria were present. Microscopic examination of the appositions revealed they were indistinguishable from those in wild type plants, except that they contained no callose (*Appendix D*).

The formation of wound callose in *AtGSL5*-dsRNAi lines was also greatly reduced or absent when compared with levels in the *AtGSL6*-, *AtGSL11*-dsRNAi and control lines (*Figure 6.5a and 6.5b*). Leaves from both the *AtGSL5* independent dsRNAi lines failed to produce callose at wound sites at a level comparable to that seen in wild type plants in all cases. Thus, gene silencing experiments clearly demonstrate a role for the *AtGSL5* gene in the deposition of wound and papillary callose. More generally, the data provide strong genetic evidence that the products of glucan synthase-like (*GSL*) genes are essential for callose formation in higher plants.

When pollen grains germinating on the style of the three dsRNAi transgenic lines were examined with the aniline blue fluorochrome, callose deposits in all lines appeared normal (*Figure 6.6*). In addition, no differences were observed in any of the *AtGSL* dsRNAi lines for callose deposits found at the cell plate, although background fluorescence in these images was high (*Figure 6.7*).

6.3.5 Microscopic analysis of callose deposits in mutant lines

To confirm that the effects in the *GSL5*-dsRNAi lines were specific to the lack of the GSL5 callose synthase isoform, a T-DNA insertion line (GABI-KAT 089H05) containing an insertion in the second exon of *GSL5* was examined. The *GSL5* insertion line did not exhibit the slow growth phenotype or show the epinastic leaves of the dsRNAi lines, which suggests there is some vector effect. The *AtGSL5*-dsRNAi vector was shown to alter the mRNA levels of the other most closely related *AtGSL* genes by quantitative PCR reinforcing the need to assess the callose deposits in other *AtGSL5* mutants. Dr. Volker Lipka (Max-Planck-Institute for Plant Breeeding Research, Cologne, Germany) analysed eighteen independent lines segregating for a T-DNA insertion in *AtGSL5* and inoculatied them with conidiospores of the grass powdery mildew *Blumeria graminis*. *Blumeria graminis* failed to produce

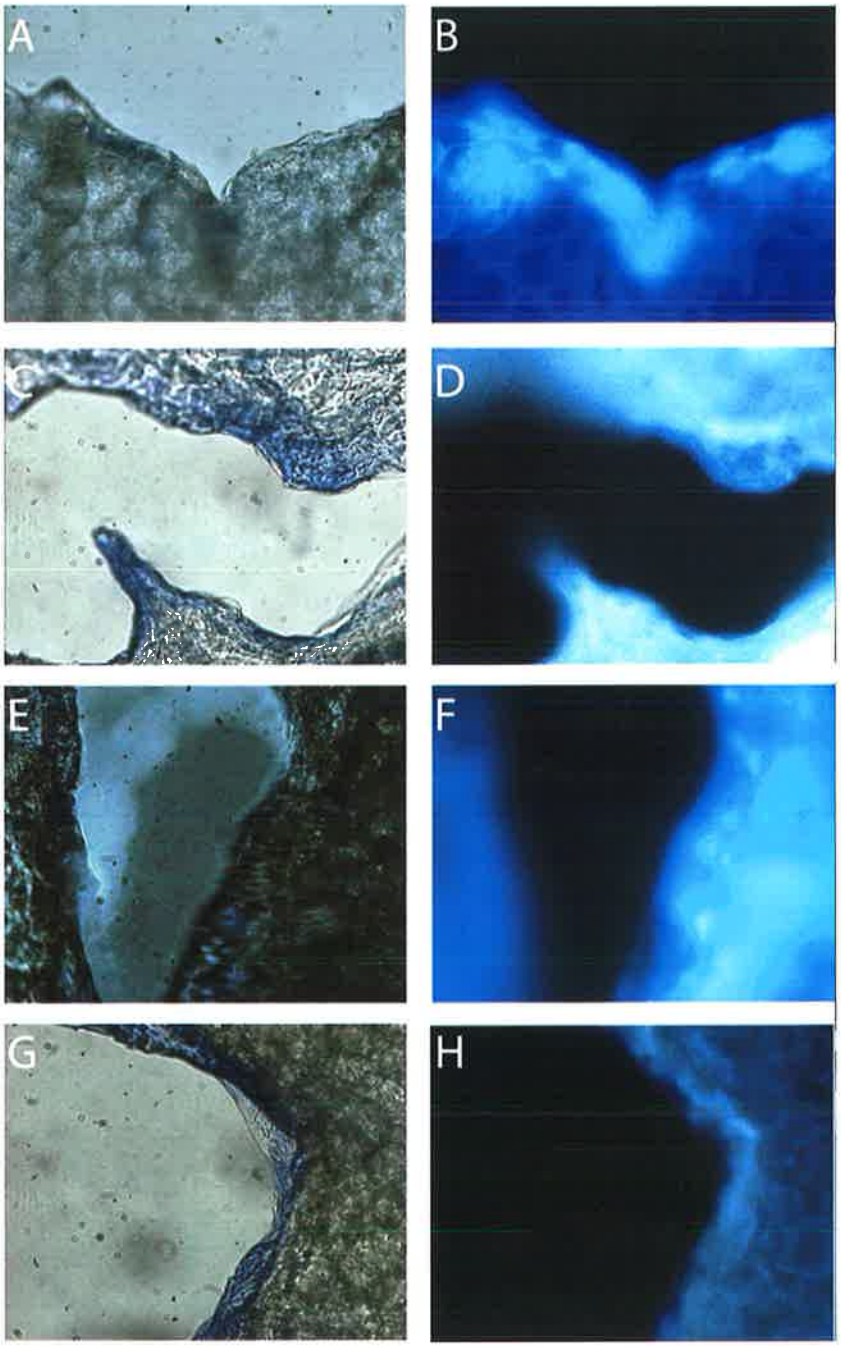

Figure 6.5a Microscopic analyses of wounded leaves from *AtGSL*-dsRNAi transgenic lines of *Arabidopsis*. Paired images in the left and right hand columns show bright field, Coomassie blue-stained leaf surfaces in parallel with fluorescence images of exactly the same regions of the leaves after staining with the aniline blue fluorochrome, respectively. (**A/B**) Empty vector control. (**C/D**) An *AtGSL6*-dsRNAi transgenic line. (**E/F**) An *AtGSL11*-dsRNAi transgenic line. (**G/H**) An *AtGSL5*-dsRNAi transgenic line. Brightly fluorescing callose deposits can be seen in the empty vector control and the *AtGSL6*- and *AtGSL11*-dsRNAi lines, but is absent in the *AtGSL5* -dsRNAi line. The dark regions of the sections correspond to the holes punched in the leaves during wounding.

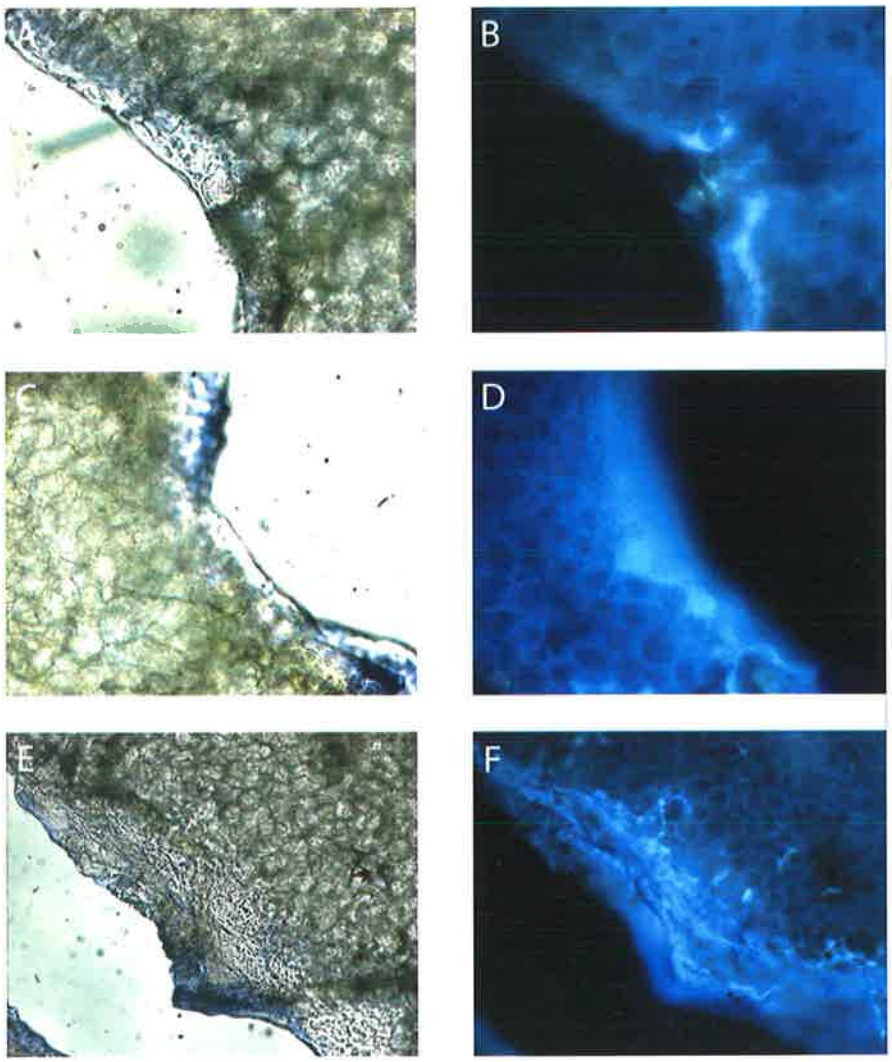

Figure 6.5b Microscopic analyses of wounded leaves from *AtGSL5*-dsRNAi transgenic lines of *Arabidopsis*. Paired images in the left and right hand columns show bright field, Coomassie blue-stained leaf surfaces in parallel with fluorescence images of exactly the same regions of the leaves after staining with the aniline blue fluorochrome, respectively. **(A/B, C/D, E/F)** *AtGSL5*-dsRNAi transgenic lines. Brightly fluorescing callose deposits seen in the empty vector control and the *AtGSL6*- and *AtGSL11*-dsRNAi lines (Figure 6.5a) are absent in the *AtGSL5*-dsRNAi lines.

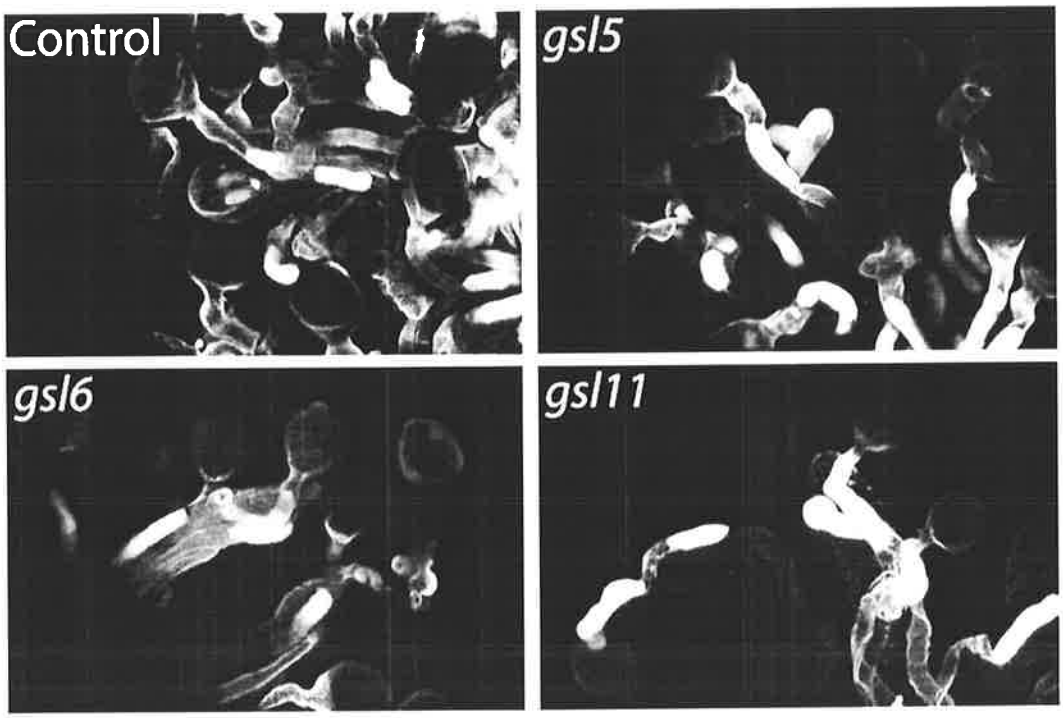

Figure 6.6 Confocal analyses of pollen tubes growing on the style of *AtGSL*-dsRNAi transgenic lines of *Arabidopsis*. No obvious aberrations in callose deposits found in pollen tubes were detectable in any of the *AtGSL* dsRNAi transgenic lines.

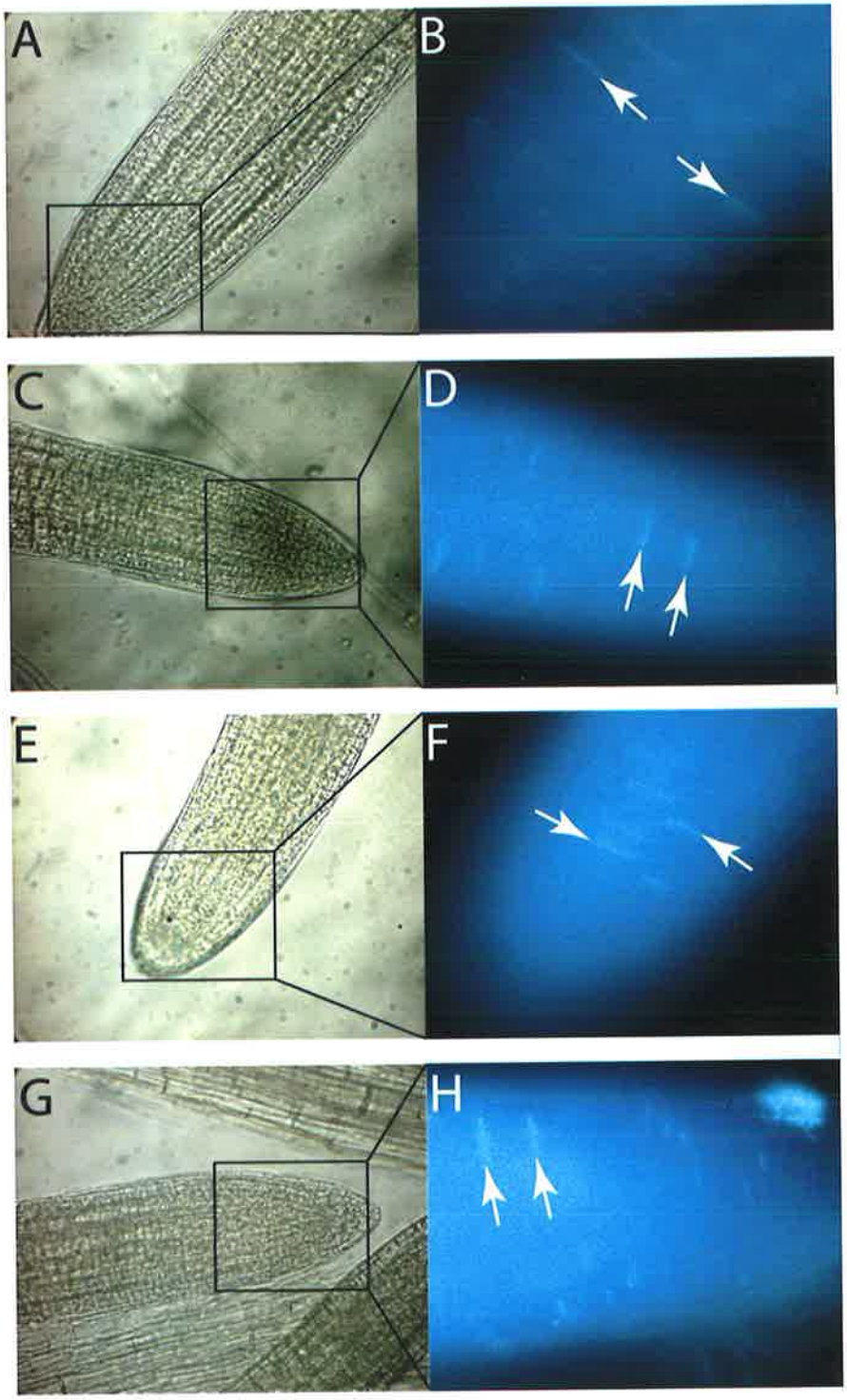

Figure 6.7 Microscopic analyses of root meristems from *Arabidopsis* transgenic plants. Paired images in the left and right hand columns show bright field illuminated root meristems in parallel with fluorescence images of a higher magnification of areas indicated by rectangles after staining with the aniline blue fluorochrome, respectively. **(A/B)** Empty vector control. **(C/D)** An *AtGSL6*-dsRNAi transgenic line. **(E/F)** An *AtGSL11*-dsRNAi transgenic line. **(G/H)** An *AtGSL5*-dsRNAi transgenic line. The bright regions in the fluorescence images indicated with arrows correspond to newly formed crosswalls and the cell plates of dividing cells.

disease on non-host wildtype *Arabidopsis* leaves. Microscopic examination revealed normal conidiospore germination with production of primary and differentiated appressorial germ tubes in contact with the leaf surface (Dr. Volker Lipka, personal communication). However, the germ tubes typically failed to enter the non-host epidermal cells (92% of interaction sites) and were accompanied by the formation of callosic papillae (Dr. Volker Lipka, personal communication). This infection phenotype is similar to other reported non-host interactions between plants and fungal pathogens (Kobayashi *et al.,* 1997; Heath, 2002). Dr. Lipka used PCR procedures to determine whether each line was homozygous or hemizygous with respect to the insertion of T-DNA into the *AtGSL5* gene (*Figure 6.8*). Independent line 10 appeared to carry a T-DNA insert outside the *AtGSL5* gene (*Figure 6.8*), but the absence of callosic papillae in five of the remaining 17 lines was close to the expected ratio of 1:3, bearing in mind that the insertion lines had been pre-selected for sulfadiazine resistance (http://www.mpizkoeln.mpg. de/~GABI-Kat/ GABI-Kat_homepage.html). Thus, callosic papillae deficiency co-segregated with homozygous T-DNA insertion in the *AtGSL5* gene. *B. graminis* penetration indices were only slightly higher in *gsl5* mutant plants than in wild type plants (Dr. Volker Lipka, personal communication), suggesting that callose plays a minor role in resistance to wall penetration.

A cell death response was observed in epidermal cells that were penetrated by *B. graminis* sporelings approx. 48 h after spore inoculation (~15% of interaction sites; Dr. Volker Lipka, personal communication). Cell death was accompanied by an intense aniline blue fluorochrome staining pattern along the entire cell margin in wild type plants, whereas dead epidermal cells in *AtGSL5* insertion lines showed only a punctate callose staining pattern at the cell periphery (Dr. Volker Lipka, personal communication). Thus, GSL5 callose synthase activity not only deposits callose at the papillae and haustoria early in the infection process, but also deposits callose around cell margins during epidermal cell death as the infection proceeds. This implies that significant changes in GSL5 callose synthase levels, activity and/or subcellular location occur during the infection process.

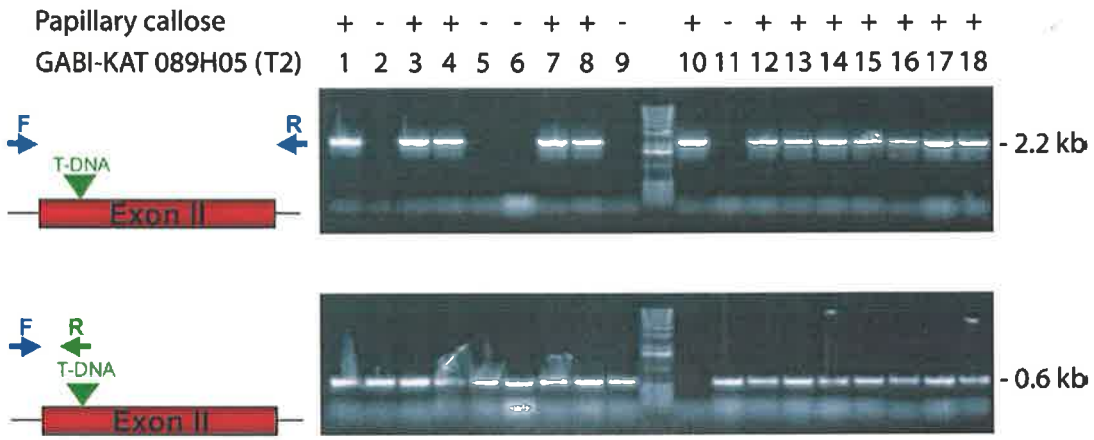

Figure 6.8 Segregation of callose deficiency in independent GABI-KAT 089H05 T-DNA insertion lines. The formation of papillary callose (+ or -) was compared with PCR products generated from genomic DNA preparations. In the top panel, the forward (F) and reverse (R) primers were positioned as shown in the diagram, such that the absence of a T-DNA insert in the *AtGSL5* gene would result in an amplified product of about 2.2 kb. No PCR product is obtained if the approx. 6 kb T-DNA is inserted in the gene. In the lower panel, PCR primers were as shown, with the reverse primer (R) sequence located near the left border of the T-DNA. Thus, PCR products of 0.6 kb would be produced if the T-DNA insert in located the *AtGSL5* gene. Lines homozygous for the T-DNA insert in the *AtGSL5* gene therefore will show no PCR product in the top panel and a positive PCR product in the bottom panel, while hemizygous lines would show PCR products in both panels. Line 10 produces callosic papillae and its *GSL5* gene appears to lack a T-DNA insertion, but the fact that it survived kanamycin selection suggests it has a T-DNA insert outside the *AtGSL5* gene. Image coutesy of Dr. Volker Lipka.

The Arabidopsis *pmr4-1* mutant was previously shown to be resistant against *Erysiphe cichoracearum* and to lack callose at fungal penetration sites. Leaves of the *Arabidopsis* mutant *pmr4-1* were compared to leaves from the *AtGSL5*-dsRNAi line and the *AtGSL5* T-DNA insertion line following inoculation with *Blumeria graminis* and showed similar, dramatic reductions in papillary callose (*Appendix D*). Furthermore, no callose deposits were detected in the leaves of either the T-DNA insertion line or the *pmr4-1* mutant after wounding (*Appendix D*). The phenotypes were exactly the same as those observed in the *AtGSL5*-dsRNAi lines. Together, these data suggest that AtGSL5 is involved in the formation of callose at wound sites and in papillae, and that the genetic basis for the lack of callose in the *pmr4-1* mutant is likely to be a mutation in the *AtGSL5* gene. To investigate this hypothesis, the *AtGSL5* gene of the *pmr4-1* mutant was sequenced.

6.3.6 Sequence analysis of AtGSL5 *in the* pmr4-1 *mutant line*

Phenotypic symptoms similar to those observed here for the *AtGSL5*-dsRNAi lines and the T-DNA line were reported by Vogel and Somerville (2000) in an *Arabidopsis* powdery mildew resistant mutant *pmr4-1*. The *pmr4-1* mutant was originally generated by chemical mutagenesis with methanesulphonic acid ethyl ester and did not form callosic plugs when challenged with several fungal pathogens. Furthermore, the *pmr4-1* gene mapped to chromosome 4 (Vogel and Somerville, 2000) in a position close to the *AtGSL5* gene. To investigate the possibility that *PMR4* was in fact *AtGSL5*, the *AtGSL5* gene in the *pmr4-1* line was sequenced by PCR-based methods. The *AtGSL5* gene in the *Arabidopsis* mutant *pmr4-1* was identical to the *AtGSL5* gene in the databases, except for a single base substitution (G→A) at nucleotide 2060, where numbering started at the ATG translation start codon (Dr. Volker Lipka, personal communication). This would result in the conversion of the TGG codon for Trp687 in AtGSL5 to a TAG stop codon, and the formation of a truncated primary translation polypeptide of 686 amino acid residues.

The position of the lesion in the *AtGSL5* gene of the *pmr4-1* mutant is compared with the position of T-DNA insertion in the GABI-KAT 089H05 line and the target site for the *AtGSL5*-dsRNAi construct in Figure 6.9a. The internal stop codon in the *AtGSL5* gene of the *pmr4-1* mutant and the T-DNA insertion in the GABI-KAT 089H05 line

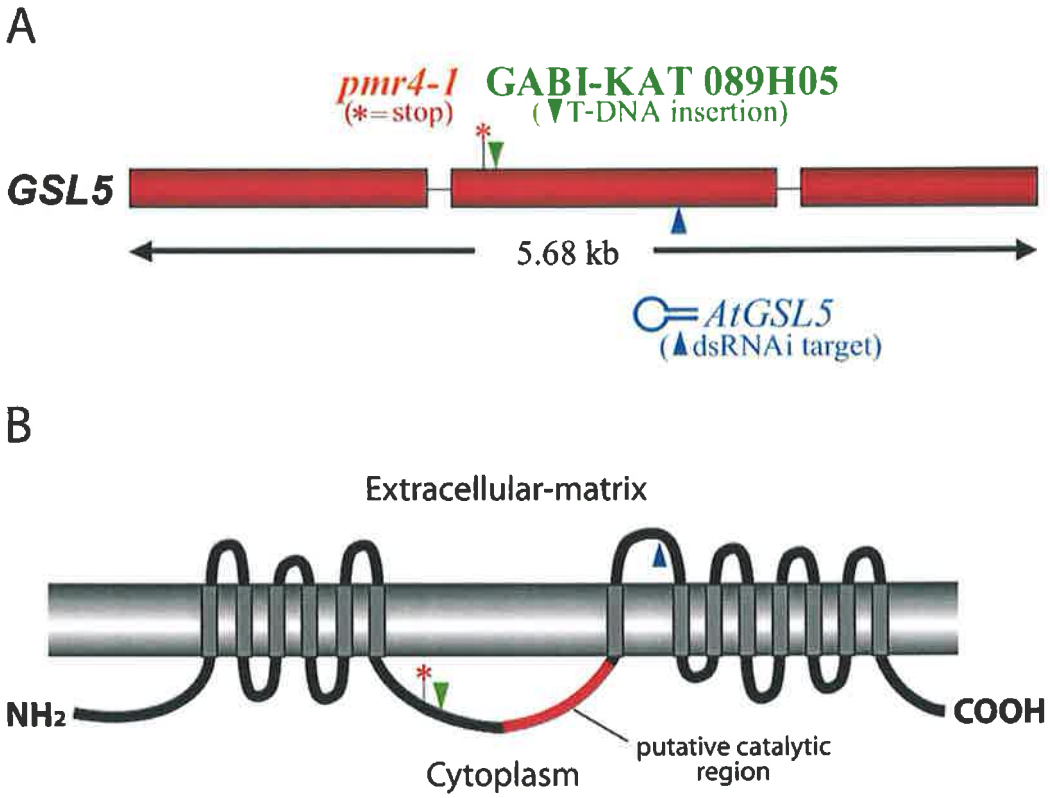

Figure 6.9 Positions of lesions in the *AtGSL5* gene. (**A**) The *pmr4-1* mutant line has a G/A substitution at nucleotide 2060 in the *AtGSL5* gene, and this results in a stop codon in the position marked with an asterisk (*). The T-DNA in the GABI-KAT 089H05 insertion line is located between nucleotides 2170 and 2171, as indicated by the arrowhead (▼). The nucleotide substitution and the T-DNA insertion therefore occur close together in the second exon of the *AtGSL5* gene. The region of the gene targeted by the dsRNAi construct (▲) is located closer to the 3'-end of the second exon. (**B**) Predicted topology of the protein product of the *AtGSL5* gene, showing the NH_2-terminal non-membrane region, six transmembrane helices, the large central non-membrane domain that is presumed to contain the catalytic site, and the multiple transmembrane helices towards the COOH-terminus. The program TopPredII was used to generate this topology diagram and predicts the extracellular and cytoplasmic orientations of the membrane. Again the positions of the *pmr4-1* stop codon (*), the T-DNA insertion (▼) and the dsRNAi target site (▲) are shown.

are located in a similar position in exon 2 of the gene (*Figure. 6.9a*). Based on a number of topology prediction programs, the lesions would disrupt the protein sequence close to the last transmembrane helix before the large, non-membrane and presumably cytoplasmic region of the protein that is widely assumed to contain the catalytic site (*Figure. 6.9b*; Cui *et al.*, 2001; Hong *et al.*, 2001; Doblin *et al.*, 2001; Østergaard *et al.*, 2002; Li *et al.*, 2003). It is highly unlikely that the truncated protein would have any callose synthase activity, although the large, non-membrane NH_2-terminal region could still be active; the role of this region in callose synthase activity has not been defined.

6.3.7 Pathogenicity assays

The *AtGSL5*-dsRNAi lines and the GABI-KAT 089H05 T-DNA insertion line, collectively referred to here as *gsl5* mutants, were inoculated with the fungal pathogens *Sphaerotheca fusca*, *Blumeria graminis*, *Erisyphe cichoraceum*, *Golovinomyces orontii* and the oomycete *Peronospora parasitica* pv *Cala2* to ascertain whether these *gsl5* mutants, like the *pmr4-1* mutant, exhibited any enhanced disease resistance phenotype. Pathogenicity assays were conducted by Dr Volker Lipka at the Max Planck Institute for Plant Breeding Research in Cologne.

In contrast to the susceptible *AtGSL5* wild type plants, leaves of both the *gsl5* mutants showed no obvious symptoms of fungal colonization (*Appendix D*), consistent with resistant phenotypes that were previously reported for *pmr4-1* mutants (Vogel and Somerville, 2000). In addition, when *pmr4-1* plants were inoculated with *B. graminis* spores, the infection phenotype was indistinguishable from that observed in *gsl5* plants, and callosic papillae could not be detected. Enhanced disease resistance phenotypes were also found on *pmr4-1* and *gsl5* mutants 10 days after challenge with the powdery mildew species *S. fusca* and *G. orontii* (Dr. Volker Lipka, personal communication). Microscopic inspection of either mutant revealed greatly reduced hyphal growth and sporangiophore formation, in comparison to wild type leaves (*Appendix D*). This indicates that pathogen growth on *gsl5* mutant plants is much slower than on wild type plants, but is not completely inhibited. A striking encapsulation of haustorial complexes with callose was found in wild type but not in *gsl5* mutant leaves, suggesting that *AtGSL5* participates in callose synthesis both in

papillae and at haustoria, before and after fungal entry into epidermal cells (Dr. Volker Lipka, personal communication). In time course experiments, differential infection phenotypes on mutant and wild type leaves became recognizable at the commencement of callose encasement of haustorial complexes, about 72 h after inoculation. This corroborates the earlier observations that dynamic changes in AtGSL5 activity or location occur as the infection process progresses.

The data collected from these experiments indicate that AtGSL5 may play a crucial role in the maintenance of fungal biotrophy but the mechanism for this is unclear. In *gsl5* mutants callose is absent from papillae, which still form in response to fungal penetration, but the plants are more resistant to a range of fungal pathogens.

6.4 DISCUSSION

The mRNA levels for the specific *AtGSL* genes were lower in each of the corresponding dsRNAi transgenic lines but they were not completely abolished presumably because dsRNAi silencing occurs post-transcriptionally (Fire *et al.*, 1998) or because of potential cell type-specific differences in the activity of the 35S promoter, which was driving the expression of the dsRNAi constructs (Sunilkumar *et al.*, 2002). The regulation of the CaMV 35S promoter may also be affected by infection or wounding leading to an alteration in the level of silencing in cells at different time points. Because dsRNAi plants are expressing this construct constitutively and plants are assayed 24-48 hours post inoculation it seems unlikely that there would be a dramatic change in the level of active GSL protein resulting from minor alterations in expression of the dsRNAi silencing construct.

The *AtGSL6* gene has been implicated in the development of the cell plate during the process of cell division (Hong *et al.*, 2001a). A recombinant AtGSL6:GFP fusion protein was located at the cell plate in transgenic tobacco BY-2 cells and the cells were also found to have elevated levels of callose synthase activity when compared with wild type cells. The AtGSL6 protein also interacts with two cell plate associated proteins, phragmoplastin and a UDP-glucose transferase, and the three proteins are likely to form part of a larger complex that assembles at the cell plate (Hong *et al.*, 2001a, 2001b). However, the *AtGSL6* gene failed to complement a yeast *fks1* mutant (Hong *et al.*, 2001a). Given the apparent involvement of AtGSL6 in the process of cell division, one might reasonably expect that silencing this gene would be lethal, because the process of cell division may be disrupted. Four independent dsRNAi lines targeting *AtGSL6* were followed through to the T_4 stage. None of these lines showed any phenotypic abnormalities or detectable alterations in the process of cell division when dividing cells in root meristems of transgenic plants were analysed after staining with the aniline blue fluorochrome, even though mRNA levels for the *AtGSL6* gene were reduced substantially in the transgenic lines. These data indicate that AtGSL6 may not be the only GSL protein involved in the formation of callose deposits at the cell plate. The plant might be able to compensate for low levels of AtGSL6 in these tissues through the upregulation of other *GSL* genes.

Papillae in *gsl5* mutants were indistinguishable from those in wild type plants, except that they contained no callose. It therefore seems unlikely that callose serves as an essential structural scaffold in papillae (cf. Smart *et al.,* 1986; Bolwell, 1993). The formation of non-callosic papillae in *gsl5* plants indicates that the accumulation of papillae components other than callose continues. Since papillae appear multilayered at the ultrastructural level (Hippe-Sanwald *et al.,* 1992), it is possible that the absence of AtGSL5 activity eliminates only one of the wall apposition layers or components.

In other studies on the *Arabidopsis AtGSL5* gene, Østergaard *et al.* (2002) showed *AtGSL5* partially complements a yeast *fks1* mutant, is likely to be a target of salicylic acid-dependent systemic acquired resistance and that transcriptional activity of the gene was relatively high in flowering tissues. Here, pollen tube callose depositions appear unaffected in plants where *AtGSL5* mRNA levels are substantially reduced. However, the callose deposits in the specialised tissues of flowers that are involved in microsporogenesis or macrosporogenesis were not examined.

The punctate staining pattern in the *AtGSL5* insertion line was reminiscent of plasmodesmata that are known to contain callose (Itaya *et al.,* 1998; Northcote *et al.,* 1989) and it would appear that the absence of heavy GSL5 callose deposition at cell margins exposes the underlying plasmodesmatal callose. This indicates that massive GSL5 callose accumulation normally occurs along the cell margin during pathogen-triggered cellular suicide and that the GSL5 cell margin callose and the plasmodesmata callose are synthesized by different callose synthase isoforms of the same cell.

The different spatial and temporal accumulation pattern of AtGSL5 callose at different subcellular sites in single cells, namely at papillae and haustorial complexes, as well as along the entire cellular periphery following pathogen-provoked cell death, might reflect local stimulation of the activity of pre-existing callose synthase enzyme, or the specific targeting of newly synthesized enzyme to cellular 'stress sites'. Each of the three pathogen-triggered AtGSL5 callose accumulation patterns is consistent with a plasma membrane location for the callose synthase, given that the extra-haustorial membrane is thought to be continuous with the plasma membrane (Giese *et al.,* 1997; Mendgen and Hahn, 2002). The presence of AtGSL5 callose at different

subcellular sites combined with data from transient gene silencing assays in *Arabidopsis* suggests the existence of a mechanism that mediates tight subcellular control of the activity of pre-existing callose synthase.

Wounding of the cell wall is a feature of pathogenesis by biotrophic microorganisms that must enter plant cells for nutrient supply. A rapid rise in cytoplasmic free Ca^{2+} levels ($[Ca^{2+}]$cyt) is a common response of plant cells to wounding (Leon *et al.,* 1998, 2001) and pathogen challenge (Blume *et al.,* 2000; Grant *et al.,* 2000), and it is therefore conceivable that local increases in Ca^{2+} concentrations at wound sites and beneath fungal appressoria contribute to local AtGSL5 stimulation.

There are several possible explanations for the observed increase in fungal resistance if papillary callose is not deposited following the tissue wounding caused by fungal penetration. Wounding is an inherent feature of fungal infection and biotrophic fungi like *Peronospora, Sphaerotheca* and *Golovinomyces* might have exploited components of the wound response for the establishment of compatible interactions. Firstly, callose might be needed as a physical support for fungal development, either as a structural scaffold to accommodate haustoria or to allow optimal nutrient uptake *via* haustoria (cf. Smart *et al.*, 1986; Bolwell, 1993). The presence of round wall appositions beneath fungal appressoria in *gsl5* mutants that are much like those in wild type plants does not support this theory. Secondly, signalling oligosaccharides released from the linear (1→3)-β-D-glucan of callosic plugs by (1→3)-β-D-glucanases or other components of callosic plugs, such as phenolic compounds, might be needed for fungal development, or as effectors of the host's defense responses. Because fungal penetration is not enhanced or inhibited in the absence of callosic plugs, one might conclude that these structural and chemical possibilities are not important for initial penetration and for the formation of haustoria. They might still be important for nutrient uptake by haustoria after successful penetration.

Perhaps a more likely explanation is that the absence of papillary callose that normally encases invading fungal pathogens would lead to the unmasking of fungal cell wall polysaccharides. Unmasking hyphal walls would presumably expose the (1→3, 1→6)-β-D-glucans, chitin and chitosan polysaccharides that are structural

components of walls of many fungi (Bartnicki-Garcia, 1968) to the action of pathogenesis-related hydrolases such as (1→3)-β-D-glucanases and chitinases that are induced *via* jasmonic acid defence pathways following wounding (Rakwal *et al.*, 2001; Sano *et al.*, 1996). Certain branched (1→3, 1→6)-β-D-oligoglucosides and chitin/chitosan oligosaccharides released from these polysaccharides by partial endohydrolysis are highly active elicitors of phytoalexin accumulation in plants, even at concentrations as low as 10 nM (Côté and Hahn, 1994) and stimulate salicylic acid defence pathways which may lead to resistance (Hunt *et al.*, 1996; Ryals *et al.*, 1996; van Wees and Glazebrook, 2003). Linear (1→3)-β-D-oligoglucosides of the type that would be released from callose itself by the (1→3)-β-D-glucanases are not active in eliciting phytoalexin accumulation (Côté and Hahn, 1994). Thus, unmasking the hyphal walls could facilitate the release of oligosaccharides that would enhance or accelerate the plant's defensive responses to fungal attack.

The evolution of (1→3)-β-D-glucanase inhibitors by pathogenic fungi implies that inhibiting the release of (1→3, 1→6)-β-D-oligoglucosides is important for the establishment of fungal infection (Rose *et al.*, 2002). Similarly, when the promoter of the *AtGSL5* gene was examined for pathogen-inducible *cis*-acting elements, a W box sequence of TTGACC was found about 1.4 kb upstream from the ATG translation start point of the gene (data not shown). This is believed to be a binding site for the WRKY family of transcription factors (Rushton *et al.*, 2002). A related promoter element GGTCAGTAAGTC, located about 1 kb upstream from the ATG codon of the *AtGSL5* gene (data not shown), corresponds closely with other plant gene elements that are inducible by elicitor oligosaccharides from fungal cell walls (Fukuda, 1997). The latter element is not present in any of the other *AtGSL* genes.

If unmasking fungal wall polysaccharides were the mechanism of increased resistance observed in the dsRNAi *AtGSL5* silenced plants here and in the *pmr4-1* mutant, one would not expect to see enhanced resistance to bacterial pathogens, which have no (1→3, 1→6)-β-D-glucan or chitin in their cell envelopes. This would explain why Vogel and Somerville (2000) could find no increase in resistance against the Gram negative bacterial pathogen *Pseudomonas syringae* in the *Arabidopsis pmr4-1* mutant. However, some pathogenesis-related chitinases produced by plants in response to

pathogen attack can hydrolyse murein, a polysaccharide homomorphous with chitin that constitutes the backbone of bacterial cell wall peptidoglycans (Stone and Svensson, 2001). If the peptidoglycan were exposed to the action of the plant chitinase, as might be expected in Gram positive pathogens, partial endo-hydrolysis of murein could release oligosaccharides that might elicit an incompatible response (Côté and Hahn, 1994; Felix and Boller, 2003).

Finally, it is possible that the enhanced resistance to fungal pathogens seen here with mutants of the *AtGSL5* callose synthase gene could result from disruption of a cell wall integrity pathway in the plant host. In *Saccharomyces cerevisiae* there appears to be a complex system that monitors cell wall integrity and is thought to involve the (1→3)-β-D-glucan synthase *FKS* genes, cell surface proteins that act as mechanosensors of changes in wall shape, and a signalling cascade (Philip and Levin, 2001). In contrast to the abundance of (1→3)- and (1→3, 1→6)-β-D-glucans in yeast cell walls, plant cell walls generally contain no (1→3)-β-D-glucan. It is nevertheless possible that a related cell wall or callose integrity pathway exists in plants and might have been corrupted during evolution by biotrophic fungi for invasive growth. The absence of callose might prevent the fungus from using this pathway for pathogenesis.

6.5 SUMMARY AND CONCLUSIONS

Levels of individual mRNA transcripts were reduced in all transgenic lines in which specific *AtGSL* genes were silenced with dsRNAi constructs. Both papillary callose and wound callose were absent in lines transformed with the *AtGSL5*-dsRNAi construct but were unaffected in *AtGSL6*- and *AtGSL11*-dsRNAi lines. Callose at the cell plate in dividing cells and in germinating pollen tubes appeared normal in all dsRNAi lines.

The role of *AtGSL5* in papillae and wound callose formation was confirmed in T-DNA insertional mutants of the *AtGSL5* gene and it was further shown that the callose deficiency co-segregated with homozygous *AtGSL5* T-DNA insertion (*Appendix D*). Phenotypic symptoms similar to those observed here for the *AtGSL5*-dsRNAi lines and the T-DNA lines were reported by Vogel and Somerville (2000) in an *Arabidopsis* powdery mildew resistant mutant *pmr4-1*. Furthermore, the *pmr4-1* gene mapped to chromosome 4 (Vogel and Somerville, 2000) in a position close to the *AtGSL5* gene. To investigate the possibility that the *pmr4-1* gene was in fact *AtGSL5*, the *AtGSL5* gene in the *pmr4-1* line was sequenced. A nucleotide substitution that would introduce an internal stop codon and shorten the protein from 1,780 amino acid residues to 686 amino acid residues was detected in the *AtGSL5* gene of *pmr4-1*. It is highly likely therefore that *pmr4-1* and *AtGSL5* are the same gene. Gene silencing experiments and the mutant data clearly demonstrate a role for the *AtGSL5* gene in the deposition of wound and papillary callose. More generally, the data provide strong genetic evidence that the products of glucan synthase-like (*GSL*) genes are essential for callose formation in higher plants.

Perhaps the most surprising observation with the *AtGSL5*-dsRNAi lines, the *pmr4-1* mutant and related T-DNA insertion line is their enhanced resistance to attack by various fungal pathogens (*Appendix D*). A longstanding and well-documented belief that the callosic papillae physically inhibit fungal penetration and the establishment of a compatible interaction (Stone and Clarke, 1992), is not supported by these results, because the removal of callose would be expected to facilitate fungal penetration and infection.

CHAPTER 7

SUMMARY AND FUTURE WORK

7.1 SUMMARY OF EXPERIMENTAL RESULTS

Callose is a (1→3)-β-D-glucan that is widely distributed in higher plants and is readily recognizable in tissue sections through the formation of an intense yellow, UV-induced fluorescence with the aniline blue fluorochrome (Stone *et al.,* 1985). During normal plant growth and development, callose is found as a transitory component of the cell plate in dividing cells, it is a major component of pollen mother cell walls and pollen tubes, and is found as a structural component of plasmodesmatal canals. Callose is also observed in abscission zones and in the phloem of dormant tissues (Stone and Clarke, 1992). In addition to its role in normal growth and development, callose is deposited between the plasma membrane and the cell wall following exposure of plants to a range of abiotic and biotic stresses, including wounding, desiccation, metal toxicity and microbial attack (Stone and Clarke, 1992).

The central importance of callose deposition in several key plant processes, both under normal growth conditions and following abiotic or biotic stress, has prompted many attempts to purify and characterize callose synthases from plants. So far, no highly purified callose synthase preparations have been reported, but there is accumulating evidence that they are encoded by a family of glucan synthase-like genes (*GSL*) (Cui *et al.,* 2001; Hong *et al.,* 2001; Doblin *et al.,* 2001; Østergaard *et al.,* 2002), based on the homology of these plant genes with yeast *FKS* genes that are also believed to be involved in (1→3)-β-D-glucan biosynthesis (Douglas *et al.,* 1994; Coutinho and Henrissat, 1999). It is important to note that to date only Hong *et al.* (2001a) have demonstrated, albeit circumstantially by detection of elevated callose synthase activity of a fusion protein in a heterologous plant and the location of the fusion protein at a site of known (1→3)-β-D-glucan synthase activity, that any kind of (1→3)-β-D-glucan synthase activity is associated with *GSL* genes. No group has provided unequivocal genetic evidence that (1→3)-β-D-glucan synthase activity is specifically associated with a single gene. However, the gene silencing experiments and mutant data presented here clearly demonstrate a role for the *AtGSL5* gene in the deposition of wound and papillary callose. More generally, the data provide strong genetic evidence that the products of glucan synthase-like (*GSL*) genes are essential for callose formation in higher plants.

The isolation and functional analysis of *GSL* genes was pursued in three different plant species, namely *Lolium multiflorum*, *Hordeum vulgare* and *Arabidopsis thaliana*. A *GSL* gene was initially isolated from *L. multiflorum* because the biochemical properties of (1→3)-β-D-glucan synthases from *L. multiflorum* were well characterised. The functional analyses were subsequently focussed on *H. vulgare*, for a number of reasons. Firstly, a homologue of the *LmGSL1* gene had been isolated from barley by a colleague (Li *et al.*, 2003). Secondly, more genetic information in terms of EST data, *GSL* gene numbers and chromosomal locations was available for barley when compared with *L. multiflorum*. Thirdly, there was an existing barley cDNA library that could be screened for protein-protein interactions and finally, a transient gene silencing system was available in barley. The reasons for then shifting the functional analyses to *Arabidopsis* were three-fold. Firstly, the full genome sequence for *Arabidopsis* was publicly available and this meant that the expression of the twelve putative *AtGSL* genes could be analysed and secondly, because of the ease and speed at which transgenic plants could be generated for functional analysis of the *GSL* genes through gene silencing experiments. Finally, superior genetic resources are available for *Arabidopsis*, including gene mapping data, microarray expression data and access to defined mutants.

A *GSL* gene, designated *LmGSL1*, encoding 1906 amino acid residues was isolated from *Lolium multiflorum*. The function of a homologous gene, *HvGSL1*, identified in barley was studied in an attempt to directly demonstrate (1→3)-β-D-glucan synthase activity in two heterologous expression systems. Two polypeptides corresponding to the larger predicted cytoplasmic domains of the barley HvGSL1 protein were expressed in *E. coli* and in the human embryonic kidney cell line, 293T. No (1→3)-β-D-glucan synthase activity could be attributed to the expressed polypeptides when enzyme assays on partially purified and crude cellular extracts were conducted. The HvGSL1 protein was further investigated using the yeast two-hybrid system. The two HvGSL1 polypeptides corresponding to the larger predicted cytoplasmic domains of the barley HvGSL1 protein were used as baits to screen an *Arabidopsis* whole plant cDNA library, a barley inflorescence cDNA library and a wheat early developing endosperm cDNA library. The NH_2-terminal cytoplasmic domain of the HvGSL1 protein was found to interact with an *Arabidopsis* protein that shared homology to an

unknown rice protein and to a barley protein that shared homology to a tryptophan synthase α-subunit-like protein.

The barley *HvGSL1* gene was targeted for silencing in a loss-of-function approach, using dsRNAi constructs in transient assays. No differences between wild type and transformed barley cells were found when the callose deposits resulting from fungal challenge were examined. Phylogenetic analyses of the barley *HvGSL1* gene shows that this gene is most closely related to the *Arabidopsis AtGSL10* gene that contains multiple introns whereas *AtGSL5* contains only two introns. If the genomic structure of the *GSL* genes is related to their function then it would be unlikely that *HvGSL1* is involved in the formation of papillary or wound callose. The transient gene silencing experiments were therefore unlikely to have an effect on the formation of wound or papillary callose. Transient dsRNAi silencing assays using a newly developed technique for the bombardment of intact *Arabidopsis* plants targeted three *Arabidopsis* genes, namely *AtGSL5*, *AtGSL6* and *AtGSL11*. Results of these assays were inconclusive and further experimentation into the function of these genes was performed in stably transformed *Arabidopsis* plants.

The *Arabidopsis AtGSL5*, *AtGSL6* and *AtGSL11* genes were silenced in transgenic plants expressing dsRNAi vectors. The *AtGSL5* gene was found to be involved in the formation of callose at wound sites and in papillae that form as a result of fungal challenge. A T-DNA insertion line in which *AtGSL5* was disrupted and a previously identified powdery mildew resistant mutant line of *Arabidopsis* that had reduced callose deposits was also found to have a lesion in the *AtGSL5* gene. Both these mutants exhibited the same phenotype as the dsRNAi lines. Counter-intuitively, the abolition of papillae enhanced the resistance of *gsl5* mutants to fungal infection, suggesting that callose deposits at the sites of fungal penetration may mask the presence of fungal hyphae and may be a hindrance to plant defences. Perhaps by limiting access of plant hydrolytic enzymes, such as glucanases and chitinases, to it's cell wall, fungi have exploited the wound response to circumvent plant defence responses.

7.2 FUTURE WORK

The identification of specific functions for the *LmGSL1*, *HvGSL1*, *AtGSL6* and *AtGSL11* genes have been assessed to some extent here, but present opportunities for further studies. Insights into the function of the *LmGSL1* and *HvGSL1* genes of ryegrass and barley, respectively, might be best achieved by the production of transgenic plants that over-express or no longer express the *GSL* genes. Transgenic *Arabidopsis* plants in which the *AtGSL6* and *AtGSL11* genes have been silenced were produced for this study but no function for these genes was immediately evident in the transgenic plants. Over-expression of these genes in transgenic plants might therefore be useful in assigning a biological function to the genes. The generation of GFP fusions to both the promoters and intact proteins of the four genes may also aid in the identification of a function by providing information about when and where the genes are transcribed, and their subcellular locations.

Results presented from the heterologous expression of polypeptides from the barley HvGSL1 protein and from the analysis of the protein interactions did not link HvGSL1 to the production of callose and the role of this protein in barley is not yet understood. Having clearly demonstrated that the AtGSL5 protein is involved in the formation of wound and papillary callose in *Arabidopsis*, it would be useful to conduct expression and protein-protein interaction experiments like those conducted on the *HvGSL1* gene. The information gained from these studies would further our understanding of the process of callose deposition at wound sites and in response to fungal challenge, possibly by enabling the kinetics and 3D structure of the enzyme to be studied and by the identification of interacting proteins that may play a role in callose deposition. The *AtGSL5* gene would be particularly conducive to these studies, because of the limited number of introns that are contained in the genomic sequence of this gene and because the sequence is accessible *via* DNA databases. A full-length cDNA could be produced with relative ease.

Finally, *Arabidopsis* transgenic plants, in which the expression of the *AtGSL5* gene has been disrupted, are more resistant to fungal challenge. The identification of *AtGSL5* homologues in economically important crop species and the subsequent determination of whether the disruption of this gene has an effect upon pathogen

susceptibility might prove to be a major contribution to crop science, particularly if *GSL5* knockout lines showed broad spectrum resistance to a range of fungal pathogens.

7.3 CONCLUDING REMARKS

Molecular techniques that alter the expression of a single gene within a complex biological system can be used to elucidate gene function through detection of an altered phenotype. The biological function of a plant (1→3)-β-D-glucan synthase, namely AtGSL5, has been demonstrated in transgenic plants utilising a post-transcriptional gene silencing approach and the results were confirmed by comparison to a T-DNA insertional mutant and another mutant that was also found to contain a lesion in the *AtGSL5* gene. *AtGSL5* is one of twelve genes in *Arabidopsis* that have been identified on the basis of sequence homology to the yeast *FKS1* gene and appears to have a distinct and limited biological role within the plant. The functions of the other *GSL* genes of *Arabidopsis* have yet to be discovered but the approach for assigning gene function described here might be employed equally well to uncover functions of the other genes. The availability of genome sequence data and other tools such as mutant lines for the model plant *Arabidopsis* has enabled the rapid identification of the function of the *AtGSL5* gene and provides a starting point for isolating homologous genes in other economically important plant species.

Appendices

Appendix A. Liquid hydroponic media

Used in the cultivation of various plant species. Concentrations represent those in the complete final media.

Macro nutrients	mM
KNO_3	1.25
$Ca(NO_3)_2$	1.50
$MgSO_4.7H2O$	0.75
KH_2PO_4	0.50

Micronutrients	µM
KCl	50
H_3BO_3	50
$MnSO_4.H2O$	10
$ZnSO_4.7H2O$	2
$CuSO_4.5H2O$	1.5
$(NH_4)_6Mo_7O_{24}$	0.075
$Na_2O_3Si.5H2O$	0.1 mM
$C_{10}H_{12}O_8N_2FeNa.H2O$	72 µM

Appendix B. Oligonucleotides used in PCR

Primer	Sequence 5' → 3'
dsRNAi1	GAGCTCATATTACGAGGCGCGCCGGCATCAG
dsRNAi1R	GCCGTTTCCTGCAGCAAGCTTT
dsRNAi2	TTTCATATTACCCGGGGTGGGATCCG
dsRNAi2R	GCCGATATCCTACGCGTCAACTTT
dsRNAi3	TGAGAGCTCAGGGAATCTGGCGCGCCTTC
dsRNAi3R2	TCCCTGCAGCAAGCTTTTCCA
dsRNAi4	TGAAGCTGAGGGGATCCCGGGTGTGTTC
dsRNAi4R	TCCTTGCCGATATCACGCGTTCCA
pUBI-NOS MCSF	AGCTTCTGCAGAGCTCGGCGCGCCCGGGATCCACGCGTGGAT
pUBI-NOS MCSR	ATCCACGCGTGGATCCCGGGCGCGCCGAGCTCTGCAGA
Y1F	GGGGACAAGTTTGTACAAAAAAGCAGGCTACCGGATGGGCGGCGTCTACGGG
Y1R	GGGGACCACTTTGTACAAGAAAGCTGGGTTCCAGACAGGACGCAGTGGTAA
Y2F	GGGGACAAGTTTGTACAAAAAAGCAGGCTGCCTGGGAGAGATTAGGTCTGTT
Y2R	GGGGACCACTTTGTACAAGAAAGCTGGGTAGTCAAAAAGTTGCCCAAGTCT
Ent3	GGCCAGAGCTGCAGCTGGAT
Ent5	CTCGGGCCCCAAATAATGAT
UAP	CUACUACUACUAGGCCACGCGTCGACTAGTACGGGIIGGGIIGGGII
AAP	CUACUACUACUAGGCCACGCGTCGACTAGTAC
UBI3'seq1	AGCCCTGCCTTCATACGCTATTT
NOS5'seq1R	ATAATCATCGCAAGACCGGCAAC
AtdsRNAi1	ATCGGATTAAGCTTCCGGGACCA
AtdsRNAi1R	CCGTCCATAAAGAAACACATACACCGTAA
RiCS2F	TTCATGGCGGCGCAGAATACAGA
RiCS2R	TGCCACTCGAAACCAGAGGGATTG
RiCS3F	TGGCTTTTTGCTCCCTTCCTCTTCA
RiCS3R	ATCTCCGCCTTCCAACCGAAACA
RiCS4F	AGGGAGAGATGTGGGACTCAACCAA
RiCS4R	CGAACGACTGCGAAGCAAGGATAA
RiCS5F	TGGGTTTGAGCAGCACCGAAAGA
RiCS5R	GCTGACATTTCCAGCCAAGAGACCA
RiCS6F	TGGGAATCGTGGTGGAACGTAGA
RiCS6R	TGACTGACAAAAAGCCGAGGAAGAGA
RiCS7F	TGTGGTTCCTGGTGACTTCTTGGTTGT
RiCS7R	GGCGAGCGATGTTGAGGTGGTAG
RiCS8F	CGGGAGGGGTCAGGAGAAGACAC
RiCS8R	CGTACTTTCGGAGCATCGGGCATA
RiCS9F	AAGGGAAGGTTGCTGGTGGGAATG
RiCS9R	TCAAGGCGGCGCTAAGTGCAGTA
RiCS10F	GTCGTGGTGGGAGGAAGAACAGG
RiCS10R	CGGTCGGGATAAAACCAAGGACAC
RiCS11F	CACGAGGAGATGCGATTCAGACCA
RiCS11R	CACCCCGAGGCACAAACCAAAAC
RiCS12F	GGAAGGGACGGGATGTTGGATTG
RiCS12R	CGGCGTTGGTGTCCGTACTGTCT

RiCS1R	CCATCGATAAAGGATCCCATACACCGTAA
RiCS1b	CATCCATGGGATTAAGCTTCCCGGGCCA
2HRev	AGATGGTGCACGATGCACAG
MlaF	CCCAAGCTTCTGCAGAGCTCGGCGCGCCGTATGCATCAATTTAGAAAAAA GT
MlaR	GGATATCCACGCGTGGATCCCGGGCTACATTAGTTCAGAGTGTCAGTGTA
HvGSL1	GACCCCATGGGCGGCGTCTACG
HvGSL1R	TCCAGACAGGACCCCGGGGTAAA
HvGSL2	GCCTGGGAGAGCATATGTCTGTT
HvGSL2R	AGTCAAAAGGATCCCCAAGTCTG
HvGSL3	CCGAAGGCCGCCATATGAGTAATC
HvGSL3R	TGTCTGCTGCATTTGGATCCCTGTTG
HvGSL1XhoI	CTCGAGCCACCATGGACCGGATGGGCGGCGTCTACGGG
HvGSL2XhoI	CTCGAGCCACCATGGGCCTGGGAGAGATTAGGTCTGTT
HvGSL1REagI	CGGCCGTCACAGATCCTCTTCAGAGATGAGTTTCTGCTCCCAGACAGGAC GCAGTGGTAA
HvGSL2REagI	CGGCCGTCACAGATCCTCTTCAGAGATGAGTTTCTGCTCGTCAAAAAGTT GCCCAAGTCT
T3	AATTAACCCTCACTAAAGGGAA
T7	GTAATACGACTCACTATAGGGC
SP6	ATTTAGGTGACACTATAG
AP1	GGATCCTAATACGACTCACTATAGGG
AP2	AATAGGGCTCGAGCGGC
Anchor primer	CTGGTTCGGCCCACCTCTGAAGGTTCCAGAATCGATAG
LM5.8sF	TTGCAATTCTATATAATCCACACGA
LM5.8sR	TCCGCTTATTGATATGCTTAAATTC
lmgapdhF	CCACCGGTGTCTTCACTGACAAGG
lmgapdhR	GCCTTAGGATCAAAGATGCTGG
CS6Hind	TGGGAAGCTTGGTGGAACGTAGA
CS6RBam	TGACTGACAAGGATCCGAGGAAGAG
CS12Xma	GGAAGGCCCGGGATGTTGGATTG
CS12RSpe	CGGCGTTGGTGTCCGTACTAGT
CalS1Rb	CCGTCCATAAAGGATCCCATACACTAGT
AtGSL5-ex2F	CGCAGATGCTGCATATAA
AtGSL5-ex2R	CAGTATAGTTAGTTAGAAATAATCC
AtGSL5-ex3F	GGATTATTTCTAACTAACTATACTG
GABI T-DNA LB	CCCATTTGGACGTGAATGTAGACAC
AtGAPDHF	TGGTTGATCTCGTTGTGCAGGTCTC
AtGAPDHR	GTCAGCCAAGTCAACAACTCTCTG
AtCycloF	TGGCGAACGCTGGTCCTAATACA
AtCycloR	CAAAAACTCCTCTGCCCCAATCAA
AtGSL5F	TCTGGAATGCTGTTGTCTCTGTTG
AtGSL5R	TCGCCTTTTGATTTCTTCCCAGT
AtGSL6F	GTGAAGGGTTTGGGCGTTGGAAG
AtGSL6R	CAATGAGAAGCATTCCCCATCCAGTT
AtGSL11F	TTTAGGGGTTTGGGACTCGGTGAAA
AtGSL11R	TGTCTTTCCGACCAGCGAGAATCA
lmgsl15'-1	CCCCGTCGAGTGAGATG
lmgsl15'-2	ATGGCGAGGGCGGAGGCCAA
lmcasyn1	CAAGCGAACCAAGTACAGCA
lmcasyn2	TAYGATGATTTYAAYGARTTYTTYTGG
lmcasyn1R	ATAGTCGCGTCTGGAAGGTG

lmcasyn2R	TGCTGTACTTGGTTCGCTTG
lmcasyn3R	CCAGTATCCTCCCACGAAAA
lmcasyn7R	TCTTTGTCTTAAAACTACCTTTGTTGAA
lmcasyn8R	GTGGTAAAGATGGAGAAAAGTTCTGT
lmcasyn9R	CCAAAAAAACTCGTTAAAATGCATCGTA
lmcasyn10R	CAGCCTCTCCCCAGATCA
lmcasyn11R	CACACATATAGCAACTTTTTCTC
lmcasyn22R	GCGTTAAGATCCCTAAAAGGTTG
lmcasyn23R	TGGCTAACAGATACAGTGAAAACA
lmcasyn26R	GCATTAGTTGTAGACACGGCATC
lmcasyn27R	CCCTATGGTACTGCAAAGCTGAT
lmcasyn30R	TTTATCTGCATCCTCAGGGGAAA
lmcasyn31R	GCTTCAGAGTTTTGCGCTCCAG
lmcasyn38R	GCCAGAGCGAAAAGTAGTAACACACA
lmcasyn39R	CGAAAATCAGAATCAAGCCGTGTA
atgsl5e1	ATTGGTTTCTTCAGTGAAGCT
atgsl5e1r	TCAAGTCAAGCGTTGTAC
atgsl5e2	CGCAGATGCTGCATATAA
atgsl5e2r	CAGTATAGTTAGTTAGAAATAATCC
atgsl5e3	GGATTATTTCTAACTAACTATACTG
atgsl5e3r	GAACAAGGAGCTTTACCGT
atgsl5e1s	GTAAGTGGAGGAACTACGA
atgsl5e1rs	AGCCAGGATTTAGGGCACC
atgsl5e2s	GATTCTCACCTCTAGGGAC
atgsl5e2rs	CTCACGGAACTACTTGCTC
AtGSL1F	CACGAGGAGATGCGATTCAGACCA
AtGSL1R	CACCCCGAGGCACAAACCAAAAC
AtGSL3F	TTCATGGCGGCGCAGAATACAGA
AtGSL3R	TGCCACTCGAAACCAGAGGGATTG
AtGSL7F	TGTGGTTCCTGGTGACTTCTTGGTTGT
AtGSL7R	GGCGAGCGATGTTGAGGTGGTAG

Appendix C. White's media (modified)

Used in the cultivation of *Lolium multiflorum* endosperm suspension cultures. Concentrations represent those in the complete final media.

Macro nutrients	mM
$MgSO_4$	2.96
Na_2SO_4	1.42
$Ca(NO_3)_2.4H2O$	1.23
KCl	0.94
NaH_2PO_4	11.6
KNO_3	0.79

Micronutrients	µM
$MnSO_4.4H2O$	17.75
$ZnSO_4.7H2O$	1.74
H_3BO_3	8.08
$CuSO_4.5H2O$	0.10
CoCl.6H2O	0.11
Ferric citrate	40.70

Vitamins	µM
Nicotinic acid	0.01
Thiamaine hydrochloride	0.71
Calcium pantothenate	0.53
Pyridoxine	1.21

Sugar and Hormone	
Sucrose	117 mM
Indole acetic acid	5.70 µM

pH 5.5

Yeast Extract 0.5% (w/v)

Appendix D. Published AtGSL5 manuscript

This article is published in *The Plant Cell* Online, *The Plant Cell* Preview Section, which publishes manuscripts accepted for publication after they have been edited and the authors have corrected proofs, but before the final, complete issue is published online. Early posting of articles reduces normal time to publication by several weeks.

RESEARCH ARTICLES

An Arabidopsis Callose Synthase, GSL5, Is Required for Wound and Papillary Callose Formation

Andrew K. Jacobs,[a,b,1] Volker Lipka,[b,1] Rachel A. Burton,[a] Ralph Panstruga,[b] Nicolai Strizhov,[c] Paul Schulze-Lefert,[b,2] and Geoffrey B. Fincher[a]

[a] Australian Centre for Plant Functional Genomics, University of Adelaide, Waite Campus, Glen Osmond, South Australia 5064, Australia

[b] Department of Plant Microbe Interactions, Max-Planck-Institute for Plant Breeding Research, D-50892 Cologne, Germany

[c] Max-Planck-Unit for Structural Molecular Biology, 22607 Hamburg, Germany

Arabidopsis was transformed with double-stranded RNA interference (dsRNAi) constructs designed to silence three putative callose synthase genes: *GLUCAN SYNTHASE-LIKE5* (*GSL5*), *GSL6*, and *GSL11*. Both wound callose and papillary callose were absent in lines transformed with *GSL5* dsRNAi and in a corresponding sequence-indexed *GSL5* T-DNA insertion line but were unaffected in *GSL6* and *GSL11* dsRNAi lines. These data provide strong genetic evidence that the *GSL* genes of higher plants encode proteins that are essential for callose formation. Deposition of callosic plugs, or papillae, at sites of fungal penetration is a widely recognized early response of host plants to microbial attack and has been implicated in impeding entry of the fungus. Depletion of callose from papillae in *gsl5* plants marginally enhanced the penetration of the grass powdery mildew fungus *Blumeria graminis* on the nonhost Arabidopsis. Paradoxically, the absence of callose in papillae or haustorial complexes correlated with the effective growth cessation of several normally virulent powdery mildew species and of *Peronospora parasitica*.

INTRODUCTION

Callose is a (1→3)-β-D-glucan that is widely distributed in higher plants and is readily recognizable in tissue sections through the formation of an intense yellow, UV light–induced fluorescence with the aniline blue fluorochrome (Stone et al., 1985). During normal plant growth and development, callose is found as a transitory component of the cell plate in dividing cells, is a major component of pollen mother cell walls and pollen tubes, and is found as a structural component of plasmodesmatal canals. Callose also has been observed in abscission zones and on sieve plates in dormant phloem (Stone and Clarke, 1992).

In addition to its role in normal growth and development, callose is deposited between the plasma membrane and the cell wall after exposure of plants to a range of abiotic and biotic stresses, including wounding, desiccation, metal toxicity, and microbial attack (Stone and Clarke, 1992). Particular attention has been focused on callose formation in plant–microbe interactions, during which plant host cells respond to microbial attack by rapidly synthesizing and depositing callose as plugs, drops, or plates in close proximity to the invading pathogen (Ryals et al., 1996; Donofrio and Delaney, 2001). These callosic deposits are commonly referred to as papillae and are thought to contain, in addition to (1→3)-β-D-glucan, minor amounts of other polysaccharides, phenolic compounds, reactive oxygen intermediates, and proteins (Smart et al., 1986; Bolwell, 1993; Bestwick et al., 1997; Thordal-Christensen et al., 1997; Heath, 2002). Although the precise function of callosic papillae during microbial attack has not been demonstrated unequivocally, it has been postulated that the papillae act as a physical barrier to impede microbial penetration (reviewed by Stone and Clarke, 1992). By slowing or immobilizing the invading microorganisms, the host plant could focus upon them a number of antimicrobial compounds, such as wall-degrading enzymes, phytoalexins, and active oxygen species, or initiate cascade responses involving race-specific resistance genes (Brown et al., 1998).

The central importance of callose deposition in several key plant processes, both under normal growth conditions and after abiotic or biotic stress, has prompted many attempts to purify and characterize callose synthases from plants. To date, no highly purified callose synthase preparations have been reported; therefore, it has not been possible to demonstrate a direct link between callose synthase activity and amino acid or nucleotide sequence. Nevertheless, evidence is accumulating that callose synthases are encoded by a family of glucan synthase–like (*GSL*) genes (Cui et al., 2001; Doblin et al., 2001; Hong et al., 2001a; Østergaard et al., 2002), based on the homology of these plant genes with yeast *FK506 hypersensitivity* (*FKS*) genes, which also are believed to be involved in (1→3)-β-D-glucan biosynthesis (Douglas et al., 1994; Cabib et al., 2001; Dijkgraaf et al., 2002).

[1] These authors contributed equally to this report.

[2] To whom correspondence should be addressed. E-mail schlef@mpiz-koeln.mpg.de; fax 49-221-5062313.

Article, publication date, and citation information can be found at www.plantcell.org/cgi/doi/10.1105/tpc.016097.

Twelve *GSL* genes have been identified in Arabidopsis (Richmond and Somerville, 2000; Verma and Hong, 2001; http://cellwall.stanford.edu/), in which individual members of the family presumably mediate the synthesis of callose in different tissues and/or under different environmental conditions. Very limited information is available about the biological functions of individual AtGSL family members. GSL6 (CalS1) is located at the growing cell plate and interacts with two cell plate–associated proteins, phragmoplastin and a UDP-glucose transferase (Hong et al., 2001a, 2001b). The three proteins likely form part of a larger complex that assembles at the cell plate (Hong et al., 2001b). Transgenic tobacco lines overexpressing a *GREEN FLUORESCENT PROTEIN* (*GFP*)–*AtGSL6* construct showed increased callose deposition at the cell plate, but this gene failed to complement the yeast mutant *fks1* (Hong et al., 2001a). *AtGSL5* has been shown to partially complement *fks1* and is inducible by salicylic acid (Østergaard et al., 2002). Despite these observations, direct genetic evidence linking *GSL* genes to callose biosynthesis in plants generally, or genetic evidence linking individual *AtGSL* family members to specific sites of callose deposition in Arabidopsis, has yet to be found.

The work described here was initiated in an attempt to identify members of the Arabidopsis *GSL* gene family that might be upregulated after wounding and when Arabidopsis leaves are exposed to the powdery mildew fungus *Blumeria graminis*. This ascomycete is a common fungal pathogen of grasses but fails to produce disease in nonhost interactions with Arabidopsis or other dicot plants (Braun et al., 2002). Semiquantitative reverse transcriptase–mediated PCR indicated that, of the 12 Arabidopsis *GSL* genes, transcript levels for *GSL5*, *GSL6*, and *GSL11* increased slightly after inoculation of leaves with *B. graminis* spores; on this basis, these genes were chosen for further examination (our unpublished data). Here, we assign the GSL5 isoform (referred to as CalS12 by Hong et al. [2001a]) a crucial role in inducible callose accumulation upon wounding and during biotic stress. Contrary to the common belief that callose accumulation contributes to plant defenses against pathogen attack, our data indicate that callose synthesized by the wound-responsive GSL5 might protect the fungus during pathogenesis.

RESULTS

GSL Transcript Levels Are Reduced in Double-Stranded RNA Interference Lines

Fertile transgenic T3 Arabidopsis lines were obtained for each of the three double-stranded RNA interference (dsRNAi) constructs, which targeted *GSL5*, *GSL6*, and *GSL11*. The *GSL5*, *GSL6*, *GSL11*, and empty vector control lines exhibited no obvious morphological abnormalities. DNA gel blot hybridization analyses confirmed the presence of the dsRNAi construct in each line, most of which carried single copies of the transgene (data not shown). When total RNA was extracted from young leaves and inflorescences of dsRNAi lines for quantitative real-time PCR analysis, mRNA for the three *GSL* genes was generally 3- to 10-fold less abundant than in the empty vector controls and wild-type lines (Figure 1).

Wound and Papillary Callose Are Reduced in *GSL5* dsRNAi Transgenic Lines

The formation of wound callose in *GSL5* dsRNAi lines was greatly reduced or absent compared with that in the *GSL6*, *GSL11*, and control lines (Figure 2). When germinated pollen

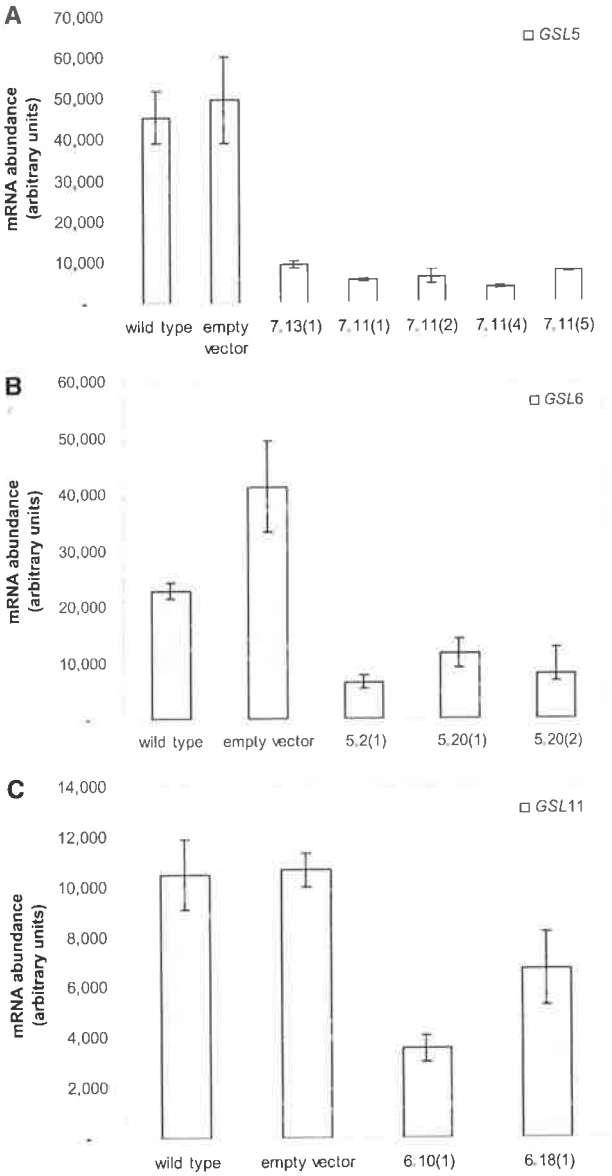

Figure 1. Transcript Accumulation of *GSL* Genes Is Reduced in Transgenic dsRNAi Lines.

Quantitative analysis of mRNA steady state levels showed a significant reduction of *GSL* transcript accumulation in transgenic lines harboring dsRNAi constructs directed against *GSL5* [lines 7.13(1), 7.11(1), 7.11(2), 7.11(4), and 7.11(5)] **(A)**, *GSL6* [lines 5.2(1), 5.20(1), and 5.20(2)] **(B)**, or *GSL11* [lines 6.10(1) and 6.18(1)] **(C)**.

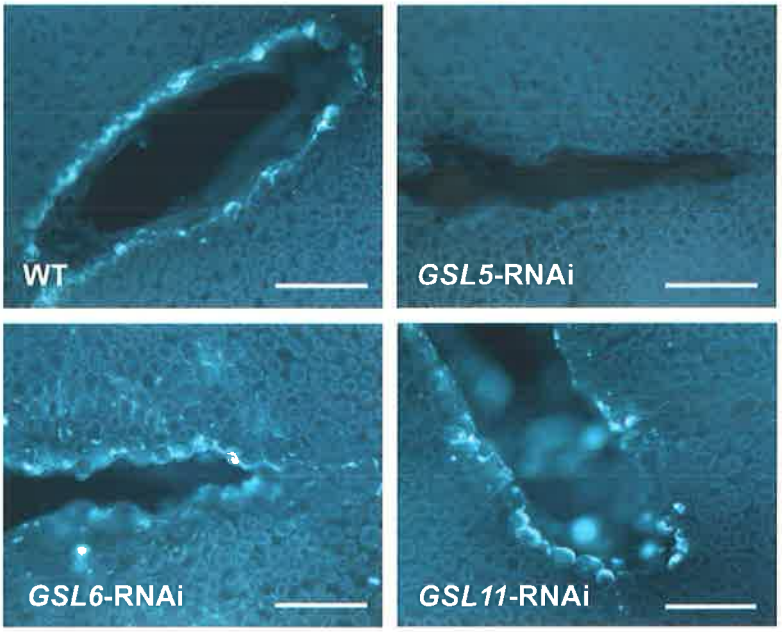

Figure 2. Reduced Callose Accumulation at Wound Sites in *GSL5* dsRNAi Lines.

Leaves of wild-type (WT) plants and *GSL5*, *GSL6*, and *GSL11* dsRNAi lines were wounded by cutting with a razor. Aniline blue fluorochrome staining of leaves revealed reduced callose accumulation at wound sites after 24 h. Bars = 200 μm.

grains in the three dsRNAi transgenic lines were examined with the aniline blue fluorochrome, callosic deposits in the *GSL5* line appeared normal (data not shown). No differences were observed in any of the *GSL* dsRNAi lines for cell plate or plasmodesmata callose (data not shown).

Given that fungal penetration is likely to cause wounding of plant cells, the formation of callosic plugs was examined in transgenic *GSL* dsRNAi lines after inoculating leaves with spores from the virulent powdery mildew fungus *Sphaerotheca fusca*. Elongating fungal hyphae were observed in all cases, and the rate of hyphal growth on the leaf surface did not differ substantially between the lines for at least 48 h after inoculation. Callosic papillae that stained brightly with the aniline blue fluorochrome were clearly evident in all independent *GSL6*, *GSL11*, and control lines (Figure 3). By contrast, in all independent *GSL5* transgenic lines, callosic plugs were completely absent, despite the fact that hyphal growth occurred (Figure 3).

Wound and Papillary Callose Also Are Reduced in a *GSL5* T-DNA Insertion Line

To confirm that the effects in the *GSL5* dsRNAi lines were specific to the lack of the GSL5 callose synthase isoform, we examined a T-DNA insertion line (GABI-KAT 089H05) containing an insertion in the second exon of *GSL5*. When leaves of homozygous T-DNA insertion siblings (referred to as *gsl5-1*) were wounded or inoculated with *S. fusca*, they showed similar, dramatic reductions in wound callose and papillary callose formation (data not shown).

Inoculation with conidiospores of the *B. graminis* powdery mildew failed to produce disease on wild-type Arabidopsis leaves. Microscopic examination revealed normal conidiospore germination, with production of primary and differentiated appressorial germ tubes in contact with the leaf surface. However, the germ tubes typically failed to enter the nonhost epidermal cells (92% of interaction sites) and were accompanied by the formation of callosic papillae (Figures 4A to 4C). This infection phenotype is similar to other reported nonhost interactions between plants and fungal pathogens (Kobayashi et al., 1997; Heath, 2002). By contrast, callosic plugs were virtually undetectable in both the homozygous *GSL5* T-DNA insertion line (*gsl5-1*) and the *GSL5* dsRNAi lines (Figures 4B and 4C). *B. graminis* penetration indices were only slightly higher in *gsl5-1* than in wild-type plants (Figure 4A), suggesting that callose plays a minor role in resistance to wall penetration. In T2 progeny obtained after selfing of the GABI-KAT 089H05 T1 line, which was hemizygous for the T-DNA insertion, siblings homozygous or hemizygous for the T-DNA insertion in *GSL5* cosegregated with the absence or presence of callosic plugs, respectively, beneath *B. graminis* appressoria (Figure 5). Despite the absence of callosic plugs in *gsl5-1* mutant plants, round papillae still were clearly recognizable beneath fungal appressoria (Figure 4C), indicating that components other than callose were present in these subcellular structures.

A cell death response was observed in epidermal cells that were penetrated by *B. graminis* sporelings at ~48 h after spore inoculation (~15% of interaction sites; Figure 4A). In contrast to epidermal cells that were not penetrated by the fungus, com-

plete collapse and browning of cytoplasm was observed in epidermal cells containing haustoria in wild-type and *gsl5-1* genotypes. Cytoplasmic collapse and browning is considered a reliable indicator of cell death (Heath, 1998). Trypan blue staining was used to confirm these observations (data not shown). Cell death was accompanied by an intense aniline blue fluorochrome staining pattern along the entire cell margin in wild-type plants, whereas dead epidermal cells in *gsl5-1* mutants showed only a punctate callose staining pattern at the cell periphery (Figure 4D). The punctate staining pattern in *gsl5-1* plants was reminiscent of plasmodesmata that are known to contain callose (Northcote et al., 1989; Itaya et al., 1998); therefore, we conclude that the absence of heavy GSL5 callose deposition at cell margins in *gsl5-1* plants reveals the underlying plasmodes-

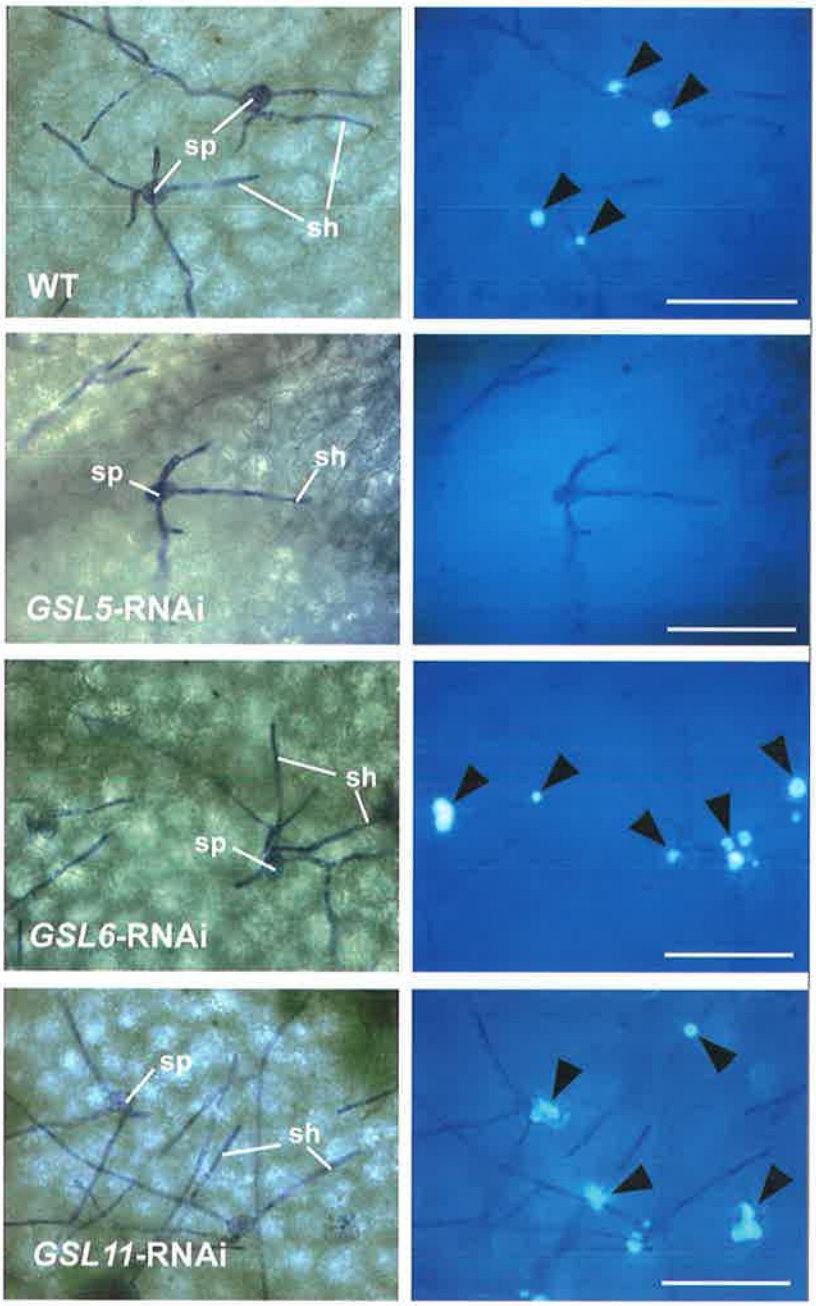

Figure 3. Absence of Callose Accumulation upon Powdery Mildew Infection in *GSL5* dsRNAi Lines.

Leaves of wild-type (WT) plants and *GSL5*, *GSL6*, and *GSL11* dsRNAi lines were challenged with the virulent powdery mildew fungus *S. fusca*. Forty-eight hours after inoculation, fungal structures (left column) and callose deposits in papillae (right column; marked by arrowheads) were stained with Coomassie blue and the aniline blue fluorochrome, respectively. sh, secondary hyphae; sp, conidiospore. Bars = 100 μm.

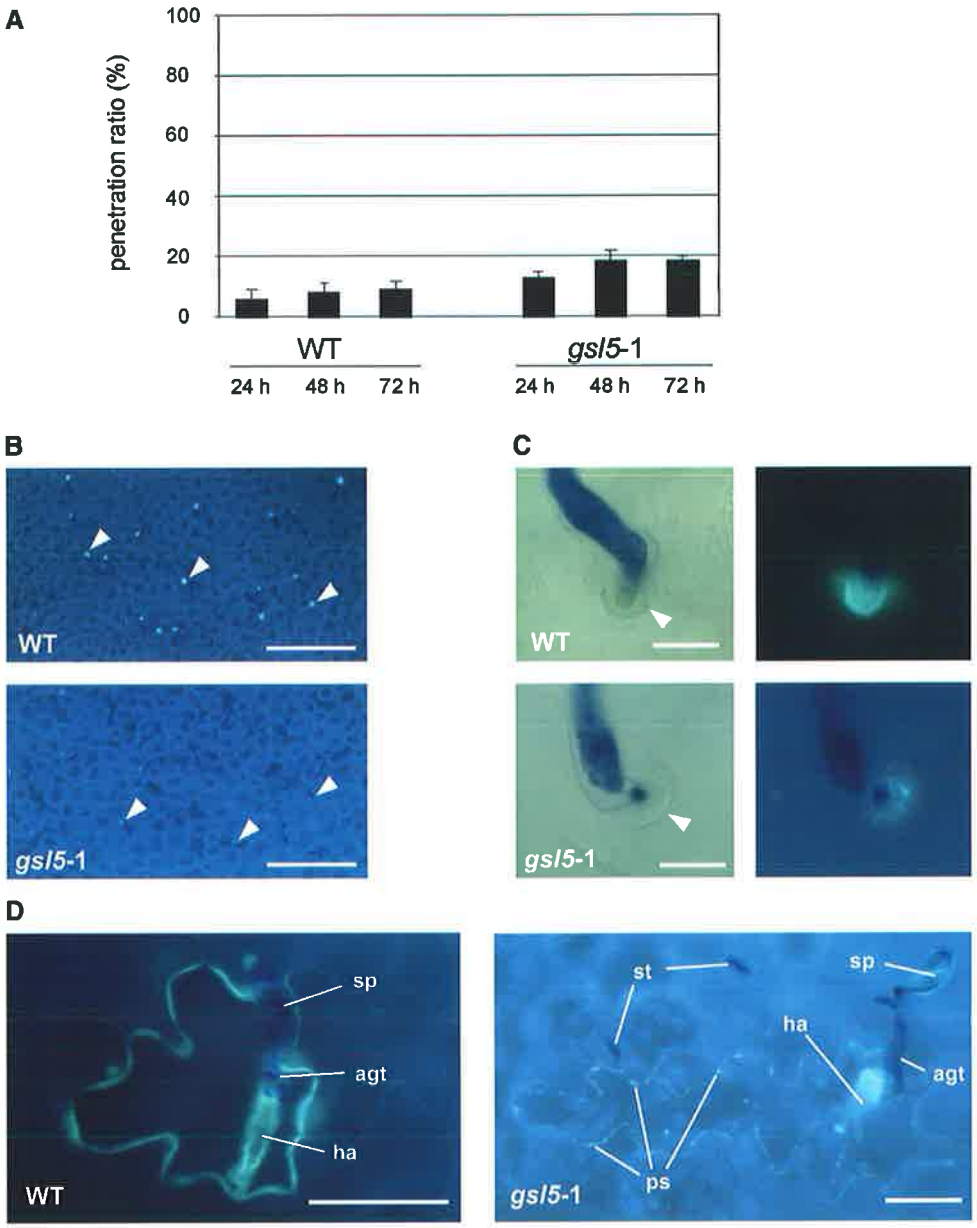

Figure 4. GSL5 Callose Accumulation Patterns upon Challenge with the Grass Powdery Mildew Fungus *B. graminis*.

Wild-type (WT) and T-DNA insertion (*gsl5-1*) plants were inoculated with *B. graminis* f. sp. *hordei* conidiospores.

(A) Quantitative analysis of *B. graminis* penetration rate. At least 300 interaction sites between *B. graminis* sporelings and leaf epidermal cells were scored for the presence or absence of fungal haustoria at the times indicated.

(B) Callose depositions at sites of attempted *B. graminis* cell wall penetration (arrowheads) are visible by fluorescence microscopy on wild-type but not *gsl5-1* plants 24 h after inoculation. Bars = 200 μm.

(C) Higher magnification views of papillae (arrowheads) beneath fungal appressoria in wild-type (top row) and *gsl5-1* (bottom row) plants. Light microscopy images are shown at left, and corresponding fluorescence images after aniline blue fluorochrome staining are shown at right. Bars = 10 μm.

(D) Invasive growth of *B. graminis* (successful haustorium differentiation) in single epidermal cells of wild-type leaves leads to cell death and callose deposition along the entire cell margin. Fluorescence images were taken 48 h after inoculation, and leaves were stained with the aniline blue fluorochrome. Note the relatively low-intensity punctate fluorochrome staining pattern at the cell periphery in *gsl5-1* plants. agt, appressorial germ tube; ha, haustorium; ps, punctate staining; sp, conidiospore; st, stomata. Bars = 50 μm.

mata callose. This finding indicates that massive GSL5 callose accumulation normally occurs along the cell margin during pathogen-triggered cellular suicide and that the GSL5 cell margin callose and the plasmodesmata callose are synthesized by different callose synthase isoforms of the same cell.

The Mutant *powdery mildrew resistant4-1* Contains a Defective *GSL5* Gene

The Arabidopsis mutant *powdery mildrew resistant4-1* (*pmr4-1*) was shown previously to be resistant against *Erysiphe cichoracearum* and to lack callose at fungal penetration sites; the recessive mutation was mapped to the long arm of chromosome 4 (Vogel and Somerville, 2000). We noticed that *GSL5* is located in the same chromosomal region and tested whether *pmr4-1* might contain a mutation in *GSL5*. Direct DNA sequencing revealed a single base substitution (G→A) in genomic DNA of *pmr4-1* corresponding to position 2060 in the deduced coding sequence, whereas the sequence derived from wild-type plants was identical to the *GSL5* gene in the databases. The base substitution would result in the conversion of the TGG codon for Trp-687 in *GSL5* to a TAG stop codon and the formation of a severely truncated primary translation polypeptide of 686 amino acid residues. The position of the lesion in *GSL5* of the *pmr4-1* mutant line is compared with the position of the T-DNA insertion in the GABI-KAT 089H05 line in Figure 6.

GSL5 and *PMR4* Are the Same Gene

Mutant *pmr4-1* plants were reported previously to exhibit resistance against *E. cichoracearum* and the oomycete *Peronospora parasitica* (Vogel and Somerville, 2000). We challenged *pmr4-1*, *gsl5-1*, and the GSL5 dsRNAi lines with another virulent powdery mildew species, *Golovinomyces orontii*. In contrast to susceptible wild-type Arabidopsis, comparable enhanced disease resistance was observed (Figure 7A), indicating that the absence of *PMR4* or *GSL5* confers similar broad-spectrum resistance. When *pmr4-1* plants were inoculated with *B. graminis* spores, the infection phenotype was indistinguishable from that observed in the *AtGSL5* dsRNAi and *gsl5-1* plants, and callosic papillae were not detected (see above). To determine whether *PMR4* and *GSL5* might be the same gene, we crossed the homozygous T-DNA insertion line (*gsl5-1*) with the *pmr4-1* mutant. Inspection of 15 F1 plants after fungal spore inoculation with the virulent *G. orontii* powdery mildew showed enhanced disease resistance and lack of callose accumulation at attempted infection sites. The observed infection phenotypes of the F1 plants were indistinguishable from the *pmr4-1* and *gsl5-1* parental lines (data not shown), strongly indicating that *PMR4* and *GSL5* are the same gene.

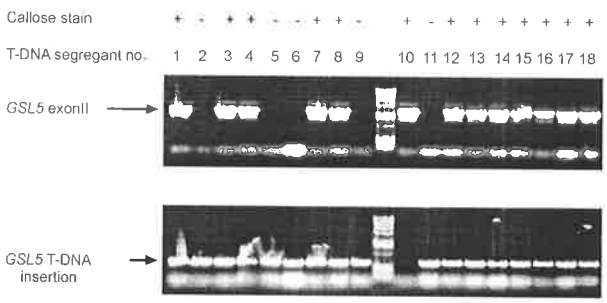

Figure 5. Lack of Callose Deposition Cosegregates with T-DNA Insertion in *GSL5*.

Absence of aniline blue fluorochrome staining after inoculation with *B. graminis* correlates with a homozygous T-DNA insertion (ins.) in *GSL5*. Segregating progeny (18 T2 siblings) of a selfed hemizygous T-DNA *GSL5* insertion line were genotyped molecularly and tested for callose deposition upon challenge with *B. graminis*. Gel electrophoretic separation of PCR products obtained with a *GSL5*– and T-DNA–specific oligonucleotide primer indicated the presence of the T-DNA insertion in all individuals except sibling 10 (bottom gel). The absence of a PCR amplification product using oligonucleotide primers designed to bind on either side of the T-DNA insertion site in *GSL5* exon 2 demonstrated that siblings 2, 5, 6, 9, and 11 are homozygous for the T-DNA insertion (top gel).

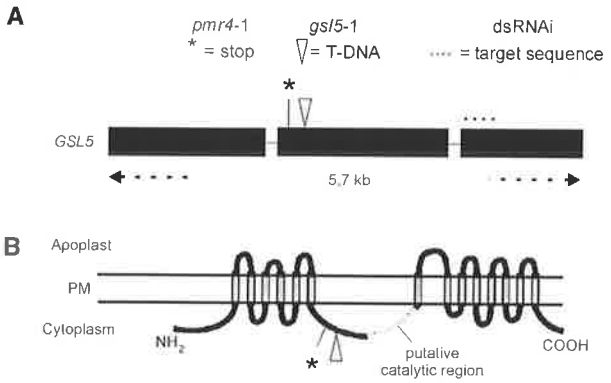

Figure 6. Scheme of *GSL5* Gene Structure and Deduced GSL5 Protein Topology.

(A) *GSL5* gene structure. Black boxes represent exons, and lines indicate introns. The asterisk indicates the mutation site in *pmr4-1* that generates a stop codon. The gray triangle represents the T-DNA insertion site in the GABI-KAT 089H05 line (*gsl5-1*). The dotted line above exon 3 shows the target sequence used to generate the *GSL5* dsRNAi construct.

(B) GSL5 is predicted to be a polytopic integral membrane protein with ~14 transmembrane helices. Both the NH_2 and COOH termini are predicted to be orientated toward the cytoplasm, as is the putative catalytic domain, which is located in an extended loop between predicted transmembrane helices 6 and 7. Mutation sites in *pmr4-1* and *gsl5-1* are indicated as described in **(A)**. PM, plasma membrane.

GSL5 Is Required for Callose Encasement of Haustorial Complexes

We examined the enhanced disease resistance phenotype to *G. orontii* (Figure 7A) in greater detail at the microscopic level (Figures 7B to 7D). This revealed indistinguishable hyphal growth on wild-type and *gsl5-1* leaves at 72 h after spore inoculation

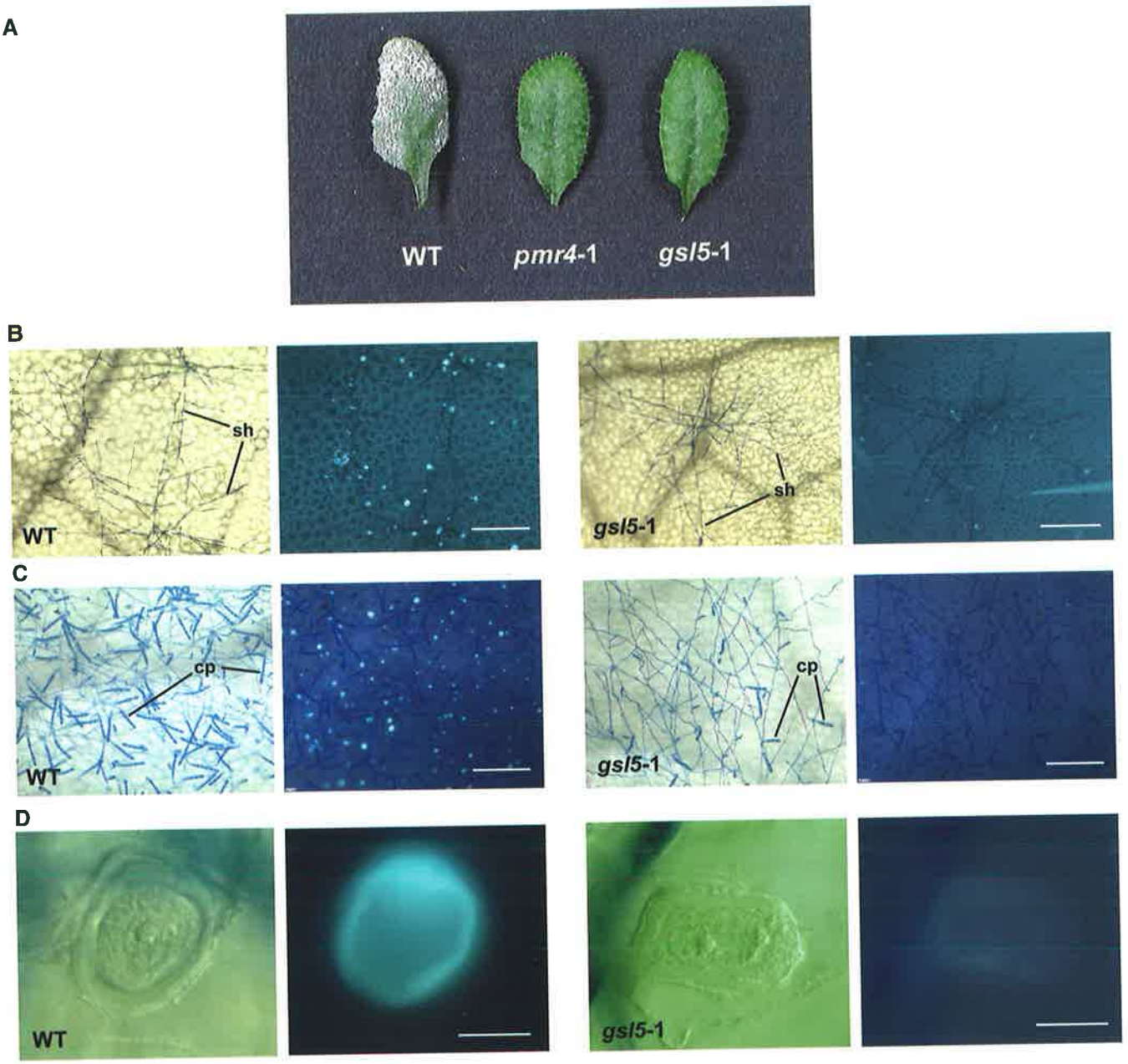

Figure 7. GSL5-Dependent Infection Phenotypes upon Challenge with the Powdery Mildew Fungus *G. orontii*.

Wild-type (WT) and T-DNA insertion (*gsl5-1*) plants were inoculated with *G. orontii* conidiospores.
(A) Single detached leaves from plants 10 days after inoculation. The surface of the leaf from the wild-type plant is covered by macroscopically visible hyphae, whereas mutants *pmr4-1* and *gsl5-1* develop no visible disease symptoms.
(B) Hyphal growth on the leaf surface at the commencement of callose encasement of haustorial complexes in wild-type and *gsl5-1* plants at 72 h after inoculation. A bright-field image is shown at left, and the corresponding fluorescence image after callose staining is shown at right. *gsl5-1* plants lack an intense aniline blue fluorochrome staining indicative of callose deposition at haustorial complexes. sh, secondary hyphae. Bars = 200 μm.
(C) A dense fungal mycelium and numerous conidiophores (cp) with long conidial chains as well as numerous local callosic deposits are visible on wild-type plants. A bright-field image is shown at left, and the corresponding fluorescence image after callose staining is shown at right. *gsl5-1* plants show significantly reduced conidiophore formation and shorter conidial chains. Bars = 200 μm.
(D) Higher magnification images of mature haustorial complexes encased by GSL5 callose from wild-type and *gsl5-1* plants. A bright-field image is shown at left, and the corresponding fluorescence microscopic image after callose staining is shown at right. Bars = 10 μm.

(Figure 7B, bright field). However, reduced hyphal growth and severely diminished conidiophore formation became detectable on *gsl5-1* leaves at 5 and 10 days after pathogen challenge (Figure 7C, bright field). This finding indicates that pathogen growth on the mutant plants is impaired significantly but is not inhibited completely. A striking encapsulation of haustorial complexes with callose was found in wild-type but not in *gsl5-1* leaves, suggesting that GSL5 participates in callose synthesis both in papillae and at haustoria before and after fungal entry into epidermal cells (Figure 7D). This encasement of haustorial complexes was recognizable as early as 72 h after spore inoculation (Figures 7B and 7C, epifluorescence). This finding corroborates our earlier observations of dynamic changes of GSL5 activity or location as the infection process progresses and might indicate a critical role for callose in the function of haustorial complexes.

DISCUSSION

To define potential roles of *GSL* genes in callose biosynthesis in plants, dsRNAi constructs that specifically target 3 of the 12 putative *GSL* genes in Arabidopsis—*GSL5*, *GSL6*, and *GSL11*—were used to generate stable transformants. Quantitative PCR showed that transcript levels of the three genes were reduced specifically in the dsRNAi transgenic lines. No evidence for compensatory upregulation of other *GSL* genes was detected. For example, in the *GSL5* lines, *GSL6* and *GSL11* mRNA remained at approximately the same levels as observed in the control and wild-type plants (data not shown). During the initial design of the dsRNAi constructs, regions in which sequences of >21 nucleotides were identical in any two different *AtGSL* genes were avoided (Hamilton and Baulcombe, 1999), but quantitative PCR showed some downregulation of *AtGSL* genes most closely related to the target genes (*AtGSL1*, *AtGSL3*, and *AtGSL7*, respectively; data not shown). Therefore, it was clear that the dsRNAi results would require independent confirmation through T-DNA insertion lines or other mutants in which a single gene had been disrupted. Although mRNA abundance for the specific *GSL* genes was lower in each of the corresponding dsRNAi transgenic lines, it was not abolished completely (Figure 1), presumably because dsRNAi silencing occurs post-transcriptionally (Fire et al., 1998) or because of potential cell type–specific differences in the activity of the 35S promoter, which drove the expression of the dsRNAi constructs (Sunilkumar et al., 2002).

In seeking a link between *GSL* expression and callose deposition, it was noticed initially that wound callose was reduced greatly, specifically in the *GSL5* dsRNAi plants (Figure 2). Wounding is an inherent consequence of fungal penetration of plant cells, so the effects of fungal challenge on the dsRNAi lines were examined. When the transgenic plants were challenged with several fungal species, the response of the dsRNAi *GSL5* lines differed markedly from that of the dsRNAi *GSL6*, dsRNAi *GSL11*, and control plants. In particular, papillary callose was absent in the dsRNAi *GSL5* line after inoculation of leaves with the fungal pathogens *S. fusca*, *G. orontii*, and *B. graminis*. Similar results were observed with the T-DNA insertion line GABI-KAT 089H05, in which the *GSL5* callose synthase gene is disrupted (Figure 6). As mentioned above, our focus was shifted from the dsRNAi lines to the homozygous GABI-KAT 089H05 T-DNA insertion line (*gsl5-1*). Although papillary callose was not detectable in *gsl5* plants, the typical round wall appositions that form beneath fungal appressoria, at least at the light microscopic level, were indistinguishable from those in wild-type plants except that they contained no callose (Figure 4C). Therefore, it seems unlikely that callose serves as an essential structural scaffold in papillae (cf. Smart et al., 1986; Bolwell, 1993). The formation of noncallosic papillae in *gsl5* plants indicates that the accumulation of papillary components other than callose continues.

The phenotypic characteristics of the *gsl5* lines were similar to those described for the powdery mildew–resistant *pmr4-1* mutant of Arabidopsis (Vogel and Somerville, 2000). We have shown here that the *pmr4-1* line has an internal stop codon in *GSL5* that is located in a similar position to the T-DNA insertion in the GABI-KAT 089H05 line in exon 2 of the gene (Figure 6). Based on a number of topology prediction programs, the lesions will disrupt the protein sequence close to the last transmembrane helix before the large, nonmembrane, and presumably cytoplasmic region of the protein that is widely assumed to contain the catalytic site (Figure 6) (Cui et al., 2001; Doblin et al., 2001; Hong et al., 2001a; Østergaard et al., 2002). It is highly unlikely that the truncated protein would have any callose synthase activity. Thus, our gene-silencing experiments and the mutant data clearly demonstrate a role for *AtGSL5* in the deposition of wound and papillary callose. More generally, the data provide strong genetic evidence that the products of *GSL* genes are essential for callose formation in higher plants.

It has long been believed that callosic papillae physically impede pathogen entry into plant cells, although this is not accepted universally (reviewed by Stone and Clarke, 1992). To test this hypothesis, we took advantage of a nonhost interaction phenotype between Arabidopsis and the grass powdery mildew fungus *B. graminis*, which is characterized by the failure of the pathogen to penetrate leaf epidermal cells on wild-type plants at most interaction sites (Figure 4A). Penetration incidence was only slightly higher in *gsl5* mutants, and infection did not occur. In other work, Arabidopsis mutants have been identified in which *B. graminis* penetration through the cell wall was increased dramatically, but none of these showed reduced callose formation at papillae (V. Lipka and P. Schulze-Lefert, unpublished data). Together, these observations indicate that resistance to wall penetration by the grass powdery mildew fungus is a plant-controlled process to which papillary callose does not contribute to any great extent. However, nonhost interactions with other fungal pathogens need to be tested on *gsl5* plants before we can generalize our observations with the *B. graminis* pathogen.

A striking finding in the present work was the different spatial and temporal accumulation patterns of GSL5 callose at different subcellular sites in single cells, namely at papillae and haustorial complexes, as well as along the entire cellular periphery after pathogen-provoked cell death (Figures 4 and 7). These changing patterns might reflect local stimulation of the activity of preexisting callose synthase enzyme or the specific targeting of newly synthesized enzyme to cellular "stress sites."

Each of the three pathogen-triggered GSL5 callose accumulation patterns is consistent with a plasma membrane location for the callose synthase, given that the extrahaustorial membrane is thought to be continuous with the plasma membrane (Giese et al., 1997; Mendgen and Hahn, 2002). At this stage, we favor the existence of a mechanism that mediates tight subcellular control of the activity of preexisting enzyme. The activity of plasma membrane–bound plant callose synthases often is dependent on Ca^{2+}, whereas in yeast, the Rho1 GTPase regulates the activity of the callose synthase homologs FKS1 and FKS2 by altering their phosphorylation status (Qadota et al., 1996; Calonge et al., 2003). A rapid increase in cytoplasmic free Ca^{2+} levels is a common response of plant cells to pathogen challenge (Blume et al., 2000; Grant et al., 2000) and wounding (Leon et al., 1998, 2001); therefore, it is conceivable that local increases in Ca^{2+} concentrations beneath fungal appressoria and at haustorial complexes contribute to local GSL5 stimulation. Subsequent increases in whole-cell cytoplasmic free Ca^{2+} levels after more widespread plasma membrane disintegration as the cell dies might contribute to GSL5 activation along the entire cell periphery.

Perhaps the most surprising observation with the *gsl5* lines is their enhanced resistance to attack by different biotrophic pathogens (Figure 7A). It was shown previously that the loss of *PMR4* function does not result in the constitutive expression of salicylic acid– or ethylene– and jasmonic acid–dependent defense pathways (Vogel and Somerville, 2000). Although Østergaard et al. (2002) showed salicylic acid–dependent *GSL5* gene expression, we have shown a link between GSL5 activity and wounding (Figure 2). Wounding of the cell wall is a feature of pathogenesis by biotrophic microorganisms that must enter plant cells for nutrient supply. Biotrophic pathogens such as *P. parasitica* and *E. cichoracearum* might have exploited components of the wound response for successful pathogenesis. It is conceivable that callose might be needed as a physical support for fungal development, either as a structural scaffold to accommodate haustorial complexes or to allow optimal nutrient uptake via this specialized feeding structure. Because cell wall penetration resistance was not altered substantially in the absence of callosic plugs and because haustorium differentiation was not impaired in any detectable manner upon challenge with the tested virulent pathogens in *gsl5* leaves (Figure 7D), a structural role of GSL5 callose for "intracellular" accommodation of fungal infection structures seems unlikely.

However, GSL5 callose might either facilitate nutrient uptake by haustoria or serve as a pathogen-induced protection barrier that prevents the recognition of pathogen-derived molecules by the host. For example, lack of callose might unmask fungal wall polysaccharides and/or secreted proteins. Certain branched (1→3,1→6)-β-D-oligoglucosides and chitin/chitosan oligosaccharides released from these fungal wall polysaccharides (Bartnicki-Garcia, 1968) by partial endohydrolysis are highly active elicitors of plant defense responses, even at concentrations as low as 10 nM (Côté and Hahn, 1994). By contrast, linear (1→3)-β-D-oligoglucosides of the type that would be released from callose itself by the (1→3)-β-D-glucanases are not active in eliciting plant defense (Côté and Hahn, 1994). The evolution of (1→3)-β-D-glucanase inhibitors by pathogenic fungi implies that inhibiting the release of (1→3,1→6)-β-D-oligoglucosides could be important for the establishment of fungal infection (Rose et al., 2002).

METHODS

Plant Lines and Growth Conditions

The *Arabidopsis thaliana GSL5* T-DNA insertion line GABI-KAT 089H05 was provided by Bernd Weisshaar (Max-Planck-Institute for Plant Breeding Research) and had been generated in the GABI-Kat program (http://www.mpiz-koeln.mpg.de/GABI-Kat/GABI-Kat_homepage.html). Oligonucleotide sequences used for T-DNA insertion detection were 5′-CGCAGATGCTGCATATAA-3′ and 5′-CAGTATAGTTAGTTAGAAATAATCC-3′ (GSL5 specific and T-DNA left border specific, respectively).

The powdery mildew–resistant line *pmr4-1* was obtained from John Vogel and Shauna Somerville (Carnegie Institution of Washington, Stanford, CA). Plants were transformed by the floral-dip method (Clough and Bent, 1998) using *Agrobacterium tumefaciens* strain GV3101::pMP90(RK) with the binary vectors pAJ5, pAJ6, and pAJ7. T3 plants used in infection experiments were grown in a glasshouse at 22°C. Seedlings (10 days old) transformed with double-stranded RNA interference (dsRNAi) constructs were selected by spraying every second day for 1 week with 100 mg/L Basta (AgrEvo, Düsseldorf, Germany).

dsRNAi Constructs

Gene-specific inverted repeats separated by an intron were inserted into plasmid pJawohl3 (AF404854) to create pAJ5 (*GSL6*; At1g05570), pAJ6 (*GSL11*; At3g59100), and pAJ7 (*GSL5*; At4g03550) dsRNAi constructs. Primer combinations used to produce the gene-specific sense and antisense *GSL* dsRNAi fragments were as follows: for *AtGSL5*, 5′-CATCGATGGGATCCGTACTGTCT-3′/5′-GGAAGGGACGGAAGCTTGAATTC-3′ and 5′-GGAAGGCCCGGGATGTTGGATTG-3′/5′-CGGCGTTGGTGTCCGTACTAGT-3′ (230-bp product); for *AtGSL6*, 5′-CATCGATAAAGGATCCCATACACCGTAA-3′/5′-CATCCATGGGATTAAGCTTCCCGGGCCA-3′ and 5′-CATCCATGGGATTAAGCTTCCCGGGCCA-3′/5′-CCGTCCATAAAGGATCCCATACACTAGT-3′ (640-bp product); and for *AtGSL11*, 5′-TGGGAAGCTTGGTGGAACGTAGA-3′/5′-TGACTGACAAGGATCCGAGGAAGAG-3′ and 5′-TGGGATCCGTGGTGGAATTCAGA-3′/5′-TGACTAGTAAAAACTCGAGGAAGAGA-3′ (280-bp product).

DNA and RNA Extractions

Genomic DNA was extracted from young leaves of Arabidopsis using the hot cetyl-trimethyl-ammonium bromide method (Lassner et al., 1989). Total RNA was extracted from young leaves and inflorescences of dsRNAi lines using the Trizol reagent (Invitrogen, Carlsbad, CA) according to the manufacturer's instructions.

Quantitative PCR Analysis of *GSL* mRNA

Total RNA (5 μg) was used in cDNA reactions using the Superscript II cDNA synthesis kit (Invitrogen). The cDNA was diluted 2.5-fold, and 1 μL was taken for quantitative real-time PCR in 20-μL reaction volumes using 10 μL of 2× Quanti-Tect PCR master mix (Qiagen, Valencia, CA), 0.3 μM gene-specific primers, and 0.6 μL of a 100-fold dilution of SYBR Green I dye (Applied Biosystems, Foster City, CA). PCR cycling and fluorescence measurements were performed with a Rotorgene 2000 Real-Time Cycler RG2072 (Corbett, Sydney, Australia), and data were normalized against glyceraldehyde phosphate dehydrogenase (*GAPDH*), actin (*Actin1*), and cyclophilin (*Cyclo*) mRNA levels (Vandesompele et al.,

2002). Primers used in the quantitative PCR were as follows: for AtGAPDH (At3g26650), 5′-TGGTTGATCTCGTTGTGCAGGTCTC-3′/5′-GTCAGCCAAGTCAACAACTCTCTG-3′; for AtActin1 (At2g37620), 5′-TGCGACAATGGAACTGGAATG-3′/5′-GGATAGCATGTGGAAGTGCATAC-3′; for AtCyclo (At2g36130), 5′-TGGCGAACGCTGGTCCTAATACA-3′/5′-CAAAAACTCCTCTGCCCCAATCAA-3′; for AtGSL5 (At4g03550), 5′-CTGGAATGCTGTTGTCTCTGTTG-3′/5′-TCGCCTTTTGATTTCTTCCCAGT-3′; for AtGSL6 (At1g05570), 5′-GAAGGGTTTGGGCGTTGGAAG-3′/5′-CAATGAGAAGCATTCCCCATCCAGTT-3′; and for AtGSL11 (At3g59100), 5′-TTTAGGGGTTTGGGACTCGGTGAAA-3′/5′-TGTCTTTCCGACCAGCGAGAATCA-3′.

Sequence Analysis of *PMR4-1*

The three exons of *GSL5* (1870, 2022, and 1448 bp, respectively) were amplified by PCR using flanking oligonucleotide primers. Purified PCR products (NucleoSpin extraction kit; Macherey-Nagel, Düren, Germany) were subjected to direct DNA sequencing. DNA sequences were determined by the MPIZ DNA core facility on Applied Biosystems (Weiterstadt, Germany) ABI Prism 377 and 3700 sequencers using BigDye-terminator chemistry. Forward/reverse primers used for *GSL5* exon amplification and sequencing from *pmr4-1* and *gsl5-1* plants were as follows: Exon1, 5′-ATTGTTTCTTCAGTGAAGCT-3′/5′-TCAAGTCAAGCGTTGTAC-3′; Exon2, 5′-CGCAGATGCTGCATATAA-3′/5′-CAGTATAGTTAGTTAGAAATAATCC-3′; and Exon3, 5′-GGATTATTTCTAACTAACTATACTG-3′/5′-GAACAAGGAGCTTTACCGT-3′. Additional sequencing primers were as follows: Exon1b-F, 5′-GTAAGTGGAGGAACTACGA-3′; Exon1b-R, 5′-AGCCAGGATTTCGGGCACC-3′; and Exon2b-F, 5′-GATTCTCACCTCTAGGGAC-3′.

Wounding

Four- to 6-week-old plants were wounded by cutting leaves with a razor. After 24 h, the leaves were detached, cleared, and stained for callose accumulation.

Pathogenicity Assays

The formation of callosic plugs was examined in 4- to 6-week-old plants 48 h after inoculating leaves with spores from the powdery mildew fungus *Sphaerotheca fusca*. Four- to 6-week-old Arabidopsis plants were inoculated with spores of *Golovinomyces orontii* and *Blumeria graminis* as described previously (Peterhänsel et al., 1997; Vogel and Somerville, 2000).

Microscopic Analyses

Tissue fixation and staining of fungal structures and callose were performed as described previously (Peterhänsel et al., 1997; Vogel and Somerville, 2000). Tissues were examined with a Zeiss Axioplan 20 fluorescence microscope (Carl Zeiss, Oberkochen, Germany). Epi-illumination was used at an excitation cutoff limit of 365 nm with barrier filter KP620.

Upon request, materials integral to the findings presented in this publication will be made available in a timely manner to all investigators on similar terms for noncommercial research purposes. To obtain materials, please contact Paul Schulze-Lefert, schlef@mpiz-koeln.mpg.de.

ACKNOWLEDGMENTS

We thank John Vogel and Shauna Somerville for providing the *pmr4-1* line, Neil Shirley for assistance with the quantitative PCR experiments, and Bruce Stone for helpful suggestions. This work was supported by grants from the Grains Research and Development Corporation and the Australian Research Council (to G.B.F.) and from the Max Planck Society (to P.S.-L.).

Received August 6, 2003; accepted September 12, 2003.

REFERENCES

Bartnicki-Garcia, S. (1968). Cell wall chemistry, morphogenesis, and taxonomy of fungi. Annu. Rev. Microbiol. **22,** 87–108.

Bestwick, C.S., Brown, I.R., Bennett, M.H.R., and Mansfield, J.W. (1997). Localization of hydrogen peroxide accumulation during the hypersensitive reaction of lettuce cells to *Pseudomonas syringae* pv *phaseolicola*. Plant Cell **9,** 209–221.

Blume, B., Nuernberger, T., Nass, N., and Scheel, D. (2000). Receptor-mediated increase in cytoplasmic free calcium required for activation of pathogen defense in parsley. Plant Cell **12,** 1425–1440.

Bolwell, G.P. (1993). Dynamic aspects of the plant extracellular matrix. Int. Rev. Cytol. **146,** 261–323.

Braun, U., Cook, R.T.A., Inman, A.J., and Shin, H.D. (2002). The taxonomy of the powdery mildew fungi. In The Powdery Mildews, R. Bélanger, A.J. Dik, and W.R. Bushnell, eds (St. Paul, MN: American Phytopathological Society Press), pp. 13–54.

Brown, I., Trethowan, J., Kerry, M., Mansfield, J., and Bolwell, G.P. (1998). Localization of components of the oxidative cross-linking of glycoproteins and of callose synthesis in papillae formed during the interaction between non-pathogenic strains of *Xanthomonas campestris* and French bean mesophyll cells. Plant J. **15,** 333–343.

Cabib, E., Roh, D.-H., Schmidt, M., Crotti, L.B., and Varma, A. (2001). The yeast cell wall and septum as paradigms of cell growth and morphogenesis. J. Biol. Chem. **276,** 19679–19682.

Calonge, T.M., Arellano, M., Coll, P.M., and Perez, P. (2003). Rga5p is a specific Rho1p GTPase-activating protein that regulates cell integrity in *Schizosaccharomyces pombe*. Mol. Microbiol. **47,** 507–518.

Clough, S.J., and Bent, A.F. (1998). Floral dip: A simplified method for *Agrobacterium*-mediated transformation of *Arabidopsis thaliana*. Plant J. **16,** 735–743.

Côté, F., and Hahn, M.G. (1994). Oligosaccharins: Structures and signal transduction. Plant Mol. Biol. **26,** 1379–1411.

Cui, X.J., Shin, H.S., Song, C., Laosinchai, W., Amano, Y., and Brown, R.M. (2001). A putative plant homolog of the yeast β-1,3-glucan synthase subunit FKS1 from cotton (*Gossypium hirsutum* L.) fibers. Planta **213,** 223–230.

Dijkgraaf, G.J., Abe, M., Ohya, Y., and Bussey, H. (2002). Mutations in Fks1p affect the cell wall content of β-1,3- and β-1,6-glucan in *Saccharomyces cerevisiae*. Yeast **19,** 671–690.

Doblin, M.S., De Melis, L., Newbigin, E., Bacic, A., and Read, S.M. (2001). Pollen tubes of *Nicotiana alata* express two genes from different β-glucan synthase families. Plant Physiol. **125,** 2040–2052.

Donofrio, N.M., and Delaney, T.P. (2001). Abnormal callose response phenotype and hypersusceptibility to *Peronospora parasitica* in defense-compromised Arabidopsis nim1-1 and salicylate hydroxylase-expressing plants. Mol. Plant-Microbe Interact. **14,** 439–450.

Douglas, C.M., et al. (1994). The *Saccharomyces cerevisiae FKS1* (*ETG1*) gene encodes an integral membrane protein which is a subunit of (1→3)-β-D-glucan synthase. Proc. Natl. Acad. Sci. USA **91,** 12907–12911.

Fire, A., Xu, S., Montgomery, M.K., Kostas, S.A., Driver, S.E., and Mello, C.C. (1998). Potent and specific genetic interference by double-stranded RNA in *Caenorhabditis elegans*. Nature **391,** 806–811.

Giese, H., Hippe-Sanwald, S., Somerville, S., and Weller, J. (1997). Plant relationships. In The Mycota V, Part B, G. Carroll and P. Tudzynski, eds (Heidelberg, Germany: Springer), pp. 55–78.

Grant, M.R., Brown, I., Adams, S., Knight, M., Ainslie, A., and Mansfield, J.W. (2000). The *RPM1* plant disease resistance gene facilitates a rapid and sustained increase in cytosolic calcium that is necessary for the oxidative burst and hypersensitive cell death. Plant J. **23,** 441–450.

Hamilton, A.J., and Baulcombe, D.C. (1999). A species of small antisense RNA in posttranscriptional gene silencing in plants. Science **286,** 950–952.

Heath, M.C. (1998). Involvement of reactive oxygen species in the response of resistant (hypersensitive) or susceptible cowpeas to the cowpea rust fungus. New Phytol. **138,** 251–263.

Heath, M.C. (2002). Cellular interactions between biotrophic fungal pathogens and host or nonhost plants. Can. J. Pl. Path. **24,** 259–264.

Hong, Z.L., Delauney, A.J., and Verma, D.P.S. (2001a). A cell plate–specific callose synthase and its interaction with phragmoplastin. Plant Cell **13,** 755–768.

Hong, Z.L., Zhang, Z.M., Olson, J.M., and Verma, D.P.S. (2001b). A novel UDP-glucose transferase is part of the callose synthase complex and interacts with phragmoplastin at the forming cell plate. Plant Cell **13,** 769–779.

Itaya, A., Woo, Y.M., Masuta, C., Bao, Y., Nelson, R.S., and Ding, B. (1998). Developmental regulation of intercellular protein trafficking through plasmodesmata in tobacco leaf epidermis. Plant Physiol. **118,** 373–385.

Kobayashi, Y., Kobayashi, I., Funaki, Y., Fujimoto, S., Takemoto, T., and Kunoh, H. (1997). Dynamic reorganization of microfilaments and microtubules is necessary for the expression of non-host resistance in barley coleoptile cells. Plant J. **11,** 525–537.

Lassner, M.W., Palys, J.M., and Yoder, J.I. (1989). Genetic transactivation of dissociation elements in transgenic tomato plants. Mol. Gen. Genet. **218,** 25–32.

Leon, J., Rojo, E., and Sanchez, S.J.J. (2001). Wound signalling in plants. J. Exp. Bot. **52,** 1–9.

Leon, J., Rojo, E., Titarenko, E., and Sanchez, S.J.J. (1998). Jasmonic acid-dependent and -independent wound signal transduction pathways are differentially regulated by Ca^{2+}/calmodulin in *Arabidopsis thaliana*. Mol. Gen. Genet. **258,** 412–419.

Mendgen, K., and Hahn, M. (2002). Plant infection and the establishment of fungal biotrophy. Trends Plant Sci. **7,** 352–356.

Northcote, D.H., Davey, R., and Lay, J. (1989). Use of antisera to localize callose, xylan and arabinogalactan in the cell-plate, primary and secondary walls of plant cells. Planta **178,** 353–366.

Østergaard, L., Petersen, M., Mattsson, O., and Mundy, J. (2002). An Arabidopsis callose synthase. Plant Mol. Biol. **49,** 559–566.

Peterhänsel, C., Freialdenhoven, A., Kurth, J., Kolsch, R., and Schulze-Lefert, P. (1997). Interaction analyses of genes required for resistance responses to powdery mildew in barley reveal distinct pathways leading to leaf cell death. Plant Cell **9,** 1397–1409.

Qadota, H., Python, C.P., Inoue, S.B., Arisawa, M., Anraku, Y., Zheng, Y., Watanabe, T., Levin, D.E., and Ohya, Y. (1996). Identification of yeast Rho1p GTPase as a regulatory subunit of (1→3)-β-D-glucan synthase. Science **272,** 279–281.

Richmond, T.A., and Somerville, C.R. (2000). The cellulose synthase superfamily. Plant Physiol. **124,** 495–498.

Rose, J.K.C., Ham, K.S., Darvill, A.G., and Albersheim, P. (2002). Molecular cloning and characterization of glucanase inhibitor proteins: Coevolution of a counterdefense mechanism by plant pathogens. Plant Cell **14,** 1329–1345.

Ryals, J.A., Neuenschwander, U.H., Willits, M.G., Molina, A., Steiner, H.Y., and Hunt, M.D. (1996). Systemic acquired resistance. Plant Cell **8,** 1809–1819.

Smart, M.G., Aist, J.R., and Israel, H.W. (1986). Structure and function of wall appositions. 1. General histochemistry of papillae in barley (*Hordeum vulgare*) coleoptiles attacked by *Erysiphe graminis* f. sp. *hordei*. Can. J. Bot. **64,** 793–801.

Stone, B.A., and Clarke, A.E. (1992). Chemistry and Biology of (1→3)-β-D-Glucans. (Victoria, Australia: La Trobe University Press).

Stone, B.A., Evans, N.A., Bonig, I., and Clarke, A.E. (1985). The application of Sirofluor, a chemically defined fluorochrome from aniline blue for the histochemical detection of callose. Protoplasma **122,** 191–195.

Sunilkumar, G., Mohr, L., Lopata, F.E., Emani, C., and Rathore, K.S. (2002). Developmental and tissue-specific expression of CaMV 35S promoter in cotton as revealed by GFP. Plant Mol. Biol. **50,** 463–474.

Thordal-Christensen, H., Zhang, Z., Wei, Y., and Collinge, D.B. (1997). Subcellular localization of H_2O_2 in plants: H_2O_2 accumulation in papillae and hypersensitive response during the barley-powdery mildew interaction. Plant J. **11,** 1187–1194.

Vandesompele, J., De Preter, K., Pattyn, F., Poppe, B., Van Roy, N., De Paepe, A., and Speleman, F. (2002). Accurate normalisation of real-time quantitative RT-PCR data by geometric averaging of multiple internal control genes. Genome Biol. **3,** 1–12.

Verma, D.P.S., and Hong, Z.L. (2001). Plant callose synthase complexes. Plant Mol. Biol. **47,** 693–701.

Vogel, J., and Somerville, S. (2000). Isolation and characterization of powdery mildew-resistant Arabidopsis mutants. Proc. Natl. Acad. Sci. USA **97,** 1897–1902.

NOTE ADDED IN PROOF

During the processing of this manuscript, Nishimura et al. (Science 301: 969–972) published work on Arabidopsis *pmr4* mutants. They showed that PMR4 encodes GSL5 callose synthase and demonstrated that resistance to powdery mildew infection is mediated through the salicylic acid pathway.

The Plant Cell

References

Aist, J.R., Kunoh, H. and Israel, H.W. (1980). Challenge appressoria of *Erysiphe graminis* fail to breach preformed papillae of a compatible barley cultivar. *Phytopath.*, **69**, 1245-1250.

Altschul, S.F., Gish, W., Miller, W., Myers, E.W. and Lipman, D.J. (1990). Basic local alignment search tool. *J. Mol. Biol.*, **215**, 403-410.

Amor, Y., Haigler, C.H., Johnson, S., Wainscott, M. and Delmer, D.P. (1995). A membrane-associated form of sucrose synthase and its potential role in synthesis of cellulose and callose in plants. *Proc. Nat. Acad. Sci. U. S. A.*, **92**, 9353-9357.

Anderson, M.A., Harris, P.J., Bonig, I. and Clarke, A.E. (1987). Immuno-gold localization of α-L-arabinofuranosyl residues in pollen tubes of *Nicotiana alata Link et Otto*. *Planta*, **171**, 438-442.

Andrawis, A., Solomon, M. and Delmer, D.P. (1993). Cotton fibre annexins - a potential role in the regulation of callose synthase. *Plant J.*, **3**, 763-772.

Arabidopsis Genome Initiative. (2000). Analysis of the genome sequence of the flowering plant *Arabidopsis thaliana*. *Nature*, **408**, 796-815.

Arellano, M., Valdivieso, M.H., Calonge, T.M., Coll, P.M., Duran, A. and Perez, P. (1999). *Schizosaccharomyces pombe* protein kinase C homologues, pck1p and pck2p, are targets of rho1p and rho2p and differentially regulate cell integrity. *J. Cell Sci.*, **112**, 3569-3578.

Arioli, T., Peng, L.C., Betzner, A.S., Burn, J., Wittke, W., Herth, W., Camilleri, C., Hofte, H., Plazinski, J., Birch, R., Cork, A., Glover, J., Redmond, J. and Williamson, R.E. (1998). Molecular analysis of cellulose biosynthesis in *Arabidopsis*. *Science*, **279**, 717-720.

Barnes, H.J., Jenkins, C.M. and Waterman, M.R. (1994). Baculovirus expression of bovine cytochrome P450c17 in Sf9 cells and comparison with expression in yeast, mammalian cells, and *E. coli*. *Arch. Biochem. Biophys.*, **315**, 489-494.

Bartnicki-Garcia, S. (1968). Cellwall chemistry, morphogenesis, and taxonomy of fungi. *Annu. Rev. Microbiol.*, **22**, 87-108.

Baulcombe, D.C. (1996). RNA as a target and an initiator of post-transcriptional gene silencing in transgenic plants. *Plant Mol. Biol.*, **32**, 79-88.

Beauvais, A., Bruneau, J.M., Mol, P.C., Buitrago, M.J., Legrand, R. and Latge, J.P. (2001). Glucan synthase complex of *Aspergillus fumigatus*. *J. Bacteriol.*, **183**, 2273-2279.

Beffa, R.S., Hofer, R.M., Thomas, M. and Meins, F., Jr. (1996). Decreased susceptibility to viral disease of beta-1,3-glucanase-deficient plants generated by antisense transformation. *Plant Cell*, **8**, 1001-1011.

Blume, B., Nuernberger, T., Nass, N. and Scheel, D. (2000). Receptor-mediated increase in cytoplasmic free calcium required for activation of pathogen defense in parsley. *Plant Cell*, **12**, 1425-1440.

Bolwell, G.P. (1993). Dynamic aspects of the plant extracellular matrix. *Int. Rev. Cytol.*, **146**, 261-323.

Brett, C.T. and Waldron, K.W. (1996). Physiology and biochemistry of plant cell walls, Chapman and Hall, London.

Brown, I., Trethowan, J., Kerry, M., Mansfield, J. and Bolwell, G.P. (1998). Localization of components of the oxidative cross-linking of glycoproteins and of callose synthesis in papillae formed during the interaction between non-pathogenic strains of *Xanthomonas campestris* and french bean mesophyll cells. *Plant J.*, **15**, 333-343.

Bucher, G.L., Tarina, C., Heinlein, M., Di, S.F., Meins, F., Jr. and Iglesias, V.A. (2001). Local expression of enzymatically active class I beta-1,3-glucanase enhances symptoms of TMV infection in tobacco. *Plant J.*, **28**, 361-369.

Bulone, V., Fincher, G.B. and Stone, B.A. (1995). *In vitro* synthesis of a microfibrillar (1→3)-β-D-glucan by a ryegrass (*Lolium multiflorum*) endosperm (1→3)-β-D-glucan synthase enriched by product entrapment. *Plant J.*, **8**, 213-225.

Burge, C. and Karlin, S., (1997). Prediction of complete gene structures in human genomic DNA. *J. Mol. Biol.*, **268**, 78-94.

Burton, R.A., Gibeaut, D.M., Bacic, A., Findlay, K., Roberts, K., Hamilton, A., Baulcombe, D.C. and Fincher, G.B. (2000). Virus-induced silencing of a plant cellulose synthase gene. *Plant Cell*, **12**, 691-705.

Bush, S.M., Folta, S. and Lannigan, D.A. (1996). Use of the yeast one-hybrid system to screen for mutations in the ligand-binding domain of the estrogen receptor. *Steroids*, **61**, 102-109.

Cabib, E., Roh, D.H., Schmidt, M., Crotti, L.B., and Varma, A. (2001). The yeast cell wall and septum as paradigms of cell growth and morphogenesis. *J. Biol. Sci.*, **276**, 19679-19682.

Cahill, D. and Weste, G. (1983). Formation of callose deposits as a response to infection with *Phytophthora cinnamomi*. *Trans. Brit. Mycol. Soc.*, **80**, 23-30.

Castro, C., Ribas, J.C., Valdivieso, M.H., Varona, R., Del, R.F. and Duran, A. (1995). Papulacandin B resistance in budding and fission yeasts: Isolation and characterization of a gene involved in (1,3)-β-D-glucan synthesis in *Saccharomyces cerevisiae*. *J. Bacteriol.*, **177**, 5732-5739.

Catala, C., Rose, J.K.C., York, W.S., Albersheim, P., Darvill, A.G. and Bennett, A.B. (2001). Characterization of a tomato xyloglucan endotransglycosylase gene that is down-regulated by auxin in etiolated hypocotyls. *Plant Phys.*, **127**, 1180-1192.

Chang, H.C. and Bush, D.R. (1997). Topology of NAT2, a prototypical example of a new family of amino acid transporters. *J. Biol. Chem.*, **272**, 30552-30557.

Charnock, S.J. and Davies, G.D. (1999). Structure of the nucleotide-diphospho-sugar transferase, SpsA from *Bacillus subtilis*, in native and nucleotide-complexed forms. *Biochem.*, **38**, 6380-638.

Chen, Z.L., Schuler, M.A. and Beachy, R.N. (1986). Functional analysis of regulatory elements in a plant embryo-specific gene. *Proc. Nat. Acad. Sci. U. S. A.*, **83**, 8560-8564.

Chory, J., Ecker, J.R., Briggs, S., Caboche, M., Coruzzi, G.M., Cook, D., Dangl, J., Grant, S., Guerinot, M.L., Henikoff, S., Martienssen, R., Okada, K., Raikhel, N.V., Somerville, C.R. and Weigel, D. (2000). National Science Foundation-Sponsored Workshop Report: "The 2010 Project": Functional genomics and the virtual plant. A blueprint for understanding how plants are built and how to improve them. *Plant Phys.*, **123**, 423-425.

Chuang, C.F. and Meyerowitz, E.M. (2000). Specific and heritable genetic interference by double-stranded RNA in *Arabidopsis thaliana*. *Proc. Nat. Acad. Sci. U. S. A.*, **97**, 4985-4990.

Clough, S.J. and Bent, A.F. (1998). Floral dip: A simplified method for *Agrobacterium*-mediated transformation of *Arabidopsis thaliana*. *Plant J.*, **16**, 735-743.

Cosgrove, D.J. (1997). Relaxation in a high-stress environment - The molecular bases of extensible cell walls and cell enlargement. *Plant Cell*, **9**, 1031-1041.

Côté, F. and Hahn, M.G. (1994). Oligosaccharins: Structures and signal transduction. *Plant Mol. Biol.*, **26**, 1379-1411.

Coutinho, P.M. & Henrissat, B. (1999). in *Recent Advances in Carbohydrate Bioengineering*, eds. Gilbert, H.J., Davies, G., Henrissat, B. & Svensson, B., The Royal Society of Chemistry, Cambridge, pp 3-12.

Cui, X.J., Shin, H.S., Song, C., Laosinchai, W., Amano, Y. and Brown, R.M. (2001). A putative plant homolog of the yeast beta-1,3-glucan synthase subunit FKS1 from cotton (*Gossypium hirsutum* L.) fibers. *Planta*, **213**, 223-230.

Czempinski, K., Zimmermann, S., Ehrhardt, T. and Mueller, R.B. (1997). New structure and function in plant K+ channels: KCO1, an outward rectifier with a steep Ca^{2+} dependency. *EMBO J.*, **16**, 2565-2575.

Czernilofsky, A.P., Hain, R., Baker, B. and Wirtz, U. (1986). Studies of the structure and functional organization of foreign DNA integrated into the genome of *Nicotiana tabacum*. *DNA*, **5**, 473-482.

Daniel, T. and Carling, D. (2002). Expression and regulation of the AMP-activated protein kinase-SNF1 (sucrose non-fermenting 1) kinase complexes in yeast and mammalian cells: Studies using chimaeric catalytic subunits. *Biochem. J.*, **365**, 629-638.

Delmer, D.P. (1987). Cellulose biosynthesis. *Ann. Rev. Plant Phys.*, **38**, 259-290.

Delmer, D.P. (1999). Cellulose biosynthesis: Exciting times for a difficult field of study. *Ann. Rev. Plant Phys. & Plant Mol. Biol.*, **50**, 245-276.

Delmer, D.P., Pear, J.R., Andrawis, A. and Stalker, D.M. (1995). Genes encoding small GTP-binding proteins analogous to mammalian *Rac* are preferentially expressed in developing cotton fibres. *Mol. & Gen. Genet.*, **248**, 43-51.

Delmer, D.P., Solomon, M. and Read, S.M. (1991). Direct photolabelling with ^{32}P-UDP-glucose for identification of a subunit of cotton fibre callose synthase. *Plant Phys.*, **95**, 556-563.

Delmer, D.P., Volokita, M., Solomon, M., Fritz, U., Delphendahl, W. and Herth, W. (1993). A monoclonal antibody recognizes a 65 kDa higher plant membrane polypeptide which undergoes cation-dependent association with callose synthase *in vitro* and co-localizes with sites of high callose deposition *in vivo*. *Protoplasma*, **176**, 33-42.

Deng, W., Grayburn, W.S., Hamilton, K.T.R., Collins, G.B. and Hildebrand, D.F. (1992). Expression of soybean-embryo lipoxygenase 2 in transgenic tobacco tissue. *Planta*, **187**, 203-208.

Devereux, J., Haeberli, P. and Smithies, O. (1984). A comprehensive set of sequence analysis programs for the VAX. *Nuc. Acids Res.*, **12**, 387-395.

Dhugga, K.S. and Ray, P.M. (1994). Purification of (1→3)-β-D-glucan synthase activity from pea tissue - Two polypeptides of 55 kDa and 70 kDa copurify with enzyme activity. *Eur. J. Biochem.*, **220**, 943-953.

Dijkgraaf, G.J.P., Abe, M., Ohya, Y. and Bussey, H. (2002). Mutations in *Fks1p* affect the cell wall content of beta-1,3- and beta-1,6-glucan in *Saccharomyces cerevisiae*. *Yeast*, **19**, 671-690.

Dinar, M., Rudich, J. and Zamski, E. (1983). Effects of heat stress on carbon transport from tomato (*Lycopersicon esculentum*) leaves. *Ann. Bot.*, **51**, 97-104.

Doblin, M.S., De Melis, L., Newbigin, E., Bacic, A. and Read, S.M. (2001). Pollen tubes of *Nicotiana alata* express two genes from different beta-glucan synthase families. *Plant Phys.*, **125**, 2040-2052.

Donofrio, N.M. and Delaney, T.P. (2001). Abnormal callose response phenotype and hypersusceptibility to *Peronospora parasitica* in defense-compromised *Arabidopsis* nim1-1 and salicylate hydroxylase-expressing plants. *Mol. Plant Microbe Int.*, **14**, 439-450.

Douglas, C.M., Dippolito, J.A., Shei, G.J., Meinz, M., Onishi, J., Marrinan, J.A., Li, W., Abruzzo, G.K., Flattery, A., Bartizal, K., Mitchell, A. and Kurtz, M.B. (1997). Identification of the *Fks1* gene of *Candida albicans* as the essential target of (1→3)-β-D-glucan synthase inhibitors. *Antimicrob. Ag. & Chemo.*, **41**, 2471-2479.

Douglas, C.M., Foor, F., Marrinan, J.A., Morin, N., Nielsen, J.B., Dahl, A.M., Mazur, P., Baginsky, W., Li, W.L., Elsherbeini, M., Clemas, J.A., Mandala, S.M., Frommer, B.R. and Kurtz, M.B. (1994). The *Saccharomyces cerevisiae Fks1 (Etg1)* gene encodes an integral membrane protein which is a subunit of (1→3)-β-D-glucan synthase. *Proc. Nat. Acad. Sci. U. S. A.*, **91**, 12907-12911.

Downey, P., Szabo, I., Ivashikina, N., Negro, A., Guzzo, F., Ache, P., Hedrich, R., Terzi, M. and Schiavo, F.L. (2000). KDC1, a novel carrot root hair K^+ channel. Cloning, characterization, and expression in mammalian cells. *J. Biol. Chem.*, **275**, 39420-39426.

Dreyer, I., Horeau, C., Lemaillet, G., Zimmermann, S., Bush, D.R., Rodriguez, N.A., Schachtman, D.P., Spalding, E.P., Sentenac, H. and Gaber, R.F. (1999). Identification and characterization of plant transporters using heterologous expression systems. *J. Exp. Bot.*, **50**, 1073-1087.

Drgonova, J., Drgon, T., Tanaka, K., Kollar, R., Chen, G.C., Ford, R.A., Chan, C.S.M., Takai, Y. and Cabib, E. (1996). Rho1p, a yeast protein at the interface between cell polarization and morphogenesis. *Science*, **272**, 277-279.

Edwards, D.R. and Denhardt, D.T. (1985). A study of mitochondrial and nuclear transcription with cloned cDNA probes. Changes in the relative abundance of mitochondrial transcripts after stimulation of quiescent mouse fibroblasts. *Exp. Cell Res.*, **157**, 127-143.

Eschrich, W. (1954). Ein beitrag zur kenntnis der kallose. *Planta*, **44**, 532-542.

Fashena, S.J., Serebriiskii, I. and Golemis, E.A. (2000). The continued evolution of two-hybrid screening approaches in yeast: how to outwit different preys with different baits. *Gene*, **250**, 1-14.

Felix, G. and Boller, T. (2003). Molecular sensing of bacteria in plants. The highly conserved RNA-binding motif RNP-1 of bacterial cold shock proteins is recognized as an elicitor signal in tobacco. *J. Biol. Chem.*, **278**, 6201-6208.

Fields, S. and Song, C. (1989). A novel genetic system to detect protein-protein interactions. *Nature*, **340**, 245-246.

Fields, S. and Sternglanz, R. (1994). The two-hybrid system: An assay for protein-protein interactions. *Trends in Genet.*, **10**, 286-292.

Fincher, G.B. and Stone, B.A. (1981). in *Encyclopaedia of Plant Physiology*, eds Tanner W. and Loewus F.A., Springer-Verlag, Berlin, pp 68-132.

Fink, J., Jeblick, W. and Kauss, H. (1990). Partial purification and immunological characterization of (1→3)-β-D-glucan synthase from suspension cells of *Glycine max*. *Planta*, **181**, 343-348.

Fire, A., Xu, S., Montgomery, M.K., Kostas, S.A., Driver, S.E. and Mello, C.C. (1998). Potent and specific genetic interference by double-stranded RNA in *Caenorhabditis elegans*. *Nature*, **391**, 806-811.

Frohman, M.A., Dush, M.K. and Martin, G.R. (1998). Rapid production of full-length complementary DNA species from rare transcripts: Amplification using a single gene-specific oligonucleotide primer. *Proc. Nat. Acad. Sci. U. S. A.*, **85**, 8998-9002.

Frommer, W.B. and Ninnemann, O. (1995). Heterologous expression of genes in bacterial, fungal, animal, and plant-cells. *Ann. Rev. Plant Phys. & Plant Mol. Biol.*, **46**, 419-444.

Fukuda, Y. (1997). Interaction of tobacco nuclear protein with an elicitor-responsive element in the promoter of a basic class I chitinase gene. *Plant Mol. Biol.*, **34**, 81-87.

Geisse, S., Gram, H., Kleuser, B. and Kocher, H.P. (1996). Eukaryotic expression systems: A comparison. *Prot. Exp. & Pur.*, **8**, 271-282.

Gibeaut, D., Hulett, J., Cramer, G.R. and Seemann, J.R. (1997). Maximal biomass of *Arabidopsis thaliana* using a simple, low-maintenance hydroponic method and favorable environmental conditions. *Plant Phys.*, **115**, 317-319.

Giese, H., Hippe-Sanwald, S. and Weller, J. (1997). in *The Mycota V Part B,* eds Carroll, G. and Tudzynski, P., Springer, Heidelberg, pp 55-78.

Goff, S.A., Ricke, D., Lan, T.H., Presting, G., Wang, R.L., Dunn, M., Glazebrook, J., Sessions, A., Oeller, P., Varma, H., Hadley, D., Hutchinson, D., Martin, C., Katagiri, F., Lange, B.M., Moughamer, T., Xia, Y., Budworth, P., Zhong, J.P., Miguel, T., Paszkowski, U., Zhang, S.P., Colbert, M., Sun, W.L., Chen, L.L. and *et al.* (2002). A draft sequence of the rice genome (*Oryza sativa* L. ssp japonica). *Science*, **296**, 92-100.

Gold, R.E., Aist, J.R., Hazen, B.E., Stolzenburg, M.C., Marshall, M.R. and Israel, H.W. (1986). Effects of calcium nitrate and chlortetracycline on papilla formation, ml-o resistance and susceptibility of barley to powdery mildew. *Phys. & Mol. Plant Path.*, **29**, 115-129.

Goodall, G.J. and Filipowicz, W. (1989). The AU-rich sequences present in the introns of plant nuclear pre-messenger RNA are required for splicing. *Cell*, **58**, 473-484.

Goodall, G.J. and Filipowicz, W. (1991). Different effects of intron nucleotide composition and secondary structure on precursor-messenger RNA splicing in monocot and dicot plants. *EMBO J.*, **10**, 2635-2644.

Goubet, F. and Morvan, C. (1995). Effects of calcium ions on β-D-glucan synthase activities in suspension-cultured cells of flax. *Plant Phys. & Biochem.*, **33**, 433-441.

Grant, M.R., Brown, I., Adams, S., Knight M., Ainslie, A. and Mansfield, J.W. (2000). The *RPM1* plant disease resistance gene facilitates a rapid and sustained increase in cytosolic calcium that is necessary for the oxidative burst and hypersensitive cell death. *Plant J.*, **23**, 441-450.

Green, R., Szostak, J.W., Benner, S.A., Rich, A. and Usman, N. (1991). Synthesis of RNA containing inosine: Analysis of the sequence requirements for the 5' splice site of the Tetrahymena group I intron. *Nuc. Acids Res.*, **19**, 4161-4166.

Guan, D.C., Li, P., Riggs, P.D. and Inouye, H. (1998). Vectors that facilitate the expression and purification of foreign peptides in *Escherichia coli* by fusion to maltose-binding protein. *Gene*, **67**, 21-30.

Hackett, R.W. and Lis, J.T. (1981). DNA sequence analysis reveals extensive homologies of regions preceding hsp70 and alpha-beta heat shock genes in *Drosophila melanogaster*. *Proc. Nat. Acad. Sci. U. S. A.*, **78**, 6196-6200.

Hamilton, A.J. and Baulcombe, D.C. (1999). A species of small antisense RNA in posttranscriptional gene silencing in plants. *Science*, **286**, 950-952.

Han, K.G., Lee, S.S. and Kang, C. (1999). Soluble expression of cloned phage K11 RNA polymerase gene in *Escherichia coli* at a low temperature. *Prot. Exp. & Pur.*, **16**, 103-108.

Hanfrey, C., Sommer, S., Mayer, M.J., Burtin, D. and Michael, A.J. (2001). *Arabidopsis* polyamine biosynthesis: Absence of ornithine decarboxylase and the mechanism of arginine decarboxylase activity. *Plant J.*, **27**, 551-560.

Hayashi, T., Read, S.M., Bussell, J., Thelen, M., Lin, F.C., Brown, R.M. and Delmer, D.P. (1987). UDP-Glucose: (1→3)-β-D-glucan synthases from mung bean and cotton. *Plant Phys.*, **83**, 1054-1062.

Heath, M.C. (2002). Cellular interactions between biotrophic fungal pathogens and host or non-host plants. *Can. J. Plant Path.*, **24**, 259-264.

Heid, C.A., Stevens J., Livak, K.J. and Williams, P.M. (1996). Real time quantitative PCR. *Genome Res.*, **6**, 986-994.

Heitefuss, R. and Ebrahim-Nesbat, F. (1986). Ultrastructural and histochemical studies on mildew of barley (*Erysiphe graminis* DC. f. sp. *hordei* Marchal). III. Ultrastructure of different types of papillae in susceptible and adult plant resistant leaves. *J. Phytopath.*, **116**, 358-373.

Henry, R.J. and Stone, B.A. (1982a). Solubilization of β-D-glucan synthases from the membranes of cultured ryegrass endosperm cells. *J. Biochem.*, **203**, 629-636.

Henry, R.J. and Stone, B.A. (1982b). Factors influencing β-D-glucan synthesis by particulate enzymes from suspension-cultured *Lolium multiflorum* endosperm cells. *Plant Phys.*, **69**, 632-636.

Hippe-Sanwald, S., Hermanns, M. and Somerville, S.C. (1992). Ultrastructural comparison of incompatible and compatible interactions in the barley powdery mildew disease. *Protoplasma*, **168,** 27-40.

Hong, Z.L., Delauney, A.J. and Verma, D.P.S. (2001a). A cell plate specific callose synthase and its interaction with phragmoplastin. *Plant Cell*, **13**, 755-768.

Hong, Z.L., Zhang, Z.M., Olson, J.M. and Verma, D.P.S. (2001b). A novel UDP-glucose transferase is part of the callose synthase complex and interacts with phragmoplastin at the forming cell plate. *Plant Cell*, **13**, 769-779.

Horst, W.J., Asher, C.J., Cakmak, I., Szulkiewicz, P. and Wissemeier, A.H. (1992). Short-term responses of soybean roots to aluminium. *J. Plant Phys.*, **140**, 174-178.

Horst, W.J., Pueschel, A.K. and Schmohl, N. (1997). Induction of callose formation is a sensitive marker for genotypic aluminium sensitivity in maize. *Plant & Soil*, **192**, 23-30.

Huang, K.X., Huang, Q.L., Wildung, M.R., Croteau, R. and Scott, A.I. (1998). Overproduction, in *Escherichia coli*, of soluble taxadiene synthase, a key enzyme in the taxol biosynthetic pathway. *Prot. Exp. & Pur.*, **13**, 90-96.

Hunt, M.D., Neuenschwander, U.H., Delaney, T.P., Weymann, K.B., Friedrich, L.B., Lawton, K.A., Steiner, H.Y. and Ryals, J.A. (1996). Recent advances in systemic acquired resistance research: A review. *Gene*, **179**, 89-95.

Iglesias, V.A. and Meins, F., Jr. (2000). Movement of plant viruses is delayed in a beta-1,3-glucanase-deficient mutant showing a reduced plasmodesmatal size exclusion limit and enhanced callose deposition. *Plant J.*, **21**, 157-166.

Immink, R.G.H., Gadella, T.W.J., Jr., Ferrario, S., Busscher, M. and Angenent, G.C. (2002). Analysis of MADS box protein-protein interactions in living plant cells. *Proc. Nat. Acad. Sci. U. S. A.*, **99**, 2416-2421.

Inoue, S.B., Aist, J.R. and Macko, V. (1994). Earlier papilla formation and resistance to barley powdery mildew induced by a papilla-regulating extract. *Phys. & Mol. Plant Path.*, **44**, 433-440.

Inoue, S.B., Qadota, H., Arisawa, M., Anraku, Y., Watanabe, T. and Ohya, Y. (1996). Signaling toward yeast 1,3-beta-glucan synthesis. *Cell Struc. & Func.*, **21**, 395-402.

Inoue, S.B., Takewaki, N., Takasuka, T., Mio, T., Adachi, M., Fujii, Y., Miyamoto, C., Arisawa, M., Furuichi, Y. and Watanabe, T. (1995). Characterization and gene cloning of 1,3-β-D-glucan synthase from *Saccharomyces cerevisiae*. *Eur. J. Biochem.*, **231**, 845-854.

Israel, H.W., Wilson, R.G., Aist, J.R. and Kunoh, H. (1980). Cell wall appositions and plant disease resistance: Acoustic microscopy of papillae that block fungal ingress. *Proc. Nat. Acad. Sci. U. S. A.*, **77**, 2046-2049.

Itaya, A., Woo, Y.M., Masuta, C., Bao, Y., Nelson, R.S., and Ding, B. (1998). Developmental regulation of intercellular protein trafficking through plasmodesmata in tobacco leaf epidermis. *Plant Phys.*, **118,** 373–385.

Jako, C., Kumar, A., Wei, Y., Zou, J., Barton, D.L., Giblin, E.M., Covello, P.S. and Taylor, D.C. (2001). Seed-specific over-expression of an *Arabidopsis* cDNA encoding a diacylglycerol acyltransferase enhances seed oil content and seed weight. *Plant Phys.*, **126**, 861-874.

Janknecht, R. and Nordheim, A. (1991). Affinity purification of histidine-tagged proteins transiently produced in HeLa cells. *Gene*, **121**, 321-324.

Jarillo, J.A., Gabrys, H., Capel, J., Alonso, J.M., Ecker, J.R. and Cashmore, A.R. (2001). Phototropin-related NPL1 controls chloroplast relocation induced by blue light. *Nature*, **410**, 952-954.

Jørgensen, J.H. (1992). Discovery, characterisation and exploitation of Mlo powdery mildew resistance in barley. *Euphytica*, **63**, 141-152.

Jorns, A.C., Hecht, B.C. and Wissemeier, A.H. (1991). Aluminium-induced callose formation in root tips of Norway spruce (*Picea abies* (L.) Karst.). *Zeit. Pflanzen. Und Bodenkunde*, **154**, 349-354.

Kammerloher, W., Fischer, U., Piechottka, G.P. and Schaffner, A.R. (1994). Water channels in the plant plasma membrane cloned by immunoselection from a mammalian expression system. *Plant J.*, **6**, 187-199.

Kapoor, S. and Bhatla, S.C. (1998). Indole-3-acetic acid elicits Ca^{2+}-dependent callose synthesis in the protonema of *Funaria hygrometrica*. *J. Plant Phys.*, **153**, 520-522.

Kelly, R., Register, E., Hsu, M.J., Kurtz, M. and Nielsen, J. (1996). Isolation of a gene involved in 1,3-beta-glucan synthesis in *Aspergillus nidulans* and purification of the corresponding protein. *J. Bacteriol.*, **178**, 4381-4391.

Kessler, G. (1958). Zur charakterisierung der siebrohrenkallose. *Ber. Schwiez. Bot. Ges.* **68**, 5-43.

Kim, M.C., Panstruga, R., Elliott, C., Muller, J., Devoto, A., Yoon, H.W., Park, H.C., Cho, M.J. and Schulze-Lefert, P. (2002). Calmodulin interacts with MLO protein to regulate defence against mildew in barley. *Nature*, **416**, 447-450.

Kobayashi, Y., Kobayashi, I., Funaki, Y., Fujimoto, S., Takemoto, T., and Kunoh, H. (1997). Dynamic reorganization of microfilaments and microtubules is necessary for the expression of non-host resistance in barley coleoptile cells. *Plant J.*, **11**, 525-537.

Konarska, M.M., Padgett, R.A. and Sharp, P.A. (1985). Trans splicing of messenger RNA precursors *in vitro*. *Cell*, **42**, 165-172.

Kristoffersen, P., Teichmann, T., Stracke, R. and Palme, K. (1996). Signal sequence trap to clone cDNAs encoding secreted or membrane-associated plant proteins. *Anal. Biochem.*, **243**, 127-132.

Laemmli, U.K. (1970). Cleavage of structural proteins during the assembly of the head of bacteriophage T4. *Nature*, **227**, 680-685.

Lal, S., Choi, J.H. and Hannah, L.C. (1999). The AG dinucleotide terminating introns is important but not always required for pre-mRNA splicing in the maize endosperm. *Plant Phys.*, **120**, 65-72.

Lassner, M.W., Palys, J.M. and Yoder, J.I. (1989). Genetic transactivation of dissociation elements in transgenic tomato plants. *Mol. & Gen. Genet.*, **218**, 25-32.

Lawson, S.G., Mason, T.L., Sabin, R.D., Sloan, M.E., Drake, R.R., Haley, B.E. and Wasserman, B.P. (1989). UDP-glucose: (1→3)-β-D-glucan synthase from *Daucus carota* L. Characterisation, photoaffinity labelling and solubilisation. *Plant Phys.*, **90**, 1149-1156.

Leemans, J., Deblaere, R., DeGreve, H., Hernalsteens, J.P., Maes, M., van Montagu, M. and Schell, J. (1981). Site-specific mutagenesis of *Agrobacterium tumefaciens* Ti plasmids and transfer of genes to plant cells. *J. Mol. & App. Gen.*, **1**, 149-164.

Leon, J., Rojo, E. and Sanchez, S.J.J. (2001). Wound signalling in plants. *J. Exp. Bot.*, **52**, 1-9.

Leon, J., Rojo, E., Titarenko, E. and Sanchez, S.J.J. (1998). Jasmonic acid-dependent and -independent wound signal transduction pathways are differentially regulated by Ca^{2+}/calmodulin in *Arabidopsis thaliana*. *Mol. & Gen. Genet.*, **258**, 412-419.

Li, H., Lin, Y., Heath, R.M., Zhu, M.X. and Yang, Z. (1999). Control of pollen tube tip growth by a Rop GTPase-dependent pathway that leads to tip-localized calcium influx. *Plant Cell*, **11**, 1731-1742.

Li, H.J., Bacic, A. and Read, S.M. (1997). Activation of pollen tube callose synthase by detergents - Evidence for different mechanisms of action. *Plant Phys.*, **114**, 1255-1265.

Li, H.W., Lucy, A.P., Guo, H.S., Li, W.X., Ji, L.H., Wong, S.M. and Ding, S.W. (1999). Strong host resistance targeted against a viral suppressor of the plant gene silencing defence mechanism. *EMBO J.*, **18**, 2683-2691.

Li, J., Burton, R.A., Harvey, A.J., Hrmova, M., Wardak, A.Z., Stone, B.A. and Fincher, G.B. (2003). The product of a callose synthase gene from barley synthesises (1→3)-β-D-glucan. *In preparation*.

Maina, C.V., Riggs, P.D., Grandea, A.G.I., Slatko, B.E., Moran, L.S., Tagliamonte, J.A., McReynolds, L.A. and Guan, C.D. (1988). An *Escherichia coli* vector to express and purify foreign proteins by fusion to and separation from maltose-binding protein. *Gene*, **74**, 365-374.

Mangin, L. (1890). Sur la callose, novelle substance fondamentale existant dans la membrane. Compt. *Rend. Hebd. Séances Acad. Sci.*, **110**, 644-647.

Matthews, D.E., Carollo, V.L., Lazo, G.R. and Anderson, O.D. (2003). GrainGenes, the genome database for small-grain crops. *Nuc. Acids Res.*, **31**, 183-186.

Mazur, P. and Baginsky, W. (1996). *In vitro* activity of (1→3)-β-D-glucan synthase requires the GTP-binding protein Rho1. *J. Biol. Chem.*, **271**, 14604-14609.

Mazur, P., Morin, N., Baginsky, W., Elsherbeini, M., Clemas, J.A., Nielsen, J.B. and Foor, F. (1995). Differential expression and function of two homologous subunits of yeast (1→3)-β-D-glucan synthase. *Mol. & Cell. Biol.*, **15**, 5671-5681.

McCormac, A.C., Cherry, J.R., Hershey, H.P., Vierstra, R.D. and Smith, H. (1991). Photoresponses of transgenic tobacco plants expressing an oat phytochrome gene. *Planta*, **185**, 162-170.

McCormack, B.A., Gregory, A.C.E., Kerry, M.E., Smith, C. and Bolwell, G.P. (1997). Purification of an elicitor-induced glucan synthase (callose synthase) from suspension cultures of french bean (*Phaseolus Vulgaris* L.) - Purification and immunolocation of a probable M_r-65 000 subunit of the enzyme. *Planta*, **203**, 196-203.

Mendgen, K. and Hahn, M. (2002). Plant infection and the establishment of fungal biotrophy. *Trends in Plant Sci.*, **7**, 352-356.

Meikle, P.J., Ng, K.F., Johnson, E., Hoogenraad, N.J. and Stone, B.A. (1991). The beta - glucan synthase from *Lolium multiflorum* : Detergent solubilization, purification using monoclonal antibodies, and photoaffinity labeling with a novel photoreactive pyrimidine analogue of uridine 5'-diphosphoglucose. *J. Biol. Chem.*, **266**, 22569-581.

Meir, S., Philosoph, H.S. and Aharoni, N. (1984). Role of IAA conjugates in inducing ethylene production by tobacco (*Nicotiana tabacum* cultivar Xanthi) leaf discs. *J. Plant Growth Reg.*, **3**, 169-182.

Mio, T., Adachishimizu, M., Tachibana, Y., Tabuchi, H., Inoue, S.B., Yabe, T., Yamadaokabe, T., Arisawa, M., Watanabe, T. and Yamadaokabe, H. (1997). Cloning of the *Candida albicans* homolog of *Saccharomyces cerevisiae Gsc1/Fks1* and its involvement in beta-1,3-glucan synthesis. *J. Bacteriol.*, **179**, 4096-4105.

Mol, P.C., Park, H.M., Mullins, J.T. and Cabib, E. (1994). A GTP-binding protein regulates the activity of (1→3)-beta-glucan synthase, an enzyme directly involved in yeast cell wall morphogenesis. *J. Biol. Chem.*, **269**, 31267-31274.

Molendijk, A.J., Bischoff, F., Rajendrakumar, C.S.V., Friml, J., Braun, M., Gilroy, S. and Palme, K. (2001). *Arabidopsis thaliana* Rop GTPases are localized to tips of root hairs and control polar growth. *EMBO J.*, **20**, 2779-2788.

Moore, M.J. and Sharp, P.A. (1993). Evidence for two active sites in the spliceosome provided by stereochemistry of pre-mRNA splicing. *Nature*, **365**, 364-368.

Nasmyth, K.A. and Reed, S.I. (1980). Isolation of genes by complementation in yeast (*Saccharomyces cerevisiae*): Molecular cloning of a cell-cycle gene. *Proc. Nat. Acad. Sci. U. S. A.*, **77**, 2119-2123.

Nass, M.M.K. (1981). Restriction endonuclease analysis of mitochondrial DNA from virus-transformed tumor and control cells of human, hamster and avian origin: Sequence conservation and intraspecific variation. *Biochim. Biophys. Acta*, **655**, 210-220.

Northcote, D.H., Davey, R. and Lay, J. (1989). Use of antisera to localize callose, xylan and arabinogalactan in the cell-plate, primary and secondary walls of plant cells. *Planta*, **178**, 353-366.

Oono, Y., Suzuki, T., Toki, S. and Uchimiya, H. (1993). Effects of the over-expression of the *rolC* gene on leaf development in transgenic periclinal chimeric plants. *Plant & Cell Phys.*, **34**, 745-752.

Osmond, R.I.W. (2000). Barley family five pathogenesis-related proteins. *PhD Thesis*, University of Adelaide, Glen Osmond, Australia.

Østergaard, L., Petersen, M., Mattsson, O. and Mundy, J. (2002). An *Arabidopsis* callose synthase. *Plant Mol. Biol.*, **49**, 559-566.

Otegui, M.S., Mastronarde, D.N., Kang, B.H., Bednarek, S.Y. and Staehelin, L.A. (2001). Three-dimensional analysis of syncytial-type cell plates during endosperm cellularization visualized by high resolution electron tomography. *Plant Cell*, **13**, 2033-2051.

Ouellet, F., Overvoorde, P.J. and Theologis, A. (2001). IAA17/AXR3: Biochemical insight into an auxin mutant phenotype. *Plant Cell*, **13**, 829-841.

Pear, J.R., Kawagoe, Y., Schreckengost, W.E., Delmer, D.P. and Stalker, D.M. (1996). Higher plants contain homologs of the bacterial *CelA* genes encoding the catalytic subunit of cellulose synthase. *Proc. Nat. Acad. Sci. U. S. A.*, **93**, 12637-12642.

Peterbauer, T., Mucha, J., Mayer, U., Popp, M., Gloessl, J. and Richter, A. (1999). Stachyose synthesis in seeds of adzuki bean (*Vigna angularis*): Molecular cloning and functional expression of stachyose synthase. *Plant J.*, **20**, 509-518.

Philip, B. & Levin, D.E. (2001). Wsc1 and Mid2 are cell surface sensors for cell wall integrity signaling that act through Rom2, a guanine nucleotide exchange factor for Rho1. *Mol. Cell. Biol.*, **21**, 271-280.

Piao, H.L., Lim, J.H.; Kim, S.J., Cheong, G.W. and Hwang, I. (2001). Constitutive over-expression of *AtGSK1* induces NaCl stress responses in the absence of NaCl stress and results in enhanced NaCl tolerance in *Arabidopsis*. *Plant J.*, **27**, 305-314.

Pierrugues, O., Brutesco, C., Oshiro, J., Gouy, M., Deveaux, Y., Carman, G.M., Thuriaux, P. and Kazmaier, M. (2001). Lipid phosphate phosphatases in *Arabidopsis*: Regulation of the *AtLPP1* gene in response to stress. *J. Biol. Chem.*, **276**, 20300-20308.

Qadota, H., Python, C.P., Inoue, S.B., Arisawa, M., Anraku, Y., Zheng, Y., Watanabe, T., Levin, D.E. and Ohya, Y. (1996). Identification of yeast *Rho1p* GTPase as a regulatory subunit of (1→3)-β-D-glucan synthase. *Science*, **272**, 279-281.

Quail, P.H. (2000). Phytochrome-interacting factors. *Sem. Cell & Dev. Biol.*, **11**, 457-466.

Radford, J.E., Vesk, M. and Overall, R.L. (1998). Callose deposition at plasmodesmata. *Protoplasma*, **201**, 30-37.

Radwanski, E.R., Barczak, A.J. and Last, R.L. (1996). Characterization of tryptophan synthase alpha subunit mutants of *Arabidopsis thaliana*. *Mol. and Gen. Genet.*, **253**, 353-361.

Rakwal, R., Kaku, H. and Komatsu, S. (2001). Immunological evidence for induction of pathogenesis related proteins by jasmonic acid and blast infection in rice (*Oryza sativa* L.). *Res. Comm. Biochem. Cell Mol. Biol.*, **5**, 3-25.

Richmond, T.A. and Somerville, C.R. (2000). The cellulose synthase superfamily. *Plant Phys.*, **124**, 495-498.

Riehl, T.E. and Jaffe, M.J. (1984). Physiological studies on pea (*Pisum sativum* cultivar Alaska) tendrils: 14. Effects of mechanical perturbation, light, and 2-deoxy-D-glucose on callose deposition and tendril coiling. *Plant Phys.*, **75**, 679-687.

Rose, J.K.C., Ham, K.S, Darvill, A.G. and Albersheim, P. (2002). Molecular cloning and characterization of glucanase inhibitor proteins: Coevolution of a counterdefense mechanism by plant pathogens. *Plant Cell*, **14**, 1329-1345.

Rossmann, C., Sharp, N., Allen, G. and Gewert, D. (1996). Expression and purification of recombinant, glycosylated human interferon alpha 2b in murine myeloma NSo cells. *Prot. Exp. & Pur.*, **7**, 335-342.

Rozen, S. and Skaletsky, H.J. (1996, 1997, 1998). Primer3. Code available at http://www.genome.wi.mit.edu/genome_software/other/primer3.html

Rushton, P.J., Reinstädler, A., Lipka, V., Lippock, B. and Somssich, E. (2002). Synthetic plant promoters containing defined regulatory elements provide novel insights into pathogen- and wound-induced signaling. *Plant Cell*, **14**, 749-762.

Ryals, J.A., Neuenschwander, U.H., Willits, M.G., Molina, A., Steiner, H.Y. and Hunt, M.D. (1996). Systemic acquired resistance. *Plant Cell*, **8**, 1809-1819.

Sakamoto, A., Ueda, M. and Morikawa, H. (2002). *Arabidopsis* glutathione-dependent formaldehyde dehydrogenase is an S-nitrosoglutathione reductase. *FEBS Letters*, **515**, 20-24.

Sambrook, J., Fritsch, E.F. and Maniatis T. (1987). Molecular cloning: a laboratory manual, Cold Spring Harbor Laboratory Press, Cold Spring Harbor, NY.

Sano, H., Seo, S., Koizumi, N., Niki, T., Iwamura, H. and Ohashi, Y. (1996). Regulation by cytokinins of endogenous levels of jasmonic and salicylic acids in mechanically wounded tobacco plants. *Plant Cell Phys.*, **37**, 762-769.

Sauer, N., Friedlaender, K. and Graeml, W.U. (1990). Primary structure, genomic organization and heterologous expression of a glucose transporter from *Arabidopsis thaliana*. *EMBO J.*, **9**, 3045-3050.

Saxena, I.M., Lin, F.C. and Brown, R.M.J. (1990). Cloning and sequencing of the cellulose synthase catalytic subunit gene of *Acetobacter xylinum*. *Plant Mol. Biol.*, **15**, 673-684.

Sayanova, O., Beaudoin, F., Libisch, B., Castel, A., Shewry, P.R. and Napier, J.A. (2001). Mutagenesis and heterologous expression in yeast of a plant DELTA6-fatty acid desaturase. *J. Exp. Bot.*, **52**, 1581-1585.

Schlüpmann, H., Bacic, A. and Read, S.M. (1993). A novel callose synthase from pollen tubes of *Nicotiana*. *Planta*, **191**, 470-481.

Schlüpmann, H., Bacic, A. and Read, S.M. (1994). Uridine diphosphate glucose metabolism and callose synthesis in cultured pollen tubes of *Nicotiana alata* Link Et Otto. *Plant Phys.*, **105**, 659-670.

Schweizer, P., Pokorny, J., Schulze-Lefert, P. and Dudler, R. (2000). Double-stranded RNA interferes with gene function at the single-cell level in cereals. *Plant J.*, **24**, 895-903.

Sen Gupta, D.J., Zhang, B., Kraemer, B., Pochart, P., Fields, S. and Wickens, M. (1996). A three-hybrid system to detect RNA-protein interactions *in vivo*. *Proc. Nat. Acad. Sci. U. S. A.*, **93**, 8496-8501.

Shea, E.M., Gibeaut, D.M. and Carpita, N.C. (1989). Structural analysis of the cell walls regenerated by carrot protoplasts. *Planta*, **179**, 293-308.

Shimomora, T. (1982). Effects of boron on the formation of local lesions and accumulation of callose in French bean (*Phaseolus vulgaris* cultivar Gintebo) and tobacco (*Nicotiana tabacum*) cultivar Samsun NN leaves inoculated with tobacco mosaic virus. *Phys. Plant Path.*, **20**, 257-262.

Shirasu, K., Nielsen, K., Piffanelli, P., Oliver, R. and Schulze-Lefert. P. (1999). Cell-autonomous complementation of mlo resistance using a biolistic transient expression system. *Plant J.*, **17**, 293-299.

Siebert, P.D., Chenchik, A., Kellogg, D.E., Lukyanov, K.A. and Lukyanov, S.A. (1995). An improved PCR method for walking in uncloned genomic DNA. *Nuc. Acids Res.*, **23**, 1087-1088.

Skou, J.P., Jorgensen, J.H. and Lilholt, U. (1984). Comparative studies on callose formation in powdery mildew compatible and incompatible barley (*Hordeum vulgare*). *Phytopathologische Zeitschrift*, **109**, 147-168.

Slakeski, N., Baulcombe, D.C., Devos, K.M., Ahluwalia, B., Doan, D.N.P. and Fincher, G.B. (1990). Structure and tissue-specific regulation of genes encoding barley (1→3, 1→4)-beta-glucan endohydrolases. *Mol. & Gen. Genet.*, **224**, 437-449.

Smart, M.G., Aist, J.R. and Israel, H.W. (1986a). Structure and function of wall appositions: 1. General histochemistry of papillae in barley (*Hordeum vulgare*) coleoptiles attacked by *Erysiphe graminis* f. sp. *hordei*. *Can. J. Bot.*, **64**, 793-801.

Smart, M.G., Aist, J.R. and Israel, H.W. (1986b). Structure and function of wall appositions: 2. Callose and the resistance of oversize papillae to penetration by *Erysiphe graminis* f. sp. *hordei*. *Can. J. Bot.*, **64**, 802-804.

Smith, N.A., Singh, S.P., Wang, M.B., Stoutjesdijk, P.A., Green, A.G. and Waterhouse, P.M. (2000). Gene expression - Total silencing by intron-spliced hairpin RNAs. *Nature*, **407**, 319-320.

Soellick, T.R., Uhrig, J.F., Bucher, G.L., Kellmann, J.W. and Schreier, P.H. (2000). The movement protein NSm of tomato spotted wilt tospovirus (TSWV): RNA binding, interaction with the TSWV N protein, and identification of interacting plant proteins. *Proc. Nat. Acad. Sci. U. S. A.*, **97**, 2373-2378.

Southern, E. (1975). Detection of specific sequences among DNA fragments separated by gel electrophoresis. *J. Mol. Biol.*, **98**, 503-517.

Steer, M.W. and Steer, J.M. (1989). Pollen tube tip growth. *New Phytol.*, **111**, 323-358.

Stone, B.A. and Clarke, A.E. (1992) Chemistry and biology of (1→3)-β-D-glucans. La Trobe University Press, Victoria, Australia.

Stone, B.A. and Svensson, B. (2001). Biosynthesis and Degradation, in *Glycoscience: Chemistry and Chemical Biology*, Vol. III, eds Fraser-Reid, B., Tatsuta, K. and Thiem, J., Springer-Verlag, Heidelberg, pp 1905-1989.

Stone, B.A., Evans, N.A., Bonig, I. and Clarke, A.E. (1985). The application of Sirofluor, a chemically defined fluorochrome from aniline blue for the histochemical detection of callose. *Protoplasma*, **122**, 191-195.

Sunilkumar, G., Mohr, L., Lopata, F.E., Emani, C. and Rathore, K.S. (2002). Developmental and tissue-specific expression of CaMV 35S promoter in cotton as revealed by GFP. *Plant Mol. Biol.*, **50**, 463-474.

Thelen, M.P. and Delmer, D.P. (1986). Gel-electrophoretic separation, detection, and characterization of plant and bacterial UDP-glucose glucosyltransferases. *Plant Phys.*, **81**, 913-918.

Thomas, B. and Hall, M.A. (1979). The control of wound callose formation in willow (*Salix viminalis*) phloem. *J. Exp. Bot.*, **30**, 449-458.

Thompson, C.J., Movva, N.R., Tizard, R., Crameri, R., Davies, J.E., Lauwereys, M. and Botterman, J. (1987). Characterization of the herbicide-resistance gene *bar* from *Streptomyces hygroscopicus*. *EMBO J.*, **6**, 2519-2524.

Thompson, J.D., Higgins D.G. and Gibson, T.J. (1994). CLUSTAL W: improving the sensitivity of progressive multiple sequence alignment through sequence weighting, position-specific gap penalties and weight matrix choice. *Nuc. Acids Res.*, **22**, 4673-4680.

Thompson, J.R., Douglas, C.M., Li, W.L., Jue, C.K., Pramanik, B., Yuan, X.L., Rude, T.H., Toffaletti, D.L., Perfect, J.R. and Kurtz, M. (1999). A glucan synthase *Fks1* homolog in *Cryptococcus neoformans* is single copy and encodes an essential function. *J. Bacteriol.*, **181**, 444-453.

Tourneur, C., Jouanin, L. and Vaucheret, H. (1993). Over-expression of acetolactate synthase confers resistance to valine in transgenic tobacco. *Plant Sci.*, **88**, 159-168.

Tsugita, A. and Kamo, M. (1999). 2-D electrophoresis of plant proteins. *Meth. Mol. Biol.*, **112**, 95-97.

Tucker M.R., Paech, N.A., Willemse, M.T.M., and Koltunow, A.M.G. (2001). Dynamics of callose deposition and beta-1,3-glucanase expression during reproductive events in sexual and apomictic *Hieracium*. *Planta*, **212**, 487-498.

Turner, A., Bacic, A., Harris, P.J. and Read, S.M. (1998). Membrane fractionation and enrichment of callose synthase from pollen tubes of *Nicotiana alata* Link Et Otto. *Planta*, **205**, 380-388.

Uozumi, N., Kim, E.J., Rubio, F., Yamaguchi, T., Muto, S., Tsuboi, A., Bakker, E.P., Nakamura, T. and Schroeder, J.I. (2000). The *Arabidopsis HKT1* gene homolog mediates inward Na^+ currents in *Xenopus laevis* oocytes and Na^+ uptake in *Saccharomyces cerevisiae*. *Plant Phys.*, **122**, 1249-1259.

Vandesompele, J., De Preter, K., Pattyn, F., Poppe, B., Van Roy, N., De Paepe, A. and Speleman, F. (2002). Accurate normalisation of real-time quantitative RT-PCR data by geometric averaging of multiple internal control genes. *Genome Biol.*, **3**, 1-12.

van Wees. S.C.M. and Glazebrook, J. (2003). Loss of non-host resistance of *Arabidopsis NahG* to *Pseudomonas syringae* pv. *phaseolicola* is due to degradation products of salicylic acid. *Plant J.*, **33**, 733-742.

Verma, D.P.S. (2001). Cytokinesis and building of the cell plate in plants. *Ann. Rev. Plant Phys. & Plant Mol. Biol.*, **52**, 751-784.

Verma, D.P.S. and Hong, Z.L. (2001). Plant callose synthase complexes. *Plant Mol. Biol.*, **47**, 693-701.

Vogel, J. and Somerville, S. (2000). Isolation and characterization of powdery mildew-resistant *Arabidopsis* mutants. *Proc. Nat. Acad. Sci. U. S. A.*, **97**, 1897-1902.

von Heijne, G. (1992). Membrane protein structure prediction: hydrophobicity analysis and the 'positive inside' rule. *J. Mol. Biol.*, **225**, 487-494.

Walhout, A.J.M. and Vidal, M. (2001). High-throughput yeast two-hybrid assays for large-scale protein interaction mapping. *Methods*, **24**, 297-306.

Wallroth, M., Gerats, A.G.M., Rogers, S.G., Fraley, R.T. and Horsch, R.B. (1986). Chromosomal localization of foreign genes in *Petunia hybrida*. *Mol. & Gen. Genet.*, **202**, 6-15.

Waterkeyn, L. (1981). Cytochemical localization and function of the 3-linked glucan callose in the developing cotton (*Gossypium hirsutum* cultivar B49) fiber cell wall. *Protoplasma*, **106**, 49-68.

Waterkeyn, L. and Bienfeit, A. (1979). Production et dégradationde callose dabs les stomates des Fougéres. *Cellule*, **73**, 83-97.

Weickert, M.J., Pagratis, M., Curry, S.R. and Blackmore, R. (1997). Stabilization of apoglobin by low temperature increases yield of soluble recombinant hemoglobin in *Escherichia coli*. *App. & Env. Microbiol.*, **63**, 4313-4320.

Wenzl, H. and Wodicka, B. (1981). The etiology of the occurrence of callose in the tubers of stolbur-diseased potato plants. *Zeitschrift fuer Pflanzenkrankheiten und Pflanzenschutz*, **88**, 584-587.

Wesley, S.V., Helliwell, C.A., Smith, N.A., Wang, M., Rouse, D.T., Liu, Q., Gooding, P.S., Singh, S.P., Abbott, D., Stoutjesdijk, P.A., Robinson, S.P., Gleave, A.P., Green, A.G. and Waterhouse, P.M. (2001). Construct design for efficient, effective and high-throughput gene silencing in plants. *Plant J.*, **27**, 581-590.

Wingfield, P.T., Sax J.K. Stahl, S.J., Kaufman, J., Palmer, I., Chung, V., Corcorans, M.L., Kleiners, D.E. and Stetler-Stevenson, W.G. (1999). Biophysical and functional characterization of full-length, recombinant human tissue inhibitor of metalloproteinases-2 (TIMP-2) produced in *Escherichia coli*. Comparison of wild type and amino-terminal alanine appended variant with implications for the mechanism of TIMP functions. *J. Biol. Chem.*, **274**, 21362-21368.

Wissemeier, A.H. and Horst, W.J. (1987). Callose deposition in leaves of cowpea (*Vigna unguiculata* (L.) Walp.) as a sensitive response to high manganese supply. *Plant & Soil*, **102**, 283-286.

Wissemeier, A.H. and Horst, W.J. (1995). Effect of calcium supply on aluminium-induced callose formation, its distribution and persistence in roots of soybean (*Glycine max* (L.) Merr.). *J. Plant Phys.*, **145**, 470-476.

Wissemeier, A.H., Hergenroeder, A., Mix, W.G. and Horst, W.J. (1993). Induction of callose formation by manganese in cell suspension culture and leaves of soybean (*Glycine max* L.). *J. Plant Phys.*, **142**, 67-73.

Wu, A. and Wasserman, B.P. (1993). Limited proteolysis of (1→3)-β-D-glucan (callose) synthase from *Beta vulgaris* L - Topology of protease-sensitive sites and polypeptide identification using pronase E. *Plant J.*, **4**, 683-695.

Yu, J., Hu, S.N., Wang, J., Wong, G.K.S., Li, S.G., Liu, B., Deng, Y.J., Dai, L., Zhou, Y., Zhang, X.Q., Cao, M.L., Liu, J., Sun, J.D., Tang, J.B., Chen, Y.J., Huang, X.B., Lin, W., Ye, C., Tong, W., Cong, L.J., Geng, J.N., Han, Y.J., Li, L., Li, W., Hu, G.Q., Yuan, L.P. and *et al.* (2002). A draft sequence of the rice genome (*Oryza sativa* L. ssp indica). *Science*, **296**, 79-92.

Zhang, Y., Olsen, D.R., Nguyen, K.B., Olson, P.S., Rhodes, E.T. and Mascarenhas, D. (1998). Expression of eukaryotic proteins in soluble form in *Escherichia coli*. *Prot. Exp. & Pur.*, **12**, 159-165.

Zhou, F., Kurth, J., Wei, F., Elliott, C., Vale, G., Yahiaoui, N., Keller, B., Somerville, S., Wise, R. and Schulze-Lefert. P. (2001). Cell-autonomous expression of barley *Mla1* confers race-specific resistance to the powdery mildew fungus via a *Rar1*-independent signaling pathway. *Plant Cell.*, **13**, 337-350.

Zimmermann, S., Talke, I., Ehrhardt, T., Nast, G. and Mueller, R.B. (1998). Characterization of SKT1, an inwardly rectifying potassium channel from potato, by heterologous expression in insect cells. *Plant Phys.*, **116**, 879-890.